The Pennsylvania State University

The Graduate School

College of Medicine

ALTERATIONS IN *FOXA1* AND *PTEN* EXPRESSION CONTRIBUTE TO MORPHOLOGIC AND MOLECULAR HETEROGENEITY IN BLADDER CANCER

A Dissertation in

Biomedical Sciences and Clinical and Translational Sciences

by

Vasty Osei Amponsa

Submitted in Partial Fulfillment
of the Requirements
for the Degree of

Doctor of Philosophy

May 2019

The dissertation of Vasty Osei Amponsa was reviewed and approved* by the following:

David J DeGraff
Assistant Professor of Pathology
Dissertation Advisor
Co-Chair of Committee

Kent E Vrana
Professor and Chair of Pharmacology
Co-Chair of Committee

Lisa M Shantz
Associate Professor of Cellular and Molecular Physiology

James R Broach
Professor and Chair of Biochemistry and Molecular Biology
Director of the Institution of Personalized Medicine

Ralph L Keil
Associate Professor of Biochemistry and Molecular Biology
Chair of Biomedical Sciences Graduate Program

*Signatures are on file in the Graduate School

ABSTRACT

Bladder cancer is a heterogeneous malignancy at both morphologic and genetic levels. The most common morphologic variant of bladder cancer is urothelial cell carcinoma, which is often admixed with other histologic variants including squamous differentiation and glandular differentiation. To improve therapeutic decision making, several molecular subtypes that can be broadly subdivided into basal subtype and luminal subtype based on gene expression patterns have been described. In addition to morphologic heterogeneity, evidence shows that bladder cancer can be heterogeneous in regards to molecular subtypes, challenging the effectiveness of therapies. Therefore, identifying the molecular signatures and the genetic alterations contributing to bladder cancer heterogeneity is of utmost importance.

Loss of the transcription factor, *FOXA1*, and the tumor suppressor, *PTEN*, has been reported in muscle invasive bladder cancer exhibiting heterogeneity in the form of squamous differentiation. Because this suggests that *FOXA1* and *PTEN* may play a role in bladder cancer pathogenesis, we hypothesized that loss of *FOXA1* and *PTEN* might cooperate to promote the development of heterogeneous bladder cancers.

To test our hypothesis, we integrated publicly available clinical data with *in vivo* and *in vitro* studies. Clinical data showed that concurrent loss of *FOXA1* and *PTEN* is a common event in muscle invasive bladder cancer. Supporting previous reports, *FOXA1* loss was associated with basal subtype bladder cancer whereas *PTEN* loss was independent of molecular subtype or presence of squamous differentiation. We identified copy number alterations and DNA promoter hypermethylation as significant contributors of *PTEN* and *FOXA1* expression, respectively. Moreover, bladder-specific knockout of *Foxa1* and *Pten* in mice resulted in carcinoma *in situ* with squamous differentiation, and in muscle invasive bladder cancer with extensive squamous differentiation when combined with carcinogen exposure. Expanding on the findings implicating

deletion of *Foxa1* and *Pten* in bladder tumorigenesis, overexpression of *FOXA1* and not of *PTEN* in UMUC3 bladder cancer cell lines resulted in a reduction of cell viability and induction of apoptosis supporting the idea of a protective role for *FOXA1* in bladder tumorigenesis.

Overall, our data show that genetic alterations of *FOXA1* and *PTEN* contribute to morphologic heterogeneity of bladder cancer in the form of squamous differentiation, and potentially drive the development of a basal molecular subtype disease. Future investigations on the molecular mechanisms between these two genes will provide further insight into their role in bladder cancer heterogeneity.

TABLE OF CONTENTS

LIST OF FIGURES

LIST OF TABLES

LIST OF ABBREVIATIONS

7-AAD	7-Aminoactinomycin D
AC	Adenocarcinoma
AKT	AKT Serine/Threonine kinase
APC	Adenomatosis polyposis coli tumor suppressor
APOBEC3B	Apolipoprotein B mRNA editing enzyme catalytic subunit 3B
AR	Androgen receptor
ARID1A	AT-Rich Interaction domain 1A
AUM	Asymmetric unit membrane
BBN	N-butyl-N-(4-hydroxybutyl) nitrosamine
BCG	Bacillus Calmette-Guérin
BCL-2	Apoptosis regulator
BCL2L1	BCL2 Like 1
BRCA1	Breast cancer 1, early onset
CCND1	Cyclin D1
CCND3	Cyclin D3
CCNE	Cyclin E1
CD24	Small cell lung carcinoma cluster 4 antigen
CD44	Cell surface glycoprotein CD44
CD80	Cluster of differentiation 80
CD86	Cluster of differentiation 86
CDH1	Cadherin 1
CDKN1A	Cyclin-dependent kinase inhibitor 1A
CDKN2A	Cyclin-dependent kinase inhibitor 2A
CDX2	Caudal type homeobox 2
CHD6	Chromodomain helicase DNA binding protein 6
CHGA, B	Chromogranin A, B
CIS	Carcinoma *in situ*
CRE	Cre recombinase
CTNNB1	Catenin beta 1
DAPK1	Death-associated protein kinase 1
DNMT1	DNA methyltransferase 1
DNMT3A	DNA methyltransferase 3 alpha
DNMT3B	DNA methyltransferase 3 beta
DSC3	Desmocollin 3
E2F3	Transcription factor 3
EGFR	Epidermal growth factor receptor

ELF3	E74 Like ETS transcription factor 3
EP300	E1A binding protein P300
EPCAM	Epithelial cell adhesion molecule
Epi-Inf	Epithelial-infiltrated
ER	Estrogen receptor
ERBB2	Erb-B2 receptor tyrosine kinase 2
ERCC2	Excision repair cross-complementation group 2
ERT2	Mutated estrogen receptor
FABP	Fatty acid binding protein
FACS	Flow cytometry
FAK	Focal adhesion kinase
FGFR3	Fibroblast growth factor receptor 3
FOXA1	Forkhead box A1
FOXQ1	Forkhead box Q1
GATA3	GATA binding protein 3
GD	Glandular differentiation
GEMs	Genetically engineered models
GU	Genomically unstable
HG	High grade
HRAS	Harvey rat sarcoma viral oncogene homolog
IHC	Immunohistochemistry
KDM6A	Lysine demethylase 6A
KLF5	Kruppel like factor 5
KMT2D	Lysine methyltransferase 2D
KRAS	Kirsten rat sarcoma viral proto-oncogene
KRTs	Cytokeratin 5, 6, 7, 8, 14, 16,17, 19, 20
IL	Interleukin 5, 6, 7, 17
ITP	Immune thrombocytopenia
LG	Low grade
LKB1	Liver kinase B1
LOH	Loss of heterozygosity
MAPK	Mitogen-activated protein kinase
MDA	MD Anderson Cancer Center
MDM2	Proto-oncogene, E3 ubiquitin protein ligase
MIBC	Muscle invasive bladder cancer
MLH1	MutL homolog 1
MMAC1	Mutated in multiple advanced cancers
mTORC1, 2	Mammalian target of Rapamycin complex 1, 2

MTT	3-(4,5-dimethylthiazol-2-yl)-2,5-diphenyltetrazolium bromide
MXI1	Max-interacting protein 1
NFE2L2	Nuclear Factor, erythroid 2 Like 2
NMIBC	Non-muscle invasive bladder cancer
PARP	Poly(ADP-ribose) polymerase 1
PD1	Programmed cell death protein
PDK1	Phosphatidylinositol-dependent kinase 1
PDL-1	Programmed cell death protein-ligand 1
PDX	Patient-derived xenograft
PI3	Peptidase Inhibitor 3
PI3K	phosphatidylinositol triphosphate kinase
PIK3CA	Phosphatidylinositol-4,5-bisphosphate 3-kinase catalytic subunit alpha
PIP2	Phosphatidylinositol 4,5 bisphosphate
PIP3	Phosphatidylinositol 3,4,5 triphosphate
PPARG	Peroxisome proliferator-activated receptor gamma
PTEN	Phosphatase and tensin homolog on chromosome ten
PTM	Post-translational modifications
RASSF1A	Ras association domain family member 1
RB1	Retinoblastoma 1
RXRA	Retinoid X receptor alpha
Sc/NE	Small-cell/neuroendocrine-like
SCC	Squamous cell carcinoma
SCCL	Squamous cell carcinoma-like
SCCL/Mes-Inf	Squamous cell carcinoma-like/mesenchymal-infiltrated
SCG2	Secretogranin 2
SCID	Severe combined immunodeficiency
SNAI2	Snail family transcriptional repressor 2
SqD	Squamous differentiation
STAG2	Stromal antigen 2
TCGA	The Cancer Genome Atlas
TEP1	TGF-β-regulated and epithelial cell-enriched phosphatase
TGM1	Transglutaminase 1
Tis	Tumor *in situ*
TNM	Tumor-Node-Metastasis
TP53/Tp53	Tumor protein P53
TP63/Tp63	Tumor protein P63
TSC1, 2	Tuberous sclerosis complex 1, 2
TUBB2B	Tubulin beta 2B class IIb

TUR	Transurethral resection
TWIST1, 2	Twist basic helix-loop-helix transcription factor 1, 2
TXNIP	Thioredoxin-interacting protein
UBC	Ubiquitin C
UCC	Urothelial cell carcinoma
UNC	University of North Carolina
UPI, -II, -III,	Uroplakin 1, 2, 3
uroA	Urobasal A
uroB	Urobasal B
VIM	Vimentin
WEE1	WEE1 G2 Checkpoint Kinase
ZEB2	Zinc finger E-Box binding homeobox 2

ACKNOWLEDGEMENTS

First and foremost, I owe my deepest gratitude to Lord Jesus Christ for taking me this far. *Lord, thank you! Awurade, medasi! Signore, Grazie!*

I am profoundly grateful to my supervisor, Dr. DeGraff for his patience, encouragement, constant support and intellectual guidance. Dr. DeGraff showed genuine interest in helping me shape my career goals and allowing me to explore and grow as a scientist. He took the risk of admitting me as his first graduate student, and for that, I am truly thankful for the opportunity he gave me in working in his Lab.

I am immensely grateful to my dissertation committee, Drs. Kent Vrana, James Broach, and Lisa Shantz, for their invaluable intellectual input throughout this project and for challenging me to become a well-rounded scientist. Drs. Vonn Walter, Joshua Warrick, and Jay Raman, thank you for all your feedback and insightful guidance through these years. My sincere thanks go to Drs. Douglas Stairs, Amanda Nelson and Ryan Hobbs for their constructive advice during the joint lab meetings.

This dissertation would have been impossible without the aid and support of the members of the DeGraff Lab. With their expertise, Lauren, Jenna, Justine, and Zongyu contributed bringing to light the work presented in this dissertation successfully. A special thank you to Hiro for being a fantastic friend and mentor; thanks for the laughter, the enjoyable discussions on a variety and weirdest of topics, and for always lending an open ear. I would also like to thank Bob for all his suggestions and support.

I extend my sincere gratitude to Dr. Ralph Keil and the BMS program for the support and encouragement through these years. I would also like to thank Drs. Jim Pawelczyk and Gail Thomas in the CTS program for giving me the opportunity to explore clinical research. To Ms. Karen Shields, I am forever thankful for your encouragement and support, for leaving your door always open especially in times of dejection.

Importantly, I dedicate this dissertation to my three extraordinary women, my grandmothers, Eno Mary and Abena Pokua, and my great-grandmother, Eno Yaa, for their constant prayers and support. *Medamo asi! Nyame nyira mo!* My sincerest gratitude to my parents, Kwadwo and Faustina Osei, I am genuinely grateful to have you guys. Thank you for your unconditional support, encouragement, and faith in me. To Maa Julie, thank you for your kindness and unwavering support; you literally walked with me through this experience encouraging and helping me put things in perspective. To my Italian families, Gianni and Luigia, Gaetano and Eria, thank you immensely for believing in me and unfailingly lifting me even from far away. To my sisters, Isabella and Jennifer, you are my reason, thank you for always cheering me up. A special thank you to my uncles, Albert and Francis, and my aunties Veronica and Maa Akua Achian.

Last but not least, I want to thank the rest of my family and friends in Italy, Ghana, and US. Special thanks to Ester, Gifty, Angela, Akua, Kodjo, Clement, Kwame Asante, Kwame Teye, Simi, Nana Marfo, Jeffrey, Yomi, Wale, Nana Ama, Leah, Frank, PJ, Chiara, Samuele, Matilde and Amanda for their constant support and for always keeping me grounded. It's never a dull moment with you guys. Indeed, we are not just friends: we are family. *Thank you!*

Chapter 1

Literature Review

The Bladder Urothelium

The urinary bladder (hereafter simply bladder) is a hollow organ composed of four different tissue layers including the mucosa, submucosa, muscularis propria and the peritoneal membrane (adventitia). Facing the lumen of the bladder is the mucosa, which consists of transitional epithelium (urothelium). Immediately adjacent and inferior to the urothelium lies a basement membrane, which connects to the submucosa (lamina propria), consisting of fibroblasts, blood vessels, nerves and immune cells (Figure 1-1). The lamina propria and submucosa form together the connective tissue that supports the bladder wall. The muscularis propria also referred to as detrusor muscle is a lining smooth muscle surrounding the bladder, which is covered by a layer of perivesical fat[1, 2].

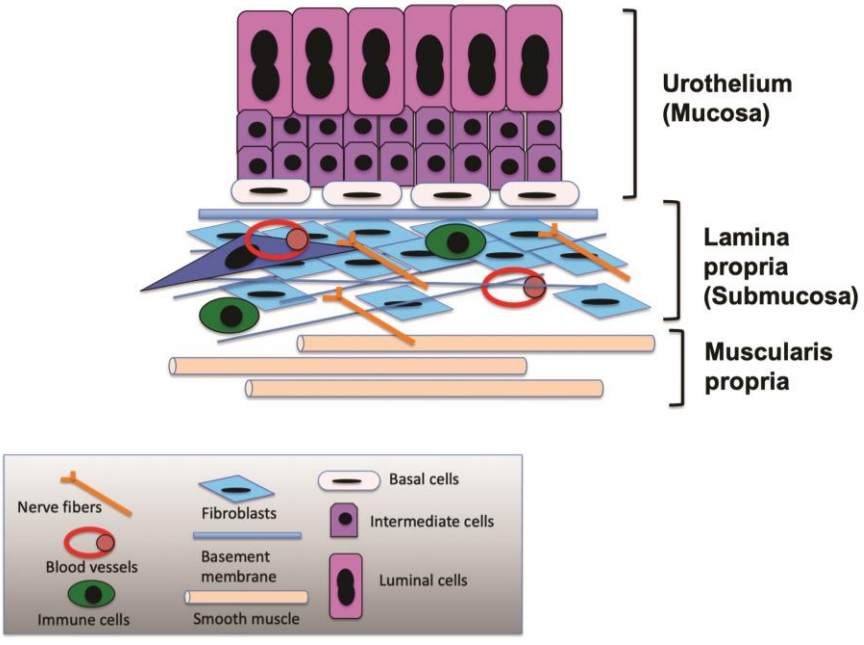

Figure 1-1. The bladder urothelium and associated connective tissue.

This cartoon represents the architecture of the bladder urothelium and additional cell types localized to the lamina propria and muscularis propria. Shown is the multilayered/stratified urothelium (mucosa) with luminal, intermediate and basal cells connected to the lamina propria (submucosa) through the basement membrane. The connective tissue enriched with different cells (such as fibroblasts, immune cells, and nerves) is adjacent to the smooth muscle (muscularis propria).

Three different cell populations constitute the bladder urothelium, including the basal cells, intermediate cells, and the luminal (superficial or umbrella) cells. The three cell populations differ in their shape, size, and urothelial marker expression[3, 4], and are structurally organized to form three to six layers of cells depending on the mammalian species. Hence the bladder urothelium is said to be a stratified epithelium[5]. The basal layer, similar in all species, consists of a single layer of cells adjacent to and connected to the basement membrane. It is constituted by small (10-20 μm in diameter), polygonal and mononucleated cells enriched of the expression of high molecular weight cytokeratins (KRT) including KRT5/6 and KRT14. Intermediate cells are similar in size to basal cells and are also mononucleated cells. While these cells are present as a single layer of cells in mouse urothelium, they can form up to five layers of cells in human urothelium[3]. Conversely, the luminal cell layer is composed of a single layer of large (20-40 μm in diameter), cuboidal, multinucleated and polarized cells, abundant in the expression of low molecular weight cytokeratins such as KRT20 and uroplakin proteins[6, 7].

Two major characteristics related to the functionality of the bladder urothelium are its impermeability and compliance. In addition to its barrier function, which is essential in limiting the exchange of substance between blood and urine, the “transitional” nature of the urothelium enables it to distend in the presence of bladder filling as well as to shrink during voiding[8, 9]. The permeability function of the urothelium is controlled by the activity of specialized urothelial plaques forming an asymmetric unit membrane (AUM) on the apical membrane of luminal cells

and by the presence of tight junctions, glycocalyx, and specialized lipids[4, 8]. The AUM is composed of uroplakin proteins (UPIa, UPIb, UPII, UPIIIa, and UPIIIb) synthesized by the luminal cells as they undergo urothelial terminal differentiation and specialization[10, 11].

Moreover, the cells of adult urothelium are quiescent cells exhibiting a slow proliferation rate. Evidence shows that in the absence of stimulation, while human adult urothelium has a cell cycle time of approximately 3 to 6 months[4], the turnover time of mouse adult urothelium is about 40 weeks[12]. However, experimental studies in rodents show that following acute injury from exposure to cyclophosphamide or the uropathogenic Escherichia *coli*, the bladder urothelium can rapidly proliferate and remarkably regenerate itself within 72 hours[13, 14]. Similar experimentation in rats exposed to protamine sulfate revealed the ability of urothelial cells to restore and form an intact urothelium by day 10[15]. Lineage tracing studies in mouse show that basal cells are capable of repopulating and restoring all three cell layers of the urothelium following pathogenic induced injury[16]. For this reason, basal cells are said to be progenitor cells of the urothelium. Nevertheless, contrasting evidence by a separate lineage tracing study revealed that intermediate cells rather than basal cells regenerate adult urothelium upon injury[17]. Additionally, developmental studies in mice deficient for tumor protein 63 (*Tp63*) showed that although these mice are deprived of basal and intermediate cells, they still develop a single layer of luminal/umbrella cells enriched of UpII expression[18, 19]. Thus, these studies suggest that umbrella cells may develop separately from intermediate and basal cells, and indicate the existence of potentially different processes driving urothelial cells differentiation, although further investigations are required.

Epidemiology

Bladder cancer is the second most common genitourinary malignancy after prostate cancer and is the sixth most common cancer worldwide with approximately 430,000 diagnoses in 2012[20]. Bladder cancer is also the third most common cancer among men, and it is the eleventh most common among women[21]. Although predominantly diagnosed in western and industrialized countries of Europe and North America, an increase in bladder cancer morbidity has been reported for North Africa and Middle East countries (i.e., Algeria, Egypt, Syria, Iraq) and also for Asia[22, 23]. According to the American Cancer Society estimates, approximately 81,190 people will have been newly diagnosed with bladder cancer in 2018 in the United States (US). Additionally, it is estimated that 17,340 people will have died in the US in 2018[21]. Evidence shows that incidence and mortality of bladder cancer are associated with socioeconomic, environmental and occupational factors, which differ based on demographics such as age, gender, ethnicity, and geographic location[24].

Among the most significant risk factors for bladder cancer are environmental factors including tobacco and occupational exposure to carcinogen. Over the past decades, the incidence of bladder cancer has remained stable in parallel with a decrease in the rates of tobacco smoking. However, with the event of new forms of tobacco smoking (i.e., electronic cigarette smoking), the composition of cigarettes has also changed leading to decreased concentrations of tar and nicotine but increased amount of tobacco-derivative carcinogens such as nitrosamines[25]. Thus, these changes in cigarette content may over time strengthen the association of tobacco smoking and the risk of bladder cancer[26, 27]. Moreover, a recent study shows that the contents of electronic cigarette possess carcinogenic properties and can induce tumorigenic transformation of urothelial cells and bronchial cells in both *in vivo* and *in vitro* studies[28].

Epidemiologic studies show that workers in the rubber industry and hairdressers are at higher risk of developing bladder cancer due to occupational exposure to industrial chemicals and

dye products containing aromatics amine (benzidine, naphthylamine, and nitrosamines)[29-31]. Moreover, dietary sources of nitrate, nitrite, and arsenic have also been associated with bladder cancer development[32-34]. Epidemiologic evidence indicates that genetic differences in carcinogen metabolism could be drivers of the differences in bladder cancer susceptibility among populations[35-37].

Age is also a significant risk factor, with the median age being 70 years old at the time of diagnosis[20, 38]. For reasons that are still unclear, men are approximately three times more likely to be diagnosed with bladder cancer[39], even upon stratification for other well-known risk factors such as age, cigarette smoking and occupational exposure to carcinogen[40]. Notably, women present a more advanced and aggressive disease than men at the time of diagnosis[41], but the sex-dependent nature of clinical outcomes is less clear. While some studies show that men have a superior rate of survival than women following treatment[42], other studies show no sex differences relative to treatment outcome and management[43, 44]. Steroid hormone receptors such as androgen receptor (AR) and estrogen receptor alpha (ESR1) are central to the molecular pathogenesis of prostate and breast cancer[45, 46] as well as a subset of other malignancies including lung and liver cancer[47, 48]. Indeed, a role for AR and ESR1 and estrogen receptor beta (ESR2) has been suggested in bladder cancer[49], but more research is required.

Ethnicity is also an established risk factor for bladder cancer. Likewise gender, racial disparities have also been noted, with African descendants presenting lower incidence but more advanced stage disease than other races (Caucasians, Asians) at diagnosis[50, 51]. However, in developing countries of the Middle East and Africa, the leading cause of bladder cancer is parasitic infection by *Schistosoma haematobium*, which causes the formation of non-urothelial cell carcinoma as described in a later section of this chapter[23, 52].

Clinicopathologic Features of Bladder Cancer

The majority of bladder cancers arise following neoplastic transformation of the urothelium[53] resulting in eventual disruption of the urothelial plaque and subsequent loss of differentiation and proper functionality of the bladder urothelium[54-56]. At the time of clinical presentation, most of the patients (80-90%) exhibit gross or microscopic painless hematuria (blood in urine), whereas 20-30% of patients present signs and symptoms of bladder irritations such as dysuria, frequency and urge incontinence[57]. When there is suspicion of bladder cancer, the bladder of a patient is assessed via cystoscopy. When abnormal lesions are detected, histological evaluation of transurethral biopsy in addition to bladder wash cytology is performed[58]. These procedures provide information about tumor biology in terms of morphology, grade and stage of disease, which are all key determining factors for risk stratification and the development of a treatment plan. Additionally, radiographic imaging of the upper urinary tract (the renal system and the ureter) using computed tomography (CT) or magnetic resonance imaging is used to stage patients with confirmed bladder cancer[59]. CT scan of the chest and bone is usually performed to rule out metastasis.

Staging of bladder cancer

Histopathological analysis of bladder cancer specimen is used for disease staging and risk stratification, and can often have value for prognostication. Generally speaking, bladder cancer staging consists of the evaluation of the tumor size and location within the bladder wall. The tumorous cells can be confined within the urothelial lining (mucosa), extended into the bladder wall (lamina propria and muscularis propria), into adjacent organs (i.e., vagina and uterus in women, and prostate in men), or to distant organs. The staging of bladder cancer follows the Tumor-Node-Metastasis (TNM) classification system developed by the American Joint Commission on Cancer

and the Union for International Cancer Control[60, 61]. Staging of bladder cancer is shown in detail in Table 1-1. The Tumor-classification (pT0, pTa, pTis, pT1, pT2, pT3 and pT4) refers to the size and the extent of the primary tumor growth into the nearby tissues. The higher is the number, the bigger the tumor size and the depth of infiltration in the bladder wall. The Tumor-classification is the staging system that will be used as reference throughout this dissertation.

Based on disease presentations and early tumor genetics studies, several lines of evidence suggest that bladder cancer arises along two divergent largely non-overlapping pathways. These pathways include (1) the development of urothelial hyperplasia, which may progress into papillary tumors (pTa), and (2) the development of urothelial dysplasia and carcinoma *in situ* (CIS or pTis) followed by progression to invasive disease (≥ pT1)[62, 63].

Approximately 70% of diagnosed cases of bladder cancer are non-invasive superficial papillary (pTa) variants, which encompass urothelial papilloma, papillary urothelial neoplasms of low malignant potential and papillary carcinoma. Morphologically, papillary variants are exophytic structures with tumor cells growing outwards into the bladder lumen, and are comprised of fibrovascular cores[64]. Non-invasive tumors also include pTis disease, a subset of superficial tumors confined in the inner lining of the urothelium. The pTis tumors are, by definition, the occurrence of neoplastic changes within the urothelium, and have a high risk of progression into the bladder wall[65]. In fact, invasive bladder cancer, which accounts for about 30% of presented cases is thought to derive from flat CIS[66]. Invasive tumors are aggressive and have a high tendency of progression and mortality[67]. These tumors can be localized tumors with invasion either into the lamina propria (pT1) or the muscularis propria (pT2), regional tumors with invasion into the perivesical fat (pT3) and distant tumors with invasion into other organs such as lymph node, bones, lung, liver and peritoneum[68, 69]. Evidence shows that genetic and epigenetic alterations are potential drivers of these divergent urothelial tumor pathways[70-73] as shown in Figure 1-2.

Additionally, accurate pathologic grading of malignant urothelium is essential, as tumor grade is associated with disease aggressiveness. Histological grading of bladder cancer, which is based on cytologic evidence (cellular and architectural atypia), describes the extent of differentiation of cells and follows the World Health Organization and International Society of Urologic Pathologist classification criteria[74, 75]. Grading is particularly crucial for papillary (pTa) tumors for the distinction of well-differentiated (low-grade) tumors from poorly differentiated (high-grade) tumors, as high-grade tumors are particularly high-risk for recurrence[76, 77]. While early-stage tumors (pTa and pT1) can be divided into low-grade and high-grade lesions, generally CIS (pTis) and advanced tumors (≥ pT2) tend to be graded into high-grade[78].

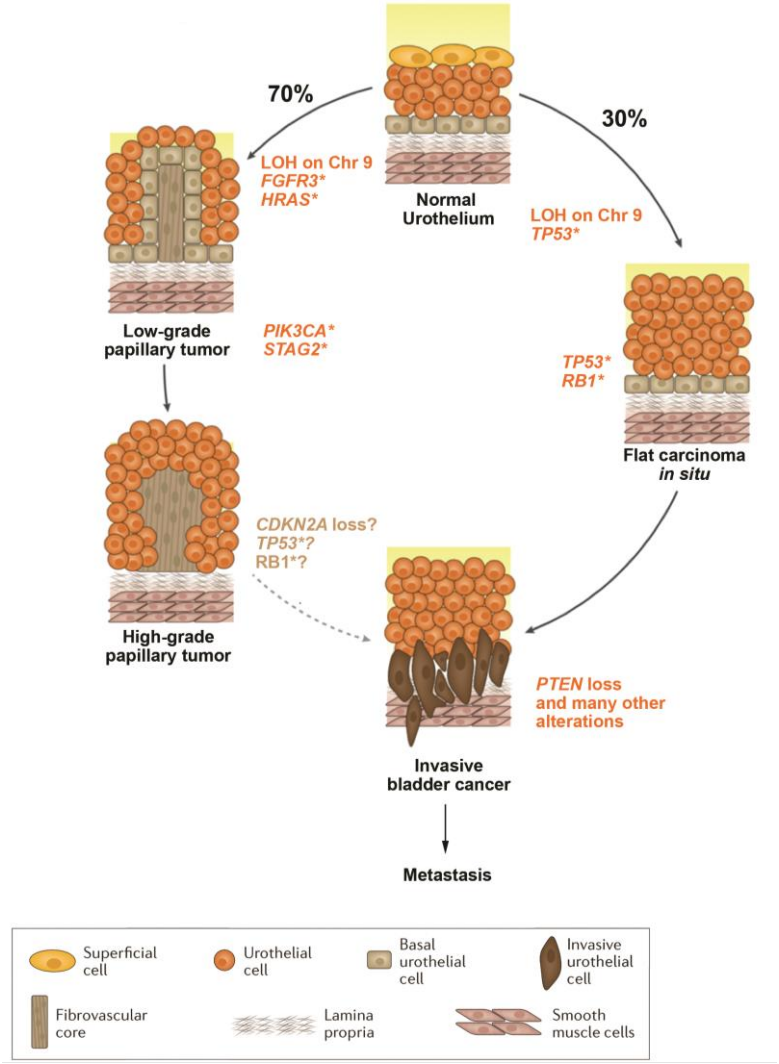

Figure 1-2. Schematic representation of the potential molecular pathways involved in bladder cancer pathogenesis.

Histopathological changes of the urothelium are believed to arise following the clonal expansion of a preneoplastic cell within a normal urothelium. As the clone expands, the occurrence of genetic alterations such as loss of heterozygosity (LOH) of genes on chromosome 9 or activating mutations in fibroblast growth factor receptor 3 (*FGFR3*), Harvey rat sarcoma viral oncogene homolog (*HRAS*), phosphatidylinositol-4,5-bisphosphate 3-kinase catalytic subunit alpha (*PIK3CA*) or stromal antigen 2 (*STAG2*) leads to the formation of non-invasive superficial papillary tumors, which accounts for 70% of all bladder cancer[70, 71]. These tumors have a high propensity to recur and progress into invasive bladder cancer potentially following the loss of cyclin-dependent kinase inhibitor 2A (*CDKN2A*) and mutations in tumor protein 53 (*TP53*) or retinoblastoma 1 (*RB1*) as indicated by the dashed arrows. Invasive tumors accounting for 30% of all bladder cancer are believed to originate from flat carcinoma *in situ* (CIS; pTis) upon LOH of genes on chromosome 9 and mutations in *TP53* and *RB1*. Additional genomic changes including LOH of phosphatase and tensin homolog (*PTEN*) promote tumor invasion and metastasis[72, 73]. Adapted from Yamashita *et al*[79].

Treatment options for bladder cancer

Current guidelines from the National Comprehensive Cancer Network[80] recommend transurethral resection (TUR) as front-line treatment for early-stage diseases (pTa, pTis, and pT1), generally categorized as non-muscle invasive bladder cancer (NMIBC). When early-stage diseases with high-grade lesions (suggesting a high risk of recurrence) are detected, the standard treatment is TUR with immediate postoperative intravesical delivery of chemotherapy (i.e., epirubicin, or mitomycin C)[81]. Additional treatment options for NMIBC include adjuvant intravesical chemotherapy (mitomycin C or gemcitabine) or Bacillus Calmette-Guérin (BCG)[82]. BCG is an attenuated mycobacterium vaccine that is used to treat tuberculosis and has been reported to be superior to chemotherapy in preventing disease recurrence and delaying its progression to advanced stage lesions[82, 83]. Patients who fail to respond to BCG therapy undergo local adjuvant chemotherapy or radical cystectomy (complete removal of the bladder)[84-86]. All patients with early-stage bladder cancer experience frequent clinical follow-up consisting of periodic cystoscopy and cytological analysis for disease surveillance. Although the five-year survival of pTa cancer is close to 90%, up to 70% of these tumors recur[76] and up to 40% of patients progress to invasive disease

following recurrence[77]. Therefore, follow-up and management of superficial disease is a lifetime commitment, explaining why bladder cancer is one of the most expensive cancer in terms of cost per patient[87].

Current guidelines for the treatment of patients with muscle invasive bladder (MIBC; ≥ pT2 disease) include neoadjuvant, cisplatin-based chemotherapy followed by radical cystectomy with concomitant urinary tract diversion[80]. Radical cystectomy is a morbid procedure, and while often saving the life of a patient, it often negatively influences the quality of life of patients in terms of sexual, urinary and bowel functionality[88]. Adjuvant therapy namely systemic cisplatin-based chemotherapy or radiotherapy can also be employed[89]. Cisplatin-based chemotherapy consists either of cisplatin alone as a single agent or combined with other agents like cyclophosphamide, doxorubicin and cisplatin (CAP); methotrexate, vinblastine, Adriamycin, and cisplatin (MVAC); or methotrexate, vinblastine, epirubicin, and cisplatin (MVEC)[80]. Survival for MIBC patients is stage dependent with a five-year survival rate of 69% for pT2 lesions, 35% for pT3 diseases, decreasing to 5% when metastasis (pT4) has occurred[68, 90]. Since radical cystectomy is reported to be of no benefit for metastatic patients, the first-line regimen for this group of patients is systemic chemotherapy such as MVAC and gemcitabine-cisplatin (GC) or radiotherapy. Because these therapies fail in 95% of cases, novel and effective treatment strategies are of utmost importance, and the expansion of the genetic and molecular evidence of bladder cancer sets the basis for the development of targeted therapies[91]. Mainly, molecular pathways identified to be altered in bladder cancer and have clinically available inhibitors include the phosphatidylinositol 3-kinase (PI3K) pathway and tyrosine kinase pathways such as the fibroblast growth factor receptor 3 (FGFR3) and epidermal growth factor receptor (EGFR)[92-94]. Nonetheless, current clinical investigations with inhibitors of the PI3K pathway such as Alpelisib and Buparlisisb or with EGFR inhibitors such as Cetumximab, Erlotinib, and Gefitinib are yet to prove clinical efficacy superior to cisplatin-based chemotherapy. Therefore, more investigations of new therapies are required. Additionally, clinical

trials based on systemic immunotherapies using programmed cell death protein (PD1) and programmed cell death protein ligand (PDL-1) inhibitors have shown promising outcomes with increased overall survival highlighting the clinical significance of immune checkpoint blockades in bladder cancer[95, 96]. Currently approved immunotherapies by the Food and Drug Administration as second-line of treatment for advanced disease patients that do not respond to chemotherapy include Atezolizumab, Nivolumab, Durvalumab, and pembrolizumab.

Table 1-1. Clinicopathologic stages of bladder cancer.

Stage	Tumor-classification	Node-classification	Metastasis-classification	Tumor Grade	Tumor Invasion	Therapy[80]
0	pT0	N0	M0	-	Normal urothelium (no tumor)	-
0a	pTa	N0	M0	LG or HG	Non-invasive papillary tumor	TUR for LG; TUR with intravesical chemotherapy or BCG for HG
0is	pTis	N0	M0	HG	Flat CIS	TUR with intravesical BCG
I	pT1	N0	M0	LG or HG	Invasion into the lamina propria (connective tissue)	TUR (with intravesical chemotherapy or BCG) or cystectomy
II	pT2	N0	M0	HG	Invasion into the muscle (depth of invasion indicated as pT2a and pT2b)	Radical cystectomy with or without neoadjuvant chemotherapy
III	pT3	Any N	M0	HG	Invasion into the perivesical tissue (extent of invasion indicated as pT3a and pT3b)	Radical cystectomy followed by adjuvant chemotherapy
IV	pT4	Any N	M0	HG	Invasion into nearby organs	Chemotherapy; radiotherapy
	Any T	Any N	M0	HG	Invasion into nearby organs	Chemotherapy; radiotherapy
	Any T	Any N	M1	HG	Distant metastasis	Chemotherapy; radiotherapy

The Tumor-classification (pT0, pTa, pTis, pT1, pT2, pT3 and pT4) refers to the size and the extent of the primary tumor growth into the nearby tissues. pT0 refers to no detection of the primary tumor. The Node-classification (N0, N1, N2, N3) indicates the spread of the tumor into regional lymph nodes and the number of lymph node affected. N0 refers to no detection of lymph node invasion. The Metastasis-classification (M0, M1) indicates the migration of the tumor to other organs of the body. M0 refers to no detection of distant. LG = low-grade tumor; HG = high-grade tumor; CIS = carcinoma *in situ*; TUR = transurethral resection; BCG = Bacillus Calmette-Guérin vaccine. Adapted from Sobin *et al*[60].

Histomorphology

Invasive bladder cancers (≥ pT1) exhibit a wide range of morphologic phenotypes, of which the most common is urothelial cell carcinoma (UCC). While UCC accounts for approximately 90% of bladder cancer diagnoses, the remaining 10% of cases are non-urothelial cell carcinoma classified as pure squamous cell carcinoma, pure adenocarcinoma, small cell carcinoma, large cell neuroendocrine carcinoma and other morphologic variants[74, 97]. While prognosis of UCC is widely dependent on tumor stage, the pure forms of bladder cancer histologic variants often present at an advanced stage disease and are considered, generally, to have poor prognosis[97-100]. However, conclusions drawn from retrospective studies examining the correlation between tumor morphology and clinical outcome, after adjusting for stage, have been conflicting[99, 101, 102]. While the reasons for this are several (i.e., a non-uniform cutoff for variant morphology between studies or selection bias among many), additional prospective studies on the pure histology forms are needed to clarify prognosis of patients with this form of disease[103].

Urothelial cell carcinoma

Tumorous cells in UCC have marked nuclear atypia, increased amount of cytoplasm and are poorly differentiated. The UCC lesions may grow into the bladder wall as diffuse single cells, nests or trabeculae, and are often characterized by increased inflammatory infiltration[104].

A subset (40%) of UCC malignancies present mixed histology and are suggested to have poor outcome and reduced survival rate owing to their association with high grade and advanced stage disease[98, 105]. These lesions appear as UCC commonly admixed with focal or extensive squamous differentiation (60%), glandular differentiation (10%), sarcomatoid (7%), micropapillary (3.7%), plasmacytoid and other rarer histological variants[101, 106]. The rest of this section will focus on the squamous and glandular histologic variants of UCC and their related pure forms.

Squamous differentiation

The coexistence of UCC with squamous differentiation (SqD) can be distinguished from pure UCC by characterizing features such as the presence of intercellular bridging, desmosomes, keratin pearl formation, and superficial keratinization[104].

When SqD is detected throughout the tumor, these malignant bladder cancers are characterized as pure squamous cell carcinoma (SCC), which accounts for about 5% of non-urothelial carcinoma in western countries. Interestingly, SCC is the predominant type of bladder cancer diagnosed in Middle East countries where it develops as a result of chronic urinary tract infection by *Schistosoma haematobium*[52]. Among the most commonly believed causes of SCC in western countries are chronic irritation, often due to catheterization of the bladder, and spinal cord injuries that lead to the activation of inflammatory response[107]. When adjusted for stage and other prognostic factors, pure SCC appears to have a more aggressive nature and a high degree of local recurrence than pure UCC[108].

Glandular differentiation

On the other hand, distinct features of UCC with glandular differentiation (GD) include the formation of gland-like or small tubular structures, often with the presence "signet ring" cells[104]. The pure form of glandular differentiation is adenocarcinoma (AC) accounting for about 2-3% of non-urothelial cell carcinoma. Similarly to SqD and SCC, the presence of GD and AC is associated with advanced disease with adverse prognostic outcome[109]. Nonetheless, additional studies are required to firmly establish a link between clinical outcome and GD/AC[103, 110].

Cell of Origin of Bladder Cancer

By definition, a cell of origin of cancer is the normal cell type that following neoplastic transformations gives rise to tumor formation[111]. Cancer can arise from any cell type within a tissue. This cell may acquire tumorigenic properties following the accumulation of genetic and epigenetic alterations leading to tumor development. These genetic alterations contribute to morphologic and molecular heterogeneity of cancer disease.

Tumor cells of origin can be identified experimentally through lineage tracing studies in mouse models. Several studies using genetically engineered mice model bearing a Cre driver specifically expressed in the cell type of interest (i.e., *Krt5-Cre* for basal cells or *UpII-Cre* for luminal/intermediate cells) in combination with Rosa26 reporters suggest that the urothelial cell types may give rise to different lesions of bladder cancer. The findings from one study indicate that luminal/umbrella urothelial cells are, likely, the cells of origin of non-invasive superficial papillary tumors whereas basal urothelial cells are, likely, the progenitors of CIS lesions, MIBC and SCC[112]. In line with these findings, studies in a carcinogen mouse model of bladder cancer suggest basal urothelial cells are tumor-initiating cell populations that give rise to CIS and muscle invasive

disease upon deletion of the Sonic hedgehog gene, the expression of which is restricted to basal cells[113]. In conjunction with clinical studies showing a high degree of concomitant CIS in patients with MIBC, these studies suggest CIS is a precursor to the development of a majority of tumors displaying frank invasion. Nonetheless, clinical data show that CIS lesions are enriched with KRT20 expression, which is a luminal urothelial specific marker[114]. Additionally, besides from CIS, invasive diseases in humans may derive from high-grade recurrent superficial papillary tumors, which conversely appear to have luminal cells as cellular progenitors based on lineage tracing studies[112]. Therefore, contradicting data exit regarding the cellular origin of CIS and invasive diseases warrantying further studies to define the cell of origin for invasive bladder cancer accurately. Nevertheless, the findings of different progenitors for development of non-invasive superficial and invasive bladder cancer support the idea of divergent mechanisms behind these two types of bladder cancer as also supported by molecular and genomic evidence[62, 115].

Bladder Cancer Heterogeneity: Clonality and Multifocality

Clinical evidence shows that bladder cancer is a multifocal and heterogeneous disease with a spectrum of pathological behavior. In a wide variety of cancers, tumor heterogeneity has significant clinical implications in terms of treatment and prognosis. Several tumor characteristics including genetic alterations, gene expression patterns and morphology contribute to tumor heterogeneity and influence tumor clinical behavior. There are two types of tumor heterogeneity: intertumoral heterogeneity, which refers to differences in tumor characteristics across patients populations[116], and intratumoral heterogeneity, which describes regional variability in morphologic and molecular features within an individual patient[117]. Put differently, a patient exhibiting intratumoral heterogeneity could present with multiple, unique subpopulations of cells with different genomic profiles[117]. Although the exact mechanisms that drive intratumoral heterogeneity

are almost certainly cancer-specific and largely unknown, two theoretical models have been proposed. These models include (1) the "field of cancerization" (also known as "field effect") model and (2) the "clonal evolution" model. In the "field of cancerization" model, independent cellular clones within a primary tumor give rise to distinct, individual tumors[118-120]. These individual tumors exhibit unique genetic alterations and gene expression patterns within the same organ. The "clonal evolution" model describes the clonal expansion of an individual/single cell as the result of adaption to tumor-intrinsic or extrinsic (i.e., therapeutically-induced) selective pressures[118]. During the expansion, a clone might undergo divergent evolution in which selective pressure promotes additional diversity at the genetic and epigenetic levels, and may cause genomic instability[72, 121, 122], a proposed significant contributor of the development of intratumoral heterogeneity[123, 124]. The spatial-temporal accumulations of genomic and epigenomic defects as the tumor progresses lead to phenotypic changes reflected in metastatic colonization, chemotherapeutic response and clinical outcome[123].

The Genomic Landscape of Bladder Cancer

The identification of the genomic events potentially driving clonal selection and the diverse phenotypes in bladder cancer has been possible by the application of a variety of molecular genetic techniques. These methods include conventional approaches such as polymerase chain reaction single-strand conformation polymorphism analysis, DNA sequencing used for assessment of genetic mutations and polymorphisms[125]. Loss of heterozygosity (LOH) analysis at microsatellite marker loci is used for detection of allelic deletion[126]. Fluorescence *in situ* hybridization and comparative genomic hybridization are applied for detection of gains and losses of regions at each chromosome[127, 128]. X-chromosome inactivation analysis is often used for assessment of DNA methylation status[129]. Up-to-date high-throughput methodologies including next-generation

sequencing of whole genome and whole exome are also utilized[130]. The use of these tools has led to the identification of somatic genetic alterations frequently implicated in urothelial carcinogenesis and to the definition of the mutational genomic landscape of bladder cancer[131, 132]. Although important caveats exist, information about specific genetic alterations can be inferred by analysis at the transcript level using RNA-sequencing (RNA-seq) and at the protein level using immunohistochemistry (IHC) although for a limited subset of gene products[133, 134].

Genetic alterations

After melanoma, lung SCC and lung AC, bladder cancer is the fourth cancer with the highest mutational load[135]. Chromosomal changes and copy number alterations resulting in aneuploidy and increased level of genomic instability are also frequent mainly in MIBC[73, 136]. Genetic analyses in combination with gene expression studies have led to the identification of candidate genes and their related molecular pathways affected by genomic alterations. The impact of genomic changes is mainly evident in the activation of oncogenes and inactivation of tumor suppressor genes. The molecular pathways frequently altered in bladder cancer include cell cycle regulation, receptor tyrosine kinase pathways, the mitogen-activated protein kinase (MAPK) pathway, phosphatidylinositol triphosphate kinase (PI3K) pathways and chromatin remodeling pathways[137]. The most frequent genetic aberrations are observed on chromosome 9 and 17[71, 138]. The following sections will cover the mutational landscape of bladder cancer followed by the copy number alterations landscape of bladder cancer.

The mutational landscape of bladder cancer

Although tobacco exposure is a major risk factor for urothelial carcinoma, the recent molecular analyses of MIBC by The Cancer Genome Atlas (TCGA), together with the analyses of NMIBC by the European multicenter (UROMOL) research team did not identify well known tobacco-related DNA alterations[133, 137]. Nonetheless, in the TCGA cohort, tumors from patients with smoking history were enriched of epigenetic alterations, consisting mainly in changes in DNA methylation pattern[137]. Several studies show that bladder cancer is enriched for mutations in genes such as *NFE2L2* and *TXNIP*, both of which are involved in the response to free radicals, and also the *ERCC2* gene, which plays a role in DNA repair process[139, 140]. However, further studies are needed to confirm an association between mutations in these genes and smoking status.

The majority (65%) of mutations in bladder cancer are attributable to the activity of the APOBEC cytosine deaminase, which promotes deamination of cytosine in favor of cytosine to thymine (C-T) transitions or cytosine to guanine (C-G) transversions[141, 142]. APOBEC-mediated mutations have been associated with high risk tumors in NMIBC, although these mutations are prevalent in tumors of both NMIBC and MIBC[133, 137].

The most commonly observed mutations in NMIBC are activating mutations in *PIK3CA, AKT1*, *FGFR3* and *HRAS* genes, and inactivating mutations in *TSC1* and *PTEN* resulting in alterations of the PI3K and the MAPK pathways[143-146]. Additionally, inactivating mutations in genes involved in chromatin remodeling such as *KDM6A*, *ARID1A* and *EP300* are frequent in bladder cancer[133, 137, 142]. Similarly, inactivating mutations in *STAG2*, which is involved in chromosome segregation, are common in bladder cancer[147].

The frequency of mutations in the *TP53* gene is generally detected at high levels (~ 50%) in MIBC[137, 148]. Nonetheless, NMIBC including pTis and pT1 disease also exhibit a high frequency of *TP53* mutations (detected in 65% of pTis[62] and 50% of pT1[149]). Whereas the rate of inactivating

mutations in *RB1* is relatively higher in MIBC than in NMIBC. Concurrent inactivation of *TP53* and *RB1* is frequently detected in MIBC and has a disease progression significance[150]. The timing and order of occurrence of these genetic mutations appear to be a determinant in clonal selection and expansion. Compelling evidence showing the presence of *TP53* mutations and chromosome 9 alterations in early-stage diseases[62, 121, 128] suggest that these genes may play a role in tumorigenesis and disease progression by acting in concert with late genetic aberrations such as point mutations or copy number alterations of other tumor suppressor genes including *RB1* and *PTEN*[151, 152].

Additionally, mutations in epithelial differentiation transcription factors such as *FOXA1* *ELF3* and *KLF5* are also frequently observed in MIBC[137]. Alterations in these genes may promote loss of urothelial differentiation resulting in poorly differentiated tumor and therefore the development of aggressive cancer types[56]. The frequency of the most common alterations in bladder cancer is shown in Table 1-2.

Copy number alterations of bladder cancer

LOH of chromosome 9 is detected in all stages of bladder cancer[121]. Among the genes altered on chromosome 9 is *CDKN2A*, which encodes for the alternatively spliced products p14 and p16 known repressors of TP53 and RB pathways, hence deletions of this locus leads to dysregulation of the cell cycle pathway. Contributing to cell cycle dysfunction in bladder cancer are also amplifications of genes with oncogenic functions such as *CCND1*, *E2F3*, *MDM2*, *EGFR* and *ERBB2*[137] (Table 1-2). Additionally, LOH of *PTEN* is observed in MIBC with consequent alteration of the PI3K pathway[126, 152, 153]. Moreover, amplification of urothelial differentiation transcription factors such as *PPARG* and *GATA3* have been observed in MIBC[137], and as abovementioned, alterations in urothelial differentiation factors genes may have implication on the differentiation status of the tumor.

Table 1-2. List of genes frequently mutated in bladder cancer.

	Hedegaard *et al.*, 2016[133]	**Hurst *et al.*, 2017[154]**	**TCGA, 2014[137]**	**Robertson *et al.*, 2017[155]**
Sample stage and size	**NMIBC** pTa (n = 345); pTis (n = 3); pT1 (n = 112) **MIBC** pT2-pT4; n = 16	**NMIBC** pTa; n = 140	**MIBC** pT2-pT4; n = 131	**MIBC** pT2-pT4; n = 412
Gene symbol	**Mutation frequency**	**Mutation frequency**	**Mutation frequency**	**Mutation frequency**
FGFR3	53%	79%	12%	14%
PIK3CA	23%	54%	20%	22%
KDM6A	22%	52%	24%	26%
TP53	8%		49%	48%
ERBB2	8%		9%	12%
STAG2	18%	37%	11%	14%
EP300	15%	18%	15%	15%
ARID1A	13%	18%	25%	25%
ELF3	8%		8%	12%
RB1	7%		13%	17%
MDM2	5%			
PTEN	8%		3%	
ERBB3			11%	10%
RXRA			9%	
CDKN2A			5%	
HRAS		12%	5%	
KLF5			8%	
ERCC2			12%	9%
NFE2L2			8%	
TXNIP			7%	
TSC1		11%	8%	8%
CDKN1A			14%	9%
FOXA1			5%	
	CNA frequency	**CNA frequency**	**CNA frequency**	**CNA frequency**
CDKN2A			47% (del.)	22% (del.)
CCND1			10% (amp.)	
RB1			14% (del.)	4% (del.)
EGFR			11% (amp.)	
PPARG			17% (amp.)	6% (amp.)
MDM2			9% (amp.)	6% (amp.)
ERBB2			7% (amp.)	
FGFR3			3% (amp.)	
PTEN			13% (del.)	
BCL2L1			11% (amp.)	
E2F3			20% (amp.)	12% (amp.)
TP53			21% (amp.)	

CNA = Copy Number Alterations; amp = amplification; del = deletion

Epigenetic alterations

Besides genetic alterations, epigenetic alterations also play a critical role in human cancer[156, 157]. The epigenetic networks, which encompass DNA methylation, histone modifications, and nucleosome positioning, promote changes in gene expression and function without affecting the coding sequence[158]. The most frequently altered epigenetic mechanism is DNA methylation. Changes in the DNA methylation patterns of the genome result in severe pathophysiological changes owing to the critical role of DNA methylation in development, genomic imprinting, and X-chromosome inactivation[159]. This epigenetic process is orchestrated by DNA methyltransferase enzymes (DNMT1, DNMT3A, and DNMT3B) and consists of the establishment and maintenance of methyl groups on cytosine residues within cytosine-guanine dinucleotide (CpG) sites. DNA methylation patterns occur in a tissue-specific manner and are dictated by the distribution of CpG sites across the genome. Although CpG sites are sparsely found on gene bodies, they cluster to form CpG islands of 150-200 base pair long, which are concentrated within or close to the promoter regions of genes[160]. In general, CpG sites in gene bodies are hypermethylated to block the expression of repetitive DNA and transposable elements; however, alterations in the methylation patterns of gene bodies can lead to upregulation of genes and increased levels of disease-related mutations. Conversely, most of promoter CpG islands are, in general, in an unmethylated state to protect gene expression. Nonetheless, during oncogenic transformation, CpG islands may undergo hypermethylation that results in transcriptional inactivation and loss of gene function[159, 160].

Altered expression related to promoter hypermethylation has been reported in the tumorigenesis of several cancer types including breast, colon and bladder cancer, and has been associated with loss of expression of tumor suppressor genes implicated in cell cycle and genes involved in DNA repair[161, 162]. In bladder cancer, the molecular pathways significantly affected by aberrant gene promoter methylation include cell cycle (*CDKN2A*), DNA repair process (*BRCA1*,

MLH1, and *RASSF1A*), epithelial-mesenchymal transition (*CDH1*), apoptosis (*DAPK*), and Wnt signaling pathway (*APC*) among others[163-166]. Nonetheless, well-established tumor suppressors that are genetically altered in bladder cancer namely *TP53*, *PTEN*, *TSC1*, and *RB1* are reported not to be affected by gene silencing through DNA hypermethylation[155].

Even though promoter hypermethylation of CpG islands is observed in both NMIBC and MIBC disease types, the frequency of hypermethylation in MIBC is higher and significantly associated with tumor stage and grade[167, 168] as opposed to NMIBC, which often exhibit hypomethylation of CpG sites in gene bodies[155, 169, 170].

In addition to alterations in DNA methylation patterns, aberrations in chromatin remodeling regulators (*KDM6A, ARID1A, EP300,* and *CHD6*) also contribute to tumorigenesis[137, 171].

Molecular Subtypes of Bladder Cancer

In an attempt to enhance disease risk stratification and the prognostic value of tumor staging as well as to develop new effective and targeted therapies, molecular sub-classifications of bladder cancer based on gene expression analyses have been undertaken by several groups. In this regard, studies by research teams at Lund University, the University of North Carolina (UNC) and MD Anderson Cancer Center (MDA) as well as the TCGA and the UROMOL cooperative research group have identified unique mRNA and protein expression patterns resulting in the identification of several molecular subtypes of bladder cancer[133, 134, 137, 172, 173]. The next paragraphs will describe first the molecular subtypes identified in NMIBC followed by the molecular subtypes identified in MIBC.

The UROMOL group study utilized RNA-seq data to characterize the gene expression pattern in NMIBC. The group identified three distinct subtypes based on tumor histopathological

features: class 1, class 2 and class 3[133]. Class 1 and class 2 tumors were characterized by expression of early cell cycle genes (*CCND1, CCND2, CCND3, WEE1)* and exhibited luminal-like characteristics consisting of the expression of luminal urothelial cell differentiation-associated markers (*PPARG, FOXA1, GATA3, UPIA, UPIB, UPII, UPIIIA, UPIIIB*). Class 3 tumors exhibited basal-like features for the presence of basal urothelial cell-associated markers. Interestingly, class 2 tumors showed high levels of *KRT20* expression, which is highly expressed in pTis disease[114]. Additionally, a subset of class 2 tumors exhibited the expression of basal-associated genes such as *KRT5* and *KRT14*, which were highly expressed in class 3 tumors. Furthermore, both class 2 and class 3 diseases had a poor prognosis with respect to progression-free survival.

The classification by the Lund group based on IHC analysis of tumors of both NMIBC and MIBC identified five major molecular subtypes that differ in survival rates: urobasal A (uroA), urobasal B (uroB), SCC-like (SCCL), genomically unstable (GU) and a heterogeneous infiltrated class of tumors (infiltrated)[134]. Tumors classified as uroA and uroB commonly shared high CCND1, FGFR3, PIK3CA, and TP63 expression, but exhibited different disease-specific survival pattern. While uroA diseases had a relatively favorable prognosis, uroB diseases were characterized by a worse prognosis associated with the presence of *TP53* mutations and by moderate expression of basal cytokeratins (KRT4, KRT5, KRT6, KRT14, and KRT16) that have been associated with SqD[174]. Approximately, 50% of the uroB tumors were MIBC cases. Tumors with SCCL subtype presented similarities with uroB but were characterized by high basal/squamous signatures with adverse prognosis. The GU subtype was characterized by *TP53* mutations, low expression of PTEN and high expression of CCNE, ERBB2, and KRT20, and about 40% of these tumors were MIBC. Both GU and infiltrated subtypes, with the latter characterized by increased expression of immune and stromal markers, had an intermediate prognosis in terms of disease-specific survival rate.

A recent revision of the Lund molecular classifications based on the integration of gene expression profiling analysis and IHC analysis has led to the expansion of the Lund taxonomy into

six subgroups[175]. The Lund's latest tumor classification includes urothelial-like (Uro) previously classified as UroA; the GU category; epithelial-infiltrated (Epi-Inf) tumors, which exhibited infiltration of non-tumor cells. The new categorization also includes squamous cell carcinoma-like/mesenchymal-infiltrated (SCCL/Mes-Inf) tumors enriched of the expression of *ZEB2* and *VIM* promoting a mesenchymal phenotype; SCCL/UroB, which included tumors previously categorized as uroB and were characterized by basal urothelial markers (*KRT5* and *KRT14*); and small-cell/neuroendocrine-like (Sc/NE), which exhibited increased expression of *TUBB2B* and *EPCAM* associated with neuroendocrine cell phenotype. Based on their expression signatures enriched of *PPARG, FOXA1, RXRA, GATA3, KRT20, UPIII*, tumors in the Uro, GU and Epi-Inf classification have been associated with a luminal-like subtype, whereas tumors in the SCCL/Mes-Inf, SCCL/UroB and Sc/NE subgroups exhibited heterogeneous signatures contributing to a basal-like subtype, and were enriched of other signatures that drive mesenchymal or neuroendocrine phenotypes.

Unlike the Lund classification, the analyses by the UNC, the MDA, and the TCGA groups were focused solely on MIBC, and the overlap between the subtyping schemas of these groups and the Lund group is shown in Figure 1-3. The UNC study revealed two distinct intrinsic subtypes of high-grade MIBC that differentially express signatures of urothelial differentiation: the luminal and the basal subtypes[172]. It was reported that these two subtypes strongly resembled the intrinsic molecular subtypes defined in breast cancer in regards to their gene expression patterns. A simultaneous and independent study by the MDA team proposed three subgroups of disease including luminal, "p53-like" and basal subtypes[176]. The molecular signatures in the luminal and basal subtypes overlapped with those of the UNC group: luminal tumors were enriched of uroplakins, *KRT20, CD24, FOXA1, GATA3, ERBB2* and *PPARG* expression whereas basal tumors showed high level of basal urothelial markers such as *KRT5, KRT6, KRT14* and *EGFR,* and were often associated with the presence of SqD markers and infiltration of stromal markers (*TWIST1/2,*

SNAI2, *ZEB2*, and *VIM*). Although the "p53-like" subtype presented the same signatures as the luminal subtype, it was characterized by the presence of a wild-type *TP53* gene signature.

The TCGA group initially identified four different clusters: cluster I, cluster II, cluster III and cluster IV[137]. While cluster I and II exhibited expression consistent with luminal features (i.e., *KRT20* and *UPII*), cluster III showed basal characteristics and cluster IV had claudin-low features enriched of stromal and immune expression[177]. The TCGA analysis was subsequently repeated and confirmed by a group at the Broad Institute, which renamed the TCGA clusters as luminal (cluster I), luminal immune (cluster II), basal (cluster III) and immune undifferentiated (cluster IV)[139]. Further characterization of the TCGA classification using a larger cohort has identified five subtypes based on expression profile[155]. The five classifications consisted of luminal-papillary, luminal-infiltrated, luminal, basal-squamous and neuronal. The three luminal subtypes, which shared urothelial differentiation-associated markers such as *PPARG, FOXA1, GATA3* as well as *UPIA, UPII*, differed among each other in respect to their wild-type *TP53* signatures, immune and stromal infiltration. The basal-squamous subtype was characterized by the expression of basal urothelial markers such as *CD44, KRT5, KRT6A* and *KRT14* and squamous differentiation markers including *TGM1, DSC3*, and *PI3*; whereas the neuronal subtype was characterized by neuroendocrine signatures such as *CHGA, CHGB*, and *SCG2*.

It is noteworthy to point out that in all classifications, tumors categorized as basal-like (often enriched of SqD) were typically aggressive, and associated with advanced stage and poor prognosis when compared with tumors labeled as luminal-like.

In addition to potentially being predictive of responsive to cisplatin-based chemotherapy[178], the molecular characterization of bladder cancer provides an opportunity for improvement and development of new clinical approaches, including targeted therapies. For example, potential subtype-specific actionable targets include the tyrosine kinase receptors, FGFR3 and ERBB2 in luminal subtype tumors as well as EGFR in basal-squamous tumors. There is also

evidence that specific subtypes respond more favorably to immune checkpoint blockade[179]. However, tumor heterogeneity concerning molecular subtype is a confounding variable that could potentially render the development of clinical tests based on molecular subtype problematic[180, 181].

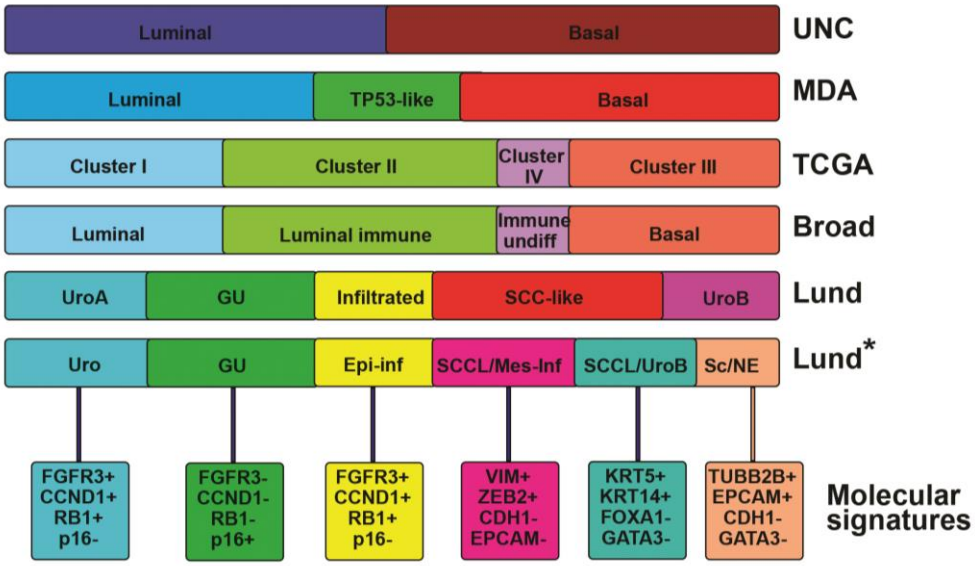

Figure 1-3. Categorization of molecular subtypes of bladder cancer.

Shown is a schematic representation of the molecular subtypes of MIBC identified by five different research teams: the University of North Carolina (UNC)[172], the MD Anderson Cancer Center (MDA)[176], The Cancer Genome Atlas Network (TCGA)[137], the Broad Institute (Broad)[139] and the Lund University[134, 175]. The approximate matching of the subtypes is shown based on the data from Aine *et al.*[182] and Choi *et al*[173]. The UNC group identified two major subtypes based on the expression of urothelial differentiation-associated markers: luminal subtypes and basal subtypes. Parallel studies by the other teams identified subgroups within the luminal and basal subtypes. The MDA team identified a third category defined as "TP53-like" enriched of stromal markers. The TCGA defined four different clusters, the nomenclatures of which were redefined by the Broad group. The Lund group initially identified five subgroups, which were re-evaluated for further categorization (as indicated by the *). The molecular signatures of the subtypes related to the Lund latest classification (*) are shown. UroA = urobasal A; UroB = urobasal B; Immune undiff = immune undifferentiated; GU = genomically unstable; SCC-like (SCCL) = squamous cell carcinoma-like; Epi–inf = epithelial infiltrated; Mes–inf = mesenchymal infiltrated; Sc/NE = small cell neuroendocrine-like. Adapted from Aine *et al*[182].

PTEN and the PI3K Pathway in Bladder Cancer

The phosphatidylinositol-3 kinase (PI3K) pathway is among the most commonly altered signaling pathway in human cancer[183]. In bladder cancer, aberrant activation of the PI3K pathway is due to genomic alterations in the pathway components including activating mutations in phosphatidylinositol-4,5-bisphosphate 3-kinase catalytic subunit alpha (*PI3KCA*), inactivating mutations in tuberous sclerosis complex 1 (*TSC1*) and LOH of phosphatase and tensin homolog on chromosome 10 (*PTEN*) (Table 1-2).

The PI3K pathway regulates multiple pivotal biologic functions, and because associated alterations result in cell growth and malignant transformation, stringent regulation of this pathway is essential. Signal transduction through the PI3K pathway is controlled by the regulatory activity of the lipid kinase, PI3K, and the lipid phosphatase, PTEN[184]. Upon growth factor stimulation, PI3K phosphorylates phosphatidylinositol 4,5 bisphosphate (PIP2) to form phosphatidylinositol 3,4,5 triphosphate (PIP3), which subsequently recruits phosphatidylinositol-dependent kinase 1 (PDK1) and the serine/threonine kinase (AKT) to the plasma membrane where AKT is then activated by dual phosphorylation on threonine 308 (Thr308) residue by PDK1 and on serine 473 (Ser473) residue by the mammalian target of Rapamycin complex 2 (mTORC2). Once activated, AKT blocks the inhibitory activity of the tuberous sclerosis complex (TSC1-TSC2) and promotes activation of mTORC1, and thus the synthesis of proteins involved cellular survival, growth, proliferation, angiogenesis and metabolism[185, 186]. mTORC1 exerts negative feedback control on PI3K activity, which is also negatively regulated by PTEN activity. PTEN promotes dephosphorylation of PIP3 to PIP2, and thus inhibits AKT downstream signaling (Figure 1-4). In addition to its lipid phosphatase activity against serine/threonine phosphorylated substrates, a protein phosphatase activity against tyrosine phosphorylated substrates has been described for PTEN[186]. By dephosphorylating focal adhesion kinase (FAK), PTEN is shown to inhibit focal

adhesion structure and cell motility[187]. Although it is suggested that the tumor suppressor activity of PTEN is primarily linked to its lipid phosphatase activity, one study in bladder cancer shows that the protein phosphatase activity of PTEN can inhibit tumor invasive phenotype[188]. In bladder cancer, activating mutations of *PIK3CA* are predominately found in non-invasive superficial bladder cancer. These mutations are considered phenocopies of the inactivation of the lipid phosphatase activity of PTEN, which leads to constitutive activation of AKT[184]. Based on that, it is suggested that the inactivation of the protein phosphatase activity of PTEN may be the driver of the invasive phenotype associated with *PTEN* loss in bladder cancer, as LOH of *PTEN* is widely detected in advanced stage and aggressive forms of bladder cancer[126, 152, 153]. However, further studies are warranted to confirm the differences between the two enzymatic activity (PIK3CA and PTEN) in the formation of different types of tumor[93].

Moreover, in a recent study based on integrative molecular subtype analysis of twelve cancer types from TCGA studies, *PTEN* loss was ranked among the genetic alterations within tumors classified as a squamous-like subtype, these tumors exhibited significantly worse prognosis in terms of overall survival[189]. Besides the clinical evidence of a role for *PTEN* in disease MIBC[190], several animal studies based on the use of genetically engineered models (GEMs) also underscore the potential role of *Pten* loss in bladder tumorigenesis[191-193]. However, the fact that most bladder-specific *Pten* knockout mice fail to recapitulate the aggressive histopathologic phenotypes typically observed in human MIBC[191, 193] suggests the existence of crosstalk between the PI3K pathway and other molecular events/pathways in promoting disease progression[192, 194, 195].

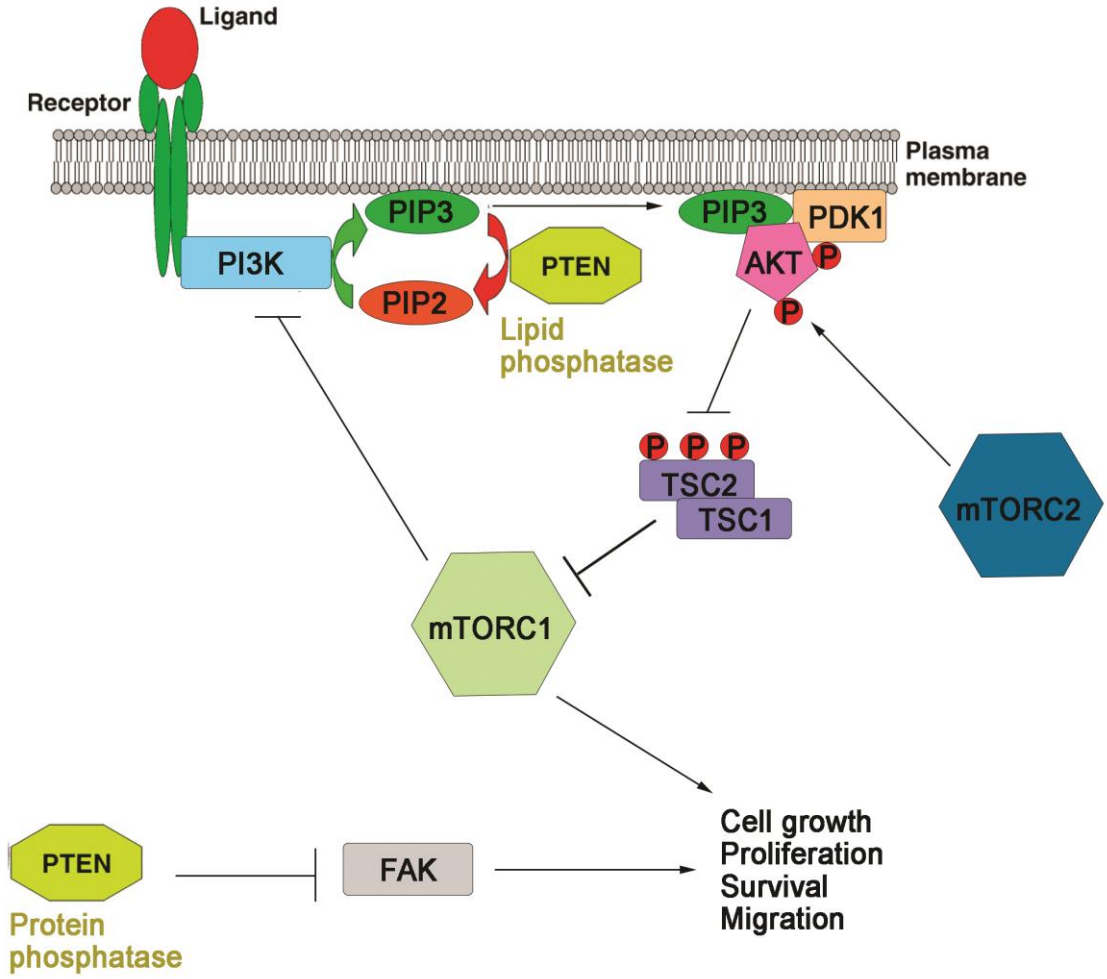

Figure 1-4. PTEN in the PI3K/AKT signaling pathway.

Upon the binding of a ligand to a receptor tyrosine kinase, the activation of phosphatidylinositol-3 kinase (PI3K) phosphorylates phosphatidylinositol 4,5 bisphosphate (PIP2) to form phosphatidylinositol 3,4,5 triphosphate (PIP3). Dephosphorylation of PIP3 to PIP2 by the lipid phosphatase activity of PTEN inhibits the downstream signaling of AKT activation mediated by the activity of PIP3, phosphatidylinositol-dependent kinase 1 (PDK1) and the mammalian target of Rapamycin complex 2 (mTORC2) complex, which phosphorylate AKT. Activated AKT blocks the inhibitory activity of tuberous sclerosis complex (TSC1-TSC2) on mTORC1 activity and promotes, therefore, cell growth, proliferation, survival, and migration. The protein phosphatase activity of PTEN also inhibits cell survival and migration by blocking, for instance, the activity of focal adhesion kinase (FAK). Adapted from Planchon *et al*[196].

FOXA1 in the Transcriptional Regulation of the Bladder Urothelium

The transcriptional factor Forkhead box A1 (FOXA1) is a key regulator of epithelial/urothelial differentiation process[197-200], and alterations in *FOXA1* expression have been implicated in several cancers including bladder cancer[201-205]. FOXA1 is a member of the Forkhead family of winged-helix transcription factors that play an essential role in the development of several organs including the liver, pancreas, lungs, breast, prostate, and bladder[198-200].

Because of its structural similarity to linker histone, FOXA1 has the intrinsic ability to stably bind to the nucleosomes and unfold the chromatin, allowing the accessibility of transcriptional machinery to locate and bind to gene regulatory regions, and promote transcription[206]. For this reason, FOXA1 is said to possess a "pioneering" function[207]. As a transcription factor, FOXA1 binds to specific DNA motifs at enhancer or promoter regions of target genes to promote gene expression. At least ten predicted motifs have been identified for FOXA1 binding site and they are all variations of this motif: TGTTTAC[208]. Like other transcription factors important for development and cell differentiation, the expression of *FOXA1* is cell-type specific[209]. The transcriptional activity of FOXA1 is dictated by recruitment and interaction with other transcriptional factors such as ER and GATA3 in the case of breast epithelium[210, 211], or AR in the case of prostate epithelium[212] (Figure 1-5). In bladder urothelium, FOXA1 was previously shown to act in concert with GATA3 and PPARG to establish a luminal differentiation phenotype[213], although the underlying mechanism is unclear.

In a manner potentially related to its role in differentiation, an impaired activity of FOXA1 has been associated with cancer development[201], poor prognosis in breast cancer[214] and disease progression in prostate cancer[215]. In bladder cancer, loss of *FOXA1* is seen in both UCC and UCC admixed with SqD of MIBC[204] and is an independent predictor of reduced overall survival[205]. In line with these findings, which support a role for *FOXA1* in urothelial differentiation and

development of SqD, inducible *Foxa1* knockout mice develop preneoplastic changes such as hyperplasia and keratinizing squamous metaplasia within the urothelium[205], which are precursors of UCC and SCC tumors, respectively. Thus, these studies indicate that while *Foxa1* is essential for maintaining urothelial differentiation, *in vivo* loss of *Foxa1* alone is insufficient to promote cancer development.

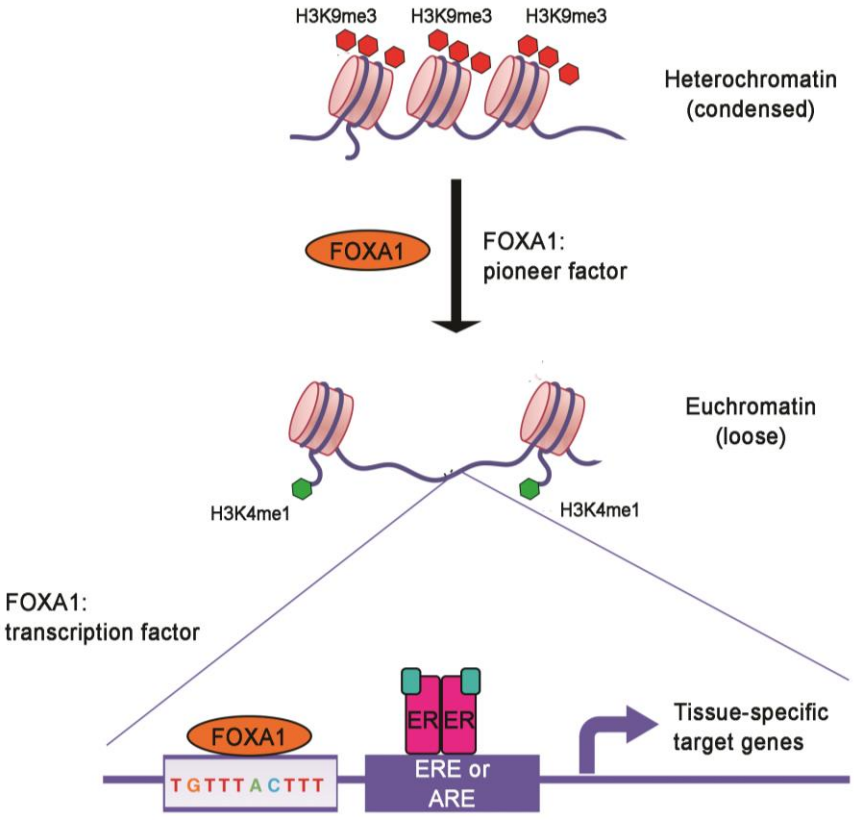

Figure 1-5. Transcription regulation by FOXA1.

Methylation of histone H3 lysine 9 (H3K9me) promotes tightening of the chromatin (heterochromatin) leading to repression of transcription[216]. The binding of pioneer factors such as FOXA1 promotes the unwinding/opening of the chromatin (euchromatin) and directs methylation of histone H3 lysine 4 (H3K4me) establishing, therefore, activation of transcription[217]. As a transcription factor, by binding to its binding site, FOXA1 recruits and interacts with other factors such as the estrogen receptor (ER) or the androgen receptor (AR) at their respective response elements and promotes transcription of tissue-specific target genes involved in developmental processes and tissue differentiation. H3K9me3 = trimethylation H3K9; H3K4me1 = monomethylation H3K4; ERE = estrogen response element; ARE = androgen response element. Adapted from Meyer and Carroll[218].

Bladder Cancer Models

Individual and collective efforts have significantly expanded our knowledge regarding common genetic alterations in bladder cancer as well as differences in molecular subtypes both across patient populations and within individual tumors. However, there is a relative lack of understanding in regards to the specific contributions of these alterations to disease pathogenesis. In addition to being useful for the functional validation of molecular changes in cancer, preclinical models are required for testing of novel therapeutic approaches. *In vitro* and *in vivo* preclinical models are available for the study of bladder cancer.

In vitro models of bladder cancer

In vitro models of bladder cancer include a variety of human cell lines as well as cell lines available from other species including mice and rats. Human bladder cancer cell lines established for the study of bladder cancer include RT4, SW780, UMUC1, T24, UMUC3, TCCSup, 5637, ScaBER, HT1197 and HT11376 among many others[219]. Additionally, cell lines from experimental bladder cancer of rat origins such as AY-27 and NBTII or mouse origins such as MB49 and MBT-2 have also been established[220-222].

Human urothelial cell lines are widely used in preclinical testing of cytotoxicity of therapeutic agents. Moreover, these cell lines can be useful tools for the study of genes of interest. When feasible, gene expression can be easily modified and this enables the performance of studies aimed to elucidate molecular mechanisms of action of candidate genes. Some advantages of human-derived cell lines are that they are somewhat representative of the phenotypic features of human disease; they replicate relatively fast and infinitely and can be easily manipulated. Disadvantages include the occurrence of spontaneous genotypic changes caused by the multiple

passaging and culturing methods. These genetic alterations are mostly unrelated to disease pathogenesis and can negatively impact cell line phenotypic behavior and relevance to the disease from which they were founded. Additionally, the potential of cross-contamination with other cells lines may occur resulting in misleading interpretations of data in a study[223]. An additional drawback of current tissue culturing methods is the traditional two-dimensional method, consisting of cell growth as monolayer deprived of an *in vivo* tumor microenvironment, and therefore unable to fully replicate the *in vivo* phenotypic behavior of a tumorous cell.

In vivo models of bladder cancer

Animal research is an integrative and complementary approach to clinical evidence for a more comprehensive knowledge of cancer disease[224, 225]. Indeed, *in vivo* studies have been a major contributor to our understanding of bladder carcinogenesis. Experimental animal models consisting of the use of mice, rats, and dogs have been applied in preclinical sets to evaluate therapies for bladder cancer. Currently, mouse models of bladder cancer include autochthonous models such as carcinogen-based models and GEMs as well as the non-autochthonous models, which include engraftment (orthotopic, renal grafting and patient-derived xenograft) models[226].

Carcinogen-based models of bladder cancer

Because of their chemical similarities to that of carcinogens found in tobacco smoke, nitrosamines such as N-butyl-N-(4-hydroxybutyl) nitrosamine (BBN), N-[4-(5-nitro-2furyl)-2-thiazolyl]formamide or N-methyl-N-nitrosourea are widely used in the carcinogen-based models of bladder cancer. This model, which consists of the exposure of mice or rats to carcinogens, exhibits a range of phenotypes including hyperplasia, dysplasia, CIS and MIBC depending on

concentration and duration of exposure as well as on the genetic background of the animal[227-229]. The ability of the BBN-model to phenocopy human bladder cancer is also evident in the mutational landscape associated with BBN. Particularly, tumors derived from the BBN-model are enriched of genetic alterations consistent with those observed in human, including genetic mutations in *Tp53, Hras, Kmt2d, Arid1a, Pik3ca, Ep300,* and *Rb1* among many others[230, 231].

Genetically engineered models of bladder cancer

Tumors in the GEM models arise from genetic manipulations in a single gene or combinations of genes in the bladder urothelium and often exhibit diverse phenotypes including both early-stage and late-stage phenotypes[192, 194, 195, 232, 233]. Several approaches are employed for the generation of GEMs. While transgenic models are generated through the expression of oncogenes such as *Hras, Egfr* or *SV40T* under the control of the *UpII* promoter[232-234], conditional and inducible knockout models are created using *Cre-loxP* system under the regulation of either a bladder-specific promoter (i.e., *UpII-Cre*) or a non-bladder-specific promoter (i.e., *Krt5-Cre, Fabp-Cre* or *UBC-Cre/ERT2*). The availability of luminal urothelial cell-specific Cre driver (i.e., *UpII-Cre*) and basal cell-specific Cre driver (i.e., *Krt5-Cre*) as well as inducible systems enables spatial and temporal control/manipulation of gene expression within the bladder urothelium by restricting gene targeting to a specific cell population. Additionally, knockout models can be obtained by intravesical delivery of *Cre*-expressing adenovirus (adeno-Cre) into the bladder lumen. These approaches are interchangeable and have been used for the generation of *Pten, Tp53, Foxa1* and many other knockout mice[191, 192, 195, 205].

Because GEMs involve genetic manipulations of candidate genes, they present as ideal models for experimental characterization of genetic impacts on disease initiation, progression, molecular subtype, heterogeneity and therapy[235, 236]. Nonetheless, the paucity of GEMs described

for bladder cancer highlights the need for more models that take into account genomic alterations relevant to human bladder cancer.

Engraftment models of bladder cancer

The engraftment models can be subdivided into three model types: the orthotopic model, the renal grafting model, and the patient-derived xenograft (PDX) model. The orthotopic model, which in turn can be subdivided into the xenograft and the syngeneic model, consists of the engraftment of tumor cells into the bladder of a host animal[237]. In the xenograft model, human cell lines are transplanted into the bladder of an immunodeficient mouse (i.e., nude or NOD/SCID mice) whereas, in the syngeneic model, mouse cell lines (i.e., MB49) are engrafted into an immunocompetent mouse[238].

In the renal grafting model, tumor cells are combined with embryonic bladder mesenchyme and grafted under the kidney capsule of a mouse recipient host[204, 239]. An advantage of the engraftment models is the ability to manipulate the expression of candidate genes and assess the impact of the altered genes on tumor behavior within the tumor microenvironment. These models are also widely used as preclinical models for intravesical therapy analysis[238]. However, a drawback of the xenograft model is the use of an immunocompromised host, which excludes the investigation of the influence of the immune system on tumor growth as immune response is reported to be a major contributor of bladder cancer[240].

In the PDX model, patients primary tumor are engrafted either subcutaneously or under the renal capsule of an immunodeficient recipient host. An advantage of this model is that the tumor maintains the genomic and molecular characteristics of the patient's tumor. Moreover, this model presents as an optimal model to test clinical response and behavior of the specific tumor[241, 242]. However, the obtainment of successful PDX models has proven to be challenging: not all tumor

samples will successfully engraft into the host. Additionally, the use of immunocompromised hosts indicates that these models may not accurately represent tumor microenvironment.

Dissertation Overview

Tumor heterogeneity consists of differences in morphology, genetic alterations, gene expression patterns and other factors within the same patient or among patients. Altogether, these elements of tumor heterogeneity make accurate diagnosis difficult and challenge the effectiveness of current therapies. Morphologically, bladder cancer is not just one disease. Indeed, the presence and often coexistence of several morphologic variants including UCC with SqD or GD may be associated with aggressive disease and adverse clinical outcomes. Also, risk stratification of bladder cancer patients is based on morphologic appearance and cellular/tumor architecture. However, stage and grade assignments are insufficient to explain the differences in the biological and clinical behaviors of urothelial tumors. Therefore, the field is now investigating the role of molecular heterogeneity in disease risk.

Transcriptomic analyses by several groups have led to the identification of multiple molecular subtypes of bladder cancer[134, 137, 172, 176]. The overlapping of signatures among the subtypes enables to group them under two subsets of disease: the luminal and the basal subtypes based on their expression of urothelial differentiation-associated markers[182]. Importantly, these subtypes present distinct clinical behaviors and sensitivities to chemotherapy with luminal subtype patients having a better prognosis than basal subtype patients[176, 243].

In two recent studies of a pan of cancer malignancies, bladder cancer emerged as the most heterogeneous cancer in terms of tumor cell of origin and molecular subtypes [189], and also as a disease with significant genomic alteration loads including alterations in pivotal cellular and molecular pathways[135]. Among the molecular processes significantly altered in bladder cancer are the PI3K pathway and the urothelial terminal differentiation process. Specifically, loss of the tumor suppressor, *PTEN*, which is a negative regulator of the PI3K pathway, has been associated with advanced and aggressive bladder cancer[126, 152, 153]. Similarly, loss of the urothelial differentiation

transcription factor, *FOXA1*, has been associated with late-stage bladder cancer and SCC disease[204]. Although, independent studies based on the use of GEMs to individually model *Foxa1* or *Pten* in bladder cancer disease implicated these two genes in preneoplastic changes of the bladder urothelium[191, 193, 205], the inability of these models to develop advanced and invasive tumors indicate that cooperativity of these genes with other genomic events are necessary for tumorigenesis and aggressive phenotypes. Based on the clinical evidence of *FOXA1* and *PTEN* association with MIBC, the goal of this dissertation is to characterize the functional interplay, if any, between *FOXA1* and *PTEN* in bladder cancer. Therefore, we hypothesized that ***FOXA1* and *PTEN* contribute to bladder cancer heterogeneity and cooperate to promote bladder tumorigenesis and progression**. To test this hypothesis, the following aims were developed and completed:

Aim 1: characterize the impact of genomic alterations on the expression of *FOXA1* and *PTEN* in bladder cancer.

The TCGA has reported a comprehensive molecular characterization of MIBC based on RNA-seq dataset[155]. Utilizing the TCGA RNA-seq data, we performed hierarchical clustering to investigate the association of *FOXA1* and *PTEN* expression with bladder cancer molecular subtypes. Using the TCGA data, we also performed correlative analyses to identify any potential contribution of genetic mutations and copy number alterations to *FOXA1* and *PTEN* expression. Furthermore, we identified CpG islands associated with *FOXA1* and used DNA methylation data from the Genomic Data Commons to correlate *FOXA1* hypermethylation with reduced *FOXA1* expression in human bladder cancer as well as in a panel of bladder cancer cell lines.

Aim 2: examine the impact of combined alterations of *FOXA1* and *PTEN* in bladder tumorigenesis.

Alterations in *FOXA1* and *PTEN* are implicated in bladder cancer. However, individual inactivation of these genes fails to result in the development of aggressive and invasive bladder cancer in animal models. As we hypothesized that *FOXA1* and *PTEN* loss cooperate to promote

tumorigenesis and tumor heterogeneity, we generated a bladder-specific *Foxa1* and *Pten* double knockout mouse model. We demonstrated that combined deletion of *Foxa1* and *Pten* in the luminal cells of mouse urothelium results in the development of CIS with SqD, which progresses to MIBC with SqD phenotype when combined with carcinogen treatment. Additionally, we performed gain of function studies by overexpressing *FOXA1* and *PTEN* in bladder cancer cell lines, and we assessed their effects on cellular viability by MTT assay and flow cytometry.

Aim 3: examine the impact of strain background on a carcinogen-based model of bladder cancer.

Generation of GEMs often requires, for breeding schemes and practicability, the use of strains with different genetic background. Two of the most commonly used mouse strain to model bladder cancer include C57BL/6 and FVB mice. To gain an understanding of how strain background may affect disease phenotype, we used a carcinogen-based model approach where C57BL/6 and FVB mice were exposed to bladder carcinogen. We demonstrated that FVB mice are more susceptible to BBN and develop aggressive phenotypes than C57BL/6. Because the *Foxa1* and *Pten* knockout model used in Aim 2 was on a mixed genetic background (C57BL/6 and FVB), these findings were complimentary to the interpretation of the data from our GEM model.

Summary and conclusions

Due to its high prevalence and recurrent characteristics demanding continuous surveillance and repeated treatment, bladder cancer has a high human and economic burden; this highlights the need for further and in-depth investigations for treatment improvement. Although, the expansion of the knowledge of the molecular pathways involved in the pathogenesis of bladder cancer opens the door for betterment of the diagnosis and management of this disease, a greater insight into these molecular processes is of utmost importance for the implementation of preventives strategies and novel therapeutics. Moreover, both *in vivo* and *in vitro* studies present as useful tools to gain an understanding of the role of several genes implicated in bladder cancer development. By addressing

the aims outlined above, we show that different genomic mechanisms contribute to *FOXA1* and *PTEN* expression in bladder cancer. Additionally, we show that while low *PTEN* expression is independent of disease molecular subtype and morphology, reduced *FOXA1* expression is associated with basal molecular subtype. Through our animal data, we report synergistic cooperation between *Foxa1* and *Pten* inactivation in bladder tumorigenesis. Specifically, alterations of *Foxa1* and *Pten* in luminal urothelial cells promote tumor heterogeneity evident in the divergent differentiation of luminal cells into tumorous cells enriched of elements of basal-squamous cell phenotype. With the cell culture studies, we provide a preliminary observation of a role for FOXA1 in apoptosis. Future directions based on this work will further elucidate the molecular mechanisms that converge PI3K pathway (*PTEN*) and urothelial differentiation process (*FOXA1*) in bladder tumorigenesis and heterogeneity and identify prognostic factors that may be critical in therapy decision making.

Chapter 2

Hypermethylation of *FOXA1* and Allelic Loss of *PTEN* Drive Squamous Differentiation and Promote Heterogeneity in Bladder Cancer

Abstract

Tumor heterogeneity in bladder cancer is a barrier to accurate molecular sub-classification and treatment efficacy. However, individual cellular and mechanistic contributions to tumor heterogeneity are controversial. We examined potential mechanisms of *FOXA1* and *PTEN* inactivation in human luminal and basal bladder cancers. We show inactivation and reduced expression of *FOXA1* and *PTEN* is prevalent in human bladder cancer. While *PTEN* is down-regulated primarily by allelic loss, *FOXA1* expression is modulated by site-specific DNA hypermethylation. These analyses were complemented with inactivation of *Foxa1* and *Pten* in intermediate and luminal mouse urothelium. Conditional knockout of both *Foxa1* and *Pten* in intermediate/luminal cells results in the development of bladder cancer exhibiting squamous features, as well as enhanced sensitivity to a bladder-specific carcinogen. By integrating human correlative and *in vivo* studies, we define a critical role for *PTEN* loss and epigenetic silencing of *FOXA1* in heterogeneous disease and show genetic targeting of luminal/intermediate cells drives squamous differentiation.

Introduction

While treatment strategies for advanced bladder cancer are largely based on pathologic stage and grade, clinical decisions also take into account the degree of morphologic heterogeneity. Morphologic heterogeneity occurs both across patient populations and within individual tumors. For example, while the most common type of bladder cancer presents morphologically as UCC, a plethora of variant "pure" morphologies have been identified (i.e., squamous cell carcinoma, adenocarcinoma, small cell/neuroendocrine carcinoma, and other rare variants). Alternatively, variant morphologies can be present and admixed within the context of conventional UCC. Elements of squamous, glandular, neuroendocrine, sarcomatoid, micropapillary and nested morphologic differentiation are relatively common in advanced UCC disease. Importantly, morphologic heterogeneity correlates with molecular subtype variation[181, 244, 245]. For this reason, intratumoral, morphology-associated molecular heterogeneity may also complicate accurate diagnosis, influence therapeutic response and contribute to chemoresistance[246, 247].

While the cellular origin of tumor heterogeneity in bladder cancer is unknown, the "cell-of-origin" and the "mutation-of-origin" models have both been proposed to explain the existence of tumor heterogeneity in a wide spectrum of malignancies (reviewed in[122]). As its name indicates, the "cell-of-origin" concept argues that cell fate is "locked" subsequent to transforming events, and therefore not further influenced during tumor development and subsequent progression. In bladder cancer, this model is supported by the observation that luminal-like and basal-like tumor subsets exhibit transcriptional patterns reminiscent of normal luminal urothelium (i.e., KRT20 and uroplakins) and basal urothelium (i.e., KRT5, KRT6, and KRT14), respectively[155].

Alternatively, the "mutation-of-origin" posits that the ultimate determining factor driving tumorigenesis and progression-associated heterogeneity is the identity of genetic or epigenetic

changes, independent of cell type. The "mutation-of-origin" implies the existence of molecular and cellular plasticity, which can contribute to the existence of morphologic and molecular subclones that share a high degree of molecular alterations[244, 245].

Although the molecular mediators of basal bladder cancer remain unidentified, studies suggest the existence of molecular parallels with basal breast cancers. For example, inactivation of the Forkhead box A1 (*FOXA1*) is implicated in basal breast cancers, and it is now well accepted that *FOXA1* loss is associated with squamous differentiation and a basal molecular subtype of bladder cancer[155, 197, 204, 205]. While the mechanisms that lead to *FOXA1* inactivation in breast cancer are documented, the same cannot be said for bladder cancer. In addition, while *Foxa1* knock-out mice develop elements of squamous differentiation, they fail to develop bladder cancer[205]; this suggests that in addition to *FOXA1* loss, further genetic alterations are required. Similar to *FOXA1*, inactivation of the Phosphatase and Tensin homolog on chromosome 10 (*PTEN*) is implicated in basal breast cancer[248, 249] with clinical and experimental evidence suggesting a similar role for *PTEN* in bladder cancer[126, 192, 193]. For example, squamous morphology can be enriched in basal bladder cancers, and a recent TCGA pan-cancer study identified a role for *PTEN* inactivation in bladder cancers with a "squamous-like" signature[189].

Based on these observations, we hypothesized that *PTEN* is inactivated in basal bladder cancers where it cooperates with *FOXA1* inactivation to promote the development of a basal transcriptional profile and squamous differentiation. Our analysis reveals that decreased *PTEN* expression occurs in both basal and luminal bladder cancers in a manner largely dependent upon copy number. We provide the first evidence that promoter hypermethylation is a major contributor to decreased *FOXA1* expression in basal bladder cancer. Moreover, our experimental *in vivo* data show that inactivation of *Foxa1* and *Pten* in luminal cells and a subset of intermediate urothelial cells results in bladder cancer with a striking degree of squamous differentiation. These results

suggest that combined inactivation of *FOXA1* and *PTEN* contributes to tumor heterogeneity in bladder cancer in a manner independent of cell of origin.

Materials and Methods

Gene expression, copy number alterations, and point mutations analyses

To explore the effect of DNA copy number alterations and somatic mutations on gene expression, we analyzed the data from the TCGA bladder cancer study[155]. Normalized RSEM gene expression values for the TCGA bladder cancer cohort were downloaded from the Broad Institute's Firehose GDAC (https://gdac.broadinstitute.org/) as were quantitative and discrete gene-level DNA copy number values produced by the GISTIC pipeline[250]. The mutation annotation file was downloaded from the Genomic Data Commons (https://gdc.cancer.gov/). Both the expression and quantitative DNA copy number data were filtered by restricting to common samples as well as genes in chromosomes 1 – 22 whose copy number values had non-zero variance; this yielded gene expression and quantitative DNA copy number values for 17,608 genes and 404 samples. The normalized RSEM values were log-transformed as log2(RSEM + 1). The MVisAGe R package[251] was applied to compute and plot gene-level Pearson correlation coefficients using the log transformed RSEM values and the quantitative DNA copy number values. Heatmaps of the quantitative DNA copy number values in select chromosomes and genomic regions of interest were also produced. Two-way tables based on the discrete gene-level DNA copy number values were used to assess the co-occurrence of DNA copy number alterations for genes of interest.

Animal studies

All animal experiments were performed in accordance with and following approval by the Institutional Animal Care and Use Committee at Pennsylvania State University College of Medicine. Previously described *Foxa1*$^{loxp/loxp}$ mice[252] maintained on a C57BL/6 were initially intercrossed with *Pten*$^{loxp/loxp}$ [253] obtained from Jackson Laboratories and maintained on a C57BL/6 background to generate *Foxa1*$^{loxp/loxp}$/*Pten*$^{loxp/loxp}$ mice. These mice were in turn intercrossed with *UpII-Cre* mice [254] generated and maintained on a FVB inbred background; this resulted in constitutive conditional knockout mice of *Foxa1* and *Pten*. A total of nine different genotypes were generated to assess the copy number contribution of each gene to phenotype development. This included genetic control (no-Cre or absence of loxp locus), *UpII-Cre/ Foxa1*^{loxp}, *UpII-Cre/Foxa1*$^{loxp/loxp}$, *UpII-Cre/Pten*^{loxp}, *UpII-Cre/Pten*$^{loxp/loxp}$, *UpII-Cre/Foxa1*^{loxp}/*Pten*^{loxp}, *UpII-Cre/Foxa1*$^{loxp/loxp}$/*Pten*^{loxp}, *UpII-Cre/Foxa1*^{loxp}/*Pten*$^{loxp/loxp}$, *UpII-Cre/Foxa1*$^{loxp/loxp}$/*Pten*$^{loxp/loxp}$. All mice were genotyped by PCR analysis (Supplemental Table 2-1). A cohort of mice (n = 101 mice total) was aged for 12 months to assess the impact of *Foxa1* and *Pten* deletion on bladder tumorigenesis. Another cohort of mice (n = 91 mice total) was used for carcinogen studies to assess the interaction between *Foxa1* and *Pten* deletion and response to *N*-butyl-*N*-(4-hydroxybutyl)-nitrosamine (BBN; TCI America; Portland OR) exposure. 8 weeks old mice were exposed to BBN (0.05% in tap water provided *ad libitum*) for 12 weeks. Water containing BBN was changed twice weekly and stored in light-protected bottles. For both aging and BBN studies, after sacrificing the animals, individual bladders were dissected and utilized for morphologic analysis and immunohistochemistry (IHC) following formalin fixation and paraffin embedding.

Methylation analysis

For analysis of *FOXA1* CpG island methylation in human bladder cancer, DNA methylation data from the Illumina HumanMethylation450K platform was downloaded from the Genomic Data Commons (https://gdc.cancer.gov/), and probes corresponding to CpG islands 99 and 143 in *FOXA1* were identified. Probe-level beta values from normal samples (n = 15) were used to compute binary unmethylated and methylated calls in the tumor samples based on a threshold of mean (normal beta) + 3*standard deviation (normal beta), which is similar to the approach presented in[255]. The EpiTect Methyl II PCR Array (Qiagen) was used to screen the DNA methylation status of CpG islands (SABioscienes CpG Island IDs: 104028, 104029, 104030) in the *FOXA1* promoter and gene body of human bladder cancer cell lines. Specifically, the bladder cancer cell lines RT4, SW780, UMUC1, UMUC3, T24, TCCSUP, SCaBER, 5637, HT1376, and HT1197 were cultured to confluency as previously described[213]. All cell lines were tested for mycoplasma contamination using the kit according to the manufacturer's instruction. After washing with PBS, cells were harvested and stored at -80°C. Samples were prepared for restriction enzyme digestion and quantitative real-time PCR according to the manufacturer's protocol. DNA and RNA were harvested in triplicate for each cell line using the AllPrep DNA/RNA Mini Kit (Qiagen) and stored at -80°C. Input DNA (250 ng) was digested using the EpiTect II DNA Methylation Enzyme Kit (Qiagen) as per manufacturer's instruction. After digestion, the enzymatic reactions were aliquoted into a 96-well plate with wells containing RT^2 SYBER Green qPCR Mastermix and EpiTect Methyl II PCR Primer Assays for Human *FOXA1* (Cat# EPHS104028-1A, EPHS104029-1A, EPHS104030-1A). PCR reactions were performed using QuantStudio7 Real-Time PCR system (Applied Biosystems) per manufacturer's instruction. The raw delta Ct values generated for each digest were used to determine the relative amount of methylated and unmethylated DNA fractions by percentage.

Morphologic and immunohistochemical analyses

All analyses of formalin-fixed, paraffin embedded tissues were completed following Institutional Review Board Approval at Pennsylvania State University College of Medicine. Hematoxylin and eosin (H&E) staining was performed as previously described[205]. For IHC, tissue sections were deparaffinized in histoclear (National Diagnostics, Atlanta GA) and rehydrated in a series of graded alcohols (Pharmaco-Aaper, Brookefield CT), and rinsed in deionized water. The slides were placed in 1% antigen unmasking solution (Vector Labs) for antigen retrieval and heated for 20 minutes at high pressure in a pressure cooker (Cuisinart, East Windsor NJ), followed by cooling at room temperature and 10 minutes washes in phosphate-buffered saline (PBS 1X, pH 7.4) for 3 times. The slides were then incubated in 1% hydrogen peroxide (Thermo Fisher Scientific) in methanol (Thermo Fisher Scientific) for 20 minutes to block endogenous peroxidase, followed by rewashes in 1X PBS (10 minutes for 3 times) and incubation for 1 hour in blocking solution 1X PBS containing horse serum (Vector Labs) to reduce nonspecific antibody binding. The mouse on mouse kit (Vector Labs) was used in conjunction with primary antibodies raised in mice to reduce nonspecific background. Slides were subsequently incubated with primary antibodies (Supplemental Table 2-2) overnight at 4°C in a humidified chamber. The following day, slides were washed in 1X PBS (10 minutes for 3 times) before incubation for 1 hour with appropriate secondary antibody (1:200; Vector Labs) diluted in blocking solution. Following additional washing, antibody binding was visualized through the Vectastain Elite ABC Peroxidase kit (Vector Labs) after addition of the chromogen 3'-diaminobenzidine (Thermo Fisher Scientific). Sections were washed in tap water for 5 minutes before counterstaining and rehydrating as previously reported[205].

Plasmid construction

FOXA1 Human Tagged ORF Clone (OriGene, Rockville MD) and *PTEN* Ultimate™ ORF (Clone ID: IOH56926, Thermo Fisher Scientific) were used as templates for PCR amplification using AccuPrime™ Pfx SuperMix (Thermo Fisher Scientific). Sequence matching primers (Supplemental Table 2-3) were designed and used to incorporate *BamHI* and *EcoRI* sites for subcloning of *FOXA1* ORF into pLVX-IRES-*ZsGreen1* (Clontech, Mountain View CA) and *PTEN* ORF into pLVX-IRES-*mCherry* (Clontech) plasmids. Subsequently, PCR products containing *FOXA1* or *PTEN* cDNA were digested with both *BamHI* and *EcoRI* restriction enzymes, and ligated into empty vector pLVX-IRES-*ZsGreen1* (hereafter EV*ZsG*) and pLVX-IRES-*mCherry* (hereafter EV*mCh*) respectively, using T4 DNA ligase (New England BioLabs, Ipswich, MA) according to the manufacturer's protocol. The sequences of pLVX-IRES-*ZsGreen1-FOXA1* (hereafter simply *FOXA1*) and pLVX-IRES-*mCherry-PTEN* (hereafter simply *PTEN*) were verified by Sanger sequencing (Supplemental Table 2-4).

Cell culture

5637 cells (ATCC. Manassas, VA) were cultured in RPMI 1640 (Corning Inc, Corning, NY) media supplemented with 10% Fetal Bovine Serum (ATLANTA biologicals, Flowery Branch GA) and 1% Penicillin/Streptomycin (Corning Inc,). UMUC3 cells (ATCC) were cultured in MEM/EBSS (HyClone, Logan UT) media complemented with 10% Fetal Bovine Serum and 1% Penicillin/Streptomycin. All cells were cultured at 37°C with 5% CO_2. Cell lines were passaged on average every 3-4 days.

Transient transfection

For transient expression of FOXA1 and PTEN, 5637 and UMUC3 cells were plated at a density of $2x10^5$ cells/ml. At 70% confluence, cells were double transfected in four different conditions as follow: with both empty vectors (EV*ZsG* and EV*mCh*); EV*mCh* and *FOXA1*; EV*ZsG* and *PTEN*; and *FOXA1* and *PTEN*. The combined empty vector transfections were used as controls. All plasmid transfections were performed at 0.5 μg/μl final concentration per each plasmid using Lipofectamine 3000 (Invitrogen, Carlsbad CA). Expression of genes of interest was determined 24 hours post-transfection using Western blot.

Western blot

For protein extraction, cell culture media was collected and centrifuged at 1200 rpm for 5 minutes at 25ºC (Sorvall ST 8R centrifuge, Thermo Fisher Scientific), while the remaining adherent cells were left on ice in 1X DPBS (Corning). The pellet was resuspended in 100 μl RIPA buffer (25mM Tris-HCl pH 7.6, 150mM NaCL, 1% NP-40, 1% sodium deoxycholate, 0.1% SDS [Thermo Fisher Scientific]) containing 1X protease (Roche, Basel, Switzerland) and phosphatase inhibitors (Roche). The cellular lysates were then transferred to the corresponding wells on the tissue culture plate to harvest the adherent cells. The cells were left on ice for 10 minutes for the lysis process and then scrapped, and collected into 1.5 ml Eppendorf tubes. Samples were then sonicated followed by microcentrifugation at 15,000xg for 30 minutes at 4°C (Centrifuge 5424 R, Eppendorf, Hamburg Germany).

Protein concentration was measured using the Pierce BCA Protein Assay Kit (Thermo Fisher Scientific) according to the manufacturer's protocol. The protein extracts were prepared with 1X NuPAGE LDS Sample buffer (Thermo Fisher Scientific) at 1 μg/μl final concentration.

Samples were boiled at 95°C for 5 minutes to reduce and denature proteins. 10 μg of protein per sample were loaded on polyacrylamide gel (Thermo Fisher Scientific) together with protein marker (BioRad, Hercules CA) for electrophoresis (BioRad) followed by blotting on PVDF membrane equilibrated earlier in 100% methanol, washed with Millipore water and then re-equilibrated with transfer buffer (Thermo Fisher Scientific). Blotting was performed using Pierce G2 Fast Blotter (Thermo Fisher Scientific). Membranes were incubated in blocking buffer (5% skim milk - Tris-buffered saline (BioRad) containing 0.1% Tween20 (TBST) for 1 hour at room temperature on a shaker to prevent nonspecific binding. Membranes were incubated overnight at 4°C with primary antibodies (Supplemental Table 2-2) diluted in blocking buffer. On the next day, the membranes were washed (5 minutes for 5 times) with TBST before incubation at room temperature on a shaker for 1 hour with appropriate secondary antibody diluted (1:2000) in blocking buffer. Membranes were rewashed (5 minutes for 5 times) with TBST followed by treatment with Amersham ECL Prime Western Blotting Detection Reagent (GE Healthcare Life Sciences, Chicago IL) for visualization of protein bands. Image J software was used to quantify protein bands.

MTT assay and apoptosis

Cell viability of 5637 and UMUC3 transfected cells with empty vectors (EV*ZsG* and EV*mCh*), *FOXA1*, and *PTEN* was assessed 24 hours post-transfection via 3-(4,5-dimethylthiazol-2-yl)-2,5-diphenyltetrazolium bromide (MTT) assay. MTT solution (Alfa Aesar, Tewksbury MA) at a final concentration of 0.5 μg/μl was added to cell culture media according to the manufacturer's protocol. The cells were incubated at dark at 37ºC with 5% CO_2 for 3 hours. Dimethyl sulfoxide (DMSO; Thermo Fisher Scientific) was added at 100% concentration to cells and incubated at dark on an orbital shaker for 2 hours to dissolve formazan crystals, and optical densitometry was measured at 570 nm wavelength.

Flow cytometry

Control and experimental 5637 and UMUC3 cells were harvested 24 hours post-transfection and washed in cold 1X PBS 3 times, each time followed by centrifugation at 200 g for 4 minutes at 4ºC before staining with the apoptotic marker, annexin V, and the necrotic marker, 7-Aminoactinomycin D (7-AAD). Flow cytometry (FACS) analysis for cell viability and apoptosis was performed using the PE Annexin V Apoptosis Detection Kit I (BD Biosciences, San Jose, CA) according to the manufacturer's instructions. FACSCalibur flow cytometer at the Pennsylvania State University College of Medicine Flow Cytometry Core was used.

Statistical analyses

Wilcoxon rank sum test in Prism version 6.0c was used for statistical analyses of PTEN IHC scores in clinical samples, and to compare *FOXA1* expression in the unmethylated and methylated tumor samples of the TCGA dataset. Two-tailed statistical tests were determined to be significant at p-value ≤ 0.05. Two-sided Fisher's exact test was used to analyze cooperativity between *Foxa1* and *Pten* inactivation in bladder tumorigenesis. Dunnett's multiple comparison test was used to statistically analyze MTT assay data, percentages and fold changes in apoptotic markers and cell viability. R 3.4.1[256] was used to perform all other data analyses and generate figures.

Results

PTEN expression is decreased in both luminal and basal bladder cancers and is independent of tumor morphology

FOXA1 expression is reduced in areas of squamous differentiation[181, 204], and is associated with the basal-squamous molecular subtype[155]. While *PTEN* mutations have been implicated in bladder cancers with a "squamous-like" signature[189], it is unknown if *PTEN* expression is reduced in basal-squamous bladder cancers or in areas of squamous differentiation. To examine *PTEN* expression in human bladder cancer and identify any associations with a molecular subtype, we performed hierarchical clustering of publicly available RNA-seq data from the TCGA bladder cancer study[155]. In agreement with previous reports[204, 205, 257], hierarchical clustering of RNA-seq data shows that tumors with decreased *FOXA1* expression cluster within the basal molecular subtype (Figure 2-1 A). However, *PTEN* expression was heterogeneous within the TCGA cohort, and reduced expression did not appear to correlate strongly with either subtypes (Table 2-1 and Figure 2-1 A). Specifically, low *FOXA1* expression (below the 0.25 quantile) was observed in 85 out of 138 cases (62%) of basal bladder cancers, but only in 10 out of 243 (4%) of luminal tumors (Table 2-1). Whereas low *PTEN* expression (below the 0.25 quantile) was observed in 26 out of 138 cases (19%) of basal tumors, and in 69 out of 243 (28%) luminal bladder cancers (Table 2-1); this suggests that decreased *PTEN* expression may not correlate with molecular subtype or could be difficult to detect from analyzing bulk tumor RNA-seq of heterogeneous tumors.

We then examined PTEN protein expression in clinical samples collected from a total of 18 bladder cancer patients from our institution, most with at least one form of morphologic heterogeneity (Supplemental Figure 2-1). Of these 18 patients, three had areas of non-invasive papillary urothelial carcinoma, 16 had areas of muscle invasive urothelial cell carcinoma (UCC), and 15 had areas of muscle invasive squamous differentiation. Two patients exhibited muscle

invasive UCC with no additional morphologies present. Interestingly, PTEN expression was frequently undetectable in regions of both UCC and squamous differentiation within the same tumor. Thus, while decreased *FOXA1* expression is related to both basal molecular subtype and squamous differentiation[204], IHC for PTEN confirms reduced expression of this tumor suppressor does not appear to be associated with molecular subtype or with the presence of squamous differentiation, suggesting its importance is not limited to one subtype of disease (*p*-value = 0.493, Wilcoxon rank sum test; Figure 2-1 B).

Table 2-1. The rate of *FOXA1* and *PTEN* expression in the basal and luminal subtypes of bladder cancer.

	***FOXA1* Expression**				***PTEN* Expression**		
mRNA subtype	**Below 25th percentile n (%)**	**Above 25th percentile n (%)**	Total	mRNA subtype	**Below 25th percentile n (%)**	**Above 25th percentile n (%)**	Total
Luminal	10 (4%)	233 (96%)	243	**Luminal**	69 (28%)	174 (72%)	243
Basal	85 (62%)	53 (38%)	138	**Basal**	26 (19%)	112 (81%)	138

	***FOXA1* Expression**				***PTEN* Expression**		
mRNA subtype	**Below 75th percentile n (%)**	**Above 75th percentile n (%)**	Total	mRNA subtype	**Below 75th percentile n (%)**	**Above 75th percentile n (%)**	Total
Luminal	150 (62%)	93 (38%)	243	**Luminal**	186 (77%)	57 (23%)	243
Basal	136 (99%)	2 (1%)	138	**Basal**	100 (72%)	38 (28%)	138

Percentage of luminal and basal patients from the TCGA MIBC cohort (n = 404) with "low expression" (below 0.25 quantile) and "high expression" (above 0.75 quantile) of *FOXA1* and *PTEN*

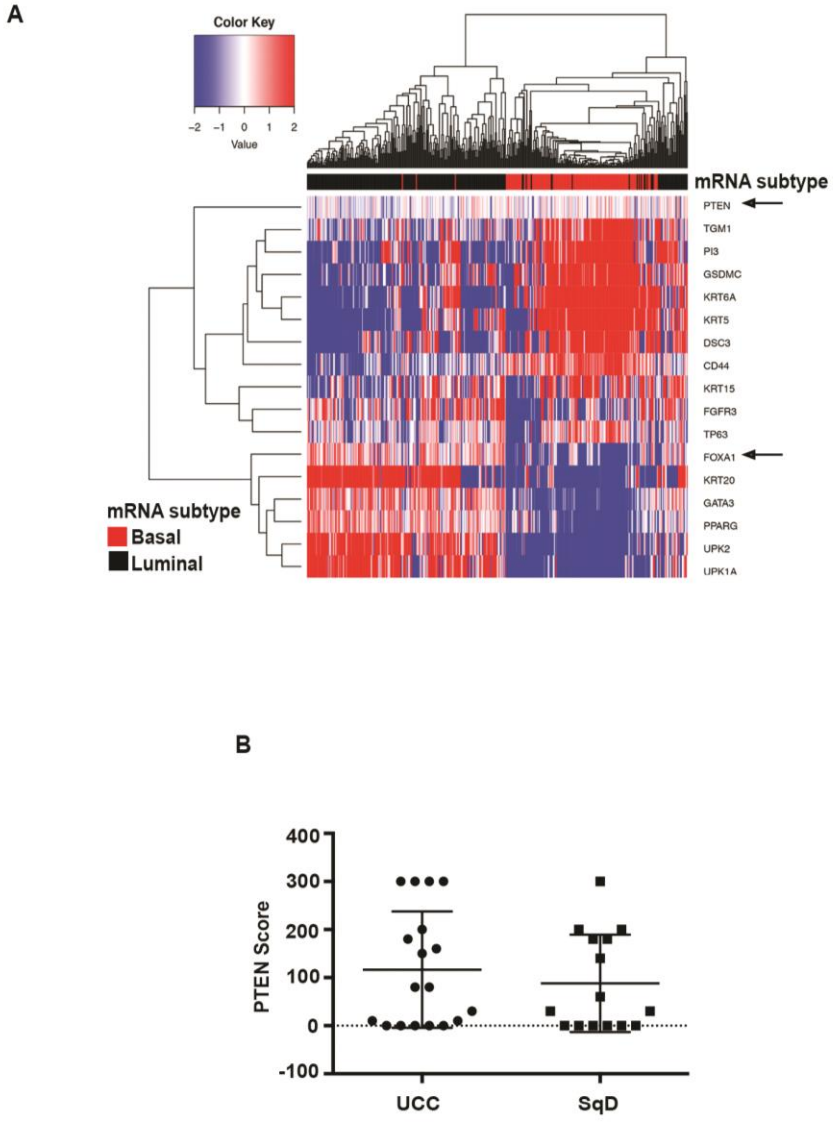

Figure 2-1. Loss of *PTEN* expression is independent of molecular subtype and specific elements of tumor heterogeneity.

(**A**) Hierarchical clustering of publicly available gene expression data from the TCGA muscle invasive bladder cancer cohort (n = 404). Each column represents a patient and genes are listed by row. Annotation bar at the top of the heatmap indicates mRNA subtype (basal versus luminal). Gene expression code: low expression (blue), neutral (white) and high expression (red).While clinical samples with low *FOXA1* expression robustly cluster with the basal group, *PTEN* low expressing tumors fail to strongly cluster with any subtype group. (**B**) Comparison of PTEN immunohistochemistry in areas of urothelial cell carcinoma (UCC) and squamous differentiation (SqD) within the same tumor revealed no significant difference between the level of PTEN expression in UCC area and in SqD areas (*p*-value = 0.4928; Wilcoxon rank sum test).

PTEN copy number loss is common and associated with reduced expression in muscle invasive bladder cancer

To gain insight into the mechanisms underlying decreased expression of *PTEN* and *FOXA1*, we next utilized the TCGA data[155] to explore the relationship between copy number status and gene expression. From the analysis of the TCGA bladder cohort (n = 404), we identified 19 and 9 patients with homozygous loss of *PTEN* or *FOXA1*, respectively (Table 2-2). A total of 68 (~ 17%) of patients exhibited at least heterozygous or homozygous loss of both *PTEN* and *FOXA1*, suggesting combined copy number loss is relatively common in advanced disease (Table 2-2). Further analysis of TCGA data also showed that copy number loss in the genomic region containing *PTEN* is common across patients and is associated with reduced expression of *PTEN* (Figure 2-2 A). Indeed, the effect of copy number loss on *PTEN* expression was quite pronounced, which is better illustrated in the plot of the unsmoothed correlation coefficients (ρ = 0.638; Figure 2-2 B). In contrast, copy number status in the genomic area containing *FOXA1* did not exhibit a consistent pattern, with amplification and deletion appearing to have similar frequencies across patients, and with no major effects on expression of regional genes (Figure 2-2 C). As a consequence, we did not observe a strong correlation between gene expression and copy number status for *FOXA1* (ρ = 0.036; Figure 2-2 D). Moreover, while *PTEN* expression correlated with copy number status in a manner apparently independent of molecular subtype (Figure 2-2 E), patients with basal bladder cancer were likely to have reduced *FOXA1* expression, independent of copy number status (Figure 2-2 F). In regards to point mutations, additional genomic analyses show *PTEN* mutations were evenly distributed across a spectrum of *PTEN* expression values (Supplemental Figure 2-2 A). However, mutations in *FOXA1* were largely found in patient tumors with high *FOXA1* expression (Supplemental Figure 2-2 B). When taken together, these findings suggest that copy number alterations in *PTEN* have a significant impact on expression of this tumor suppressor, while neither

copy number alterations nor mutations can explain alterations in *FOXA1* expression, which are commonly detected in advanced bladder cancer and associated with molecular subtype.

Table 2-2. Two-way table of discrete copy number values for *FOXA1* and *PTEN* in the TCGA cohort.

		FOXA1					
		HomDel	**HetDel**	**Neutral**	**LowGain**	**HighGain**	**Total**
PTEN	**HomDel**	1	2	12	3	1	19
	HetDel	3	62	52	31	0	148
	Neutral	5	44	132	26	0	207
	LowGain	0	11	12	5	0	28
	HighGain	0	1	1	0	0	2
	Total	9	120	209	65	1	404

Analysis of TCGA MIBC cohort (n = 404)[155]. Reported are homozygous deletion (HomDel), heterozygous deletion (HetDel), wild-type (Neutral), amplifications (LowGain and HighGain).

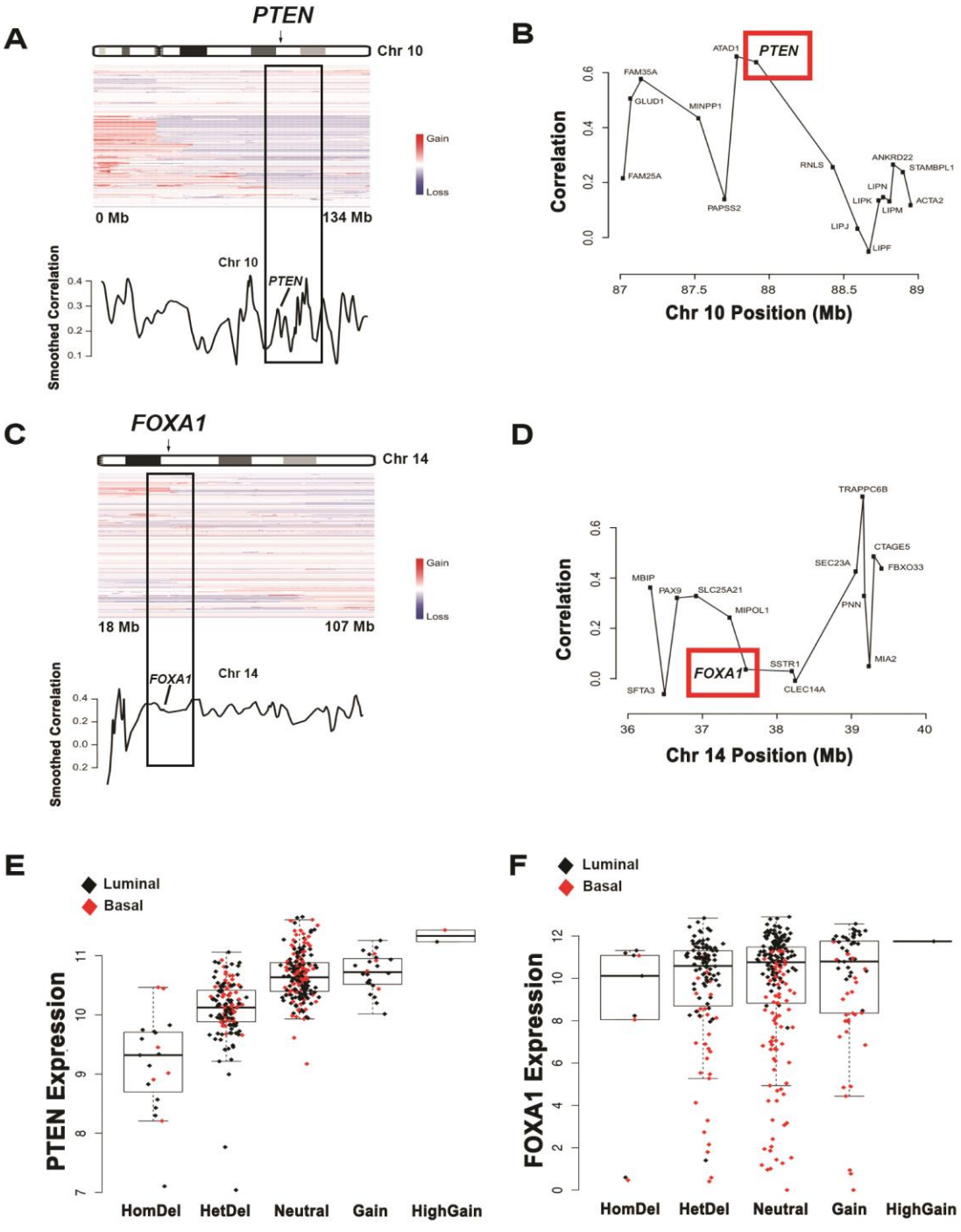
A
PTEN
Chr 10
Gain
Loss
0 Mb
134 Mb
Chr 10
PTEN
Smoothed Correlation
B
PTEN
ATAD1
FAM35A
GLUD1
MINPP1
FAM25A
PAPSS2
RNLS
ANKRD22
STAMBPL1
LIPN
LIPK
LIPM
ACTA2
LIPJ
LIPF
Correlation
Chr 10 Position (Mb)
C
FOXA1
Chr 14
Gain
Loss
18 Mb
107 Mb
FOXA1
Chr 14
Smoothed Correlation
D
TRAPPC6B
CTAGE5
SEC23A
FBXO33
MBIP
PAX9
SLC25A21
MIPOL1
PNN
MIA2
FOXA1
SSTR1
SFTA3
CLEC14A
Correlation
Chr 14 Position (Mb)
E
Luminal
Basal
PTEN Expression
HomDel
HetDel
Neutral
Gain
HighGain
F
Luminal
Basal
FOXA1 Expression
HomDel
HetDel
Neutral
Gain
HighGain

Figure 2-2. *PTEN* expression, but not *FOXA1* expression is associated with copy number status in advanced bladder cancer.

(**A**) Chromosome-wide copy number alterations (CNAs) for chromosome 10 including *PTEN*. Accompanying plot shows the correlation of CNAs with gene expression smoothed across the entire chromosome 10. Rectangle inset identifies CNAs of genomic regions next to *PTEN*. (**B**) Graph of unsmoothed Pearson correlation of CNAs with the expression of *PTEN* (ρ = 0.638) and surrounding regions on chromosome 10. (**C**) Chromosome-wide CNAs for chromosome 14 including *FOXA1*. Accompanying plot shows the correlation of CNAs with gene expression smoothed across the entire chromosome 14. Rectangle inset identifies CNAs of genomic regions next to *FOXA1*. (**D**) Unsmoothed Pearson correlation of CNAs with the expression of *FOXA1* (ρ = 0.036) and surrounding regions on chromosome 14. (**E**) Dot plot showing the correlation of *PTEN* CNAs with gene expression. Patients with luminal tumors are identified with black dots while patients with basal bladder cancer are identified with red dots. (**F**) Dot plot showing the correlation of *FOXA1* CNAs with gene expression. Patients with luminal tumors are identified with black dots while patients with basal bladder cancer are identified with red dots. CNAs indicated as homozygous deletion (HomDel), heterozygous deletion (HetDel), wild-type (Neutral), amplifications (LowGain and HighGain).

Epigenetic modification of the *FOXA1* promoter in the form of DNA methylation is associated with decreased *FOXA1* expression

Because our previous analysis showed that DNA copy number alterations and mutations do not appear to drive changes in *FOXA1* expression, we examined a potential role for epigenetic regulation of *FOXA1* in bladder cancer. Using the University of California Santa Cruz Genome Browser, we identified CpG islands 99, 123 and 143 within the *FOXA1* promoter and gene body (Figure 2-3 A). Identification of probes associated with *FOXA1* in the methylation data from the TCGA bladder study [155] resulted in probes for the analysis of CpG islands 99 (5 probes) and 143 (15 probes). There were no probes targeting CpG island 123 in the TCGA methylation data. As described in the Methods, we calculated a beta-value threshold that distinguished methylated versus unmethylated samples for each probe. Following dichotomization, statistical analyses show that methylation at probes in CpG island 99 is significantly associated with reduced *FOXA1* expression (Figures 2-3 B-D and Supplemental Table 2-5). In regards to CpG island 143, with the exception of one probe (Figure 2-3 E), *FOXA1* expression was not statistically different between methylated and unmethylated tumor samples (Figures 2-3 F and G, and Supplemental Table 2-5). In an effort

to validate these findings as well as examine the methylation profile of CpG island 123, we extended our methylation analysis to a panel of commonly used human bladder cancer cell lines previously subtyped by our group[213]. In agreement with clinical data, CpG island 99 was methylated specifically in basal bladder cancer cell lines SCaBER, 5637, HT1376, and HT1197 and in "non-type" bladder cancer cell lines UMUC3 and TCCSUP, which exhibits low *FOXA1* expression (*p*-value = 0.00285; Figure 2-4 A) while CpG island 143 was unmethylated in all cell lines except UMUC3 and HT1197 (*p*-value = 0.00336; Figure 2-4 B). Interestingly, CpG island 123 was methylated in all ten cell lines in a manner independent of molecular subtype assignment, and there was no association between methylation status at CpG island 123 and *FOXA1* expression (*p*-value = 0.0667; Figure 2-4 C).

Overall, our data indicate that *FOXA1* promoter methylation is present in clinical samples collected from patients with advanced disease as well as in cell line models of bladder cancer.

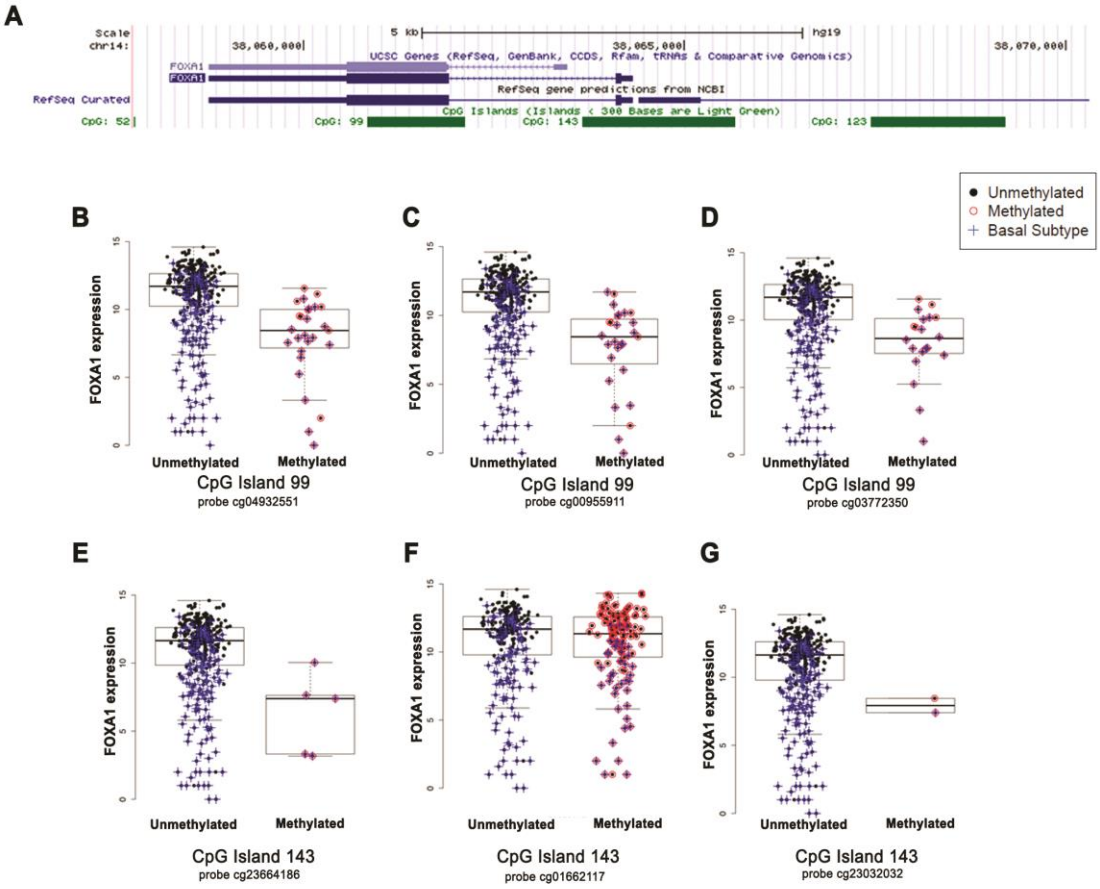

Figure 2-3. *FOXA1* is methylated in human bladder cancer.

(**A**) Screenshot of chromosome 14 showing CpG islands -99, -143 and -123, and their relationship to exons and introns of *FOXA1* gene. (**B-D**) Association of *FOXA1* expression with methylation of CpG island 99 in the bladder TCGA study. Tumors exhibiting a basal gene expression subtype are indicated with a blue cross while methylated samples are circled in red. (**E-G**) Association of *FOXA1* expression with methylation of CpG island 143 in the bladder TCGA study. Tumors exhibiting a basal gene expression subtype are indicated with a blue cross while methylated samples are circled in red.

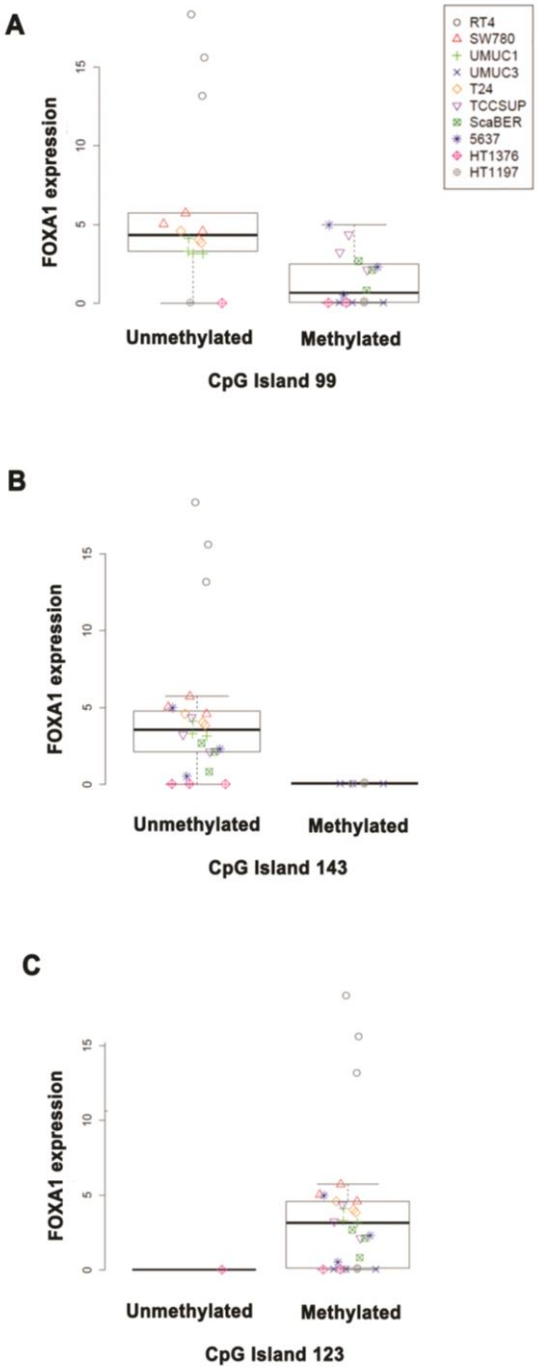

Figure 2-4. *FOXA1* is methylated in human basal-squamous bladder cancer cell lines.

(**A**-**C**) Boxplots showing *FOXA1* expression versus methylation status for CpG island 99 (**A**), island 143 (**B**) and 123 (**C**) for a panel of bladder cancer cell lines.

Knockout of *Foxa1* and *Pten* in luminal and intermediate urothelial cells results in bladder cancer

In order to test the possibility that copy number loss of *PTEN* cooperates with genetic silencing of *FOXA1* to promote bladder tumorigenesis and tumor heterogeneity, urothelium-specific *Foxa1 and Pten* knockout mice were generated by breeding *UpII-Cre* (targets superficial/luminal and a subpopulation of intermediate urothelium) with *Foxa1*$^{loxp/loxp}$ and *Pten*$^{loxp/loxp}$ mice (Figure 2-5 A). Cre-mediated deletion of *Foxa1* and *Pten* in mouse bladder was confirmed by PCR examination of DNA extracted from 4 week old mice (Figure 2-5 B). To assess the impact of *Foxa1* and *Pten* knockout on urothelial differentiation and bladder tumorigenesis, we aged control and knockout animals for 6 and 12 months. Consistent with previous studies[191-193], 6 months old *UpII-Cre/Pten*$^{loxp/loxp}$ mice developed urothelial hyperplasia, which was also observed in the combined *Foxa1* and *Pten* mice at 6 months of age (Supplemental Figure 2-3). Relative to the urothelium of the genetic controls (Figure 2-5 C) and *UpII-Cre/Foxa1*^{loxp} mice (Figure 2-5 D), urothelial hyperplasia was detected in *UpII-Cre/Pten*^{loxp} (Figure 2-5 E), *UpII-Cre/Foxa1*$^{loxp/loxp}$ (Figure 2-5 F), *UpII-Cre/Pten*$^{loxp/loxp}$ (Figure 2-5 G) and *UpII-Cre/Foxa1*^{loxp}*/Pten*^{loxp} (Figure 2-5 H) at 12 months of age. However, we detected bladder cancer in the form of focal carcinoma *in situ* (CIS) in a subset of *UpII-Cre/Foxa1*$^{loxp/loxp}$*/Pten*^{loxp} mice at 12 months of age (Figure 2-5 I) as well as in a majority of *UpII-Cre/Foxa1*^{loxp}*/Pten*$^{loxp/loxp}$ (Figure 2-5 J) and *UpII-Cre/Foxa1*$^{loxp/loxp}$*/Pten*$^{loxp/loxp}$ mice (Figure 2-5 K). Interestingly, development of bladder cancer following *Foxa1* and *Pten* knockout at 12 months of age was associated with the presence of squamous differentiation (high power image in Figure 2-5 K and low power images depicted in Figures 2-5 L and M). The number of mice that developed cancer was quantified (Figure 2-5 N), with percentages of mice developing cancer (Figure 2-5 O). Statistical analysis revealed that the development of bladder cancer was significantly associated with combined homozygous and heterozygous knockout of *Foxa1* and *Pten* in the mouse urothelium (*p*-value = 5.68e-5, Fisher's

exact test). These results indicate that ablation of both *Foxa1* and *Pten* within superficial/luminal and intermediate urothelial cells by *UpII-Cre* promote bladder cancer with elements of squamous differentiation, a common form of tumor heterogeneity.

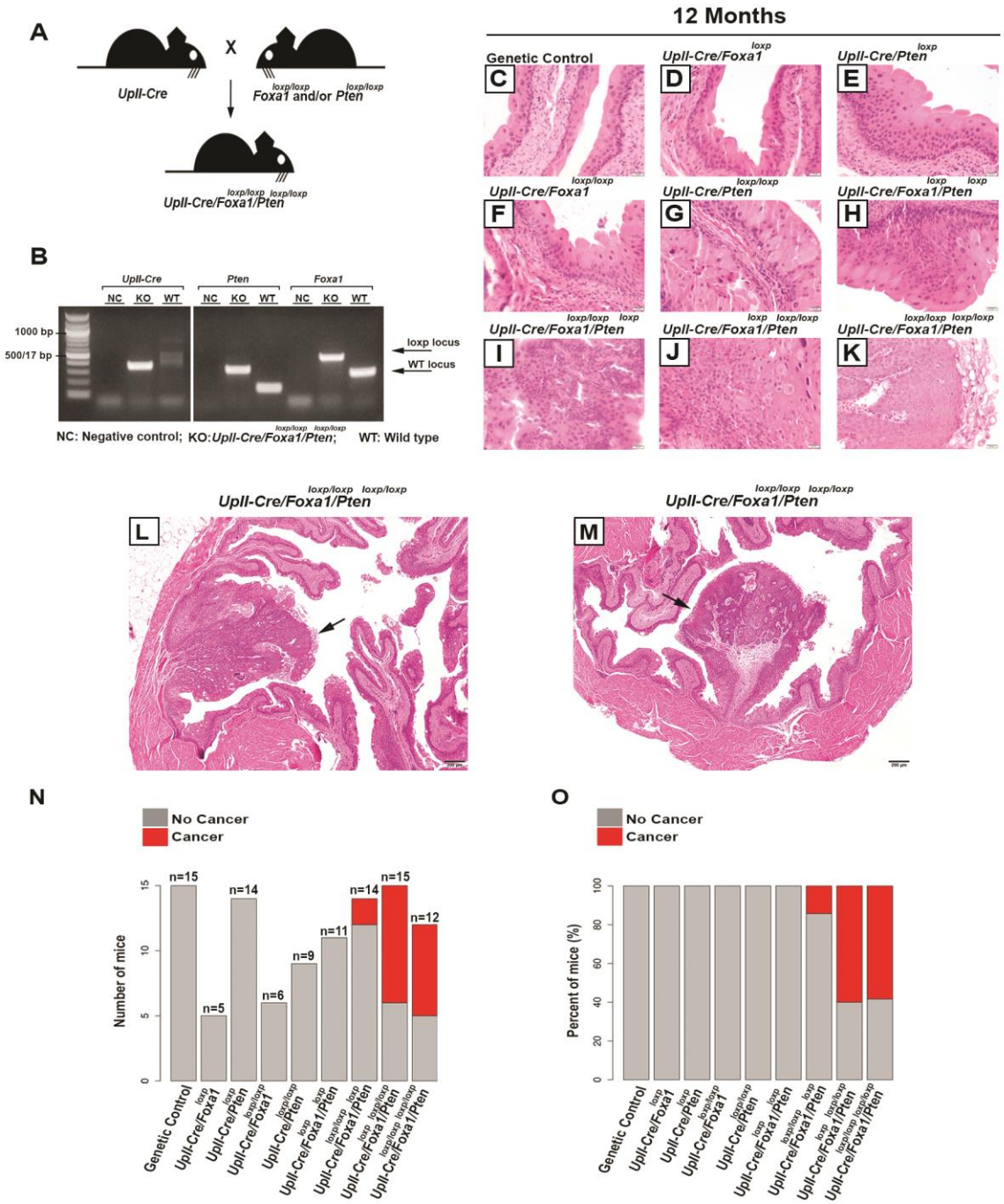

Figure 2-5. *UpII-Cre*-mediated knockout of *Foxa1* and *Pten* results in the development of bladder cancer.

(**A**) Breeding scheme for the generation of *UpII-Cre/Foxa1*$^{loxp/loxp}$*/Pten*$^{loxp/loxp}$ and the other experimental mice. (**B**) PCR analysis confirms genotype in experimental mice. (**C-K**) H&E sections show bladder tissue morphology of 12 months old control and experimental mice. All experimental genotypes are shown: (**C**) genetic controls and (**D**) *UpII-Cre/Foxa1*^{loxp} mice exhibited normal urothelium while (**E**) *UpII-Cre/Pten*^{loxp}, (**F**) *UpII-Cre/Foxa1*$^{loxp/loxp}$, (**G**) *UpII-Cre/Pten*$^{loxp/loxp}$ and (**H**) *UpII-Cre/Foxa1*^{loxp}*/Foxa1*^{loxp} exhibited urothelial hyperplasia at one year of age. Additionally, we detected bladder cancer in the form of focal carcinoma *in situ* (CIS) in (**I**) *UpII-Cre/Foxa1*$^{loxp/loxp}$*/Pten*^{loxp} (2 out of 14 mice); (**J**) *UpII-Cre/Foxa1*^{loxp}*/Pten*$^{loxp/loxp}$ (9 out of 15 mice) and (**K**) *UpII-Cre/Foxa1*$^{loxp/loxp}$*/Pten*$^{loxp/loxp}$ (7 out of 12 mice). Note presence of squamous differentiation in K. (**L-M**) Low power images of H&E sections highlighting squamous differentiation in *UpII-Cre/Foxa1*$^{loxp/loxp}$*/Pten*$^{loxp/loxp}$ mice. (**N**) Raw numbers and (**O**) percentages of mice per genotype that develop bladder cancer. Knockout of *Foxa1* and *Pten* cooperates to significantly enhance tumorigenesis (*p*-value = 5.68e-5; two-sided Fisher's exact test). Image scale bar: 20 μm (high power magnification) and 200 μm (low power magnification scale).

Immunohistochemistry confirms the presence of tumor heterogeneity in the form of squamous differentiation following *Foxa1* and *Pten* knockout in luminal and intermediate cells

While morphologic analysis shows normal urothelium in genetic control mice (Figure 2-6 A), and hyperplasia in *UpII-Cre/Foxa1*$^{loxp/loxp}$ (Figure 2-6 B) and *UpII-Cre/Pten*$^{loxp/loxp}$ (Figure 2-6 C), we consistently detected bladder cancer in the form of focal CIS in *Foxa1* and *Pten* double knockout mice (Figure 2-6 D). While Ki67 staining was undetectable in the urothelium of genetic control mice (Figure 2-6 E), but present in a subset of urothelial cells from *UpII-Cre/Foxa1*$^{loxp/loxp}$ (Figure 2-6 F) and *UpII-Cre/Pten*$^{loxp/loxp}$ (Figure 2-6 G), it was markedly increased in the urothelium isolated from *Foxa1* and *Pten* double knockout mice (Figure 2-6 H). *FOXA1* is overexpressed in luminal bladder cancers, but is recognized to be significantly decreased in areas of squamous differentiation in human bladder cancer[204]. In our study, while Foxa1 was detected in urothelium dissected from genetic control mice (Figure 2-6 I), its expression was noticeably absent in superficial/umbrella cells (targeted by *UpII-Cre*) in bladders dissected from *UpII-Cre/Foxa1*$^{loxp/loxp}$ mice (Figure 2-6 J). While Foxa1 expression was detectable in hyperplastic urothelium collected from *UpII-Cre/Pten*$^{loxp/loxp}$ mice (Figure 2-6 K), on the other hand, it was undetectable in areas of

bladder cancer in *UpII-Cre/Foxa1*$^{loxp/loxp}$/*Pten*$^{loxp/loxp}$ mice (Figure 2-6 L). Squamous differentiation is associated with increased expression of high molecular weight cytokeratins[3, 4, 7]. While a single layer of Krt5 positive cells was detected in basal urothelium of control (Figure 2-6 M), *UpII-Cre/Foxa1*$^{loxp/loxp}$ (Figure 2-6 N) and *UpII-Cre/Pten*$^{loxp/loxp}$ mice (Figure 2-6 O), there was a significant expansion in the number of Krt5 positive cells in *UpII-Cre/Foxa1*$^{loxp/loxp}$/*Pten*$^{loxp/loxp}$ mice (Figure 2-6 P), with similar results for Krt14 (Figures 2-6 Q-T). These findings confirm the presence of squamous differentiation in malignant tumors following targeted deletion of *Foxa1* and *Pten* in superficial/luminal and intermediate urothelial cells.

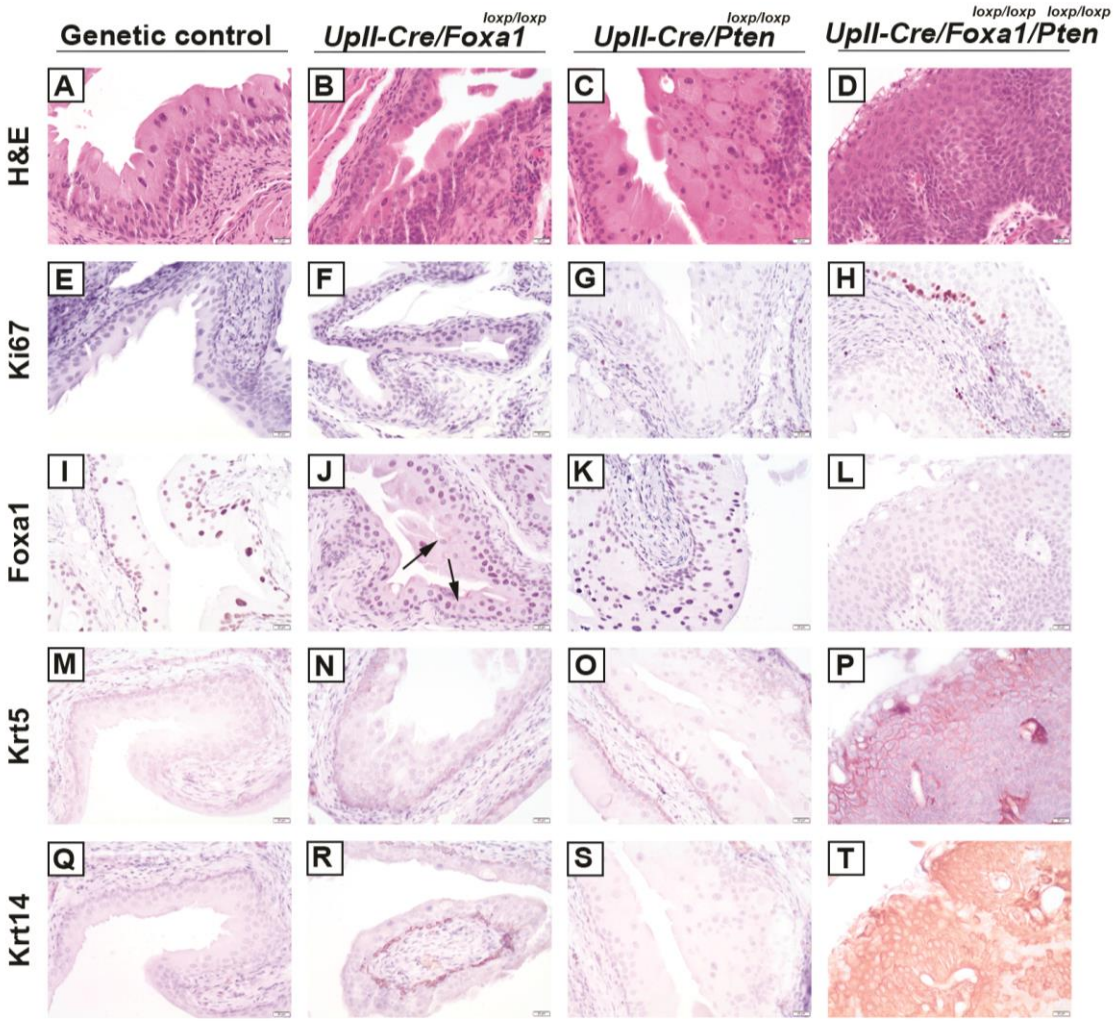

Figure 2-6. Immunohistochemical analysis confirms squamous differentiation following combined *Foxa1* and *Pten* knockout.

(**A**-**D**) H&E sections show bladder tissue morphology for (**A**) genetic controls, (**B**) *UpII-Cre/Foxa1*$^{loxp/loxp}$, (**C**) *UpII-Cre/Pten*$^{loxp/loxp}$ and (**D**) *UpII-Cre/Foxa1*$^{loxp/loxp}$*/Pten*$^{loxp/loxp}$ mice. Note presence of intercellular bridging and hyper-keratinization in (D). (**E**-**H**) Immunohistochemistry (IHC) of the proliferative marker Ki67 shows no Ki67 positive urothelium in (**E**) genetic controls and minimal positivity in (**F**) *UpII-Cre/Foxa1*$^{loxp/loxp}$ and (**G**) *UpII-Cre/Pten*$^{loxp/loxp}$ mice. Increased Ki67 levels were detected in tissue isolated from (**H**) *UpII-Cre/Foxa1*$^{loxp/loxp}$*/Pten*$^{loxp/loxp}$ mice. (**I**-**L**) IHC for Foxa1. The expression of Foxa1 is higher in (**I**) genetic control mice, absent in a subset of luminal cells (indicated by the arrows) in (**J**) *UpII-Cre/Foxa1*$^{loxp/loxp}$ mice. While we detected robust Foxa1 expression in (**K**) *UpII-Cre/Pten*$^{loxp/loxp}$ mice, we failed to detect Foxa1 in (**L**) double knockout *UpII-Cre/Foxa1*$^{loxp/loxp}$*//Pten*$^{loxp/loxp}$ mice consistent with squamous differentiation. (**M**-**T**) IHC of the markers of basal and squamous differentiation, Krt5 and Krt14. We detected a single layer of basal urothelium positive for Krt5 in (**M**) genetic controls as well as in (**N**) *UpII-Cre/Foxa1*$^{loxp/loxp}$ and (**O**) *UpII-Cre/Pten*$^{loxp/loxp}$ mice; however, we noted a significant expansion of Krt5 staining in (**P**) *UpII-Cre/Foxa1*$^{loxp/loxp}$*/Pten*$^{loxp/loxp}$ double knockout mice. An identical pattern was noted regarding Krt14 positivity in (**Q**) genetic controls, (**R**) *UpII-Cre/Foxa1*$^{loxp/loxp}$, (**S**) *UpII-Cre/Pten*$^{loxp/loxp}$ and (**T**) *UpII-Cre/Foxa1*$^{loxp/loxp}$*//Pten*$^{loxp/loxp}$ mice. Image scale bar: 20 μm.

Knockout of *Foxa1* and *Pten* increases the susceptibility of male and female mice to a bladder-specific carcinogen

Exposure of mice to BBN results in the development of bladder cancer in a sex-dependent manner[258-261], and Forkhead family members including *Foxa1* have been previously implicated in the sexual dimorphic response to carcinogens in other organ systems[47]. In an effort to test the impact of *Foxa1* and *Pten* knockout on tumorigenesis as well as sex-dependent differences in the incidence of BBN-induced bladder cancer development, adult (8 weeks old) male and female control and experimental mice were exposed to BBN. According to the literature, 12 weeks of BBN treatment of male mice results in the development of urothelial hyperplasia (Figure 2-7 A), while 16 and 20 weeks of treatment result in the development of CIS and muscle invasive disease, respectively[262]. Whereas, female mice develop extensive edema within the lamina propria after 12 weeks of BBN treatment, and hyperplasia/dysplasia after 16 weeks of BBN exposure (Figure 2-7 B) with a much lower frequency of tumor development within even extended periods of BBN exposure[263]. Consistent with previous reports[229], in our study, 12 weeks of BBN treatment resulted in urothelial

hyperplasia in male genetic control mice (Figure 2-7 C) while experimental male mice exhibited a spectrum of tumor phenotypes. A minority of *UpII-Cre/Foxa1*^{loxp} and *UpII-Cre/Foxa1*$^{loxp/loxp}$ mice developed tumors with invasion into the lamina propria (Figures 2-7 D and F), whereas *UpII-Cre/Pten*^{loxp} and *UpII-Cre/Pten*$^{loxp/loxp}$ (Figures 2-7 E and G) mice developed CIS. Most interestingly, male *UpII-Cre/Foxa1*^{loxp}*/Pten*^{loxp} (Figure 2-7 H), *UpII-Cre/Foxa1*$^{loxp/loxp}$*/Pten*^{loxp} (Figure 2-7 I), *UpII-Cre/Foxa1*^{loxp}*/Pten*$^{loxp/loxp}$ (Figure 2-7 J) and *UpII-Cre/Foxa1*$^{loxp/loxp}$*/Pten*$^{loxp/loxp}$ (Figure 2-7 K) mice developed muscle invasive bladder cancer after only 12 weeks of BBN exposure. These results indicate that knockout of *Foxa1* and *Pten* enhances sensitivity to this chemical carcinogen resulting in high rates of cancer development in male mice (Figure 2-7 L). While female control mice were resistant to BBN (Figure 2-7 M), we detected CIS in a number of *UpII-Cre/Foxa1*^{loxp}, *UpII-Cre/Pten*^{loxp}, *UpII-Cre/Foxa1*$^{loxp/loxp}$ and *UpII-Cre/Pten*$^{loxp/loxp}$ (Figures 2-7 N-Q) mice. Similar to male mice, we detected muscle invasive bladder cancer in female *UpII-Cre/Foxa1*^{loxp}*/Pten*^{loxp} (Figure 2-7 R), *UpII-Cre/Foxa1*$^{loxp/loxp}$*/Pten*^{loxp} (Figure 2-7 S), *UpII-Cre/Foxa1*^{loxp}*/Pten*$^{loxp/loxp}$ (Figure 2-7 T) and *UpII-Cre/Foxa1*$^{loxp/loxp}$*/Pten*$^{loxp/loxp}$ (Figure 2-7 U) mice after just 12 weeks of BBN exposure. Although female mice are relatively resistant to BBN-induced carcinogenesis, the incidence of tumorigenesis in experimental female mice was high (Figure 2-7 V), similar to that of male mice. Notably, tumors in both male and female mice exhibited reduced expression of Foxa1 as well as increased expression of Krt5 and Krt14 (Supplemental Figure 2-4). These results indicate that individual and combined *Foxa1* and *Pten* knockout results in enhanced susceptibility to chemical carcinogenesis in a manner that overcomes sexual dimorphism associated with this model and bladder cancer in humans.

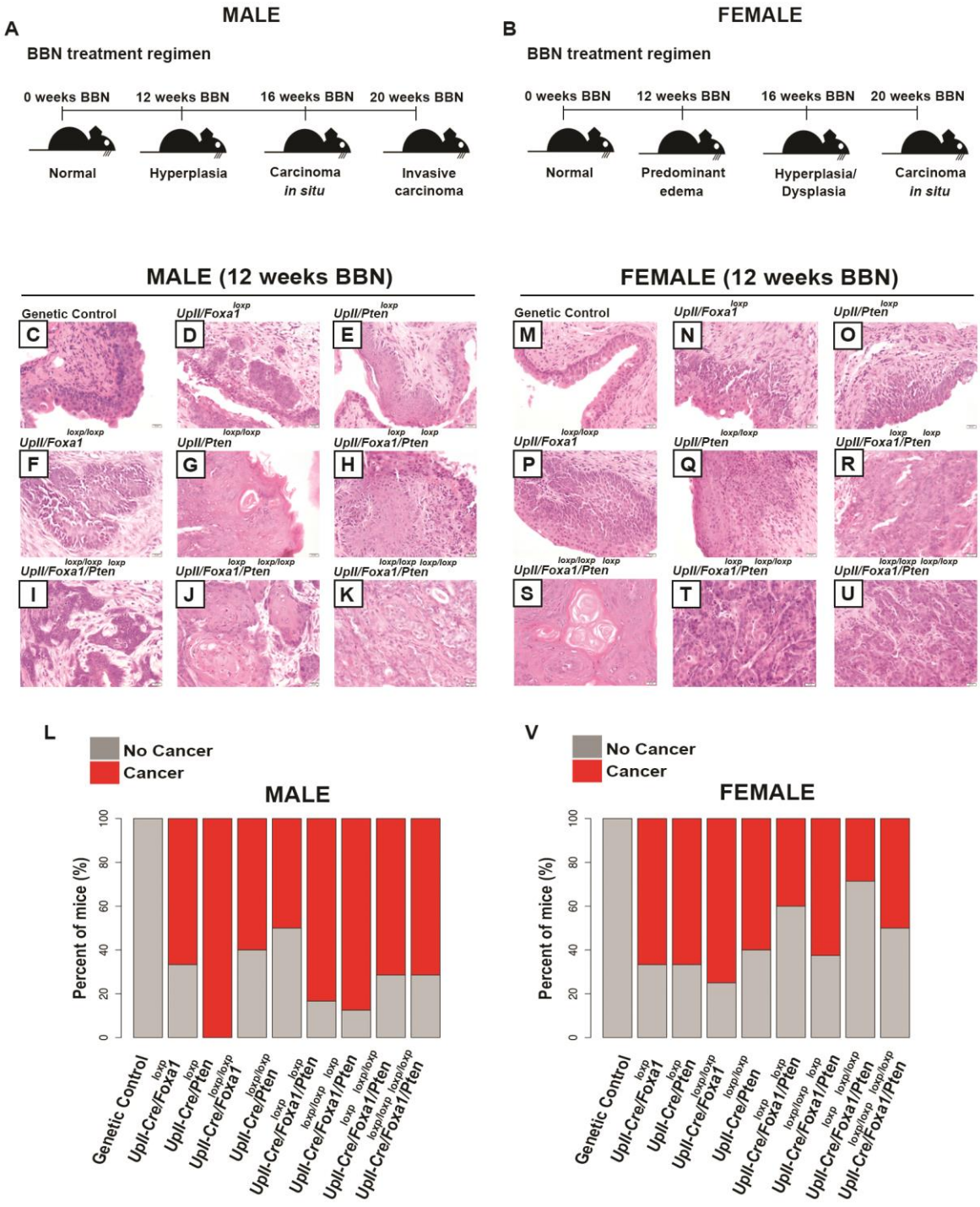
A
MALE
BBN treatment regimen
0 weeks BBN
12 weeks BBN
16 weeks BBN
20 weeks BBN
Normal
Hyperplasia
Carcinoma in situ
Invasive carcinoma
B
FEMALE
BBN treatment regimen
0 weeks BBN
12 weeks BBN
16 weeks BBN
20 weeks BBN
Normal
Predominant edema
Hyperplasia/ Dysplasia
Carcinoma in situ
MALE (12 weeks BBN)
FEMALE (12 weeks BBN)
Genetic Control
UpII/Foxa1loxp
UpII/Ptenloxp
UpII/Foxa1loxp/loxp
UpII/Ptenloxp/loxp
UpII/Foxa1loxp loxp
UpII/Foxa1/Ptenloxp loxp
UpII/Foxa1/Ptenloxp/loxp loxp
UpII/Foxa1/Ptenloxp/loxp loxp/loxp
C
D
E
F
G
H
I
J
K
M
N
O
P
Q
R
S
T
U
L
V
No Cancer
Cancer
MALE
FEMALE
Percent of mice (%)
0
20
40
60
80
100
Genetic Control
UpII-Cre/Foxa1loxp loxp
UpII-Cre/Ptenloxp loxp
UpII-Cre/Foxa1loxp/loxp
UpII-Cre/Ptenloxp/loxp
UpII-Cre/Foxa1/Ptenloxp loxp
UpII-Cre/Foxa1/Ptenloxp/loxp loxp
UpII-Cre/Foxa1/Ptenloxp loxp/loxp
UpII-Cre/Foxa1/Ptenloxp/loxp loxp/loxp

Figure 2-7. The combination of *UpII-Cre*-mediated knockout of *Foxa1* and *Pten* with BBN treatment results in rapid development of muscle invasive bladder cancer and overcomes carcinogen-associated sexual dimorphism.

(**A-B**) Cartoons provide an overview of the sex-dependent phenotypes associated with BBN exposure in wild-type (**A**) male and (**B**) female mice as well as BBN experimental regimen of our control and experimental animal groups. (**C-K**) H&E sections show morphology of control and experimental male mice following 12 weeks of BBN treatment. All experimental genotypes are shown. We detected urothelial hyperplasia in (**C**) genetic controls, (**D**) lamina propria invasion in *UpII-Cre/Foxa1*^{loxp}, (**E**) CIS in U*pII-Cre/Pten*^{loxp}, (**F**) lamina propria invasion in *UpII-Cre/Foxa1*$^{loxp/loxp}$, and (**G**) CIS in *UpII-Cre/Pten*$^{loxp/loxp}$ mice after 12 weeks of BBN treatment. However, we detected muscle invasive bladder cancer with extensive squamous differentiation in (**H**) *UpII-Cre/Foxa1*^{loxp}*/Pten*^{loxp}, (**I**) *UpII-Cre/Foxa1*$^{loxp/loxp}$*/Pten*^{loxp}, (**J**) *UpII-Cre/Foxa1*^{loxp}*/Pten*$^{loxp/loxp}$ and (**K**) *UpII-Cre/Foxa1*$^{loxp/loxp}$*/Pten*$^{loxp/loxp}$ mice. (**L**) Percentage of male mice per genotype that developed bladder cancer is reported. (**M-U**) H&E sections show morphology of control and experimental female mice following 12 weeks of BBN treatment. All experimental genotypes are shown. We detected urothelial hyperplasia in (**M**) genetic controls, (**N**) predominant CIS in *UpII-Cre/Foxa1*^{loxp}, (**O**) U*pII-Cre/Pten*^{loxp}, (**P**) *UpII-Cre/Foxa1*$^{loxp/loxp}$ and (**Q**) *UpII-Cre/Pten*$^{loxp/loxp}$ mice after 12 weeks of BBN treatment. However, we detected muscle invasive bladder cancer with extensive squamous differentiation in (**R**) *UpII-Cre/Foxa1*^{loxp}*/Pten*^{loxp}, (**S**) *UpII-Cre/Foxa1*$^{loxp/loxp}$*/Pten*^{loxp}, (**T**) *UpII-Cre/Foxa1*^{loxp}*/Pten*$^{loxp/loxp}$ and (**U**) *UpII-Cre/Foxa1*$^{loxp/loxp}$*/Pten*$^{loxp/loxp}$ mice. (**V**) Percentage of female mice per genotype that developed bladder cancer is reported. Image scale bar: 20 μm.

Overexpression of human *FOXA1* and *PTEN* genes induces apoptosis in bladder cancer cell lines

To investigate the functional impact of re-establishing *FOXA1* and *PTEN* in bladder cancer, we transiently transfected the UMUC3 cell line with plasmids encoding *FOXA1* or *PTEN* with appropriate empty vector controls (EV*ZsG* and EV*mCh*). UMUC3 cells were chosen because they do not express *FOXA1*[213], and are null for *PTEN*[146]. Confirming transfection efficiency, protein expression of FOXA1 and PTEN was detected by Western blot in transfected cells but not in EV*ZsG* and EV*mCh* transfected control cells at 24 hours post-transfection (Figure 2-8 A). After 24 hours of transfection, relative to control, overexpression of *FOXA1* alone and when combined with *PTEN* resulted in significantly decreased levels of UMUC3 cell viability measured by MTT assay ($p \leq 0.0001$, Dunnett's test; Figure 2-8 B). As these results suggested a decrease in cell proliferation and possibly increase in cell death following overexpression of *FOXA1*, further experiments were

carried out to examine the effects of these genes on the induction of apoptosis. Western blot analysis of the apoptotic marker caspase 3 revealed significantly increased levels of cleaved caspase 3 in *FOXA1* UMUC3 transfected cells ($p \leq 0.01$, Dunnett's test; Figures 2-8 C-E). The increased levels of this apoptotic protein suggested activation/induction of apoptosis in cells overexpressing *FOXA1* alone and combined with *PTEN*. Therefore, to confirm ongoing apoptosis, FACS analysis was performed to measure changes in cell plasma membrane asymmetry and permeability following *FOXA1* and *PTEN* overexpression. One early change during apoptosis involves flipping of phosphatidylserine (PS) from the inner leaflet of the plasma membrane to the outer membrane, which serves as a signal to enhance phagocytosis. Late apoptotic changes include proteolysis of death substrate and increased DNA fragmentation. Therefore, the UMUC3 transfected cells were analyzed by FACS (Figure 2-8 F) following staining with Annexin V and 7-AAD, which have an affinity for PS and fragmented DNA, respectively. The FACS analysis indicated that overexpression of *FOXA1* alone or combined with *PTEN* results in significantly increased late apoptosis ($p \leq 0.05$, Dunnett's test; Figure 2-8 G). These data suggest that *FOXA1* overexpression induces apoptosis in UMUC3 while *PTEN* expression seems to have no detectable influence on UMUC3 apoptosis. To confirm the findings in UMUC3, we further carried out the transient transfection experiments in a different bladder cancer cell line, the 5637 cells, which do not express *FOXA1* but express relatively low levels of *PTEN*[213]. Similarly to UMUC3, overexpression of *FOXA1* alone and when combined with *PTEN* (Supplemental Figure 2-5 A) resulted in significantly decreased cell viability ($p \leq 0.01$, Dunnett's test; Supplemental Figure 2-5 B) and increased levels of cleaved caspase 3, although not statistically significant (Supplemental Figures 2-5 C-E). However, FACS analysis of *FOXA1* and *PTEN* transfected 5637 cells did not confirm an induction of apoptosis in this bladder cancer cell line (Supplemental Figures 2-5 F and G). Thus, although the results in UMUC3 cells suggest that *FOXA1* and not *PTEN* reduces cell growth and promote

apoptosis, further investigations are required to implicate a role for *FOXA1* in apoptosis especially in light of the results from the 5637 cells.

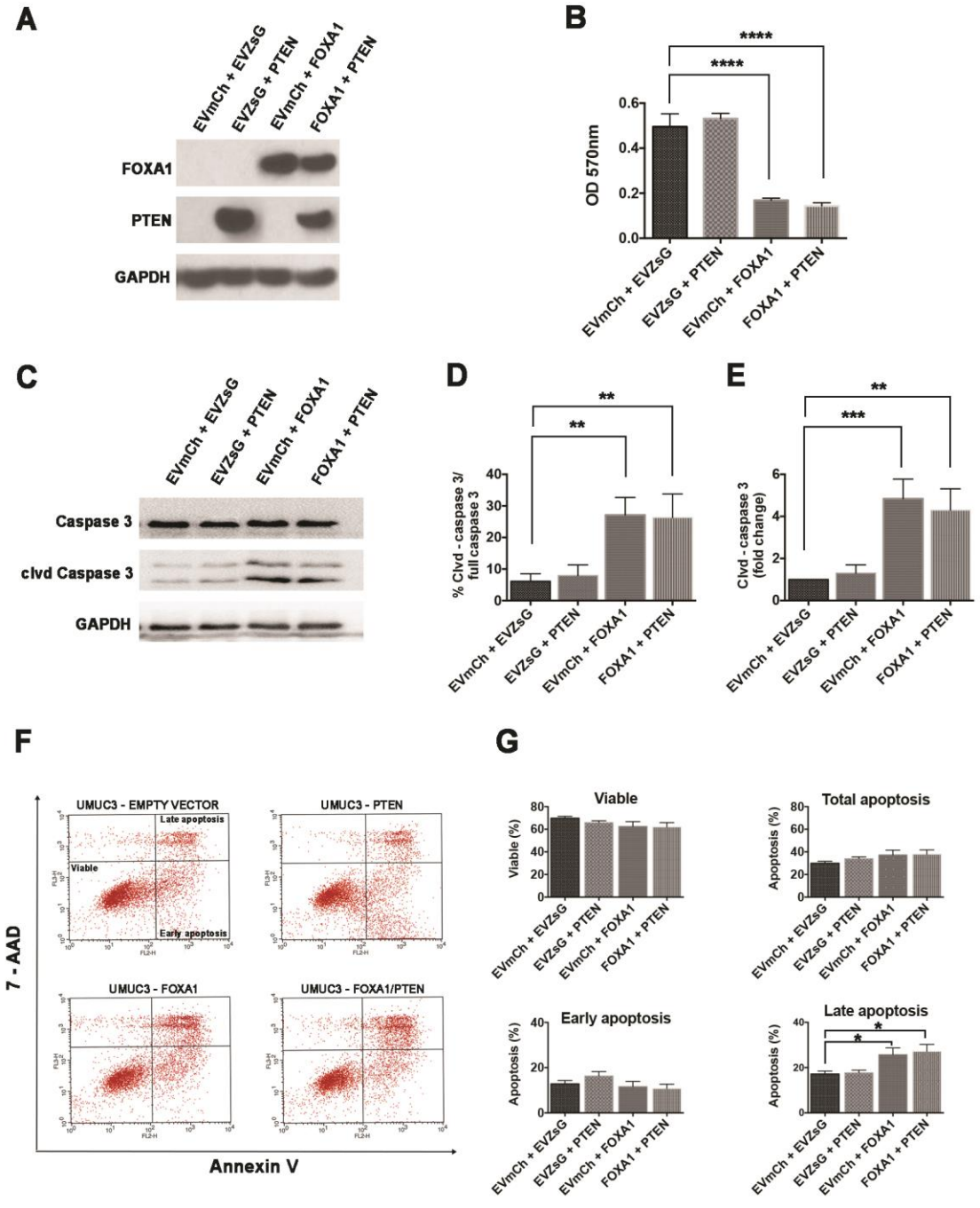

Figure 2-8. Overexpression of human *FOXA1* and *PTEN* in the UMUC3 cell line reduces cell viability and induces apoptosis.

(**A**) Western blot of FOXA1 and PTEN expression in four different conditions: empty vector (EV*mCh* and EV*ZsG*); overexpression of *PTEN* (EV*ZsG* and *PTEN*); overexpression of *FOXA1* (EV*mCh* and *FOXA1*) and overexpression of both genes (*FOXA1* and *PTEN*). GAPDH for loading control in all conditions is shown. (**B**) Reduction of cell viability in *FOXA1* overexpression alone and combined with *PTEN* measured by MTT assay. Optical densitometry (OD) measured at 570 nm. (**C**) Western blot showing cleaved (clvd) apoptotic marker, caspase 3, and GAPDH loading control. (**D**) Percentage of clvd-caspase 3 over full length caspase 3. (**E**) Fold change of clvd-caspase 3 over GAPDH. (**F**) Apoptosis analysis by FACS after staining for the apoptotic marker, Annexin V, and the necrotic marker, 7-AAD. (**G**) Percentage of viable cell and apoptotic cells per condition is shown. All experiments were performed and repeated three times. FACS experiments were performed in triplicate and repeated three times (**** = $p \leq 0.0001$; *** = $p \leq 0.001$; ** = $p \leq 0.01$ and * = $p \leq 0.05$ Dunnett's test).

Discussion

In the current study, we identify *PTEN* expression to be commonly inactivated in both luminal and basal tumors and to be strongly associated with copy number status in human bladder cancer. In regards to *FOXA1*, we confirm the association of *FOXA1* expression to molecular subtype and tissue morphology, and we provide the first evidence that epigenetic silencing is a significant contributor to decreased *FOXA1* expression in human bladder cancer. In addition, we show evidence that dual inactivation of *FOXA1* and *PTEN* (through an apparent variety of mechanisms) is relatively common in bladder cancer, and has pathophysiologic implications. Supporting this evidence, we show that combined, bladder-specific inactivation of *Foxa1* and *Pten* in luminal and intermediate urothelium results in the development of bladder cancer with a squamous phenotype. Overall, our studies support cooperativity between these molecular pathways in bladder tumorigenesis, disease progression and tumor heterogeneity.

Based on a recent report[189], we originally hypothesized that *PTEN* expression would be reduced specifically in patients with basal bladder cancer as well as in areas of squamous differentiation. However, our analysis shows that while *PTEN* is indeed frequently reduced/absent in bladder cancer, this occurs in a manner that is independent of molecular subtype (Figure 2-1).

Loss of heterozygosity of *PTEN* is a frequent event in bladder cancer[126, 152], and previous reports indicate the importance of copy number status in regards to the expression of this tumor suppressor[153, 264]. Based on our analysis, *PTEN* appears to be the prototypical example regarding the impact of copy number status on expression. For example, the correlation between copy number and expression is robust for *PTEN*, and a similar relationship is observed amongst adjacent genes on chromosome 10 (Figure 2-2). Therefore, *PTEN* expression exhibits a strong positive correlation with copy number in bladder cancer. Surprisingly, the relationship between *FOXA1* copy number and expression is much less striking. In a manner apparently independent of *FOXA1* copy number status, patients within the TCGA study displayed a broad range of *FOXA1* expression values. When viewed within the context of our DNA promoter methylation data (discussed below) as well as data indicating *FOXA1* mutant tumors express higher levels of *FOXA1* (Supplemental Figure 2-2), the data suggest that different mechanisms may coexist to maintain *FOXA1* expression in the face of genetic/epigenetic alterations as *FOXA1* is a critical urothelial differentiation factor.

Based on the relatively limited association between *FOXA1* copy number and *FOXA1* mutations with gene expression, we examined the methylation status of this transcriptional regulator within the TCGA cohort (Figure 2-3). In doing so, we provide the first evidence identifying an association between DNA methylation of CpG island 99 and decreased *FOXA1* expression in bladder cancer. We show a subset of patients exhibiting a basal-squamous transcriptional signature has specific hypermethylation of CpG island 99, which is within the gene promoter of *FOXA1*. Importantly, we also show *FOXA1* methylation at CpG island 99 in human basal-squamous bladder cancer cell lines (Figure 2-4). In addition to identifying models for the study of *FOXA1* methylation, analysis of cell line serves as an important control; this is true because inflammatory cells or stromal tissue can confound our human studies by contributing to the "methylation signature". However, there still exists a significant number of patients with a basal, *FOXA1* low expression pattern that does not exhibit *FOXA1* methylation (Figure 2-3). In these

patients, a combination of copy number loss (Figure 2-2), microRNA regulation[265] and additional post-transcriptional, and epigenetic events almost certainly play a role. Nonetheless, we identify DNA promoter methylation as a mechanism contributing to decreased *FOXA1* expression in human bladder cancer. These findings are in agreement with previous reports identifying *FOXA1* methylation in breast cancer[266-268], highlighting yet another parallel between these malignancies. A future goal will be to elucidate the mechanism(s) by which *FOXA1* becomes epigenetically silenced in this common disease, and if reversing this process has clinical utility.

Similar to other malignancies, significant clinical data support both "cell-of-origin" and "mutation-of-origin" concepts in bladder cancer. For example, supporting the "cell-of-origin" concept, several studies show that molecular subtypes appear to retain potentially vestigial expression patterns associated with normal urothelium[155, 172, 176]. On the other hand, recent clinical studies focused on characterizing spatially (and sometimes morphologically) distinct areas support a role for the "mutation-of-origin" concept[244, 245]. This is true because it is unlikely that multiple regions within the same tumor that exhibit highly similar mutational differences, yet different transcriptional programs, would arise from different progenitor clones. Put differently, it appears that areas with differing tumor morphology and transcriptional programs can share a common genetic origin. As there also exist experimental data to support both "cell-of-origin" and "mutation-of-origin" theories[112, 269], it is more than likely that these concepts are not mutually exclusive. Nonetheless, our experimental data show that inactivation of *Foxa1* and *Pten* specifically within luminal and intermediate urothelium through the action of the *UpII-Cre* results in the development of bladder cancer with elements of squamous differentiation. These results support the idea that tumors that exhibit squamous differentiation can arise following genetic events in superficial/luminal and intermediate urothelium. Interestingly, *PTEN* expression is reduced in both luminal and basal bladder cancers (Figure 2-1), and *UpII-Cre*-mediated deletion of *Pten* results in extensive urothelial hyperplasia (Figure 2-5). *FOXA1* is expressed throughout the urothelium of

humans and in mice, and the fact that *Foxa1* knockout results in squamous differentiation is in line with previous reports[205], and suggests that *Foxa1* is indeed required to maintain urothelial differentiation in luminal and intermediate urothelial cells.

While CIS can exhibit elements of squamous differentiation in humans[270], this is a relatively rare clinical entity. However, it is possible that concomitant inactivation of *PTEN* or other elements of the PI3K/AKT/mTOR pathway and gatekeepers of urothelial differentiation such as *FOXA1* could play a role in this process. More commonly, CIS in humans exhibits a hyper luminal gene expression pattern[271], which can take on squamous elements following disease progression. In these tumors, it is likely that *PIK3CA* mutations or *PTEN* loss cooperate with *TP53* mutation or other events to drive the development of CIS and further disease progression[192] while inactivation of *FOXA1* or other urothelial differentiation factors such as *PPARG* and *GATA3* promote a basal gene expression pattern with (or without) squamous differentiation. Further studies are required to identify the order in which these events occur and the mechanism by which they determine tumor "fate".

Men are more commonly diagnosed with bladder cancer, and it is well recognized that male mice exhibit enhanced sensitivity to BBN treatment relative to female mice[260]. Interestingly, we also show that individual and combined *Foxa1* and *Pten* knockout resulted in enhanced tumor development in both male and female experimental mice (Figure 2-7). These results are reminiscent of a previous study showing combined deletion of *Foxa1* and *Foxa2* reverses sexual dimorphism in response to a liver-specific carcinogen[47]. In that study, *Foxa1* and *Foxa2* knockout was shown to negatively impact *Esr1* signaling (which is protective) as well as *Ar* signaling, which promotes liver carcinogenesis in this model. *Foxa1* and *Pten* knockout in the current study markedly enhanced tumorigenesis in both male and female mice. While clinical studies suggest females are more likely to exhibit a basal molecular subtype of bladder cancer[155], future studies are required to

determine the mechanistic contributions of *Foxa1* and *Pten* inactivation to enhanced carcinogen susceptibility.

In attempt to corroborate our *in vivo* findings and identify the potential mechanism(s) by which *FOXA1* and *PTEN* cooperate in bladder tumorigenesis, *in vitro* studies based on gain-of-function approaches consisting of the overexpression of *FOXA1* and *PTEN* in two bladder cancer cell lines were performed. Overexpression of *FOXA1* in UMUC3 and 5637 bladder cancer cell lines resulted in reduced cell viability as measured by MTT assay. Western blot analysis for the biochemical marker of apoptosis, cleaved caspase-3, was suggestive of induction of apoptosis in UMUC3 and 5637 following *FOXA1* overexpression. However, while FACS analysis additionally supported apoptotic induction of UMUC3 cells, this was not the case for 5637 cells. Overexpression of *FOXA1* in 5637 cells failed to induce apoptosis in the FACS analysis. A potential explanation for this outcome could be that unlike UMUC3 cells, 5637 cells present molecular events that are preventive of the induction of apoptosis following *FOXA1* overexpression. Thus, while UMUC3 cells appear to be optimal cells for these studies, 5637 cells may not be so. Nonetheless, the finding that *FOXA1* promotes apoptosis in UMUC3 cells is in agreement with other studies implicating *FOXA1* in the apoptotic process[272, 273]. Specifically, a pro-apoptotic role for FOXA1 suppressing the expression of the anti-apoptotic gene *BCL-2* has been described[274]. Cancer cells can acquire the ability to escape stress-induced apoptosis, and this is often reflected in their resistance to chemotherapy[275]. For example, inactivating mutations in *ERCC2*, a DNA helicase that promotes nucleotide excision repair during DNA damage[276], are frequent events in bladder cancer[140] and appear to be a potential mechanism by which tumorous cells hinder the DNA repair process to promote survival and growth despite genetic damage. Interestingly, mutations in *ERCC2* also render these cells sensitive to cisplatin through mechanisms that are yet to be fully understood[277, 278]. Upregulation of *BCL-2* is an additional mechanism utilized by cancer cells to disable the pro-apoptotic circuitry[279]. To that point, treatment with pan-BCL2 inhibitors enhanced apoptosis in

established chemo-resistant bladder cancer sublines, that were derived from chemo-sensitive bladder cancer cell lines 5637 and RT4[280]. Interestingly, in our study, we did not observe changes in BCL-2 expression following overexpression of *FOXA1*, indicating that FOXA1 may be activating apoptosis through a different mechanism. In short, the results presented here suggest a potential tumor-suppressing role for FOXA1; however, additional studies are necessary to support these findings.

The fact that PTEN overexpression failed to induce measurable levels of apoptosis in either UMUC3 or 5637 cells suggests that high levels of PI3K function or other genetic alterations downstream of PTEN may drive constitutive pathway activity. Alternatively, PTEN reportedly undergoes post-translational modifications in the form of phosphorylation, which can serve to inhibit the function of PTEN[281]. Therefore, it could be that upon expression, PTEN function is inhibited by phosphorylation in these cells lines.

In conclusion, our study demonstrates that copy number alterations have important implications for *PTEN* expression in bladder cancer while methylation of *FOXA1* is almost certainly a significant contributor to reduced expression of this driver of urothelial differentiation. Additionally, we show that genetic inactivation of *Foxa1* and *Pten* in luminal/intermediate urothelium results in the development of bladder cancer with elements of squamous differentiation and enhanced sensitivity to carcinogen exposure independent of sex.

Supplemental Information

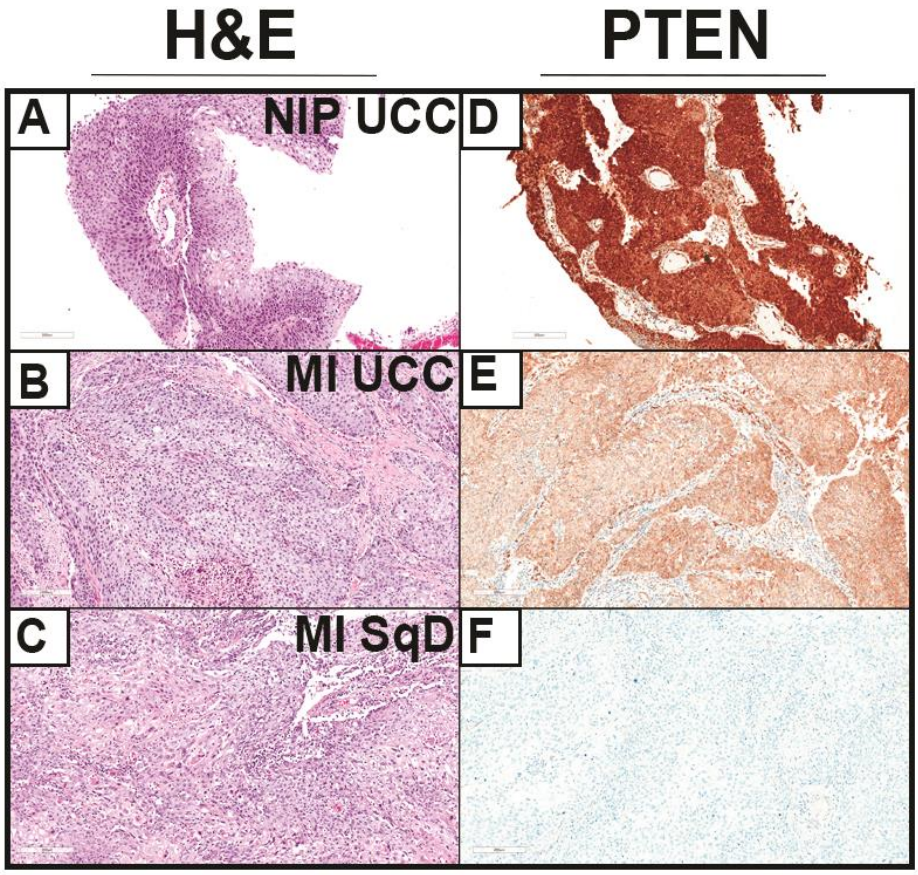

Supplemental Figure 2-1. Morphology and representative PTEN immunohistochemical analysis.

(**A-C**) H&E staining of tissue collected from areas of non-invasive papillary urothelial cell carcinoma (**A**; [NIP UCC]); muscle invasive UCC (**B**; [MI UCC]); and muscle invasive area of squamous differentiation (**C**; [MI SqD]) within the tumor of one individual. (**D-F**) Immunohistochemistry of PTEN in areas depicted in A-C. Image scale bar: 200 µm.

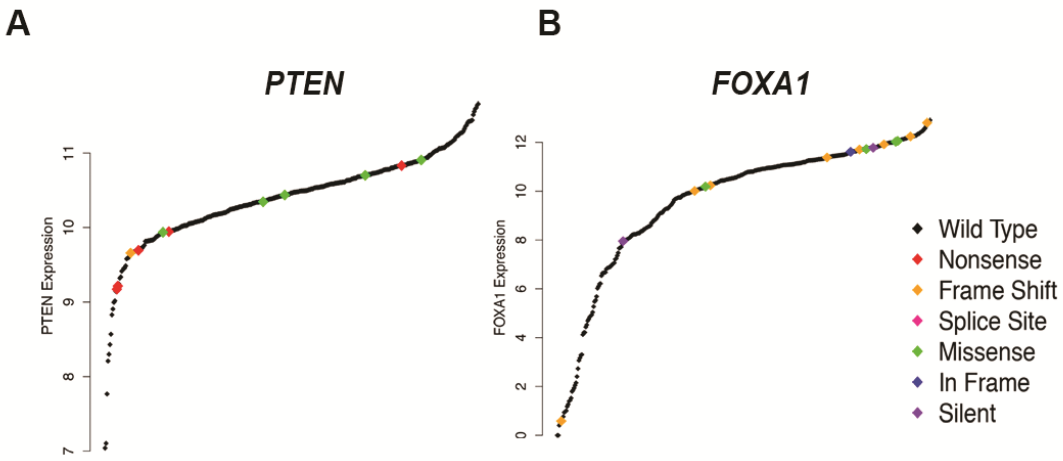

Supplemental Figure 2-2. The relationship between *FOXA1* and *PTEN* mutations and gene expression in muscle invasive bladder cancer.

Waterfall plots show the relationship between DNA mutations and expression of (**A**) *PTEN* and (**B**) *FOXA1* using publicly available data from the TCGA bladder cancer cohort (n = 404). Note that while mutations in *PTEN* are largely spread along the sigmoid curve, there is a cluster of mutations associated with low expression. Alternatively, mutations in the *FOXA1* gene appear to be associated with high gene expression.

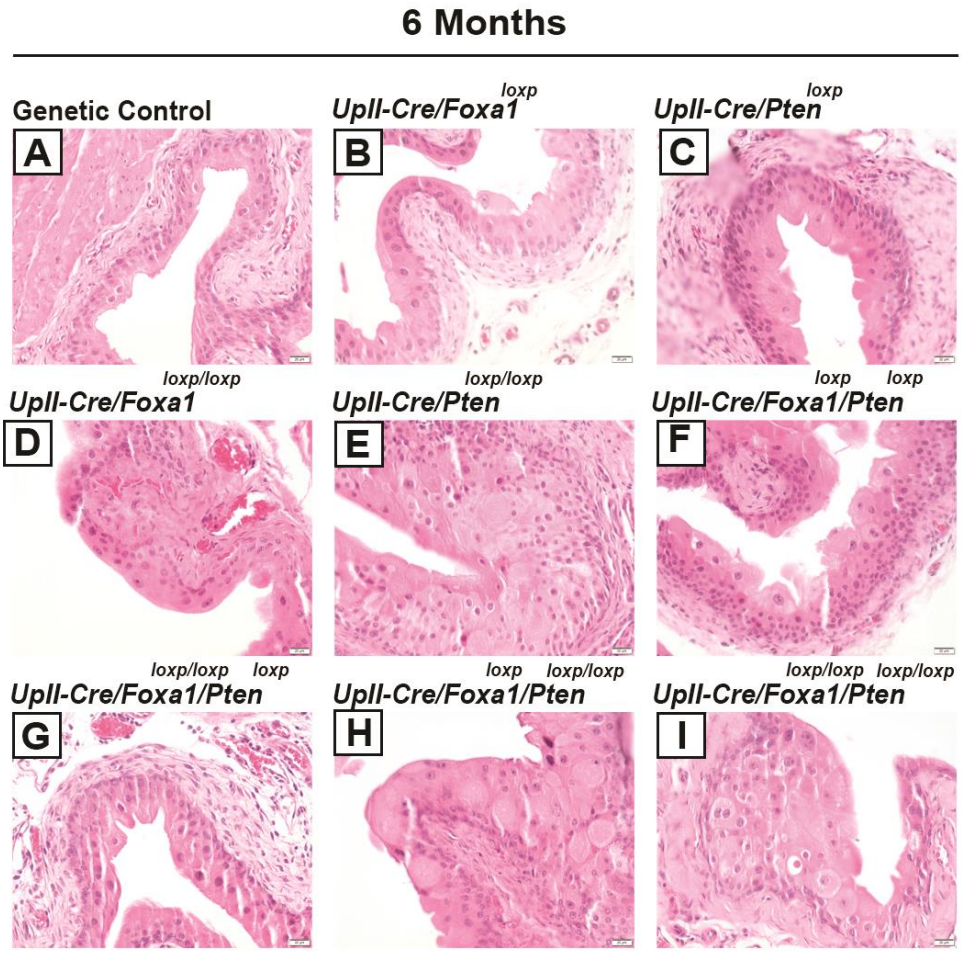

Supplemental Figure 2-3. Combined urothelial-specific deletion of *Foxa1* and *Pten* in mice results in pronounced hyperplasia at 6 months of age.

All experimental genotypes are shown. At 6 months of age, in addition to (**A**) normal urothelium present in genetic controls, (**B**) urothelium was normal in *UpII-Cre/Foxa1*^{loxp}, (**C**) *UpII-Cre/Pten*^{loxp}, (**D**) *UpII-Cre/Foxa1*$^{loxp/loxp}$. However, we detected urothelial hyperplasia in (**E**) *UpII-Cre/Pten*$^{loxp/loxp}$, (**F**) *UpII-Cre/Foxa1*^{loxp}*/Pten*^{loxp}, (**G**) *UpII-Cre/Foxa1*$^{loxp/loxp}$*/Pten*^{loxp}, (**H**) *UpII-Cre/Foxa1*^{loxp}*/Pten*$^{loxp/loxp}$ and (**I**) double knockouts *UpII-Cre/Foxa1*$^{loxp/loxp}$*/Pten*$^{loxp/loxp}$. Image scale bar: 20 µm.

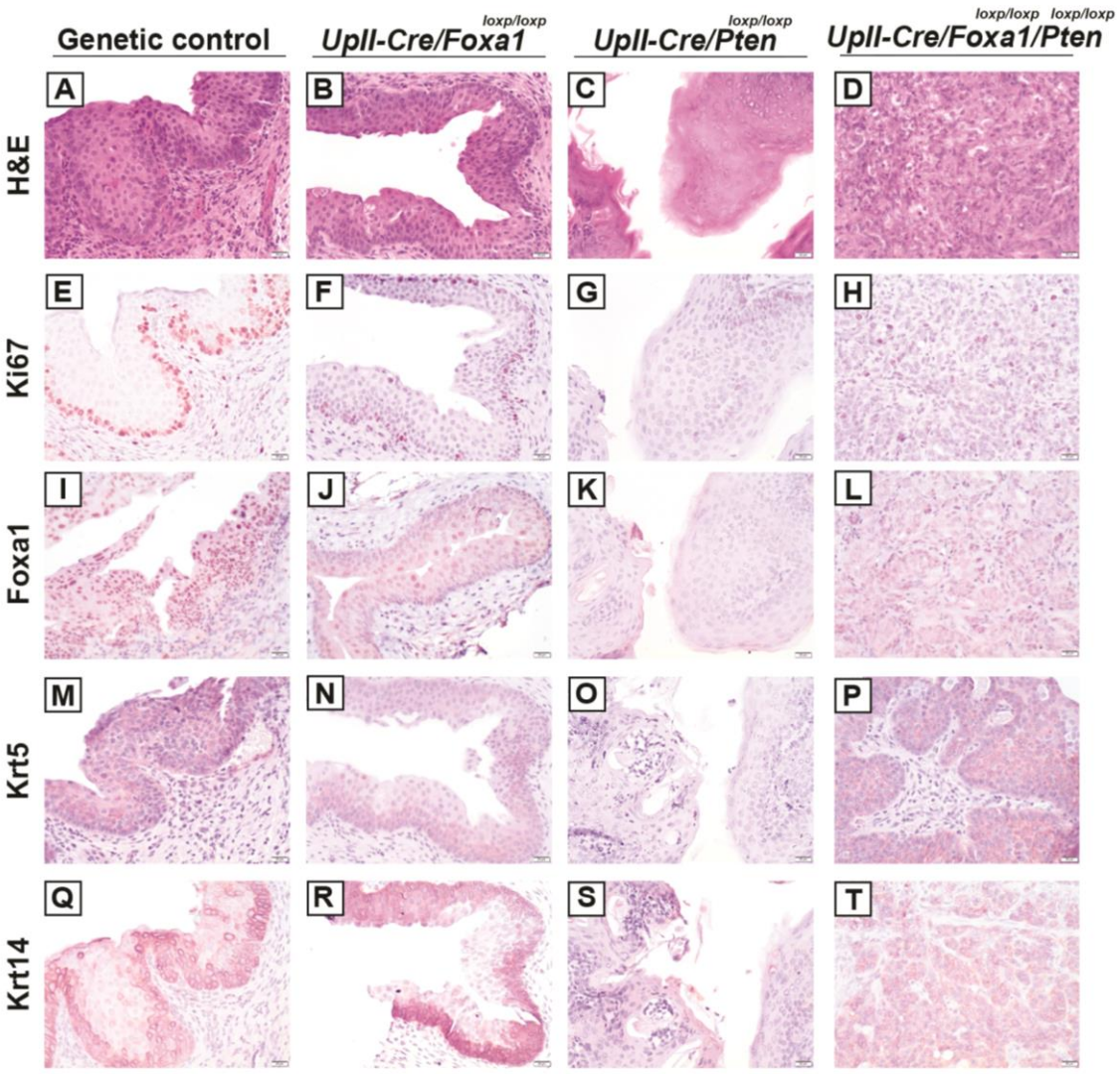

Supplemental Figure 2-4. Immunohistochemistry confirms retention of squamous differentiation following BBN treatment of urothelium-specific knockout of *Foxa1* and *Pten* mice.

Results from the immunohistochemistry (IHC) staining were identical in both male and female mice. (**A-D**) H&E sections show bladder tissue morphology for (**A**) genetic controls, (**B**) *UpII-Cre/Foxa1*$^{loxp/loxp}$, (**C**) *UpII-Cre/Pten*$^{loxp/loxp}$, and (**D**) *UpII-Cre/Foxa1*$^{loxp/loxp}$*/Pten*$^{loxp/loxp}$. (**E-H**) IHC of the proliferative marker Ki67 in (**E**) genetic controls, (**F**) *UpII-Cre/Foxa1*$^{loxp/loxp}$, (**G**) *UpII-Cre/Pten*$^{loxp/loxp}$, and (**H**) double knockout *UpII-Cre/Foxa1*$^{loxp/loxp}$*/Pten*$^{loxp/loxp}$. (**I-L**) IHC of the urothelial luminal marker, Foxa1 in (**I**) genetic controls, (**J**) *UpII-Cre/Foxa1*$^{loxp/loxp}$, (**K**) *UpII-Cre/Pten*$^{loxp/loxp}$, and (**L**) double knockout *UpII-Cre/Foxa1*$^{loxp/loxp}$*/Pten*$^{loxp/loxp}$ mice. (**M-P**) IHC of the urothelial basal-squamous marker, Krt5 in (**M**) genetic controls, (**N**) *UpII-Cre/Foxa1*$^{loxp/loxp}$, (**O**) *UpII-Cre/Pten*$^{loxp/loxp}$, and (**P**) double knockout *UpII-Cre/Foxa1*$^{loxp/loxp}$*/Pten*$^{loxp/loxp}$ mice. (**Q-T**) IHC of the urothelial basal-squamous marker, Krt14 in (**Q**) genetic controls, (**R**) *UpII-Cre/Foxa1*$^{loxp/loxp}$, (**S**) *UpII-Cre/Pten*$^{loxp/loxp}$, and (**T**) double knockout *UpII-Cre/Foxa1*$^{loxp/loxp}$*/Pten*$^{loxp/loxp}$ mice. Image scale bar: 20 µm.

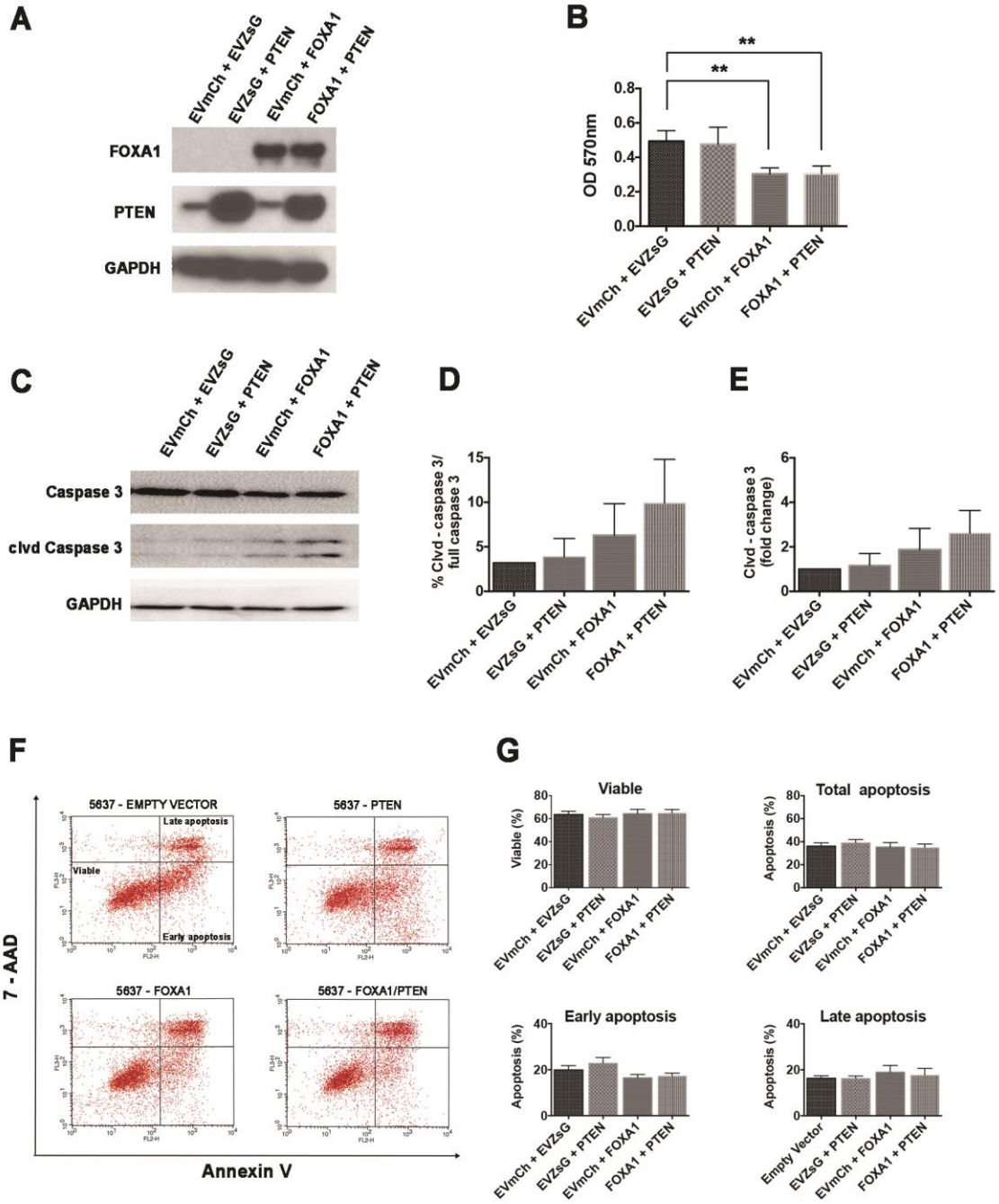
A
EVmCh + EVZsG
EVZsG + PTEN
EVmCh + FOXA1
FOXA1 + PTEN
FOXA1
PTEN
GAPDH
B
**
**
OD 570nm
0.8
0.6
0.4
0.2
0.0
EVmCh + EVZsG
EVZsG + PTEN
EVmCh + FOXA1
FOXA1 + PTEN
C
EVmCh + EVZsG
EVZsG + PTEN
EVmCh + FOXA1
FOXA1 + PTEN
Caspase 3
clvd Caspase 3
GAPDH
D
% Clvd - caspase 3/ full caspase 3
15
10
5
0
EVmCh + EVZsG
EVZsG + PTEN
EVmCh + FOXA1
FOXA1 + PTEN
E
Clvd - caspase 3 (fold change)
6
4
2
0
EVmCh + EVZsG
EVZsG + PTEN
EVmCh + FOXA1
FOXA1 + PTEN
F
5637 - EMPTY VECTOR
Late apoptosis
Viable
Early apoptosis
5637 - PTEN
5637 - FOXA1
5637 - FOXA1/PTEN
7 - AAD
Annexin V
G
Viable
Viable (%)
80
60
40
20
0
EVmCh + EVZsG
EVZsG + PTEN
EVmCh + FOXA1
FOXA1 + PTEN
Total apoptosis
Apoptosis (%)
80
60
40
20
0
EVmCh + EVZsG
EVZsG + PTEN
EVmCh + FOXA1
FOXA1 + PTEN
Early apoptosis
Apoptosis (%)
40
20
0
EVmCh + EVZsG
EVZsG + PTEN
EVmCh + FOXA1
FOXA1 + PTEN
Late apoptosis
Apoptosis (%)
40
20
0
Empty Vector
EVZsG + PTEN
EVmCh + FOXA1
FOXA1 + PTEN

Supplemental Figure 2-5. Overexpression of human *FOXA1* and *PTEN* in the 5637 cell line reduces cell viability but does not induce apoptosis.

(**A**) Western blot of FOXA1 and PTEN expression in four different conditions: empty vector (EV*mCh* and EV*ZsG*); overexpression of *PTEN* (EV*ZsG* and *PTEN*); overexpression of *FOXA1* (EV*mCh* and *FOXA1*) and overexpression of both genes (*FOXA1* and *PTEN*). GAPDH for loading control in all conditions is shown. (**B**) Reduction of cell viability in *FOXA1* overexpression alone and combined with *PTEN* measured by MTT assay. Optical densitometry (OD) measured at 570 nm. (**C**) Western blot showing cleaved (clvd) apoptotic marker, caspase 3, and GAPDH loading control. (**D**) Percentage of clvd-caspase 3 over full length caspase 3. (**E**) Fold change of clvd-caspase 3 over GAPDH. (**F**) Apoptosis analysis by FACS after staining for the apoptotic marker, Annexin V, and the necrotic marker, 7-AAD. (**G**) Percentage of viable cell and apoptotic cells per condition is shown. All experiments were performed and repeated three times. FACS experiments were performed in triplicate and repeated three times (** = $p \leq 0.01$ Dunnett's test).

Supplemental Table 2-1**.** The sequence of primers used for genotyping *Foxa1* and *Pten* knockout mice.

Foxa1 LoxP	
Forward Primer 5'-3'	CTGTGGATTATGTTCCTGATC
Reverse Primer 5'-3'	GTGTCAGGATGCCTATCTGGT
Pten LoxP	
Forward Primer 5'-3'	CAAGCACTCTGCGAACTGAG
Reverse Primer 5'-3'	AAGTTTTTGAAGGCAAGATGC
UpII-Cre	
Cre-AS Primer 5'-3'	TGCATGATCTCCGGTATTGA
Cre-S Primer 5'-3'	CGTACTGACGGTGGGAGAAT

Supplemental Table 2-2. Antibodies used for immunohistochemistry (IHC) and Western blot (WB).

Antibody	Dilutions	Catalog number	Manufacturer	Application
Caspase 3 Rabbit pAb	1:1000	# 9662	Cell Signaling Technology (Danvers, MA)	WB
FOXA1 Rabbit pAb	1:1000	# ab23738	Abcam (Cambridge, MA)	WB
FOXA1-HNF3*α*/*β* (C-20) Goat pAb	1:1000	# sc-6553	Santa Cruz Biotechnology (Santa Cruz, CA)	IIHC
GAPDH (14C10) Rabbit mAb	1:2000	# 3683S	Cell Signaling Technology (Danvers, MA)	WB
Ki67 Rabbit mAb	1:1000	# ab16667	Abcam (Cambridge, MA)	IHC
KRT14 Mouse mAb	1:200	# LL002-L-CE	Novocastra Leica Biosystems (Buffalo Grove, IL)	IHC
KRT5/6 Mouse mAb	1:200	# D5/16 B4 clone	Dako Agilent Pathology Solutions (Santa Clara, CA)	IHC
PTEN (D4.3) XP Rabbit mAb	1:1000	# 9188S	Cell Signaling Technology (Danvers, MA)	WB

Supplemental Table 2-3. The sequence of primers used for PCR.

FOXA1	
Forward Primer 5'-3'	TCTGAATTCACCATGTTAGGAACTGTAAGATGGAAG
Reverse Primer 5'-3'	TCTGGATCCCTAGGAAGTGTTTAGGACGGGTCTGGA
PTEN	
Forward Primer 5'-3'	TCTGAATTCACCATGACAGCATCATCAAAGAGATC
Reverse Primer 5'-3'	TCTGGATCCCTAGACTTTTGTAATTTGTGTATGCTG

Primers were used for incorporation of *BamHI* and *EcoRI* sites on *FOXA1* and *PTEN* inserts and subcloning into pLVX-IRES-*ZsGreen1* and pLVX-IRES-*mCherry* plasmids, respectively.

Supplemental Table 2-4. The sequence of primers used for Sanger sequencing of human *FOXA1* and *PTEN*.

CMV-Forward Primer 5'-3'	CGCAAATGGGCGGTAGGCGTG
IRES-Reverse Primer 5'-3'	CCTCACATTGCCAAAAGACG

Primer were used to assess *FOXA1* and *PTEN* insertion in pLVX-IRES-*ZsGreen1* and pLVX-IRES-*mCherry* plasmids, respectively.

Supplemental Table 2-5. Probes used to assess the methylation status of CpG island 99 and 143 on *FOXA1* promoter and gene body.

CpG Island 99		
Probe ID	***p*-value**	**Bonferroni p-value**
cg10988041	0.00000403	0.0000806
cg07940072	0.00097400	0.01948
cg04932551	0.00000001	0.0000001226
cg00955911	0.00000001	0.0000001234
cg03772350	0.00000240	0.000048
CpG Island 143		
Probe ID	***p*-value**	**Bonferroni p-value**
cg00744656	0.487	1
cg01662117	0.328	1
cg01824511	0.267	1
cg01892516	0.88	1
cg03015370	0.25	1
cg03026462	0.0557	1
cg09276158	0.296	1
cg10323697	0.457	1
cg10724086	0.0794	1
cg11260422	0.081	1
cg16527491	0.215	1
cg16581536	0.127	1
cg19802865	0.281	1
cg23032032	0.0794	1
cg23664186	0.00338	0.0676

Acknowledgements

This chapter is a manuscript co-written by Osei-Amponsa V*****, Buckwalter JM*****, Shuman L, Zheng Z, Yamashita H, Walter V, Ellis J, Liu C, Warrick J, Shantz L, Feehan R, Al-Ahmadie H, Mendelsohn C, Kaestner K, Wu XR and DeGraff D.

*****These authors contributed equally to this study.

Pathology studies including H&E staining and immunohistochemistry were performed by Osei-Amponsa V, Shuman L and Ellis J. Mouse breeding was performed by Zheng Z and Shuman L. Bioinformatic analyses were performed by Walter V. Pathological evaluations were performed by Warrick J, Osei-Amponsa V and DeGraff D. Epigenetic studies were performed by Buckwalter JM**.** Cell culture studies were performed by Osei-Amponsa V.

The work described in this chapter was supported by K99CA172122 (DJD), R00CA172122 (DJD) and startup funding from the Departments of Pathology and Surgery at Pennsylvania State University College of Medicine (DJD).

Chapter 3

Carcinogen-induced bladder cancer in the FVB mouse strain is associated with glandular differentiation and increased Cd274/Pdl-1 expression

Abstract

Creation of genetically engineered mouse models of bladder cancer often involves the use of several background strains in conjunction with the carcinogen N-butyl-N-(4-hydroxybutyl) nitrosamine (BBN). However, carcinogen susceptibility in commonly used strains as well as phenotypic differences, are not well characterized. The objectives of this study were to determine differences in sensitivity and phenotypic outcome following BBN exposure of C57BL/6 and FVB, two strains commonly used for model development.

Male C57BL/6 and FVB mice were exposed to BBN (0.05%) in drinking water for 12 and 16 weeks. Dissected bladders were characterized by histological and immunohistochemical analyses. Gene Ontology analysis was performed to identify differences in gene expression across strains following BBN exposure.

While the C57BL/6 strain developed non-invasive tumors following 12 weeks of BBN exposure, FVB mice developed muscle invasive bladder cancer with squamous and glandular differentiation. Glandular differentiation was exclusively observed in the FVB strain. FVB tumors were highly immunogenic and inflamed by the presence of high expression of Cd274 (Pdl-1), murine histocompatibility complex (H2) and pro-inflammatory cytokines (Il-5 and Il-17).

Following BBN exposure, FVB mice undergo rapid tumorigenesis and disease progression characterized by Pdl-1 expression and development of glandular differentiation. These studies identify a degree of tumor heterogeneity in the FVB tumors previously undescribed and identify

FVB mice as a potentially useful model for the study of bladder adenocarcinoma and the inflammatory tumor microenvironment.

Introduction

Bladder cancer is the second most common genitourinary malignancy in the United States with an estimated 81,190 new diagnoses and 17,340 deaths in 2018[21]. At clinical presentation, approximately 70% of bladder cancer patients are diagnosed with non-muscle invasive bladder cancer (NMIBC) while the remaining 30% of patients present with muscle invasive bladder cancer (MIBC) with or without metastasis[67]. In addition to the need for accurate tumor staging, development of a treatment strategy for bladder cancer is driven by several factors including the histopatological features of the tumor. Approximately 90% of bladder cancer cases are diagnosed primarily as urothelial cell carcinoma (UCC) while an additional 5% are identified as squamous cell carcinoma (SCC). The remainder of diagnoses includes other relatively rare pure histologic variants such as adenocarcinoma, plasmacytoid variant, small cell carcinoma, and other variants[282]. In addition to these pure histologic subtypes, variant histology is often present in a manner that is admixed with UCC. For example, up to 40% of UCC exhibits elements of squamous differentiation (SqD) or other morphologic variant patterns[204]. Recent studies show that morphologic variants of bladder cancer are associated with unique gene expression patterns and phenotypic behavior[246]. As the presence of morphologic variation is associated with differences in response to therapy [283], increased efforts are required to understand the impact of tumor heterogeneity on disease progression and clinical outcomes.

The use of carcinogen-based models of malignant disease has significantly advanced our understanding of the biologic processes underlying disease pathogenesis and tumor progression. Because of the lack of *in vivo* model systems that effectively recapitulate the heterogeneity

(morphology, genomic alterations, metastatic capacity) in human pathologic disease, preclinical models often fail in the identification of therapeutic approaches that exhibit clinical effectiveness in humans[284, 285]. As there are relatively limited *in vivo* models in bladder cancer research[224, 226, 286], the establishment of improved models suitable for therapeutic assessment is essential.

Exposure of rodents to the chemical N-butyl-N-(4-hydroxybutyl) nitrosamine (BBN) is widely used as a preclinical model for the study of bladder cancer[226, 227, 229, 258]. A derivative of the environmental carcinogen N-nitrosodi-n-butylamine, BBN is also a metabolite derived from a N-nitroso compound present in tobacco, which is a major risk factor for bladder cancer development in western countries. Oxidation of BBN in the liver generates *N*-n-butyl-*N*-(3-carboxypropyl) nitrosamine (BCPN) metabolite, which, in addition to BBN, is considered to be the driving factor for bladder tumorigenesis[287-289]. Because of these reasons and the organ-specific mutagenicity of BBN [259], the BBN-induced carcinogenesis model is particularly effective for assessing the impact of environmental carcinogen exposure on bladder cancer development.

Several studies have shown that BBN-induced bladder tumors exhibit species and strain-specific phenotypes[290-293]. For example, while administration of BBN to Wistar rats for 10 weeks results in the development of non-invasive superficial papillary bladder carcinoma, 10 weeks of BBN exposure in the BABL/C mouse strain results in the development of invasive bladder carcinoma[294]. In addition, it has been shown that strain differences within a species correlate with sensitivity to BBN-induced bladder carcinogenesis resulting in different histopathologic phenotypes[228, 262, 295, 296]. These findings are in agreement with extensive documentation regarding differential strain susceptibility in other preclinical animal systems[297, 298].

While all preclinical models have limitations, BBN treatment results in reproducible neoplastic changes in the murine urothelium. For this reason, BBN is additionally used in conjunction with genetically engineered (transgenic and knockout) mouse models to test hypotheses regarding the interplay between environmental carcinogens and underlying genetic

alterations. Nonetheless, the generation of genetically engineered mouse models often involves breeding schemes that incorporate different strains; therefore, it is crucial to understand the extent to which common mouse strains used in the creation of genetically engineered mouse models are susceptible to BBN-induced bladder cancer. Therefore, as a foundational study, we performed experiments to determine the degree to which, if any, two of the most commonly used mouse strains, C57BL/6 and FVB, exhibit differential susceptibility to BBN carcinogen.

Materials and Methods

Animals

All animal studies were approved by Institutional Animal Care and Use Committee of Pennsylvania State University College of Medicine (PSCOM). Adult male C57BL/6 and FVB mice were purchased from The Jackson Laboratory (Bar Harbor, ME) and were housed within the PSCOM animal facility with 12 hours regulated day/night cycle at 68-73°F room temperature. Mice were fed with rodent diet (2016 Teklad global 16% protein rodent diets, Madison WI), and water *ad libitum*.

Carcinogen treatment

The chemical N-butyl-N-(4-hydroxybutyl) nitrosamine (BBN; TCI America; Portland OR) was prepared at 0.05% solution in water and administered *ad libitum* in drinking water. Mouse drinking water was changed twice per week, and water bottles were covered with aluminum foil to prevent light exposure. 8 weeks old mice were exposed to BBN for 12 weeks (C57BL/6, n = 18 and FVB, n = 20), for 16 weeks (C57BL/6, n = 8 and FVB, n = 12) and for 20 weeks (C57BL/6, n

= 5). Because FVB mice were moribund after 16 weeks of BBN exposure, we did not expose these mice to further BBN treatment. A total of 6 mice (C57BL/6, n = 3 and FVB, n = 3) non exposed to carcinogen was used as control group for normal urothelium. At the specified time points, BBN treatment was discontinued, and mice were exposed to normal water *ad libitum* for one week before euthanized via isoflurane (Vedco; Saint Joseph MO) inhalation followed by cervical dislocation. Bladders were then dissected and fixed in 10% neutral-buffered formalin (VWR International; Radnor PA) and subsequently stored in 70% ethanol (Pharmaco-Aaper; Brookefield CT) prior to processing and paraffin embedding. A total of 6 mice (C57BL/6, n = 3 and FVB, n = 3) and a total of 9 (C57BL/6, n = 4 and FVB, n = 5) from the 12-weeks-BBN treated group were used for RNA-sequencing (RNA-seq) and Western blot, respectively.

Histology and immunohistochemistry

Tissue sections were deparaffinized and used for H&E staining and immunohistochemistry (IHC) as previously reported[205]. One C57BL/6 mouse treated for 12 weeks with BBN was excluded for further characterization because of the inability to define the histologic type due to small bladder size. For IHC, slides were deparaffinized in histoclear (National Diagnostics; Atlanta GA), rehydrated in a series of graded alcohols (Pharmaco-Aaper; Brookefield CT) and washed in deionized water. The slides were placed in 1% antigen unmasking solution (Vector Labs; Burlingame CA) and heated for 20 minutes at high pressure in a pressure cooker (Cuisinart; East Windsor NJ), followed by cooling at room temperature and 10 minutes washes in phosphate-buffered saline (PBS 1X, pH 7.4) for 3 times. Incubation in 1% hydrogen peroxide (Thermo Fisher Scientific; Fremont CA) in methanol (Thermo Fisher Scientific) for 20 minutes was performed to block endogenous peroxidase activity. Slides were rewashed in 1X PBS (10 minutes for 3 times) and incubated for 1 hour in blocking solution 1X PBS containing horse serum (Vector Labs) to

reduce nonspecific antibody binding. Subsequently, slides were incubated with primary antibodies overnight at 4°C in a humidified chamber. Antibodies used were diluted in blocking solution and included goat polyclonal anti-FOXA1 (1:1000; Santa Cruz Biotechnology, Santa Cruz CA; #sc-6553), rabbit monoclonal anti-Ki67 (1:1000; Abcam, Cambridge MA; #ab16667), mouse monoclonal anti-KRT5/6 (1:200; Dako, Santa Clara, CA; #D5/16 B4), mouse monoclonal anti-KRT14 (1:200; Novocastra Leica Biosystem, Buffalo Grove IL; #LL002-L-CE), rabbit polyclonal anti-PPARG (1:200; Cell Signaling; #2430S), rabbit polyclonal anti-CDX2 (1:50; Sigma; #HPA049580). Mouse intestine was used as a positive control for CDX2 IHC.

The following day, slides were washed in 1X PBS (10 minutes for 3 times) before incubation for 1 hour with appropriate secondary antibody (1:200; Vector Labs) diluted in blocking solution. Following additional washing, antibody binding was visualized through the Vectastain Elite ABC Peroxidase kit (Vector Labs) after addition of the chromogen 3'-diaminobenzidine (Dako). Sections were washed in tap water for 5 minutes before counterstaining and rehydration as previously reported[205]. To reduce potential background noise and cross-reaction on mouse tissues, the mouse on mouse kit (Vector Labs) was used for IHC staining performed with antibodies raised in mouse. For IHC quantification, percent cells positive for Foxa1 were multiplied by staining intensity (graded 0-3) to calculate H score and percent positive cells were used for Pparg, Krt5/6, Krt14, and Ki67 staining.

For morphologic characterization of the bladder tumors, the following rules were applied: variant morphology was defined as anything other than conventional UCC identified via H&E examination. Specimens with hyperplasia and nuclear atypia in the urothelial lining in the absence of observable invasion were classified either flat urothelial carcinoma *in situ* (CIS) or CIS with keratinizing squamous metaplasia (KSM) in the presence of squamous changes. However, bladder tissues exhibiting squamous elements in the setting of tumor invasion were referred to as squamous differentiation (SqD), and tumors showing glandular differentiation (GD) in the presence of

additional variant morphology were considered glandular. When multiple tumor stages were present (i.e., CIS, pTa disease or frank invasion, for example), the tumor was designated as the highest stage present. All tumor staging, morphologic characterization, and quantification of IHC were performed in a blinded manner by genitourinary pathologists (JIW and MZ).

RNA-sequencing and computational analyses

In an effort to identify differences in gene expression between strains following BBN exposure, bladders were dissected from C57BL/6 (n = 3) and FVB mice (n = 3) after 12 weeks of BBN exposure and stored in RNAlater solution (Thermo Fisher Scientific) to stabilize RNA. Extraction of RNA was performed using TriZol (Thermo Fisher Scientific) reagent according to the manufacturer's instructions. One sample from the C57BL/6 mice was omitted for further analysis because of RNA degradation. RNA-seq was performed by the Genome Sciences and Bioinformatics Facility at the Pennsylvania State College of Medicine. The RNA-seq data were normalized to fragments per kilobase of transcript per million (FPKM) and used for differential expression analysis through the limma package[299] and R Commander software version 3.3.1[256]. Differentially expressed genes between the strains were identified using a false discovery rate threshold of q = 0.05. Gene Ontology (GO) analyses were performed using the Database for Annotation, Visualization and Integrated Discovery (DAVID)[300, 301]. Genes differentially expressed in the two strains with q < 0.05 (Supplemental Tables 3-1 and 3-2) were uploaded on DAVID and analyzed on *Mus musculus* species background using the default annotation categories as defined by DAVID. A medium classification stringency was chosen for DAVID functional annotation clustering analyses, based on which, groups of terms/annotations sharing similar gene members with similar biological meaning are clustered together. For this study, we focused on the GO biological process annotations to identify pathways modulated in FVB versus C57BL/6 following

BBN exposure. Genes associated with the identified biological processes were used to generate gene expression heatmaps in which the expression values are median centered by gene.

Western blot

A total of 9 dissected mouse bladders were homogenized in radioimmunoprecipitation (RIPA) buffer (25mM Tris-HCl pH 7.6, 150mM NaCl, 1% NP-40, 1% sodium deoxycholate, 0.1% SDS [Thermo Scientific, #89901]) containing 1X protease inhibitors (Roche, #11697498001), 1X phosphatase inhibitors (Roche, #4906837001) and 1nM Dithiothreitol (DTT; Invitrogen) in microcentrifuge tubes with a pestle (USA Scientific, #1415-5390). The homogenized tissues were left on ice for 30 minutes for the lysis process and then sonicated 4 seconds (x2) before spinning at 15,000xg for 30 minutes at 4°C. Protein concentrations were measured by optical densitometry at 562 nm wavelength using Pierce BCA Protein Assay Kit (Thermo Scientific; #23225) according to the manufacturer's protocol. Lysate samples were prepared with 1X NuPAGE LDS Sample buffer (Thermo Scientific; #NP0007) at 1μg/μl final concentration. Samples were boiled at 95°C for 5 minutes to reduce and denature proteins. A total of 10 μg of proteins per sample was loaded on polyacrylamide gel (Thermo Scientific; #NP0323BOX) together with protein marker (BioRad; #1610374) for electrophoresis at 85-90 Volts power (BioRad) followed by blotting on PVDF membrane equilibrated first in 100% methanol, washed with Millipore water and then re-equilibrated with transfer buffer (Thermo Scientific; #NP0006-1). Blotting was performed using Pierce G2 Fast Blotter (Thermo Scientific) at 25 Volts power for 15 minutes. Membranes were incubated in blocking buffer (5% skim milk - Tris-buffered saline [BioRad; #170-6435] containing 0.1% Tween20 [Thermo Scientific; #BP337-500]; TBST) for 1 hour at room temperature on a shaker to block unspecific antigens. Membranes were incubated with primary antibodies overnight at 4°C. Primary antibodies used were diluted in blocking buffer: goat polyclonal anti-PDL-1 (1:400;

R&D Systems; #AF1019), rabbit monoclonal anti-CD80 (1:1000; Abcam; #ab134120), rabbit monoclonal anti-CD86 (1:5000; Abcam; #ab53004) and rabbit anti-PPARG (1:1000; Cell Signaling Technology; #2430). On the next day, membranes were washed in TBST 3 times 10 minutes each before incubation with secondary antibody (anti-goat or anti-rabbit; 1:2000) for 1 hour at room temperature on a shaker. Membranes were rewashed in TBST 3 times 10 minutes each followed by treatment with Amersham ECL Prime Western Blotting Detection Reagent (GE Healthcare Life Sciences, #RPN2232) for visualization of protein bands. Image J software was used to quantify protein bands.

Statistical analyses

The Wilcoxon rank sum test was used to identify significant differences in strain-specific bladder weights, IHC scores and protein levels of Pdl-l expression upon BBN exposure. One FVB mouse was omitted as an outlier for the statistical analysis of Pdl-1 expression in the strains. Following dichotomization to compare non-invasive (hyperplasia and pTa) to invasive (pT1 or greater) disease, Fisher's exact test was used to identify significant associations between mouse strain and tumor invasion following BBN exposure. Two-Sided exact Cochran-Mantel-Haenszel test was applied for analysis of the association between strain background and histologic differentiation. The mouse tumors were stratified by stage (pTa/pTis/pT1 versus pT2/pT3) and analyzed using a 2x2 table for the association between strain and glandular differentiation. *P*-values ≤ 0.05 were considered statistically significant. Prism version 6.0c (GraphPad Software) was used for Wilcoxon rank sum test; and R Commander software for Fisher's exact test.

Results

FVB mice exhibit rapid bladder tumorigenesis and disease progression following BBN exposure

Following 12 weeks of BBN exposure, bladders dissected from FVB mice were significantly heavier when compared with bladders dissected from C57BL/6 mice (FVB = 80 mg [median] versus C57BL/6 = 45 mg [median]; *p*-value = 0.0393, Wilcoxon rank sum test; Figure 3-1 A). The FVB bladders trended on being heavier than C57BL/6 bladders following 16 weeks of BBN exposure, but differences were not statistically significant (Figure 3-1 B). The observed tumor stage in C57BL/6 following 12 weeks of BBN exposure was predominantly urothelial pTis (CIS 100%; Figure 3-1 C). Although pTis stage disease persisted, progression to pT1 stage disease was noted in approximately 38% of C57BL/6 mice after 16 weeks on BBN (Figure 3-1 C). As previously reported[261], prolonged BBN exposure for 20 weeks led to further tumor invasion into the muscularis propria (pT2) and perivesical fat (pT3) in C57BL/6 (Supplemental Figure 3-1 A). Conversely, pT3 disease (invasion through the muscle into perivesical fat) was the most commonly observed tumor stage phenotype in FVB following 12 weeks (~ 42%) and 16 weeks (~ 58%) of BBN exposure (Figure 3-1 C). We identified co-occurrence of pTa and pTis lesions in a number of C57BL/6 mice after 12 weeks (n = 3) and 16 weeks (n = 4) of BBN treatment. After 16 weeks of BBN exposure, we also identified concomitant presence of pTa and pT1 disease (n = 1), and pTis and pT1 lesions (n = 1) in C57BL/6 mice. Multiple lesion types were also detected in FVB mice. Following 12 weeks of BBN exposure, we observed concomitant pTa and pTis disease (n = 1) as well as co-occurrence of pTis and pT1 (n = 1), and pTis and pT3 (n = 1). After 16 weeks of BBN exposure, one FVB mouse had both pTa and pT1 disease, and another FVB mouse had pTis and pT1 diseases.

Examples of normal urothelium before exposure to carcinogen (Figure 3-1 D), urothelial hyperplasia, CIS and non-invasive papillary tumors complete with a well-developed fibrovascular core in C57BL/6 are shown (Figures 3-1 E-J). In addition, we provide examples of normal urothelium before exposure to carcinogen (Figure 3-1 K), lamina propria invasion (Figures 3-1 L-M) as well as invasion into the muscularis propria and perivesical fat in FVB (Figures 3-1 N-Q). Statistical analysis shows that FVB mice were significantly more likely to develop invasive bladder cancer (tumor stage ≥ pT1) following 12 weeks of BBN exposure compared with C57BL/6 mice (*p*-value = 0.0013, Fisher's exact test; Table 3-1); however, these differences were not significant after 16 weeks of BBN exposure as C57BL/6 mice develop invasive disease from this time point.

In summary, both C57BL/6 and FVB mice exhibit multiple lesions of various stages following BBN exposure. Our data show that FVB mice develop tumors rapidly and display a significantly increased likelihood of tumor invasion at an earlier time point relative to C57BL/6 when exposed to BBN.

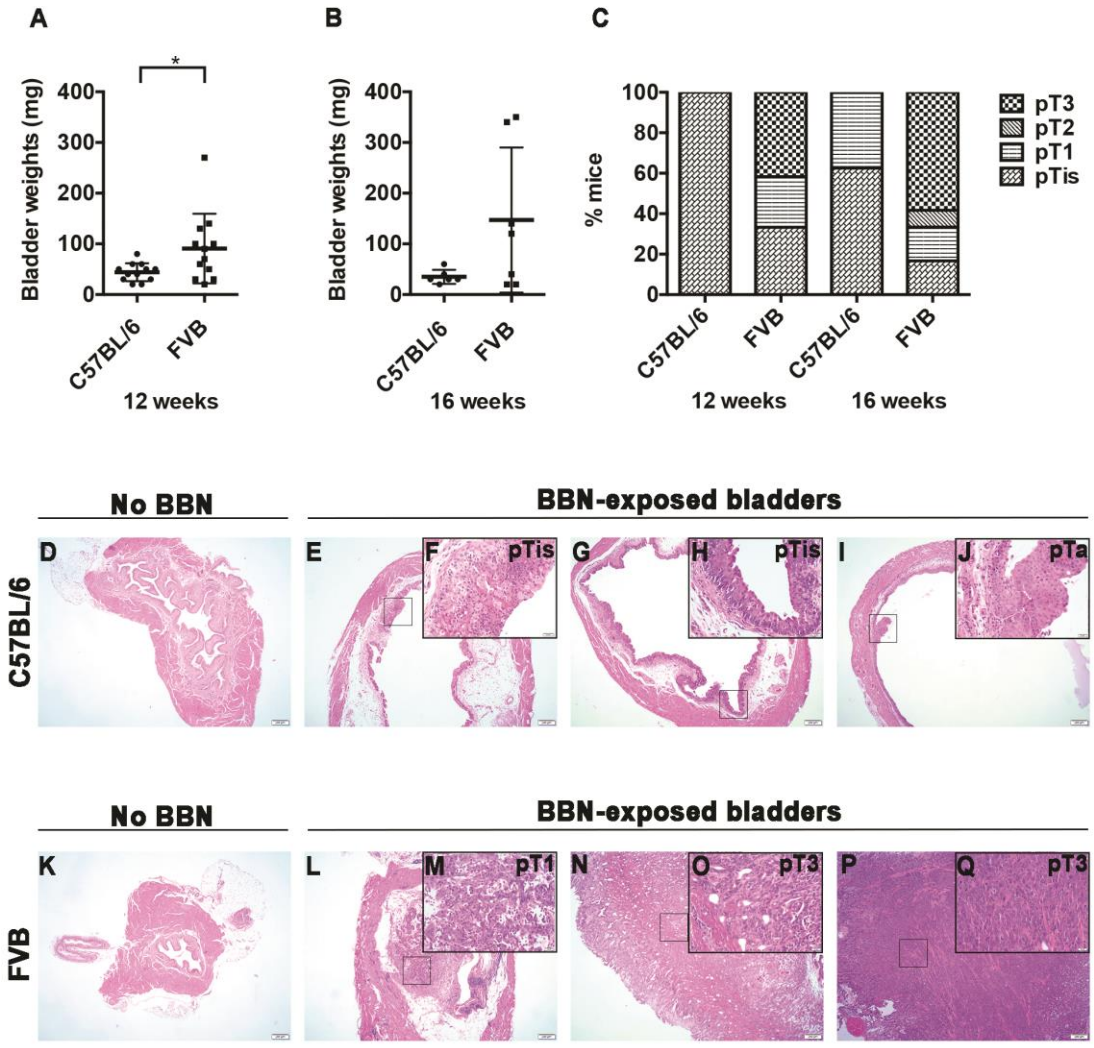

Figure 3-1. FVB strain of mice develops more advanced stage bladder cancer compared with C57BL/6 following BBN exposure.

(**A**-**B**) The weights of bladders dissected from C57BL/6 and FVB mice following (**A**) 12 weeks and (**B**) 16 weeks of BBN exposure are shown. Each dot represents one animal. After 12 weeks of BBN exposure, the bladders of FVB mice were significantly heavier than the bladders from C57BL/6 mice (*p-value = 0.0393; Wilcoxon rank sum test). Differences in bladder weights following 16 weeks of treatment were not statistically significant (p-value = 0.2442; Wilcoxon rank sum test). (**C**) Percentage of C57BL/6 and FVB mice with a given tumor stage. Following 12 weeks on BBN, C57BL/6 (n =11) developed pTis (n = 11) diseases, whereas FVB (n = 12) developed pTis (n = 4), pT1 (n = 3) and pT3 (n = 5) diseases. After 16 weeks on BBN, C57BL/6 (n = 8) developed pTis (n = 5) and pT1 (n = 3) diseases, whereas FVB (n = 12) developed pTis (n = 2), pT1 (n = 2), pT2 (n = 1) and pT3 (n = 7) diseases. (**D**-**Q**) H&E sections of normal urothelium before exposure to carcinogen and BBN-exposed bladders dissected from C57BL/6 (**D**-**J**) and FVB (**K**-**Q**) mice. Image scale bar 200 µm (low power magnification) and inset with higher magnification scale bar: 50 µm.

Table 3-1. Tumor invasion and strain dependence association following BBN exposure

	12 weeks BBN			16 weeks BBN		
STAGE	**C57BL/6** n (%)	**FVB** n (%)	TOTAL	**C57BL/6** n (%)	**FVB** n (%)	TOTAL
Non-invasive tumor (< pT1)	11 (100%)	4 (33%)	15 (65%)	5 (63%)	2 (17%)	7 (35%)
Invasive tumor (≥ pT1)	0 (0%)	8 (67%)	8 (35%)	3 (37%)	10 (83%)	13 (65%)
Significance of association *p*-value		*p*-value 1.3e-3			*p*-value 6.2e-2	

Glandular differentiation is enriched in FVB strain bladder tumors following BBN exposure

As tumor heterogeneity is reported to have prognostic significance, and bladder cancer is a highly heterogeneous disease exhibiting different response to therapy[181, 283], we next sought to define the degree of tumor heterogeneity in C57BL/6 and FVB mice following BBN-induced carcinogenesis. While FVB mice exhibited rapid tumorigenesis and disease progression in comparison to C57BL/6, the histological differences between FVB and C57BL/6 mice were also striking. Overall, C57BL/6 mice developed dramatic urothelial atypia interpreted as non-invasive flat UCC with squamous features after 12 weeks (~ 37%) and 16 weeks (~ 50%) of BBN exposure (Figure 3-2 A). Histological variants consisted of KSM complete with the presence of intercellular bridging and keratin deposition (Figures 3-2 B-G), and these findings are consistent with a recent report indicating C57BL/6 mice exposed to BBN develop basal bladder cancer[302], which is often enriched with SqD in humans[155]. Conversely, FVB mice exhibited more morphologically heterogeneous disease seen as UCC admixed with invasive SqD and GD (Figures 3-2 H-M), both of which were respectively present at a frequency of ~ 25% and ~ 17% after 12 weeks of BBN, and

each at a frequency of ~ 33% after 16 weeks of BBN exposure (Figure 3-2 A). While FVB mice developed GD and SqD following BBN exposure, we detected no GD in C57BL/6 mice after 12 and 16 weeks (Figure 3-2 A) or after prolonged exposure (Supplemental Figures 3-1 B-D). When we accounted for tumor stage, we did not observe a significant association between strain and glandular differentiation (*p*-value = 0.11, two-sided exact Cochran-Mantel-Haenszel test) suggesting that advanced tumor stage may increase the likelihood of GD phenotype, independent of strain background. However, in our study, while advanced stage diseases (pT3) in C57BL/6 at 20 weeks of BBN were associated with SqD, no GD phenotype was detected at this time point in C57BL/6 mice. Therefore, these data suggest that while FVB mice develop advanced stage bladder tumors with elements of UCC, SqD and GD as earlier as at 12 weeks of BBN exposure, C57BL/6 mice develop invasive tumors with elements of UCC and SqD at late time points such as 16 weeks and 20 weeks of carcinogen exposure (Supplemental Figure 3-1).

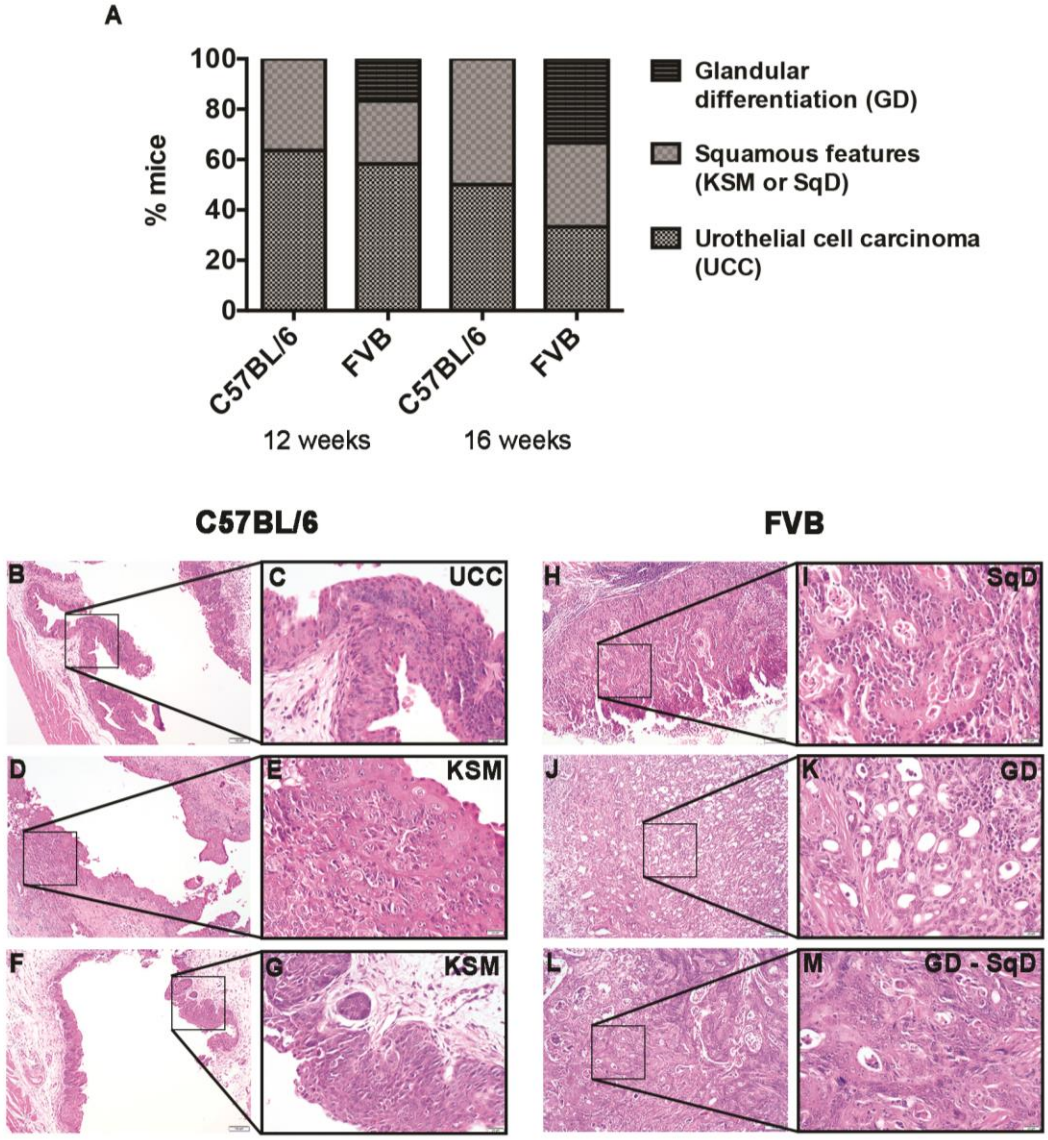

Figure 3-2. FVB mice exhibit squamous and glandular morphologic variants of urothelial carcinoma in response to BBN.

(**A**) Percentage of C57BL/6 and FVB mice with urothelial cell carcinoma (UCC), squamous features (keratinizing squamous metaplasia [KSM] or squamous differentiation [SqD]) and glandular differentiation (GD) following 12 and 16 weeks of BBN treatment. (**B-M**) H&E sections of bladders tissue dissected from (**B-G**) C57BL/6 and (**H-M**) FVB mice exposed to BBN for 12 and 16 weeks. Morphologic assessment of C57BL/6 bladders revealed non-invasive flat UCC (**B-C**; 12 weeks of BBN exposure) or KSM (**D-E**; 12 weeks of BBN exposure, and **F-G**; 16 weeks of BBN exposure) characterized by intercellular bridging and keratin deposition. Morphologic assessment of FVB bladders revealed invasive UCC with the presence of SqD (**H-I**; 12 weeks of BBN exposure) or GD (**J-K**; 12 weeks of BBN exposure) as well as mixed GD and SqD (**L-M**; 16 weeks of BBN exposure). Image scale bar 100 µm (low power magnification) and inset with higher magnification scale bar 20 µm.

Immunohistochemical analysis confirms strain-dependent influence of BBN treatment on tumor morphology

Specific morphologic variants are associated with the expression of immunohistochemical markers indicative of differentiation state. For example, while expression of high molecular weight cytokeratins including Krt5/6 and Krt14 is associated with squamous morphology[303], expression of the transcriptional regulators, peroxisome proliferator-activated receptor gamma (Pparg) and Forkhead box A1 (Foxa1) is associated with urothelial and glandular differentiation[303]. Therefore, we next explored the expression of these markers in the tumors of our experimental mice. While C57BL/6 mice exhibited moderate to high expression of Krt5 and Krt14 in their BBN-induced tumors, they exhibited mild and often undetectable nuclear Pparg or Foxa1 expression in these tumors (Figure 3-3 A). On the other hand, as BBN-associated tumors in FVB mice were characterized by SqD and GD, we observed high expression of both squamous markers (Krt5 and Krt14) and the urothelial marker (Foxa1) whereas Pparg expression was low (Figure 3-3 A). Scoring of IHC showed no significant difference between C57BL/6 and FVB tumors regarding the levels of expression of Krt5 (Figure 3-3 B) and Krt14 (Figure 3-3 C). However, the IHC scoring also showed that Pparg levels were significantly lower in FVB tumors compared with C57BL/6 tumors (Figure 3-3 D) whereas Foxa1 levels were significantly higher in FVB tumors relative to C57BL/6 tumors (Figure 3-3 E). Altogether, these findings are suggestive of the existence of divergent morphologic patterns in C57BL/6 and FVB mice following BBN exposure.

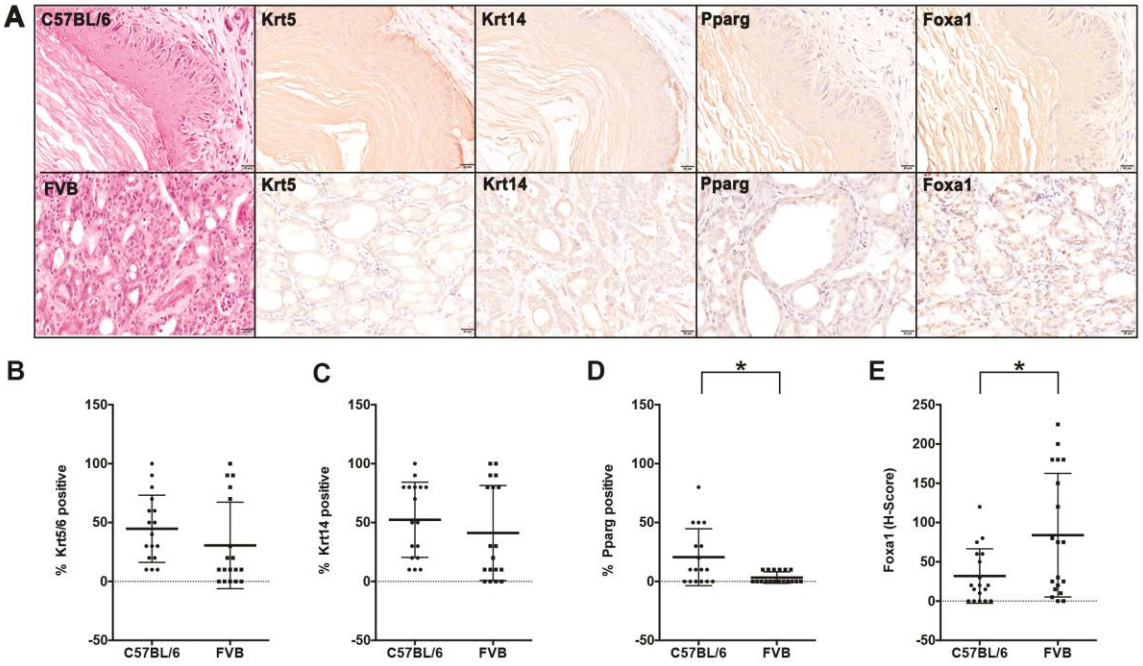

Figure 3-3. Immunohistochemical analysis suggests divergent differentiation patterns in BBN-induced bladder cancers in C57BL/6 and FVB mice.

(**A**) H&E staining and immunohistochemistry (IHC) for Krt5/6, Krt14, Pparg, and Foxa1 in C57BL/6 and FVB mice following 12 and 16 weeks of BBN exposure. (**B-C**) Tumors from FVB and C57BL/6 mice did not express significantly different levels of the basal markers, (**B**) Krt5 and (**C**) Krt14; each dot represents a mouse. (**D-E**) Quantification of IHC for Pparg and Foxa1, both associated with urothelial differentiation, revealed significantly lower expression of (**D**) Pparg, but higher expression of (**E**) Foxa1 in FVB mice (* = $p \leq 0.05$; Wilcoxon rank sum test). Each dot represents a mouse.

C57BL/6 and FVB mice exhibit differential expression of Cd274 (Pdl-1) in bladder tumors following BBN exposure

In order to develop a more in-depth understanding of the molecular differences that underlie the non-invasive tumors in C57BL/6 mice versus the invasive tumors in FVB mice, we performed RNA-seq on dissected bladders after 12 weeks of BBN exposure followed by differential expression analysis and subsequent functional annotation studies using the NIH DAVID software. We found that upregulated genes in FVB mice relative to C57BL/6 mice were associated with GO terms related to immune activities. Specifically, the FVB strain exhibited increased expression of genes related to the following biological processes: antigen processing and presentation via major histocompatibility complex (MHC/H2), immune response and proteolysis (Table 3-2). In contrast, genes differentially downregulated in FVB, but upregulated in C57BL/6 mice were involved in biological processes such as transport and GPCR signaling pathways (Table 3-2). Based on this analysis indicating important differences in the tumor microenvironment, we further examined the differential expression between C57BL/6 and FVB strains for immune markers that are associated with cancer progression. Interestingly, we found evidence that immune markers including matrix metalloprotease (Mmp2 and Mmp9), interleukins and their receptors (Il-5, Il-5ra, Il-5rb, Il-6ra, Il-17b, Il-17ra and Il-17rb) as well as immune checkpoints (Cd274, Cd80 and Cd86) are upregulated in FVB mice relatively to C57BL/6 mice after 12 weeks of BBN exposure (Figure 3-4 A); this suggests the presence of inflammation and ongoing immune reactivity in the FVB bladder tumors. Moreover, Pparg, which is known to be associated with immune suppression activity in the bladder tumor microenvironment[304], appeared to be upregulated in C57BL/6 mice compared to FVB mice at the RNA level (Figure 3-4 A) supporting our IHC analysis (Figure 3-3 D).

As the immune checkpoint pathways are major targets in cancer immunotherapy, we further examined expression differences of these pathway components at both RNA and protein levels. Contrary to Pparg expression, T-cells co-stimulatory factors such as cluster of differentiation

80 and 86 (Cd80 and Cd86) were not differentially expressed between strains at either the transcriptional (Supplemental Figure 3-2) or protein (Figure 3-4 B) levels. Nonetheless, our Western blot results and associated densitometry show significantly increased expression of T-cells inhibitory factor such as the program cell death ligand-1, Pdl-1 (Cd274), in FVB mice relative to C57BL/6 following BBN treatment (*p*-value = 0.0286, Wilcoxon rank sum test; Figure 3-4 C). Interestingly, the differences between the two strains were less pronounced when the expression of Cd274 in BBN exposed bladders from both strains were compared with normal bladders prior to BBN exposure (Supplemental Figure 3-3). Therefore, our results indicate a BBN-induced activation of immune response signatures in both strain of mice following BBN exposure, with FVB strain exhibiting relatively high levels of inflamed and immunogenic markers.

Table 3-2. List of genes differentially expressed in FVB mice versus C57BL/6 mice based on the biological process in the GOterms from DAVID analysis.

Upregulated Genes in FVB versus C57BL/6		**Downregulated Genes in FVB versus C57BL/6**	
Gene Name	**Gene Symbol**	**Gene Name**	**Gene Symbol**
Immune response:		**Transport:**	
Histocompatibility 2, class II antigen E alpha, pseudogene	*H2-Ea-ps*	Afamin	*Afm*
Histocompatibility 2, Q region locus 1	*H2-Q1*	Apolipoprotein A-II	*Apoa2*
Histocompatibility 2, Q region locus 10	*H2-Q10*	Coiled-coil domain containing 109B	*Ccdc109b*
Histocompatibility 2, Q region locus 2	*H2-Q2*	Gamma-aminobutyric acid (GABA) A receptor, subunit alpha 3	*Gabra3*
Histocompatibility 2, T region locus 3	*H2-T3*		
Predicted gene 8909	*Gm8909*		
Proteolysis:		**GPCR signaling pathways:**	
Abhydrolase domain containing 1	*Abhd1*	Olfactory receptor 1034 (Olfr1034)	*Olfr1034*
Complement component 1, r subcomponent B	*C1rb*	Selection and upkeep of intraepithelial T cells 4	*Skint4*
Complement component 1, s subcomponent 2	*C1s2*	Selection and upkeep of intraepithelial T cells 7	*Skint7*
Membrane metallo-endopeptidase-like 1	*Mmel1*		

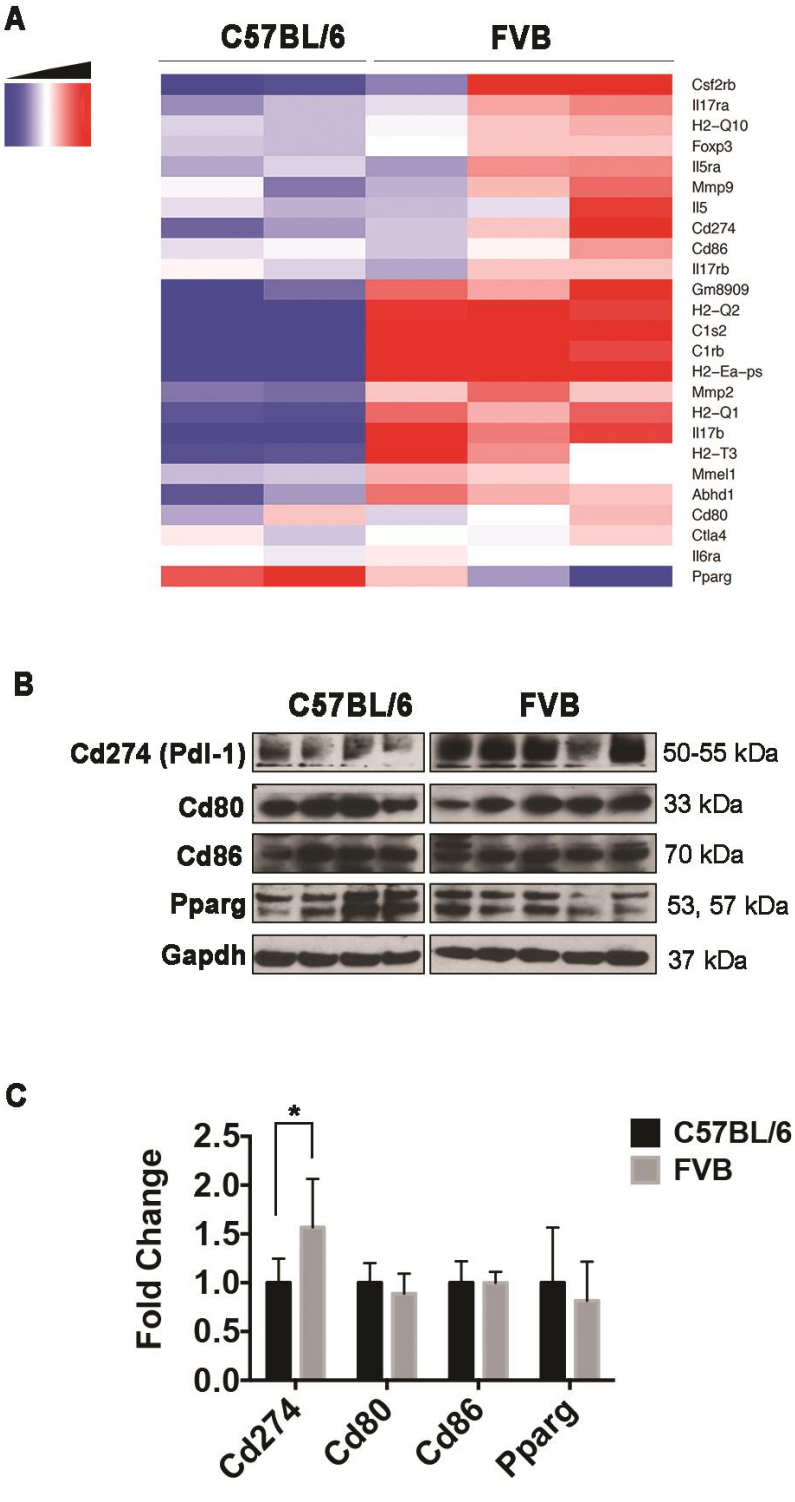
A
C57BL/6
FVB
Csf2rb
Il17ra
H2-Q10
Foxp3
Il5ra
Mmp9
Il5
Cd274
Cd86
Il17rb
Gm8909
H2-Q2
C1s2
C1rb
H2-Ea-ps
Mmp2
H2-Q1
Il17b
H2-T3
Mmel1
Abhd1
Cd80
Ctla4
Il6ra
Pparg
B
C57BL/6
FVB
Cd274 (Pdl-1)
50-55 kDa
Cd80
33 kDa
Cd86
70 kDa
Pparg
53, 57 kDa
Gapdh
37 kDa
C
Fold Change
2.5
2.0
1.5
1.0
0.5
0.0
*
C57BL/6
FVB
Cd274
Cd80
Cd86
Pparg

Figure 3-4. BBN-induced bladder tumors in FVB mice exhibit an inflamed microenvironment and increased expression of Cd274 (Pdl-1).

Both C57BL/6 and FVB mice were exposed to BBN for 12 weeks and sacrificed. Following RNA extraction, we performed RNA-seq and Gene Ontology (GO) analysis, which indicated differences in the tumor microenvironment between the two strains. (**A**) Heatmap display of immune-related genes differentially expressed in C57BL/6 and FVB mice at 12 weeks of BBN treatment and identified by GO analysis. FPKM-based gene expression measurements are median centered by row with genes listed in rows and samples (C57BL/6 n = 2; FVB n = 3) in columns. (**B**) Western blot of the immune checkpoints (Cd274/Pdl-1, Cd80 and Cd86), Pparg and Gapdh loading control. Each lane represents one bladder/mouse (C57BL/6 n = 4; FVB n = 5). (**C**) Densitometry analysis of Western blot confirmed significantly higher expression of Cd274/Pdl-1 in FVB than C57BL/6. One FVB mouse outlier (lane 4) was omitted from the densitometry analysis for statistical analysis (**p*-value = 0.0286; Wilcoxon rank sum test).

Discussion

Genetically engineered mouse models are often created through breeding strategies that incorporate various strains. While this approach can be entirely appropriate if genetically similar/identical littermates are used as controls, the association between background strain and carcinogen susceptibility is well documented throughout the field of cancer research[229, 262, 293, 294, 296]. To the best of our knowledge, no study has directly compared the impact of BBN exposure on bladder cancer susceptibility and phenotype between C57BL/6 and FVB, two commonly utilized mouse strains for the study of bladder cancer[192, 232, 253]. In this study, we showed that FVB mice are more susceptible to BBN than C57BL/6 mice and develop MIBC at just 12 weeks of BBN exposure (Figure 3-1). The BBN-induced tumors in FVB mice were poorly differentiated and morphologically heterogeneous mimicking some features of specific types of human MIBC including conventional UCC, UCC with SqD and UCC with GD (Figure 3-2). On the other hand, following 12 weeks of BBN administration, C57BL/6 mice develop NMIBC characterized by CIS and papillary tumors. However, C57BL/6 mice treated with BBN for 20 weeks develop MIBC with elements of SqD in accordance with previous studies[231, 293]. Both mouse strains exhibit increased expression of the basal markers Krt5 and Krt14 following BBN exposure (Figure 3-3). In addition,

we showed that the FVB tumor microenvironment is highly immunogenic and inflamed with increased expression of murine MHC, immune checkpoint Pdl-1 and pro-inflammatory cytokines (Il-5 and Il-17b) and their respective receptors (Il-5ra, Il-5rb, Il-17ra and Il-17rb) as shown in Figure 3-4.

While adenocarcinoma accounts for 0.5-2% of bladder cancer in the United States[305], mixed GD is the second most common morphologic subtype in cystectomy samples, and both are associated with worse clinical outcome in bladder cancer patients[99, 100]. Although current National Comprehensive Cancer Network guidelines indicate that UCC with GD should be treated similarly to conventional UCC[80], proven and effective therapeutic options for adenocarcinoma are limited and under-studied. Therefore, the development of mouse models that exhibit a rapid development of histologic variants such as UCC with GD and adenocarcinoma is crucial for the identification of novel and appropriate therapies. While GD has been previously reported following the exposure of mice on a mixed background to BBN[296], we believe this is the first report describing the presence of GD in FVB mice. As the incidence of GD in the FVB mice increases with prolonged exposure to BBN, this implies that the urothelial tissue may initially develop as UCC with GD, and then progresses in this spectrum to adenocarcinoma upon continuous carcinogen exposure. Bladder adenocarcinoma is often associated with the formation of enteric/mucinous-type glands, and the caudal type homeobox 2 (CDX2)[306] is a marker utilized for assessment of GD. Surprisingly, we failed to detect Cdx2 immunostaining in all mouse bladder tumors exhibiting any degree of GD suggesting a non-enteric route of gland development in these tumors. Similarly, Pparg expression, which is often associated with urothelial and glandular differentiation was observed to be also lower in the FVB tumors with GD as opposed to the C57BL/6 tumors.

Because human advanced bladder cancer has been associated with the presence of PDL-1 and has proven to be responsive to immune checkpoints blockade[307, 308], our results concerning Cd274/Pdl-1 are significant because of the lack of preclinical models for the study of immune

checkpoint blockade in bladder cancer. This is important because while the development of FDA approved PDL1/PD1 immune checkpoint inhibitors, including Nivolumab, Atezolizumab, Durvalumab and Avelumab, has revolutionized bladder cancer treatment and other malignancies, only a small fraction of patients benefit from these therapies, and PDL-1 detection is not always the best predictor of response. Thus, preclinical models and additional research are needed to identify ways of enhancing immune checkpoint blockade. Our differential expression analysis showed increased levels of Cd274/Pdl-1 expression in FVB than in C57BL/6 after BNN exposure. However, Western blot analysis of BBN exposed bladders of both C57BL/6 and FVB mice showed increased levels of Cd274/Pdl-1 expression when compared with normal bladders prior to BBN exposure. This result suggests that, in addition to genetic background differences, the increase in Cd274/Pdl-1 expression may be due to BBN-associated immunogenic response, and therefore, warrant further investigations.

One limitation of our model is that FVB mice become moribund at 16 weeks of BBN exposure precluding further experimentation to better characterize the natural history of glandular changes. Therefore, future approaches might “rescue” bladder tissue from BBN-treated FVB mice, followed by sub-capsular renal engraftment. This approach would enable investigators to assess the progression of cancerous bladder tissue in a syngeneic host enabling further characterization. Alternatively, this approach could potentially be useful for metastatic disease studies when the tissue is orthotopically implanted in the bladder. In addition, reduced concentrations of BBN could be employed, and it would be advantageous to create cell lines from BBN-induced FVB bladder tumors that retain elements of GD or adenocarcinoma. An additional limitation of this study is that BBN consumption by the two strains was not measured, since the rate of consumption can potentially influence tumor development. Moreover, because the RNA-seq analysis was performed solely on carcinogen exposed bladders, the differences in gene expression are assumed to be associated with strain response to BBN exposure; however, these differences could potentially also

be baseline differences between the two strains. In that regard, it is noteworthy to highlight that C57BL/6 strain was previously reported to be less immunogenic than, for instance, BABL/C strain in a mouse modeling of human immune thrombocytopenia (ITP)[309]. Although the low levels of inflammatory response in C57BL/6 in the ITP model support our observations that C57BL/6 strain is less immunogenic compared with FVB strain, further studies are warranted to confirm whether the differences in gene expression are driven by intrinsic strain response to carcinogen exposure or are baseline differences of these strains.

In conclusion, we show that FVB strain is more susceptible to BBN and develops advanced bladder cancer at earlier time point than C57BL/6 strain. We also identify important differences between the tumor microenvironments of these two strains in terms of immune signature expression following BBN exposure. The increased presence of Cd274/Pdl-1 in the FVB tumor microenvironment indicates that FVB strain can potentially be used as a model for a more in-depth characterization of (1) the interaction between immune cells and tumor cells in advanced stage tumor microenvironment and (2) the impact of histological variants on immunotherapy. Also, based on the degree to which FVB mice rapidly develop bladder cancer with unique histologic attributes following BBN exposure, the current study indicates that investigators should carefully design and interpret their research findings when utilizing genetically engineered mouse models with mixed genetic backgrounds in combination with BBN in an effort to maintain experimental rigor and enhance reproducibility.

Supplemental Information

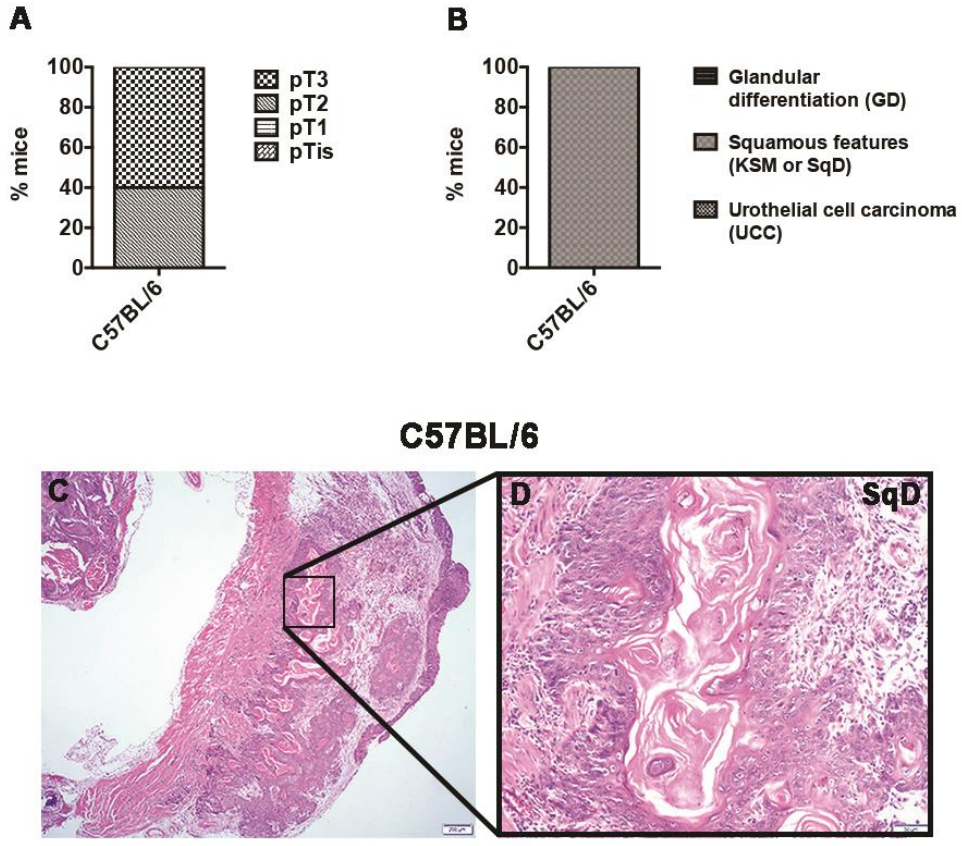

Supplemental Figure 3-1. C57BL/6 mice develop advanced bladder cancer with squamous morphologic variants upon 20 weeks of BBN.

(**A**) Percentage of C57BL/6 (n = 5) mice at different tumor stages pT2 (n = 2) and pT3 (n = 3) at 20 weeks of BBN exposure. (**B**) Percentage of C57BL/6 (n = 5) mice per morphologic variant at 20 weeks of BBN exposure: all mice developed squamous elements. (**C**) H&E of C57BL/6 bladders showing invasive UCC admixed with SqD in the presence of intercellular bridging and keratin deposition.

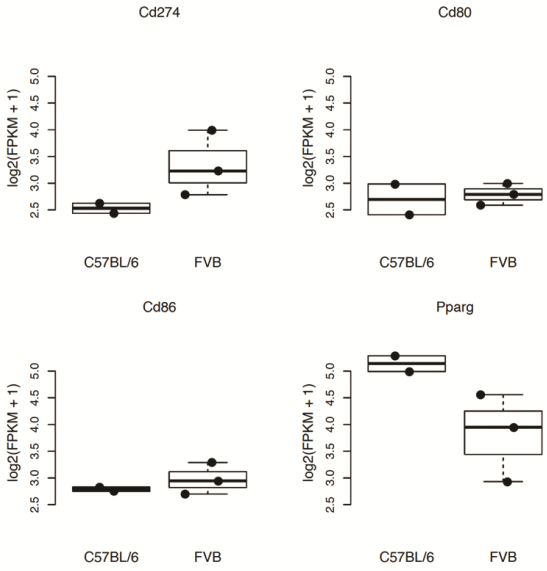

Supplemental Figure 3-2. BBN-induced bladder tumors in FVB mice exhibit an increased levels of transcripts of Cd274 (Pdl-1).

Boxplot analyses of absolute expression of transcript levels of Cd274/Pdl-1, Cd80, Cd86 and Pparg in C57BL/6 and FVB bladders exposed to BBN for 12 weeks are shown. Each dot represents a single mouse.

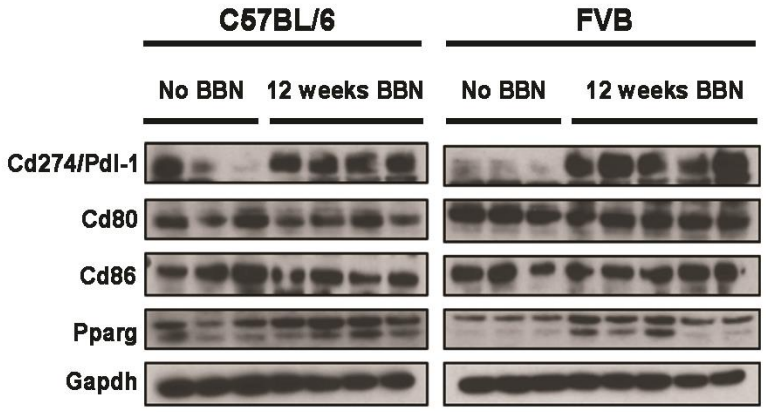

Supplemental Figure 3-3. BBN-induced immune response in C57BL/6 and FVB mice.

Western blot of the immune checkpoints (Cd274/Pdl-1, Cd80 and Cd86), Pparg and Gapdh loading control in normal urothelium prior to BBN exposure (no BBN) versus bladder tumors (12 weeks BBN) in C57BL/6 and FVB mice. Each lane represents one bladder: C57BL/6 (no BBN [n = 3] and 12 weeks BBN [n = 4]) and FVB (no BBN [n = 3] and 12 weeks BBN [n = 5]).

Supplemental Table 3-1. List of genes differentially upregulated in FVB versus C57BL/6.

C1rb	*Gm8615*	*H2-Ea-ps*	*Il17b*	*Kcns1*
Serpina1b	*Chil1*	*Gm8909*	*Gm8580*	*D030025P21Rik*
4933432I03Rik	*Gm5801*	*Xlr3c*	*H2-Q2*	*Frmpd3*
AA792892	*Sorcs3*	*Mrgprd*	*Serpina3k*	*Mup5*
Madcam1	*Apol11b*	*Trim34b*	*Ptprv*	*C1s2*
Cyp4f37	*4930565N06Rik*	*9830107B12Rik*	*A930015D03Rik*	*Zfp949*
H2-Q1	*C920025E04Rik*	*Eno1b*	*Gdpd3*	*Olfr1251*
Fam196a	*Mir6909*	*Tekt4*	*Tpte*	*C4a*
Slc6a3	*Zfp605*	*Cdh16*	*Gm17746*	*Mmel1*
Gm3558	*Tmod4*	*Mybph*	*H2-Q10*	*Ibsp*
Hal	*Slc24a1*	*Nlrp5*	*Dlx4*	*Gm10653*
Slco4c1	*H2-T3*	*Art2a-ps*	*Abhd1*	*AI506816*
Pcdhb7	*Tspan10*	*Dmp1*	*Vash2*	*Snord49b*
Ppy	*Mir7063*	*Apom*	*Dupd1*	*C330046G13Rik*
Tbr1	*1700008C04Rik*	*Scn11a*	*Tcstv3*	*Myh7b*

Supplemental Table 3-2. List of genes differentially downregulated in FVB versus C57BL/6.

Afm	*Gm14305*	*Mir7688*	*Fam47e*	*Mucl1*
Gm14393	*2310003N18Rik*	*Olfr1034*	*Rbmxl2*	*Gzmk*
D730005E14Rik	*4930481A15Rik*	*Tmem181b-ps*	*Pakap*	*Actl11*
9530027J09Rik	*4930505A04Rik*	*1110019D14Rik*	*Gm38509*	*Prr9*
Krt33a	*Nek11*	*Wfdc6b*	*Amer3*	*Gm16291*
8030455M16Rik	*Apol10a*	*Gpr150*	*Nps*	*4930546K05Rik*
4930479D17Rik	*4933427E11Rik*	*Gm5420*	*Epha10*	*Mir687*
Sun3	*Hist1h2bp*	*Mirlet7i*	*4930473A02Rik*	*Fgf4*
Mir6970	*C130060K24Rik*	*Tcaf3*	*1700125H20Rik*	*Gipr*
Snord85	*4930511A02Rik*	*H2-T23*	*Skint4*	*Skint7*
Lrrc72	*Zcchc13*	*Ankrd53*	*Gucy2d*	*Slc22a22*
Prss52	*Med9os*	*Cyp8b1*	*Sez6*	*4933433H22Rik*
Kcnj13	*Ccdc109b*	*Trim12a*	*Apoa2*	*Gabra3*
C920006O11Rik	*Cda*	*E130008D07Rik*	*Ces1f*	*4930412C18Rik*
Cd200r3	*Ttc9*	*Adgb*		

Acknowledgements

This chapter is a manuscript co-written by Osei-Amponsa V, Shuman L, Ellis J, Wang E, Walter V, Zaleski M, Warrick J, Raman J and DeGraff D.

Pathology studies including H&E staining and immunohistochemistry were performed by Osei-Amponsa V, Shuman L and Ellis J. Bioinformatic analyses were performed by Walter V and Osei-Amponsa V. Pathological evaluations were performed by Warrick J and Zaleski M.

The work described in this chapter was supported by the National Cancer Institute (R00CA172122; DJD) and the Ken and Bonnie Shockey Fund for Urologic Research (JDR).

Chapter 4

Discussion

The Role of *FOXA1* and *PTEN* in Bladder Cancer Heterogeneity

Bladder cancer presents frequent genomic and epigenomic alterations that may be associated with or be responsible for morphologic and molecular variability related to tumor heterogeneity phenotype. Because the majority of these genomic alterations are potentially actionable alterations (i.e., FGFR3, PIK3CA, EGFR and HRAS), bladder cancer presents as an ideal disease for targeted therapies regimen. However, risk stratification and treatment decisions in bladder cancer are mainly based on histological analysis (tumor stage and morphology) following initial biopsy; this can be problematic, as the degree of morphologic and molecular heterogeneity is, therefore, inferred based on the analysis of a small region of the tumor. Since the identified genetic alterations may not be fully representative of the whole tumor genomic status, analysis of biopsy samples can dangerously underestimate the degree of tumor heterogeneity. As our understanding of the role of tumor heterogeneity in disease progression and therapeutic resistance increases, it is possible that bladder cancer patients will be at increased risk of receiving inadequate (or worse) treatment. For these reasons, alternative strategies based on multiregional molecular mapping of tumor tissues and corresponding adjacent normal tissues are now being employed in order to capture the mutational load present in the entire tumor and surrounding environment[245, 310, 311]. Furthermore, our relative lack of knowledge regarding the molecular genetics of bladder cancer, as well as the utilization of genomics studies for the development of targeted therapies for breast cancer [312, 313] has prompted several studies focused on the identification of molecular subtypes of bladder cancer based on gene expression profiling. At least four different molecular subtyping schemas have been described leading to molecular phenotypes that can be broadly divided into

luminal tumors expressing markers of urothelial differentiation and basal tumors expressing markers of basal cells and squamous differentiation[134, 137, 172, 176]. While the clinical implementation of the different bladder subtyping models is currently unknown, clinical trials are now incorporating these schemas in an effort to determine their clinical significance. While this is important, the degree of tumor heterogeneity within clinical samples certainly have the potential to confound these analyses, especially, now that it is recognized that intratumoral heterogeneity exists regarding molecular subtype[181, 245]. Thus, examining the roles that cancer-associated genes may play in the mechanisms responsible for tumor heterogeneity is imperative for the generation of optimal therapies for heterogeneous diseases; this is important because various aspects of tumor heterogeneity can promote disease resistance or tumor recurrence following treatment[314].

In an effort to investigate bladder cancer heterogeneity, the work outlined in this dissertation utilizes analysis of publicly available clinical data, *in vivo* and *in vitro* approaches to analyze the role of two bladder cancer-related genes, *FOXA1* and *PTEN*, in bladder cancer tumorigenesis and heterogeneity (Chapter 2). Through the analysis of clinical data, we provided evidence of the diverse genetic mechanisms potentially regulating the expression of *FOXA1* and *PTEN* in MIBC patients. We generated a murine knockout model of *Foxa1* and *Pten* to assess the impact of genetic alterations of these genes on bladder tumorigenesis. Furthermore, we initiated gain-of-function tissue culture-based studies in an effort to elucidate the potential functional relationship between *FOXA1* and *PTEN* in bladder cancer. In addition, we performed an independent study to determine the relationship between genetic background and carcinogen susceptibility in mice (Chapter 3). For ease of discussion and reference, the data presented in this dissertation will be discussed below in separate categories, introducing first the clinical data analysis, followed by the animal data and the cell culture data.

PTEN expression correlates with copy number alterations and *FOXA1* expression is associated with promoter methylation in MIBC

Copy number variations and genetic mutations are critical events in cancer genesis and progression. Changes in the number of copies of a gene can have a significant impact on its expression[315]. Using the TCGA RNA-seq dataset[155], we investigated the correlation between gene expression and copy number alterations for *FOXA1* and *PTEN* in advanced bladder cancer. The analysis revealed a significant co-occurrence of copy number losses of both genes in muscle invasive bladder cancer.

For *PTEN* expression, we observed a prototypical positive correlation between gene expression and copy number status. While copy number losses were associated with lower expression, copy number gains resulted in increased expression. Published evidence shows that copy number variations of *PTEN* are more common events (13%) than point mutations (3%) in invasive bladder cancer[137, 153] suggesting that copy number alterations may be the predominant mechanism responsible for the decreased levels of detection of PTEN in bladder cancer. Loss of heterozygosity (LOH) is the most frequent genetic alteration type described for *PTEN* in bladder cancer[126, 152]. In a LOH condition, one locus of a gene is lost, and the retained gene copy maintains gene functionality. However, due to (1) the low levels of detection of PTEN expression by IHC in patients with *PTEN* loss and (2) the low frequency of point mutations observed in the retained allele of *PTEN* following LOH[152, 153], it was previously proposed that a different tumor suppressor gene candidate rather than *PTEN* may exist in the proximity of *PTEN* gene on chromosome 10q. One potential candidate gene was *MXI1*, which inhibits the activity of Myc oncoprotein[316]. While alterations in *MXI1* gene have been implicated, for instance, in prostate cancer[317], attempts to identify alterations in this gene in bladder cancer have not been successful[318], suggesting that *PTEN*

may be the significant tumor suppressor candidate of alterations on chromosome 10q, and that a single allele alteration may be sufficient to abrogate PTEN function in bladder cancer[153]. Alternatively, evidence shows that other mechanisms of inactivation of *PTEN* may exist.

According to Knudson's two-hit hypothesis, inactivation of both copies of tumor suppressor genes is one crucial driving force for tumorigenesis[319]. The two-hit model explains the contribution of certain tumor suppressors such as the *RB1* gene to tumorigenesis. However, this theoretical construct does not appear to explain the contribution of other suppressor genes such as *TP53* and *PTEN*. In the case of *TP53,* haploinsufficiency phenotypes have been described: a single copy loss of the gene is sufficient to promote aberrant function and increases the probability of cancer. In regards to *PTEN*, a quasi-sufficiency phenotype is defined as when the activity of the gene is coupled with gene expression dosage. Therefore, subtle changes at any level of gene expression, even without variations in either genetic loci, may lead to impaired function[319-321]. Thus, alterations in the molecular events that affect gene expression namely copy number, epigenetic regulation, transcriptional regulation and post-translational modifications (PTMs) may all have implications for subsequent gene expression and protein functionality. Whang *et al.* previously proposed gene silencing of *PTEN* at the transcriptional level by DNA methylation in advanced prostate cancer as an explanation for reduced PTEN detection in advanced disease[322]. Nonetheless, independent studies investigating epigenetic silencing of *PTEN* by Cairns *et al.* failed to detect DNA methylation as an epigenetic mechanism explaining *PTEN* inactivation in prostate cancer[323]. While *PTEN* silencing by promoter hypermethylation is reported in colorectal cancer[324] and breast cancer[325, 326], discordant studies in prostate cancer[322, 323] indicate that DNA promoter methylation may not contribute to *PTEN* inactivation in prostate cancer. Interestingly, in the TCGA cohort of MIBC, no apparent correlation was detected between DNA methylation and *PTEN* expression[155]; contrasted, however, by the findings from Agundez *et al*[327]. Thus, further investigations regarding DNA promoter methylation of *PTEN* in bladder cancer are required.

Additionally, PTMs have been also proposed as mechanisms of gene silencing for *PTEN*[328]. Abrogation of PTEN function by phosphorylation[281] has been reported in gastric cancer[329] suggesting a role in gastric tumorigenesis. Nonetheless, little is known about the role of PTMs on PTEN activity in bladder cancer. Thus, in addition to copy number variations, regulatory mechanisms associated with gene expression such as promoter hypermethylation and those associated with protein function (i.e., PTMs) also potentially contribute to *PTEN* expression and activity in bladder cancer.

On the other hand, when we looked into *FOXA1* expression, we detected a weak correlation between copy number alterations and gene expression. The discrepancy between copy number alterations and gene expression suggests the existence of additional regulatory mechanisms (as described above for *PTEN*) underlying reduced *FOXA1* expression. Moreover, although *FOXA1* has been recently reported to be mutated at a statistically significant degree (5%) in bladder cancer[137], we observed no correlation between *FOXA1* point mutations and gene expression at the transcript level. The most observed spectrum of mutations for *FOXA1* were missense and frameshift mutations. As the latter is associated with loss of function, its effects would be evident at the protein level; thus, site-directed mutagenesis in *FOXA1* studies together with reporter assays could be employed to assess if these mutations impact the transcriptional functionality of FOXA1. However, these experiments would prove difficult given the lack of chromatin structure in reporter gene assays. Therefore, the impact of *FOXA1* mutations would be more appropriately studied on endogenously-regulated genes following genome editing approaches.

Several other studies have identified a disconnect between copy number status and gene expression, and have gone on to identify a contribution for epigenetics in the form of DNA promoter methylation[159, 330-332]. Therefore, we next examined publicly available data[155] as well as a panel of human bladder cancer cell lines for a relationship between DNA promoter methylation and *FOXA1* expression. In our investigation of the DNA methylation status of the *FOXA1* promoter

in the TCGA MIBC cohort, we found that hypermethylation of the CpG island 99 within the promoter of *FOXA1* was significantly associated with decreased gene expression. Similarly, methylations of CpG island 143 within the *FOXA1* gene body was associated with reduced *FOXA1* expression but was not statistically significant. These findings were subsequently confirmed via the analysis of CpG island methylation through *in vitro* cell culture studies. The *in vitro* studies were designed also to include a probe specific for CpG island 123, which was not included in the TCGA study. Analysis of a panel of ten human bladder cancer cell lines revealed differential patterns of methylation of regulatory regions associated with the *FOXA1* gene. We previously defined the molecular subtyping of these cell lines and identified cells with luminal expression pattern (luminal-like), those with a basal expression pattern (basal-like) and those that did not rank with any subtype (no-type)[213]. As expected, hypermethylation of the promoter CpG island 99 was observed in basal-like cell lines that lack FOXA1 expression, but no evident promoter hypermethylation was detected in luminal-like FOXA1 expressing cells nor in no-type cells. On the other hand, while no methylation of CpG island 143 was detected in almost all cell lines analyzed, methylation of CpG island 123 was observed in all cell lines including luminal-like FOXA1 expressing cells. That being said, methylation of CpG island 123 within the gene body did not affect *FOXA1* expression in any of the luminal-like cell lines tested. These results indicate that while hypermethylation of CpG island 123 is not associated with reduced *FOXA1* expression, hypermethylation of CpG island 99 is associated with reduced FOXA1 expression in clinical bladder cancer samples and human cell lines. However, it is noteworthy to point out that the expression of FOXA1 may also be mediated by methylation patterns of CpG island shores, which consist of regions of low CpG density located up to 2kb distant from promoter CpG islands. Thus, further characterization is required to confirm the presence of CpG island shores in the proximity of FOXA1 gene and how they might be impacting gene expression. Moreover, the fact that nearby genes of *FOXA1* on chromosome 14 also exhibit a relatively weak correlation between copy

number status and gene expression, is suggestive that DNA methylation patterns affecting these regions may exist, and that other molecular mechanisms contribute to the silencing of *FOXA1* in MIBC patients and therefore warrant further investigation.

Many genes have been reported to be hypermethylated in bladder cancer; however, this study is the first to report an association between CpG island 99 hypermethylation and reduced *FOXA1* expression. Future characterization of the epigenetic regulation of *FOXA1* will require experimentation with a methylation inhibitor such as 5-azadeoxycytidine to assess if *FOXA1* expression can be restored in tumor cells. Alternatively, loss of function studies following knockdown or knockout of the methyltransferase enzymes, *DNMT1*, *DNMT3A*, and *DNMT3B*, followed by analysis (i.e., quantitative PCR and Western blot) of FOXA1 expression will enable us to potentially establish a cause-effect relationship between hypermethylation of CpG island 99 and *FOXA1* expression. However, a potential drawback of these experiments is that methyltransferase enzymes also mediate histone methylations in chromatin remodeling; therefore, aberrations of these genes may result in severe phenotypes preventing the assessment of a specific relationship between DNA methylation and *FOXA1* expression.

In addition to DNA methylation, microRNA regulation has been proposed as an alternative epigenetic regulator of the expression of *FOXA1* in bladder cancer[265]. Even though PTMs have been also proposed for FOXA1[333], there is no reported evidence of their impact on gene expression. Therefore, these analyses show that copy number alterations and promoter hypermethylation are alternative mechanisms for the control of *FOXA1* expression in bladder cancer heterogeneity.

PTEN expression is independent of molecular subtype and _FOXA1_ expression is associated with luminal subtype of bladder cancer

In a recent pan-cancer study, *PTEN* loss was clustered with "squamous-like" subtype tumors[189] characterized by squamous histological features and by the production of high molecular weight cytokeratins such as KRT5 and KRT14 found in basal tumor subtypes. As basal bladder cancers are often enriched of squamous differentiation and express high levels of KRT5 and KRT14, we utilized the TCGA MIBC cohort[155] to analyze *PTEN* expression in the context of molecular subtypes of bladder cancer. Surprisingly, we observed that *PTEN* expression was not associated with either basal or luminal molecular subtypes, and this was also evident in the hierarchical cluster analysis where *PTEN* expression was variable across patients from both basal and luminal subtypes. While these findings were surprising, our data suggest reduced *PTEN* expression is not associated with any specific molecular subtypes of bladder cancer.

Conversely, when we analyzed *FOXA1* expression in the context of molecular subtypes of bladder cancer using the TCGA cohort[155], we found that tumors with low *FOXA1* expression robustly clustered within the basal molecular subtype. These findings are in agreement with several previous reports in bladder cancer[172, 176]. Interestingly, reduced *FOXA1* expression is similarly associated with basal molecular subtype in breast cancer[214, 257, 334].

Urothelial differentiation is a tightly controlled process driven by a tissue-specific regulatory network in which FOXA1 and other transcriptional factors such as PPARG, GATA3, and ELF3 among other factors play a crucial role[197, 335, 336]. In keeping with their role as differentiation factors, alterations in their activity results in loss of differentiation with consequent loss of proper functionality of the urothelium[56]. Specifically, loss of *FOXA1* expression has been implicated in loss of differentiation[204, 337, 338] indicating a role for *FOXA1* in the maintenance of a differentiated status of the urothelium. Moreover, studies from Bernardo *et al.* reported a decrease in luminal-related genes with a subsequent increase in basal-related genes following silencing of

FOXA1 in several breast cancer cell lines[203]. On the other hand, Warrick *et al.* reported that combinatorial activity of the transcription factors, PPARG, FOXA1 and GATA3 in the basal-like 5637 bladder cancer cell line promoted the activation of a luminal transcriptional signature[213]. Therefore, given its functional role in urothelium, the loss of *FOXA1* appears to favor the activation and establishment of a basal expression profile, which results in an association of *FOXA1* inactivation with basal molecular subtype confirmed by our previous *in vivo* studies[205].

Bladder cancer heterogeneity is also evident through the different morphologic variants (i.e., urothelial cell carcinoma [UCC], squamous differentiation [SqD], glandular differentiation [GD], micropapillary). Co-occurrence of multiple histological variants within a single patient has also been reported posing challenges to disease treatment[181, 244, 245]. In our clinical cohort, approximately 72% (13 out of 18) of patients exhibited concomitant areas of UCC and SqD. In a recent study, Warrick *et al*. reported molecular heterogeneity among different histomorphologies[181]. Analysis of PTEN expression by IHC in our tumor samples revealed that low expression of PTEN is not associated with any particular morphology. These findings are consistent with the lack of correlation between *PTEN* expression and molecular subtype. As previously stated, the co-occurrence of multiple histology within an individual tumor can arise through the development of individual tumorigenic clones that expand in parallel, or through divergent clonal evolution. Thus, further characterizations based on phylogenetic tree studies such as those presented in Thomsen *et al.*[245] using exome-sequencing of bulk tumor may provide information about the potentially shared and unique altered molecular pathways in the morphologic variants.

Bladder-specific *Foxa1* and *Pten* knockout mice develop bladder cancer

Previous independent *in vivo* studies using GEMs have attempted to determine the functional significance of individual *Foxa1* or *Pten* loss in urothelial disease. Studies from Yoo *et al.* showed that conditional deletion of *Pten* in mouse urothelium results in a hyperplastic urothelium[191]. Similar studies from Tsuruta *et al.* showed that *Pten* deletion results in hyperplasia and promotes the development of papillary non-invasive bladder cancer after 24 weeks of BBN exposure[193]. On the other hand, Reddy *et al.* showed that inducible deletion of *Foxa1* in mouse leads to urothelial hyperplasia and keratinizing squamous metaplasia[205]. These studies indicate that, although individual ablation of *Foxa1* or *Pten* may drive pre-neoplastic changes, the interaction with other molecular events is necessary for tumorigenesis to occur. Supporting this line of reasoning, Puzio-Kuter *et al.* generated a conditional mouse model in which combined deletions of *Pten* and *Tp53* in bladder urothelium cooperate to promote invasive disease[192]. As might be expected, subsequent models investigating *Pten* deletion in combination with other molecular pathways (i.e., *Ctnnb1*, *Fgfr3*, and *Lkb1*) failed to develop phenotypes beyond hyperplasia or papillary non-invasive bladder cancer (Table 4-1). In particular, Foth *et al.* generated a conditional *Pten* knockout mouse model expressing a mutant *Fgfr3* to assess the interaction between these two pathways; however, this model developed solely hyperplasia even after 18 months[195]. Similarly, the model generated by Shorning *et al.* consisting of inducible deletion of *Pten* and *Lkb1* in the bladder urothelium developed hyperplasia[339]. On the other hand, the model created by Ahmad *et al*. consisting of a conditional knockout of *Pte*n model expressing mutant *Ctnnb1* developed hyperplasia and papillary tumors[194].

Table 4-1. *Foxa1* or *Pten* knockout models of bladder cancer.

Model name	Targeting approach	Description	Phenotype	Refs.
***Foxa1*$^{loxp/loxp}$**	*UBC-Cre/*^{ERT2}	Inducible deletion of *Foxa1*	Hyperplasia in male mice; keratinizing metaplasia in female mice	205
***Pten*$^{loxp/loxp}$**	*Fabp-Cre*	Conditional deletion of *Pten*	Hyperplasia	191
***Pten*$^{loxp/loxp}$**	*Fabp-Cre*	Conditional deletion of *Pten*	Hyperplasia, and Papillary non-invasive cancer after 24 weeks of BBN exposure	193
***p53*$^{loxp/loxp}$*; Pten*$^{loxp/loxp}$,**	Adeno-Cre (intravescical delivery)	Conditional deletion of *Pten* and *Tp53*	CIS, MIBC with SqD	192
***Ctnnb1*$^{exon3/exon3}$*; Pten*$^{loxp/loxp}$**	*UpII-Cre*	Expression of mutant (active) β-catenin combined with conditional deletion of *Pten*	Papillary non-invasive cancer	194
***Fgfr3*$^{+/K644E}$*; Pten*$^{loxp/loxp}$**	*UpII-Cre*	Expression of mutant (active) Fgfr3 combined with conditional deletion of *Pten*	Hyperplasia	195
***Lkb1*$^{loxp/loxp}$*; Pten*$^{loxp/loxp}$**	*AhCreER*	Inducible deletion of *Lkb1* and *Pten*	Hyperplasia	339

To assess if potential functional cooperativity may exist between *Foxa1* and *Pten* in urothelial tumorigenesis, we generated conditional bladder-specific *Foxa1* and *Pten* knockout mice. While single mutants of either *Foxa1* or *Pten* developed urothelial hyperplasia, mice with compound deletion of *Foxa1* and *Pten* developed focal CIS (18 out of 52 mice; 35%) after 12 months of age. Importantly, morphologic analysis of these tumors revealed a squamous differentiation phenotype, and characterization of urothelial differentiation markers by IHC indicated enrichment for basal-squamous urothelial cell markers. Thus, our results suggest that the loss of both *Foxa1* and *Pten* cooperates to promote tumorigenesis in the form of CIS with a basal-squamous phenotype.

Generally considered to be the precursor of MIBC, CIS is a high-grade aggressive non-invasive tumor. Histologically, in addition to the conventional urothelial CIS, variants of CIS with GD or SqD have been described[270, 340]. Because the occurrence of these entities is infrequent, our knowledge about the mechanisms driving these phenotypes is limited. Nonetheless, different studies have shown that CIS lesions are genetically characterized by loss of function mutations in *TP53, RB* and *PTEN*[341, 342], and are enriched of KRT20 expression, which is a luminal urothelial cell marker[133, 343]. Thus, a potential explanation for the phenotypes of our model could be that loss of *Pten* predisposes the bladder urothelium to pre-neoplastic changes, which in the absence of functional *Foxa1* progress to a malignant phenotype. Moreover, because Foxa1 is a urothelial differentiation transcription factor that promotes luminal urothelial differentiation, deletion of this gene may promote a basal expression phenotype as described in detail in the next paragraph.

In breast cancer, two models, which can be adapted to other tumors including bladder cancer, have been proposed for the description of molecular subtype heterogeneity: the "mutation-of-origin" and the "cell-of-origin". The "mutation-of-origin" model states that all subtypes of a tumor arise from any number of cellular progenitor populations. However, during neoplastic transformation, the occurrence of specific genetic or epigenetic alterations commits the tumor cell to a specific fate/lineage (i.e., luminal versus basal) in a manner independent of the cell of origin. Put simply, a specific genetic alteration always results in "luminal" tumors, while another results in "basal" tumors. On the other hand, "the cell-of-origin" model hypothesizes that transformation-inducing genetic and epigenetic alterations while resulting in tumorigenesis have no effects on the cell differentiation program. Therefore, according to the "cell-of-origin" model, the resultant tumor retains the original, lineage-related transcriptional program[122]. So, as previously described, in our clustering analysis of the TCGA dataset and the IHC analysis of clinical samples, the expression of *PTEN* did not correlate with either molecular subtype or morphology - contrary to the expression of *FOXA1*. *In vivo* experimentations using lineage-trace methods have shown that basal urothelial

cells give rise to squamous tumors exhibiting a basal gene expression profile following carcinogen exposure[113]. However, in our *Foxa1 and Pten* double mutants characterized by deletion of these genes in luminal urothelial cells, we detected higher levels of markers of basal urothelial cells and squamous elements than in the single mutants. If our reasoning that loss of the urothelial differentiation marker *Foxa1* is the driving force that promotes activation of a basal profile, and therefore determines the tumorous cell lineage fate, then our results support a "mutation-of-origin" theory in regards to the role of *FOXA1* in bladder cancer molecular subtype and squamous differentiation phenotype. Therefore, in our *Foxa1 and Pten* double mutants, while *Pten* inactivation may indeed provide the incentive for tumor growth, *Foxa1* inactivation promotes the development of squamous phenotype.

Our mouse model was generated using uroplakin 2 promoter-driven Cre (*UpII-Cre*), and because *UpII* is active in intermediate and luminal urothelial cells only, Cre expression and recombination occur in intermediate and luminal cells of the bladder. So, based on this, our results indicate that *UpII*-mediated deletion of *Foxa1 and Pten* in the intermediate and luminal urothelium results in the development of CIS with a basal-squamous phenotype. Interestingly, our findings contrast with the widespread belief that intermediate/luminal cells give rise to papillary tumors and that basal cells are likely the cell of origin for CIS and progressive tumors derived from CIS with basal phenotypes. Our study shows that upon the occurrence of certain genetic alterations in intermediate/luminal cells, these cells are capable of giving rise to CIS of the bladder with basal phenotype. However, it is also possible that ablation of *Foxa1 and Pten* in luminal urothelium may lead to loss of the luminal layer cells resulting consequently in the expansion of basal urothelial cells to differentiate and repopulate the urothelium. As the basal cells differentiate into luminal cells, *UpII-Cre* is activated and subsequently promotes deletion of *Foxa1* and *Pten*. The circling repetition of this process may eventually lead to genetic instability of the basal urothelial cells, prone to alterations that promote the development of CIS. Therefore, future studies based on

lineage-tracing approaches incorporating the use of a basal cell Cre driver (i.e., *Krt5-Cre*) and a luminal cell Cre driver (i.e., *UpII-Cre*) in combination with Rosa26 reporters will be required to definitively confirm intermediate/luminal urothelium and not basal urothelial cells as the progenitor cell population for bladder cancer development following *Foxa1 and Pten* knockout.

To definitively conclude that intermediate/luminal cell populations can serve as progenitors of CIS, one potential approach would be to perform lineage tracing studies that will enable us to track and assess the fraction of intermediate/luminal transformed cells within the tumors following *Foxa1* and *Pten* knockout. Alternatively, we could dissect and smash tumors and normal bladder from *Foxa1* and *Pten* knockout mice and genetic control mice, respectively; use FACS to sort for intermediate/luminal cell populations (using Krt20 and UpII as markers) and basal cell populations (using Krt5 and Tp63 as markers). RNA-seq analysis on RNA isolated from these cells could be informative in the assessment of similarities and changes in the expression patterns between intermediate/luminal cells and basal cells upon *Foxa1* and *Pten* deletion. Moreover, since *Foxa1* and *Pten* knockout mice develop CIS after 12 months of age, we could sort basal and intermediate/luminal cells at an earlier time point of study (i.e., from the bladders of 2 months old mice) and also at a later time point of study after tumor formation (i.e., from the bladders of 12 months old mice) and genotype them. This will enable us to show if truly *Foxa1* and *Pten* knockout cells have transitioned from luminal phenotype to basal phenotype, and whether other additional genetic events promoting basal phenotype have occurred. This is important because it will enable us to (1) directly test the ability of luminal/intermediate cells to contribute to the development of basal-squamous tumors following a known set of genetic alterations, and (2) rule out the possibility that expansion of basal bladder urothelium contributes to tumor development following genetic ablation of *Foxa1* and *Pten* in intermediate/luminal urothelium.

Sex is a widely known risk factor for bladder cancer exhibiting higher incidence rates in men than women[40]. Notably, this sexual dimorphism regarding risk is partially mirrored in chemical

carcinogenesis studies of bladder cancer. Specifically, exposure of mice or rats to BBN carcinogen results in relatively rapid tumorigenesis in male mice compared with female mice[258, 344]. However, when we combined our GEM with a carcinogenesis model, we observed an increase in susceptibility not only in male *Foxa1* and *Pten* knockout mice, but also in female mice. Specifically, both male and female mice developed MIBC with SqD in a manner apparently independent of sex. Thus, deletion of *Foxa1* and *Pten* increases mice susceptibility to BBN carcinogen and enhances the carcinogenic effects leading to more exacerbated phenotypes when compared with the genetic control.

FOXA1 plays a central role in tissue-specific gene expression. By recruiting and interacting with sex steroid receptors such as estrogen receptors (ESR1; Esr1) and androgen receptor (AR; Ar) at the promoter of their target genes, FOXA1 promotes the differentiation of mammary and prostate epithelium, respectively[209]. The role of sex hormones in bladder tumorigenesis is of a major interest in the bladder cancer field. Several studies have shown that knockout of *Esr2* in the bladder urothelium of female mice decreases tumorigenesis in a BBN-model[345]; similarly, deletion of *Ar* in the bladder urothelium of male and female mice reduces tumorigenesis in a BBN-model[260]. Together these studies implicate a role for Esr1/2 and Ar in bladder cancer development. Moreover, the evidence that ablation of *Foxa1* in mouse liver combined with deletion of *Foxa2* can reverse sexual dimorphism in response to a liver-specific carcinogen in a manner related to interactions with Esr1[47] suggests that the interaction between Foxa1 and sex steroid receptors is an important determinant in the sexual dimorphic nature of cancer incidence following carcinogen exposure. Therefore, in our model, the loss of *Foxa1* could be driving the ability of the *Foxa1* and *Pten* knockout mice to overcome sex differences when exposed to BBN. While this could be true for double mutants *Foxa1* and *Pten* and single mutants of *Foxa1*, a different mechanism has to be responsible for the phenotypes of the single mutants of *Pten*.

The activity of BBN carcinogen has been widely characterized to induce genetic alterations in genes such as *Tp53, Hras,* and *Egfr* among other genes[230, 346]. Therefore, the development of MIBC with SqD in our *Pten* knockout mice following carcinogen exposure could be the result of an aberrant PI3K pathway activity following BBN-induced mutagenesis, which potentially cooperates with conditional inactivation of *Pten.* In our *Foxa1* knockout models, the development of MIBC with SqD in male and female mice could be a result of defective urothelial differentiation process associated with inactivation of pro-apoptotic pathways following carcinogen exposure. As any number of these mechanism(s) could cooperate in our compound knockout mice, additional work is required to identify the exact pathways involved. Performance of whole genome-sequencing on DNA extracted from the murine tumors will provide insight into genes that are additionally altered in the urothelium of *Foxa1* and *Pten* mice and the related molecular pathways that might be contributing to the aggressive phenotypes.

All *Foxa1* and *Pten* knockout mice as well as all genetic controls in this study are generated and maintained on a mixed background by breeding C57BL/6 strain mice with FVB strain mice, two of the most commonly used strains for the generation of GEMs in bladder cancer. Although all controls were littermates of experimental mice, and therefore on a largely similar genetic background, we were interested in the relationship between strain genetic background and susceptibility to BBN. Thus, we initiated a tumorigenesis study based on exposure of C57BL/6 and FVB strain mice to equal concentrations of BBN carcinogen. These two mouse strains exhibited diverse phenotypic behaviors following exposure to BBN. While C57BL/6 mice developed non-invasive papillary tumors at 12 weeks of carcinogen treatment, FVB developed muscle invasive tumors with SqD and GD at 12 weeks of treatment. Nonetheless, advanced disease phenotypes were also observed in C57BL/6 at 16 and 20 weeks of BBN treatment. An RNA-seq analysis of these tumors revealed a differential expression in immune signatures with FVB mice exhibiting highly inflamed and immune reactive tumors than C57BL/6 mice. Interestingly, both C57BL/6 and

FVB showed increased levels of PDL-1 in their tumors. However, the inflamed and immunogenic tumor microenvironment of the FVB mice makes the use of this mouse strain in a carcinogen-based model optimal for the study and characterization of PDL-1 immune checkpoints inhibitors, which seems to hold promise in bladder cancer treatment based on clinical trials results[95, 179].

In the *Foxa1* and *Pten* knockout mice, the gene-targeted alleles are maintained on the C57BL/6 background whereas the *UpII-Cre* locus is maintained on the FVB background. Evidence shows that phenotypic variations on a mixed genetic background are mainly influenced by the genetic background on which the gene-targeted alleles are placed[347, 348]. Therefore, we conclude that the expressivity of FVB background in the *Pten* and *Foxa1* knockout mice is not a major cofounder of the observed phenotypes in our combined GEM-carcinogen model.

FOXA1 but not *PTEN* inhibits cell growth and promotes apoptosis in bladder cancer cell lines

To complement our clinical and *in vivo* data, we initiated *in vitro* experimental studies to identify the potential mechanism(s) through which *FOXA1* and *PTEN* loss might cooperate in bladder cancer to promote tumor progression and heterogeneity. In that regard, we performed rescue studies by overexpressing human wild-type *FOXA1* and *PTEN* in UMUC3, a cell line that does not express either *PTEN* or *FOXA1*, and in 5637, a cell line that expresses low levels of *PTEN* and undetectable levels of *FOXA1*.

The effects of *FOXA1* and *PTEN* overexpression were evident on cell viability. Specifically, overexpression of *FOXA1* alone or combined with *PTEN* resulted in decreased cell viability and induction of apoptosis. Surprisingly, overexpression of *PTEN* alone seems to have effects neither on cell viability nor apoptosis. As a tumor suppressor, PTEN inhibits the activation of AKT in the PI3K signaling pathway, and thus blocks cell proliferation and survival[349]. Potential

explanations for the inability of PTEN to suppress cell viability or induce apoptosis include (1) the PI3K pathway is constitutively activated downstream of AKT in these cell lines used; (2) a parallel pathway (i.e., MAPK pathway) serves as a strong controller of cell proliferation and survival, and therefore *PTEN* overexpression has no effect; or (3) PTEN undergoes PTMs leading to its inactivation. Overexpression of *PTEN* in bladder cancer cell lines followed by pharmacological treatment (i.e., MAPK pathway inhibitor) studies could be used to test the hypothesis of an active parallel pathway. Alternatively, knockdown of *PTEN* in bladder cancer PTEN expressing cell lines could be used to assess the impact of the decreased expression of this tumor suppressor on cell viability and apoptosis.

On the other hand, these experimental results suggest a role for the urothelial transcription factor FOXA1 in cell growth and apoptosis. Wolf *et al.* previously reported growth inhibitory activities for FOXA1 in breast cancer[350], and identified potential mechanisms by which FOXA1 exerts its inhibitory function. The two proposed mechanisms consist of (1) activation of the transcription of *CDKN1B* (p27), and (2) differential regulation of ESR1-associated pathways. Activation of p27, a cyclin-dependent kinase inhibitor involved in cell cycle regulation, promotes cell cycle arrest. Through electromobility shift assays and reporter assays, Williamson *et al.* showed that FOXA1 binds directly to the promoter of p27 and promotes its transcription contributing therefore to cell proliferation arrest[351]. The second mechanism proposed by Wolf *et al.* consists of a cell-type dependent regulation of the ESR1 pathway by FOXA1. Using an ERE-luciferase reporter in conjunction with a *FOXA1* expression construct and estrogen treatment, the authors showed that FOXA1 overexpression in ESR1 positive breast cancer cell lines (MCF-7, BT-474) inhibits ESR1 pathway and decreases cell proliferation whereas FOXA1 overexpression in ESR1 negative breast cancer cell line (MDA-MB-23) activates the ESR1 pathway[350]. Thus, our observation of FOXA1 overexpression-mediated decreases in cell viability in the bladder cancer

cell lines (UMUC3 and 5637) is in keeping with these studies, although further investigations are needed to confirm a cell growth inhibitory function for FOXA1 in bladder cancer.

Additionally, a pro-apoptotic role has been proposed for FOXA1 in bronchial cells. By using similar approaches as Koeffler and colleagues, Song *et al.* showed that FOXA1 binds directly to the promoter of *BCL-2* and inhibits its anti-apoptotic activity to induce cell death[274]. BCL-2 is a member of the BCL family of apoptosis regulatory proteins, which can be subdivided into two groups: the anti-apoptotic/pro-survival proteins and the pro-apoptotic proteins[352]. As an anti-apoptotic protein, BCL-2 is often upregulated in cancer including bladder cancer as a survival mechanism[275]. In our study, however, *FOXA1* overexpression did not affect BCL-2 expression suggesting a non-BCL-2 dependent mechanism. As further studies are required to explore the pro-apoptotic function of FOXA1, one approach could be to experimentally reduce FOXA1 expression in bladder cancer cells followed by stress-induced treatment such as treatment with cisplatin or UV radiation to activate apoptosis. Both cisplatin and UV-induced DNA damage are associated with DNA adduct formation, which, if not properly repaired, can lead to genome damage and therefore induction of cell death. Thus, the efficiency of DNA repair is critical to avoid apoptosis. If FOXA1 expression is required for the induction of apoptosis, then we would expect depletion of *FOXA1* to render cells resistant to cisplatin treatment and other forms of environmental stress, and thus block apoptosis. A mechanism by which this could potentially be occurring is through enhancement of DNA repair systems. By mapping the location of DNA damage and repair in control and knockdown cells using the "Damage-seq" and "eXcision Repair-seq" approaches[353], we could infer if a biological relationship exists between FOXA1, apoptosis and DNA repair.

Summary

By integrating *in vivo* animal experimentation with correlative human clinical data and *in vitro* cell line experimentation, we show in this dissertation that copy number alterations of *PTEN* and site-specific DNA hypermethylation of *FOXA1* are correlated with reduced gene expression, and potentially contribute to morphologic and molecular tumor heterogeneity in bladder cancer. Moreover, low *PTEN* expression is not associated with either basal or luminal molecular subtypes of bladder cancer, neither is it related to morphologic variants (UCC or SqD) of bladder cancer. On the other hand, low expression of *FOXA1* is specifically associated with basal molecular subtype of bladder cancer, and we previously reported that reduced *FOXA1* expression is associated with SqD and SCC morphologic variants[204]. We also provide evidence of cooperativity between *Foxa1* and *Pten* inactivation in the development of CIS with elements of heterogeneity in the form of SqD. Specifically, we show that genetic ablation of *Foxa1 and Pten* in intermediate/luminal cells promotes tumorigenesis in the form of CIS with a basal-squamous phenotype. Owed to its tumor suppressor function, we conclude that *Pten* inactivation promotes tumor onset while inactivation of the urothelial differentiation factor, *Foxa1*, may be supporting a divergent evolution of luminal cells into SqD with basal phenotype. Interestingly, alterations of *Foxa1 and Pten* abrogate the sexual dimorphism associated with BBN exposure, as both male and female mice develop MIBC with SqD. Additionally, we provide preliminary *in vitro* experimentation data suggesting a role for *FOXA1* in apoptosis in bladder cancer cell lines.

Based on these observations, we propose the following model (Figure 4-1) to describe the role of *FOXA1* and *PTEN* in MIBC heterogeneity. Because loss of *FOXA1* and *PTEN* is primarily detected in advanced stage bladder cancer (≥ pT2; MIBC), we propose that MIBC with a UCC phenotype can be characterized by the presence of heterogeneous cell populations where the majority of cells express wild-type *FOXA1* and *PTEN* and present a urothelial gene expression

pattern. In these cell populations, through molecular mechanisms that are yet to be unraveled, *FOXA1* and *PTEN* activities regulate urothelial differentiation and maintain homeostatic control of apoptosis and cell survival (Figure 4-1, Step 1). However, the occurrence of certain genetic and epigenetic alterations in a subset of the tumorous cells inhibits the expression of *FOXA1* and *PTEN*. These alterations lead to changes in the urothelial gene expression pattern with inhibition of apoptosis and promotion of cell survival. Importantly, the loss of the urothelial differentiation factor, *FOXA1*, commits the urothelial cells to a basal and squamous expression phenotype (Figure 4-1, Step 2). Moreover, supporting a divergent "clonal evolution" process, as the disease progresses, a subclone of cells with aberrant *FOXA1* and *PTEN* function acquires additional genetic and epigenetic alterations leading to genetic instability and increased proliferation (Figure 4-1, Step 3). The interactions between *FOXA1* and *PTEN* inactivation with other genetic alterations promote the establishment of SqD phenotype in these subclones (Figure 4-1, Step 4). Thus, *FOXA1* and *PTEN* inactivation contribute to bladder cancer tumor heterogeneity by potentially mediating divergent clonal expansion of pre-neoplastic transformed cells.

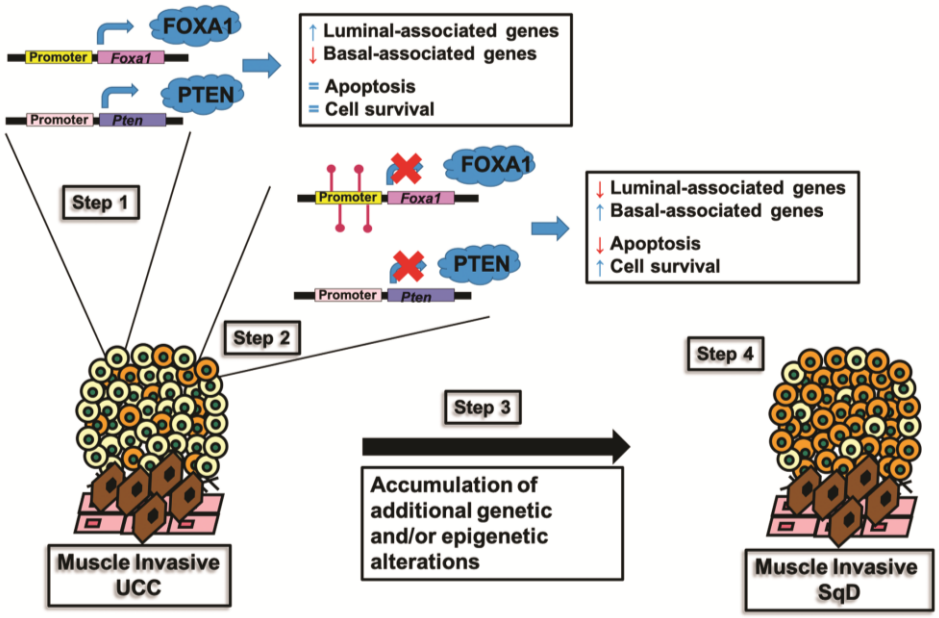

Figure 4-1. Proposed model for FOXA1 and PTEN role in MIBC heterogeneity and progression.

Moreover, we report that C57BL/6 and FVB mice, two of the commonly used mouse strains for the generation of GEMs including our *Foxa1* and *Pten* knockout model, exhibit diverse phenotypes in a BBN-model paradigm. Specifically, we observed that after 12 weeks of BBN exposure, FVB mice develop aggressive and invasive bladder tumors with SqD and GD. The FVB mice were more susceptible to BBN than C57BL/6 mice as the latter develop advanced and invasive disease after 16 and 20 weeks of BBN exposure. In our *Foxa1* and *Pten* knockout model, all controls were littermates of experimental mice, and therefore presented similar genetic background. Nevertheless, this study highlights the importance of accounting for the phenotypic variability associated with pure strain genetic background when dealing with combined GEM and carcinogen-model studies utilizing mixed genetic background.

Overall, even though additional studies are needed to unravel the functional relationship between *FOXA1* and *PTEN*, and how their molecular pathways might converge and cooperate in bladder cancer tumorigenesis and progression, this work highlights a role for *FOXA1* and *PTEN* in promoting bladder cancer heterogeneity in regards to molecular subtype, genomic alterations, and cellular phenotype.

Conclusion

Genetic and epigenetic alterations can have diagnostic value[354]. Assessment of DNA methylation is reported to be more sensitive than cytology in disease detection, and because DNA methylation can be detected in patients with early-stage disease, it presents as a useful tool for early detection of disease[355]. Therefore, the evidence from our study showing that promoter hypermethylation is potentially contributing to *FOXA1* silencing in bladder cancer tumors sets the basis for the inclusion of FOXA1 in the list of biomarkers for disease detection. Nonetheless, additional studies are required to confirm a cause-effect relationship between promoter hypermethylation and *FOXA1* inactivation.

Because most of our clinical knowledge about bladder cancer is derived from retrospective studies showing that alterations in both *FOXA1* and *PTEN* genes are detected mainly in advanced stage diseases at the time of clinical presentation, a definition of the time and order of occurrence of these alterations and how they may have affected disease initiation or progression is limited. Nonetheless, the combined *Foxa1 and Pten* knockout model in our study underscores the importance of this transcriptional regulator and this tumor suppressor in bladder tumorigenesis and provides the field with a new model for tumorigenesis and chemical carcinogenesis studies. This model could be particularly useful for the testing of targeted therapeutics such as that of the PI3K pathway.

Additionally, while more research is required, molecular subtypes of bladder cancer appear to exhibit differential sensitivities to specific therapeutic approaches. Specifically, although patients with luminal subtype disease have better clinical outcomes, patients with basal-squamous subtype of bladder cancer seem to respond to cisplatin-based chemotherapy, but poorly to immune checkpoint blockade[176, 180, 283]. Importantly, the inability to predict which patients will be responsive to multimodal chemotherapy and distinguish them from patients who will not respond highlights

the need for better prognostic factors. Although alterations in both *FOXA1* and *PTEN* have been associated with poor survival outcome[192, 205], these two genes are yet to be assigned risk and prognostic significance, which could be potentially attained through prospective studies.

Appendices

Appendix A Histology of *Foxa1* and *Pten* knockout mice at higher resolution

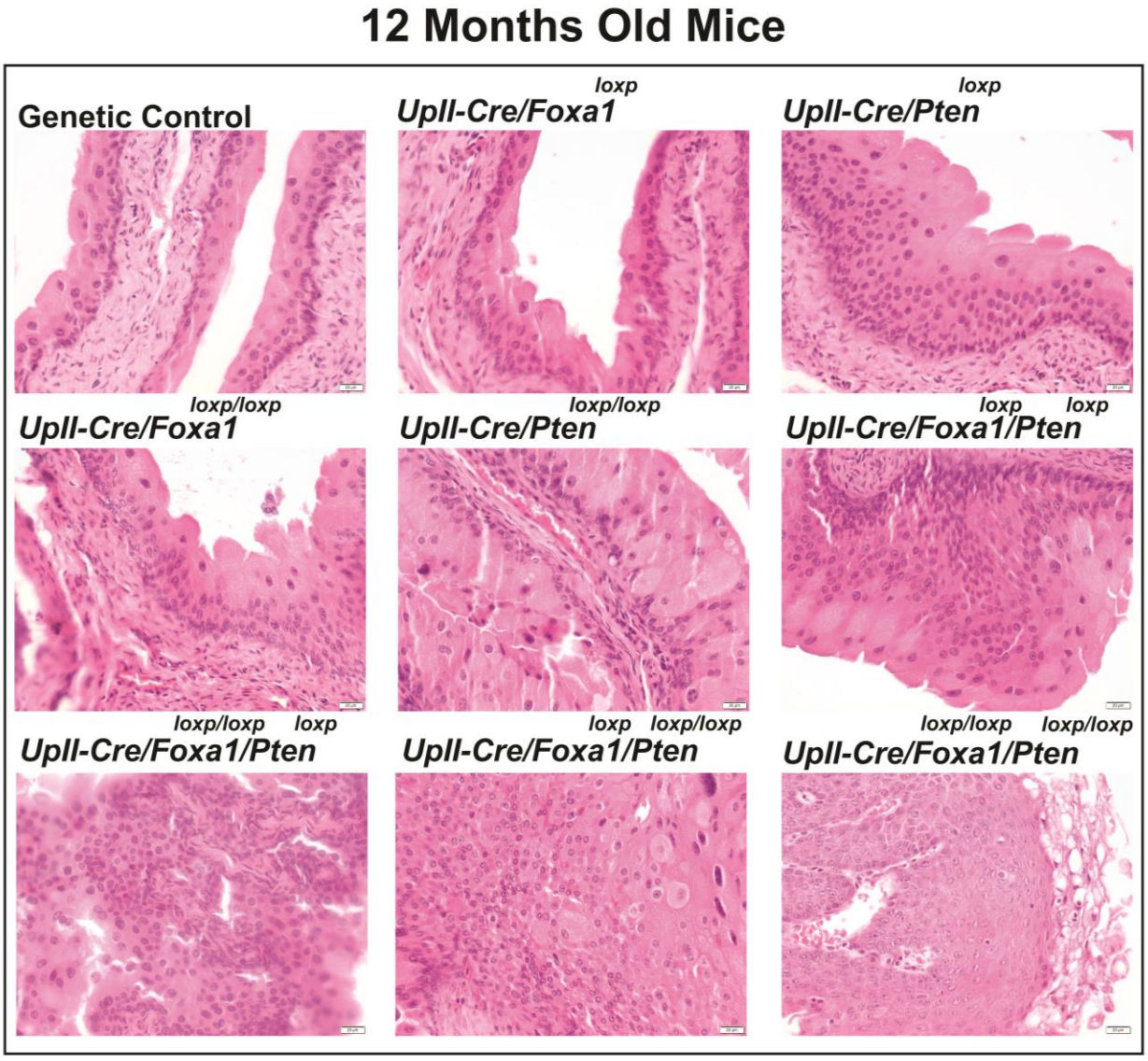

Figure A1. Histology at higher resolution of *Foxa1* and *Pten* knockout mice at 12 months old.

Shown are the histology at higher resolution of panels from C to K in Figure 2-5. Scale bar: 20 μm.

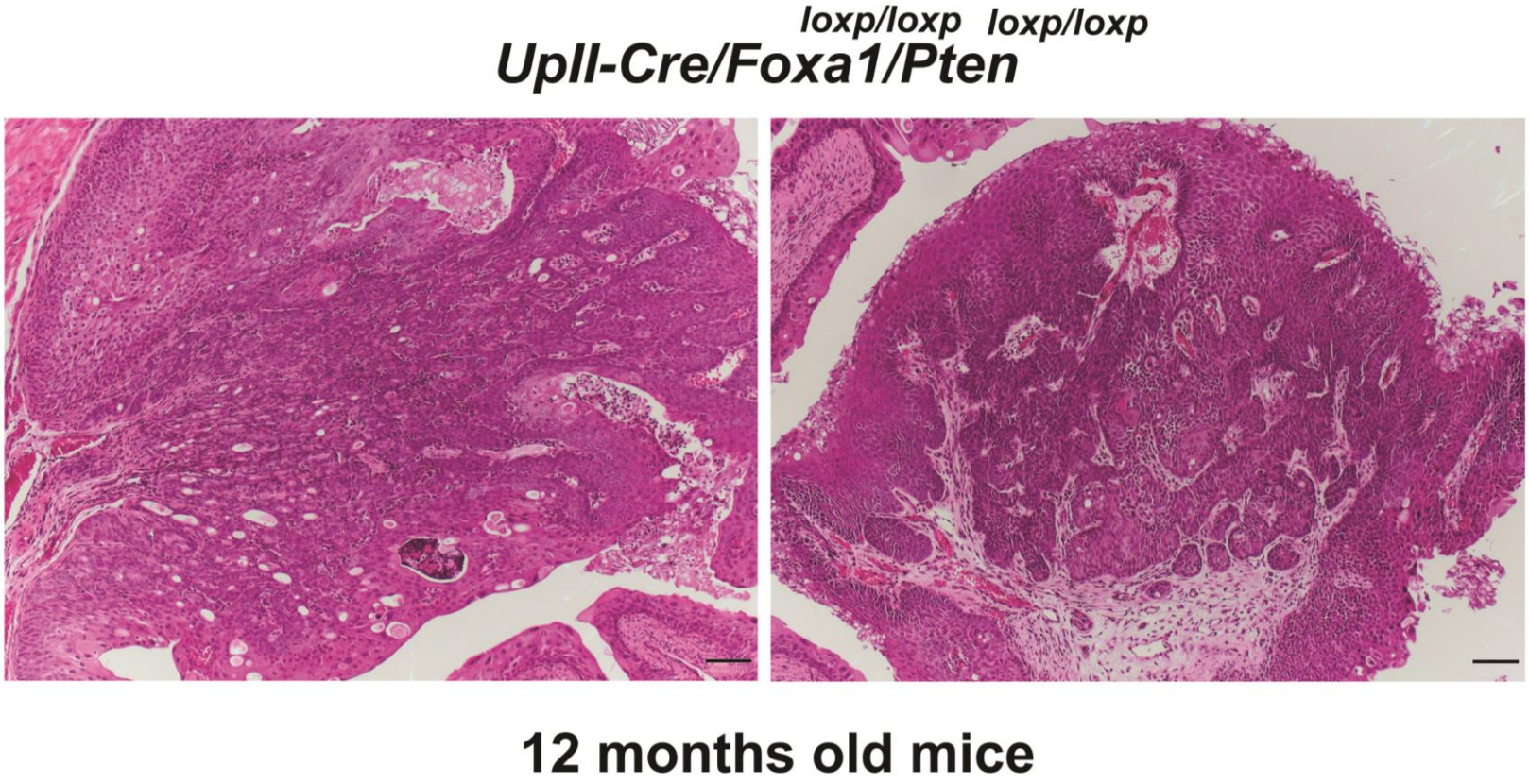

Figure A2. Histology at higher resolution of *Foxa1* and *Pten* double knockout mice at 12 months old.
Shown are the histology at higher resolution of panels L and M in Figure 2-5. Scale bar: 100 μm.

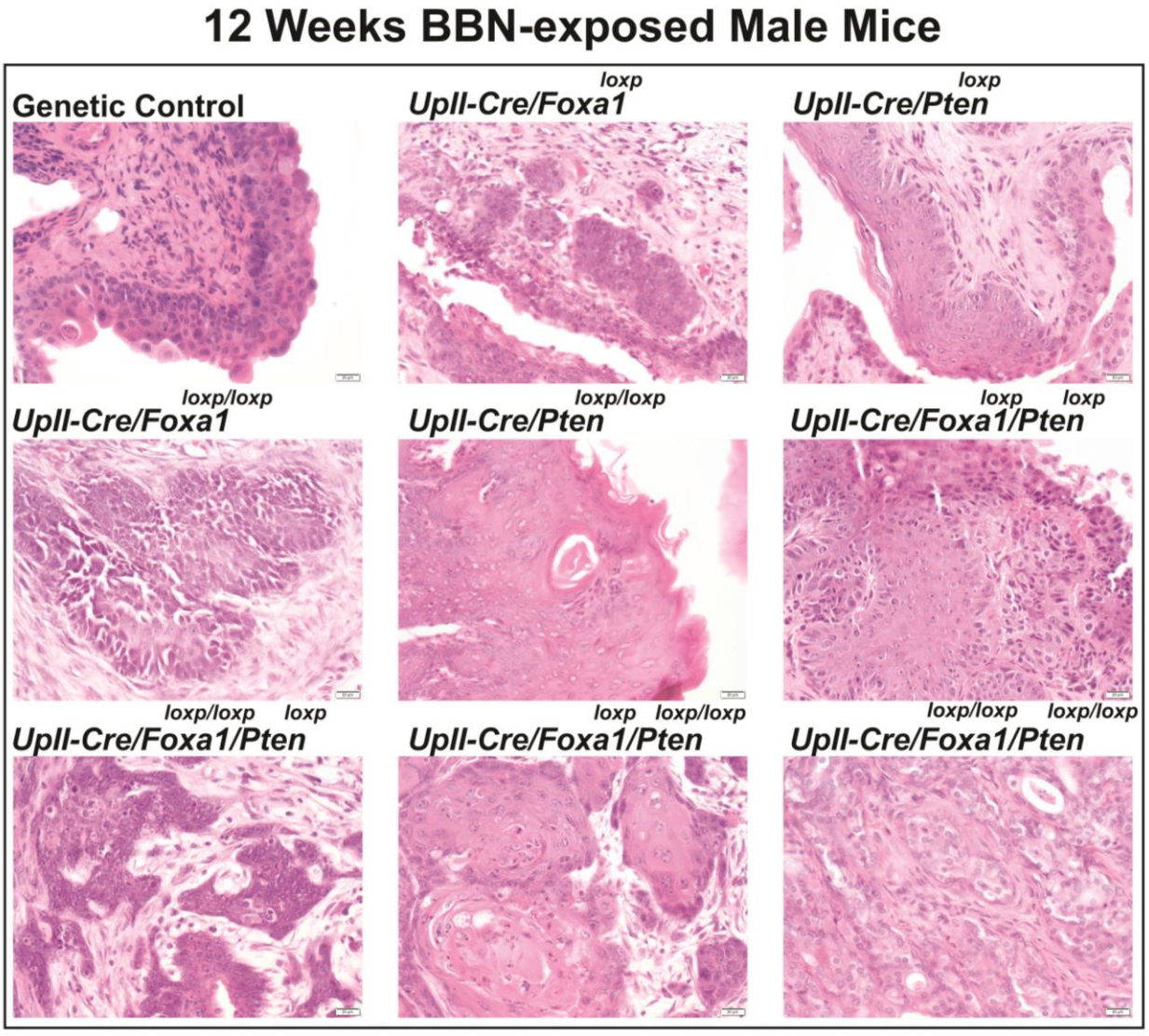

Figure A3. Histology at higher resolution of *Foxa1* and *Pten* knockout male mice after 12 weeks of BBN exposure.

Shown are the histology at higher resolution of panels from C to K in Figure 2-7. Scale bar: 20 μm.

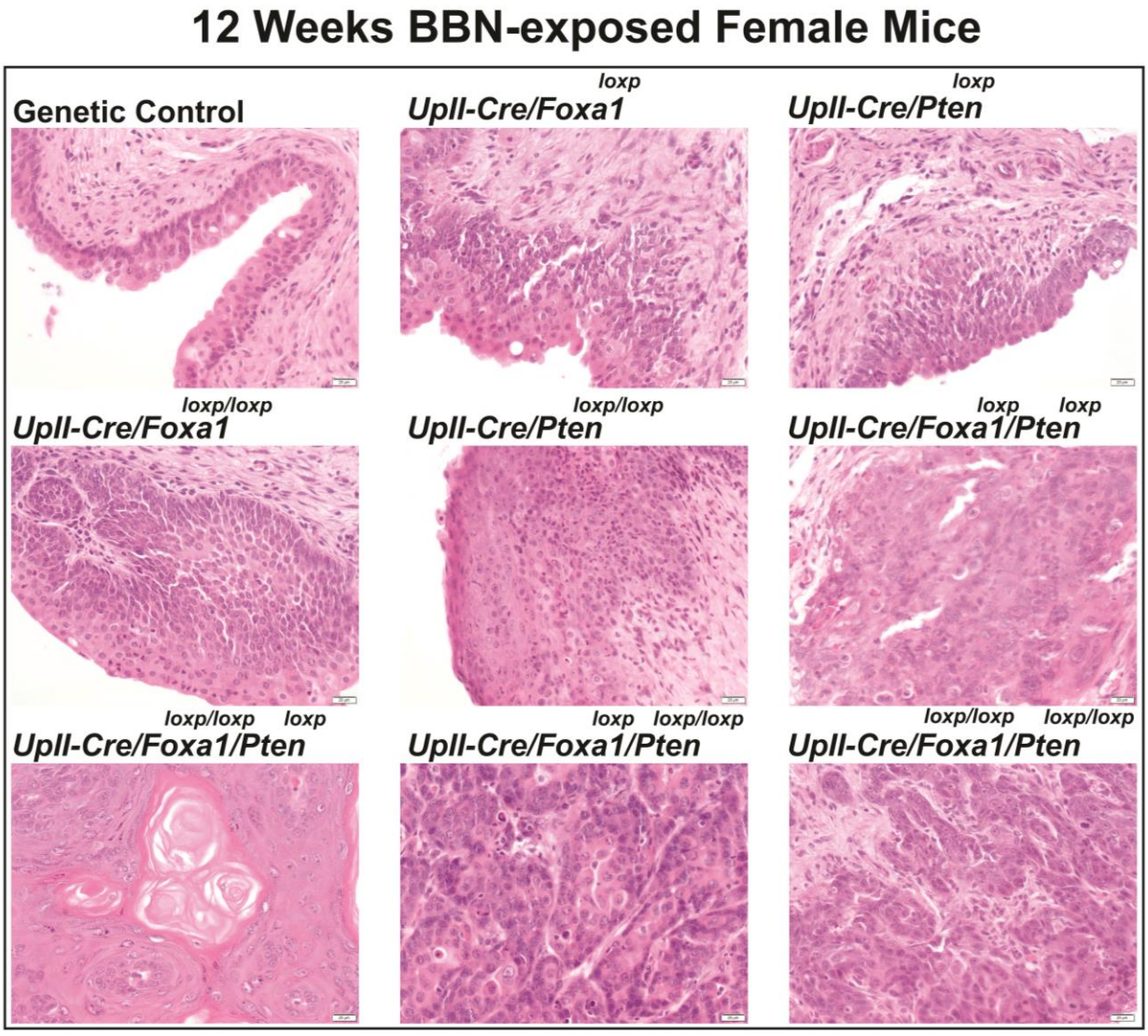

Figure A4. Histology at higher resolution of *Foxa1* and *Pten* knockout female mice after 12 weeks of BBN exposure.

Shown are the histology at higher resolution of panels from M to U in Figure 2-7. Scale bar: 20 μm.

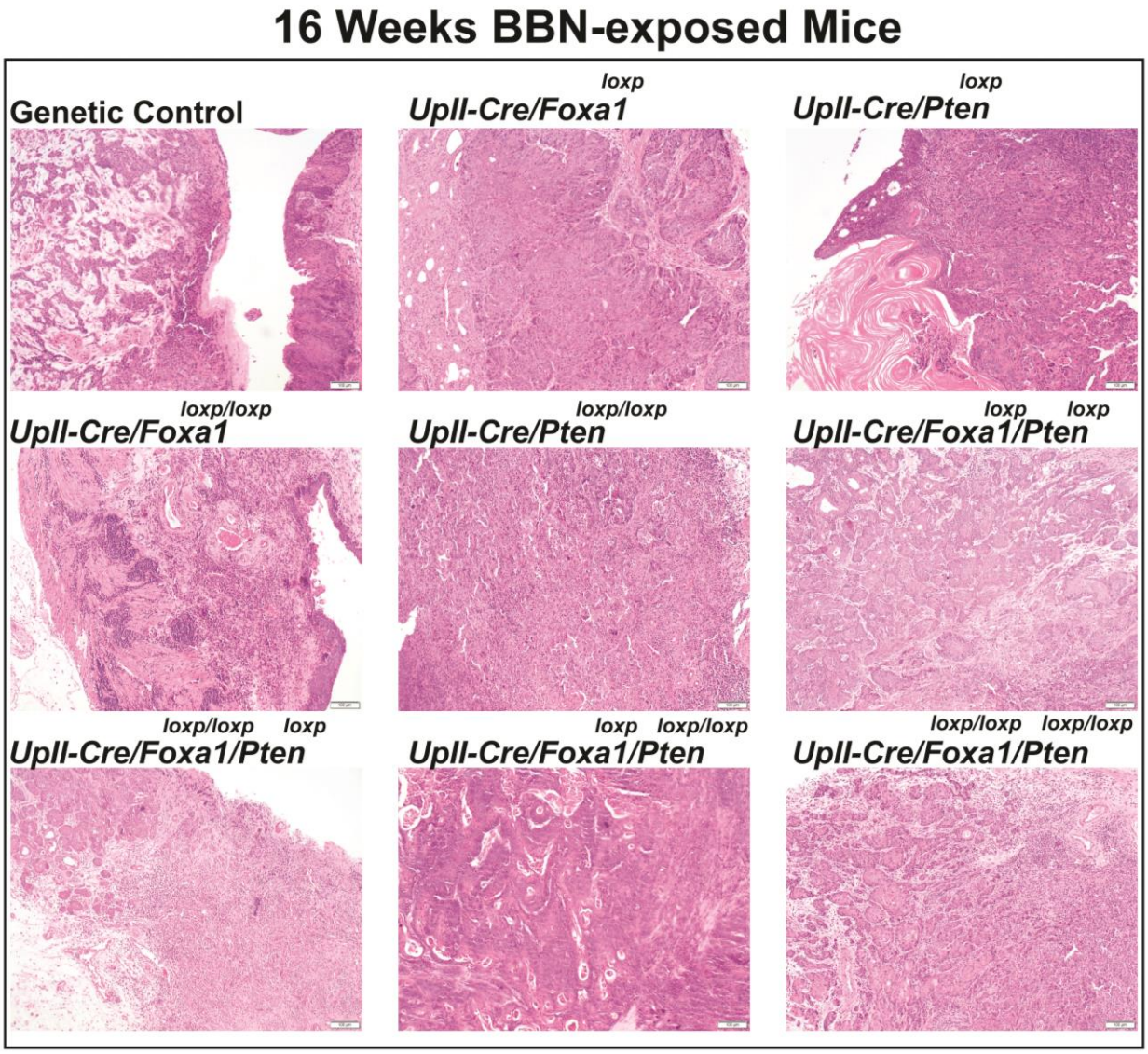

Figure A5. Histology of *Foxa1* and *Pten* knockout mice after 16 weeks of BBN exposure.

Shown are the histology of combined male and female *Foxa1* and *Pten* knockout mice. After 16 weeks of BBN exposure, genetic control mice also exhibit invasive disease (≥ pT1) as the experimental mice; this indicates that at this time point the BBN effects supersede those of the genetic alterations in *Foxa1* and *Pten*. Scale bar: 100 μm.

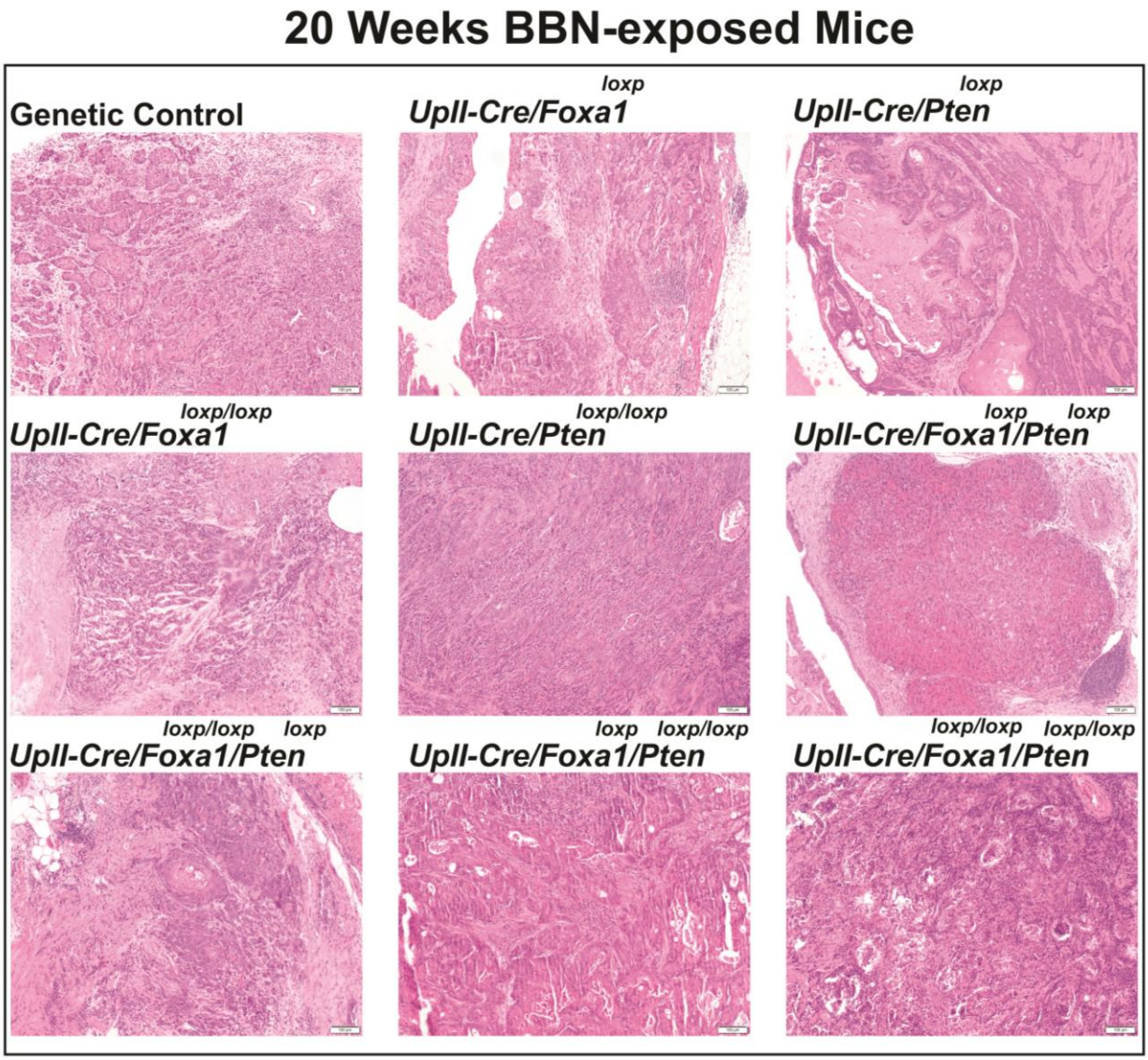

Figure A6. Histology of *Foxa1* and *Pten* knockout mice after 20 weeks of BBN exposure.

Shown are the histology of combined male and female *Foxa1* and *Pten* knockout mice. After 20 weeks of BBN exposure, genetic control mice also exhibit invasive disease (≥ pT1) as the experimental mice; this confirms that after 16 and 20 weeks exposure to BBN, the effects of this carcinogen supersede those of the genetic alterations in *Foxa1* and *Pten*. Scale bar: 100 μm.

Appendix B PARP cleavage in the UMUC3 and 5637 bladder cancer cell lines

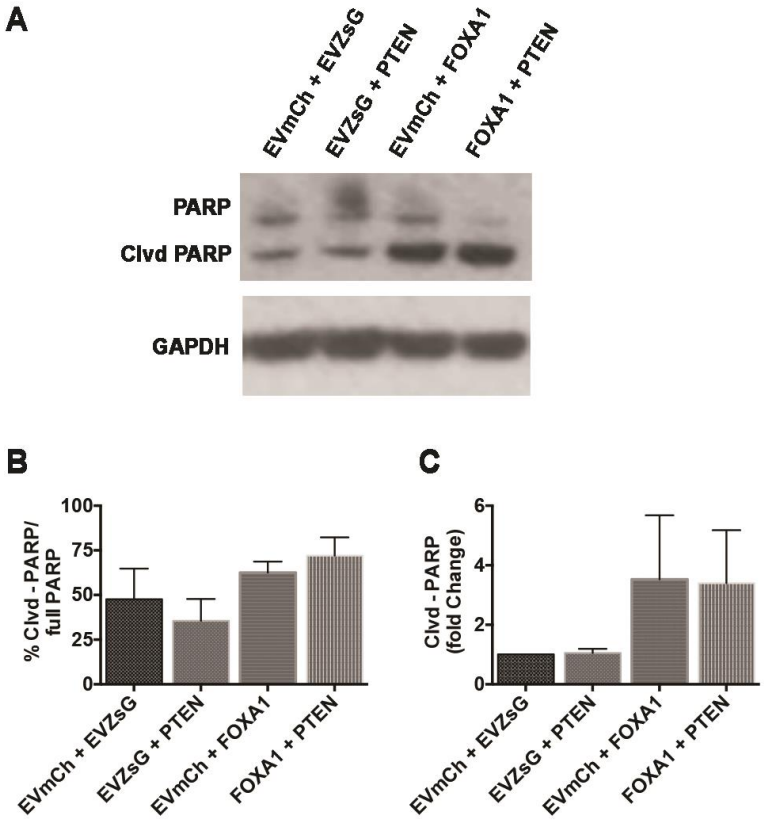

Figure B1. Overexpression of human *FOXA1* in the UMUC3 cell line promotes cleavage of PARP. (**A**) Western blot showing cleaved (clvd) apoptotic marker PARP and GAPDH loading control. (**B**) Percentage of clvd-PARP over full length PARP. (**C**) Fold change of clvd-PARP over GAPDH. All experiments were performed and repeated three times.

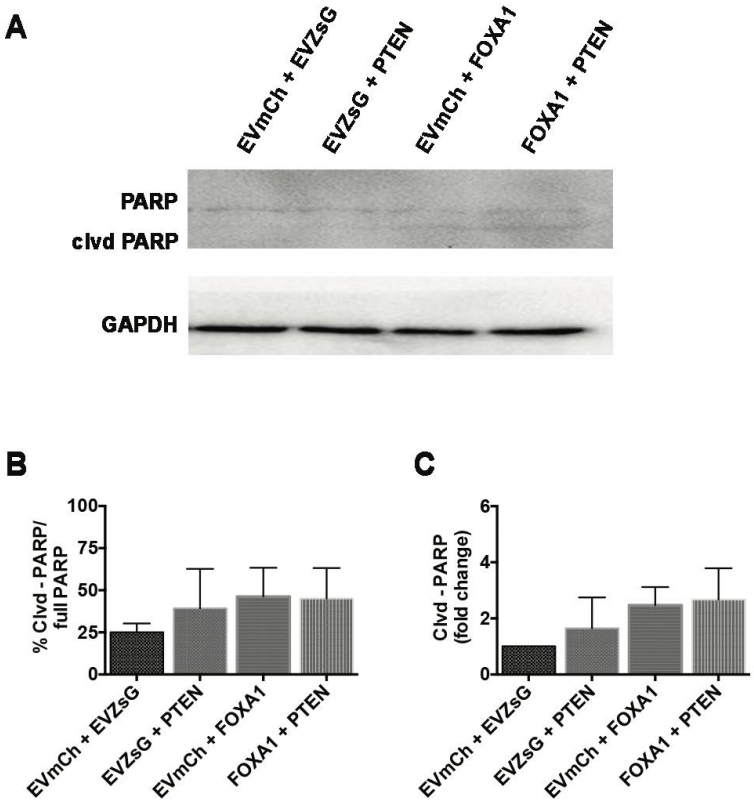

Figure B2. Overexpression of human *FOXA1* in the 5637 cell line promotes cleavage of PARP. (**A**) Western blot showing cleaved (clvd) apoptotic marker PARP and GAPDH loading control. (**B**) Percentage of clvd-PARP over full length PARP. (**C**) Fold change of clvd-PARP over GAPDH. All experiments were performed and repeated three times.

Appendix C Impact of *FOXA1* overexpression on PDL-1 expression

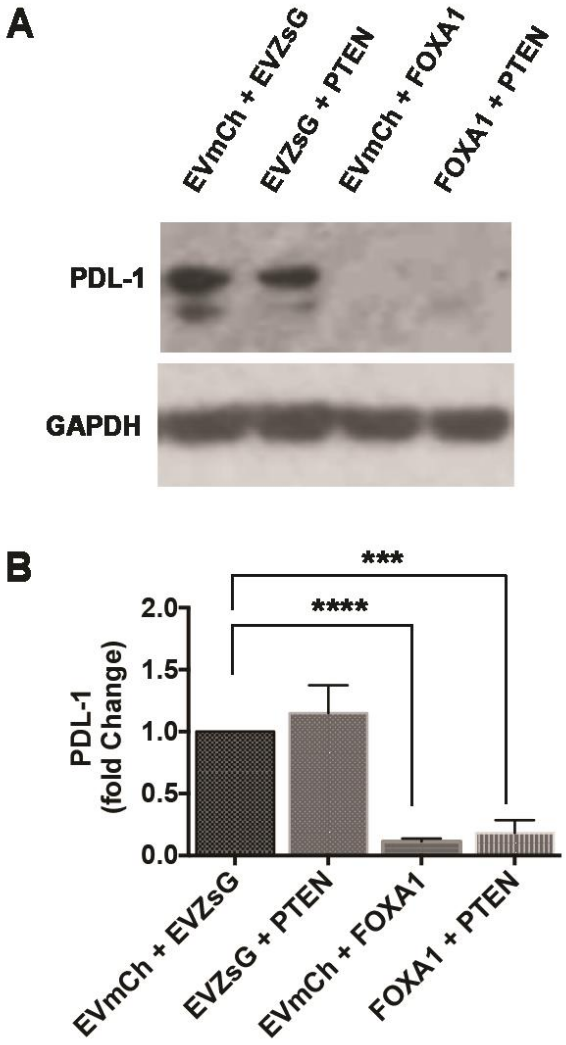

Figure C. Overexpression of human *FOXA1* in the UMUC3 cell line decreases PDL-1 expression.

(**A**) Western blot showing PDL-1 expression and GAPDH loading control. (**B**) Fold change of PDL-1 over GAPDH. All experiments were performed and repeated three times (****p-value ≤ 0.0001; *** p-value ≤ 0.001; Dunnett's test).

Appendix D Permissions

Permission to reprint published content was obtained from the following publishers through the Copyright Clearance Center system.

For Figure 1-2, the following statement was retrieved from the reprint and permission request page of **Nature Publishing Group:** "The author of articles published by Springer Nature do not usually need to seek permission for re-use of their material as long as the journal is credited with initial publication".

Figure 1-3 was reprinted by permission from the **Elsevier BV (European Association Of Urology)**.

Please find a copy of the permission below.

European urology

Billing Status: **N/A**

Order detail ID:	71745893
ISSN:	0302-2838
Publication Type:	Journal
Volume:	
Issue:	
Start page:	
Publisher:	ELSEVIER BV
Author/Editor:	EUROPEAN ASSOCIATION OF UROLOGY

Permission Status: **Granted**

Permission type: Republish or display content
Type of use: Thesis/Dissertation
Order License Id: 4500880786528

View details

Note: This item was invoiced separately through our **RightsLink service.** More info

$ 0.00

Figure 1-4 was reprinted by permission from the **Company of Biologists Ltd.**

Please find a copy of the permission below.

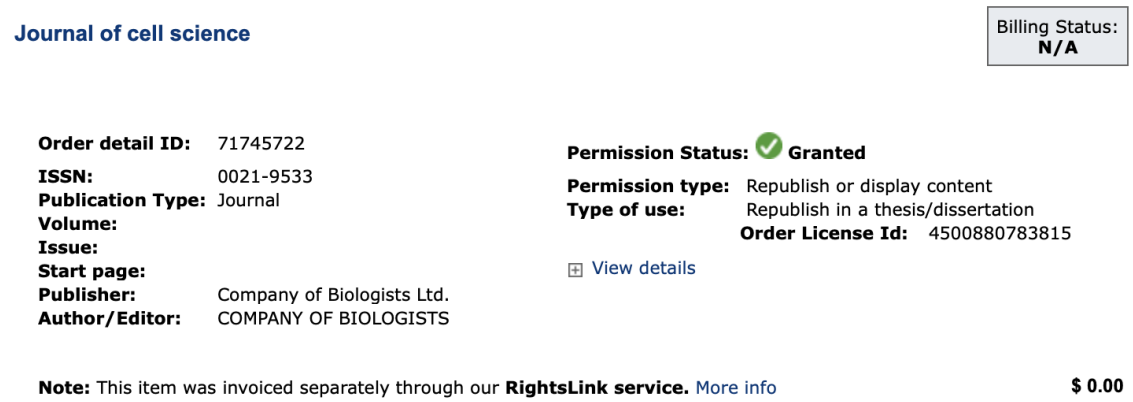

Journal of cell science

Billing Status: **N/A**

Order detail ID: 71745722
ISSN: 0021-9533
Publication Type: Journal
Volume:
Issue:
Start page:
Publisher: Company of Biologists Ltd.
Author/Editor: COMPANY OF BIOLOGISTS

Permission Status: **Granted**
Permission type: Republish or display content
Type of use: Republish in a thesis/dissertation
Order License Id: 4500880783815

View details

Note: This item was invoiced separately through our **RightsLink service.** More info **$ 0.00**

Figure 1-5 was reprinted by permission from the **Nature Publishing Group.**

Please find a copy of the permission below.

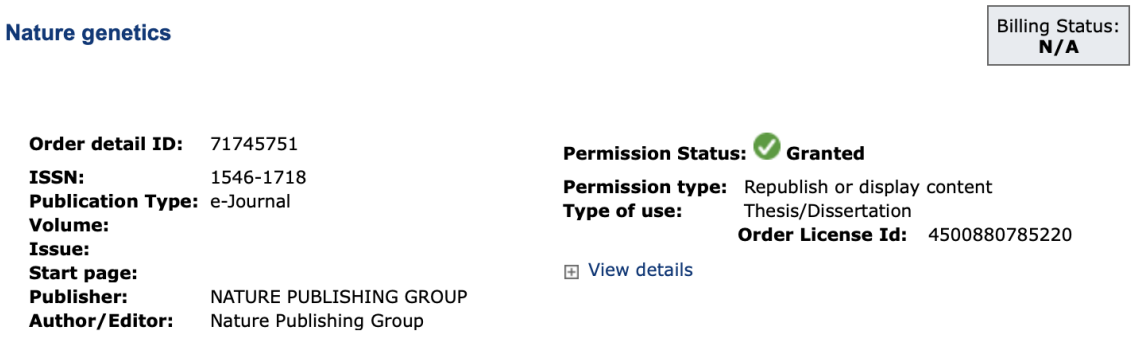

Nature genetics

Billing Status: **N/A**

Order detail ID: 71745751
ISSN: 1546-1718
Publication Type: e-Journal
Volume:
Issue:
Start page:
Publisher: NATURE PUBLISHING GROUP
Author/Editor: Nature Publishing Group

Permission Status: **Granted**
Permission type: Republish or display content
Type of use: Thesis/Dissertation
Order License Id: 4500880785220

View details

Appendix E Federal Funding Disclaimer

All federal funds used for the work described in this dissertation have been explicitly acknowledged in the document.

Disclaimer: “Any opinions, findings, and conclusions or recommendations expressed in this publication are those of the author(s) and do not necessarily reflect the views of the National Cancer Institute” (Research Terms Clarification 2 CFR§ 200.328).

References

1 Fry CH, Vahabi B. The Role of the Mucosa in Normal and Abnormal Bladder Function. *Basic Clin Pharmacol Toxicol* 2016;119 Suppl 3:57-62.

2 Lewis SA. Everything you wanted to know about the bladder epithelium but were afraid to ask. *Am J Physiol Renal Physiol* 2000;278(6):F867-874.

3 Jost SP, Gosling JA, Dixon JS. The morphology of normal human bladder urothelium. *J Anat* 1989;167:103-115.

4 Khandelwal P, Abraham SN, Apodaca G. Cell biology and physiology of the uroepithelium. *Am J Physiol Renal Physiol* 2009;297(6):F1477-1501.

5 Jost SP, Potten CS. Urothelial proliferation in growing mice. *Cell Tissue Kinet* 1986;19(2):155-160.

6 Apodaca G. The uroepithelium: not just a passive barrier. *Traffic* 2004;5(3):117-128.

7 Staack A, Hayward SW, Baskin LS, *et al.* Molecular, cellular and developmental biology of urothelium as a basis of bladder regeneration. *Differentiation* 2005;73(4):121-133.

8 Negrete HO, Lavelle JP, Berg J, *et al.* Permeability properties of the intact mammalian bladder epithelium. *Am J Physiol* 1996;271(4 Pt 2):F886-894.

9 Hicks RM. The mammalian urinary bladder: an accommodating organ. *Biol Rev Camb Philos Soc* 1975;50(2):215-246.

10 Sun TT, Liang FX, Wu XR. Uroplakins as markers of urothelial differentiation. *Adv Exp Med Biol* 1999;462:7-18; discussion 103-114.

11 Acharya P, Beckel J, Ruiz WG, *et al.* Distribution of the tight junction proteins ZO-1, occludin, and claudin-4, -8, and -12 in bladder epithelium. *Am J Physiol Renal Physiol* 2004;287(2):F305-318.

12 Jost SP. Cell cycle of normal bladder urothelium in developing and adult mice. *Virchows Arch B Cell Pathol Incl Mol Pathol* 1989;57(1):27-36.

13 Romih R, Jezernik K. Reorganisation of the urothelial luminal plasma membrane in the cyclophosphamide treated rats. *Pflugers Arch* 1996;431(6 Suppl 2):R241-242.

14 Mysorekar IU, Mulvey MA, Hultgren SJ, *et al.* Molecular regulation of urothelial renewal and host defenses during infection with uropathogenic Escherichia coli. *J Biol Chem* 2002;277(9):7412-7419.

15 Lavelle J, Meyers S, Ramage R, *et al.* Bladder permeability barrier: recovery from selective injury of surface epithelial cells. *Am J Physiol Renal Physiol* 2002;283(2):F242-253.

16 Shin K, Lee J, Guo N, *et al.* Hedgehog/Wnt feedback supports regenerative proliferation of epithelial stem cells in bladder. *Nature* 2011;472(7341):110-114.

17 Gandhi D, Molotkov A, Batourina E, *et al.* Retinoid signaling in progenitors controls specification and regeneration of the urothelium. *Dev Cell* 2013;26(5):469-482.

18 Signoretti S, Pires MM, Lindauer M, *et al.* p63 regulates commitment to the prostate cell lineage. *Proc Natl Acad Sci U S A* 2005;102(32):11355-11360.

19 Karni-Schmidt O, Castillo-Martin M, Shen TH, *et al.* Distinct expression profiles of p63 variants during urothelial development and bladder cancer progression. *Am J Pathol* 2011;178(3):1350-1360.

20 Ferlay J, Soerjomataram I, Dikshit R, *et al.* Cancer incidence and mortality worldwide: sources, methods and major patterns in GLOBOCAN 2012. *Int J Cancer* 2015;136(5):E359-386.

21 Siegel RL, Miller, K. D. and Jemal, A. Cancer statistics, 2018. Vol. 68: CA: A Cancer Journal for Clinicians, 2018.

22 Pakzad R, Mohammadian-Hafshejani A, Mohammadian M, *et al.* Incidence and Mortality of Bladder Cancer and their Relationship with Development in Asia. *Asian Pac J Cancer Prev* 2015;16(16):7365-7374.

23 Bray F, Ren JS, Masuyer E, *et al.* Global estimates of cancer prevalence for 27 sites in the adult population in 2008. *Int J Cancer* 2013;132(5):1133-1145.

24 Smith ND, Prasad SM, Patel AR, *et al.* Bladder Cancer Mortality in the United States: A Geographic and Temporal Analysis of Socioeconomic and Environmental Factors. *J Urol* 2016;195(2):290-296.

25 Hoffmann D, Hoffmann I, El-Bayoumy K. The less harmful cigarette: a controversial issue. a tribute to Ernst L. Wynder. *Chem Res Toxicol* 2001;14(7):767-790.

26 Freedman ND, Silverman DT, Hollenbeck AR, *et al.* Association between smoking and risk of bladder cancer among men and women. *JAMA* 2011;306(7):737-745.

27 Baris D, Karagas MR, Verrill C, *et al.* A case-control study of smoking and bladder cancer risk: emergent patterns over time. *J Natl Cancer Inst* 2009;101(22):1553-1561.

28 Lee HW, Park SH, Weng MW, *et al.* E-cigarette smoke damages DNA and reduces repair activity in mouse lung, heart, and bladder as well as in human lung and bladder cells. *Proc Natl Acad Sci U S A* 2018;115(7):E1560-E1569.

29 Pira E, Piolatto G, Negri E, *et al.* Bladder cancer mortality of workers exposed to aromatic amines: a 58-year follow-up. *J Natl Cancer Inst* 2010;102(14):1096-1099.

30 Takkouche B, Regueira-Méndez C, Montes-Martínez A. Risk of cancer among hairdressers and related workers: a meta-analysis. *Int J Epidemiol* 2009;38(6):1512-1531.

31 Straif K, Weiland SK, Bungers M, *et al.* Exposure to high concentrations of nitrosamines and cancer mortality among a cohort of rubber workers. *Occup Environ Med* 2000;57(3):180-187.

32 Ferrucci LM, Sinha R, Ward MH, *et al.* Meat and components of meat and the risk of bladder cancer in the NIH-AARP Diet and Health Study. *Cancer* 2010;116(18):4345-4353.

33 Michaud DS, Holick CN, Giovannucci E, *et al.* Meat intake and bladder cancer risk in 2 prospective cohort studies. *Am J Clin Nutr* 2006;84(5):1177-1183.

34 Catsburg CE, Gago-Dominguez M, Yuan JM, *et al.* Dietary sources of N-nitroso compounds and bladder cancer risk: findings from the Los Angeles bladder cancer study. *Int J Cancer* 2014;134(1):125-135.

35 Cartwright RA, Glashan RW, Rogers HJ, *et al.* Role of N-acetyltransferase phenotypes in bladder carcinogenesis: a pharmacogenetic epidemiological approach to bladder cancer. *Lancet* 1982;2(8303):842-845.

36 Risch A, Wallace DM, Bathers S, *et al.* Slow N-acetylation genotype is a susceptibility factor in occupational and smoking related bladder cancer. *Hum Mol Genet* 1995;4(2):231-236.

37 Filiadis IF, Georgiou I, Alamanos Y, *et al.* Genotypes of N-acetyltransferase-2 and risk of bladder cancer: a case-control study. *J Urol* 1999;161(5):1672-1675.

38 Garrett BE, Dube SR, Trosclair A, *et al.* Cigarette smoking - United States, 1965-2008. *MMWR Suppl* 2011;60(1):109-113.

39 Hartge P, Harvey EB, Linehan WM, *et al.* Unexplained excess risk of bladder cancer in men. *J Natl Cancer Inst* 1990;82(20):1636-1640.

40 Edgren G, Liang L, Adami HO, *et al.* Enigmatic sex disparities in cancer incidence. *Eur J Epidemiol* 2012;27(3):187-196.

41 Mungan NA, Kiemeney LA, van Dijck JA, *et al.* Gender differences in stage distribution of bladder cancer. *Urology* 2000;55(3):368-371.

42 Mungan NA, Aben KK, Schoenberg MP, *et al.* Gender differences in stage-adjusted bladder cancer survival. *Urology* 2000;55(6):876-880.

43 Konety BR, Joslyn SA. Factors influencing aggressive therapy for bladder cancer: an analysis of data from the SEER program. *J Urol* 2003;170(5):1765-1771.

44 Snyder C, Harlan L, Knopf K, *et al.* Patterns of care for the treatment of bladder cancer. *J Urol* 2003;169(5):1697-1701.

45 Schroeder A, Herrmann A, Cherryholmes G, *et al.* Loss of androgen receptor expression promotes a stem-like cell phenotype in prostate cancer through STAT3 signaling. *Cancer Res* 2014;74(4):1227-1237.

46 Fillmore CM, Gupta PB, Rudnick JA, *et al.* Estrogen expands breast cancer stem-like cells through paracrine FGF/Tbx3 signaling. *Proc Natl Acad Sci U S A* 2010;107(50):21737-21742.

47 Li Z, Tuteja G, Schug J, *et al.* Foxa1 and Foxa2 are essential for sexual dimorphism in liver cancer. *Cell* 2012;148(1-2):72-83.

48 Naugler WE, Sakurai T, Kim S, *et al.* Gender disparity in liver cancer due to sex differences in MyD88-dependent IL-6 production. *Science* 2007;317(5834):121-124.

49 Tuygun C, Kankaya D, Imamoglu A, *et al.* Sex-specific hormone receptors in urothelial carcinomas of the human urinary bladder: a comparative analysis of clinicopathological features and survival outcomes according to receptor expression. *Urol Oncol* 2011;29(1):43-51.

50 Yee DS, Ishill NM, Lowrance WT, *et al.* Ethnic differences in bladder cancer survival. *Urology* 2011;78(3):544-549.

51 Underwood W, Dunn RL, Williams C, *et al.* Gender and geographic influence on the racial disparity in bladder cancer mortality in the US. *J Am Coll Surg* 2006;202(2):284-290.

52 Gelfand M, Weinberg RW, Castle WM. Relation between carcinoma of the bladder and infestation with Schistosoma haematobium. *Lancet* 1967;1(7502):1249-1251.

53 Melicow MM. The urothelium: a battleground for oncogenesis. *J Urol* 1978;120(1):43-47.

54 Ogawa K, St John M, Luiza de Oliveira M, *et al.* Comparison of uroplakin expression during urothelial carcinogenesis induced by N-butyl-N-(4-hydroxybutyl)nitrosamine in rats and mice. *Toxicol Pathol* 1999;27(6):645-651.

55 Jacobs JB, Arai M, Cohen SM, *et al.* Early lesions in experimental bladder cancer: scanning electron microscopy of cell surface markers. *Cancer Res* 1976;36(7 PT 2):2512-2517.

56 DeGraff DJ, Cates JM, Mauney JR, *et al.* When urothelial differentiation pathways go wrong: implications for bladder cancer development and progression. *Urol Oncol* 2013;31(6):802-811.

57 Mohr DN, Offord KP, Owen RA, *et al.* Asymptomatic microhematuria and urologic disease. A population-based study. *JAMA* 1986;256(2):224-229.

58 Koss LG, Deitch D, Ramanathan R, *et al.* Diagnostic value of cytology of voided urine. *Acta Cytol* 1985;29(5):810-816.

59 Babjuk M, Böhle A, Burger M, *et al.* EAU Guidelines on Non-Muscle-invasive Urothelial Carcinoma of the Bladder: Update 2016. *Eur Urol* 2017;71(3):447-461.

60 Sobin L, Wittekind C. UICC TNM classification of malignant tumours. Vol. 6. New York: Wiley- Liss; 2002. .

61 Paner GP, Stadler WM, Hansel DE, *et al.* Updates in the Eighth Edition of the Tumor-Node-Metastasis Staging Classification for Urologic Cancers. *Eur Urol* 2018;73(4):560-569.

62 Spruck CH, Ohneseit PF, Gonzalez-Zulueta M, *et al.* Two molecular pathways to transitional cell carcinoma of the bladder. *Cancer Res* 1994;54(3):784-788.

63 Heney NM, Ahmed S, Flanagan MJ, *et al.* Superficial bladder cancer: progression and recurrence. *J Urol* 1983;130(6):1083-1086.

64 Curry JL, Wojcik EM. The effects of the current World Health Organization/International Society of Urologic Pathologists bladder neoplasm classification system on urine cytology results. *Cancer* 2002;96(3):140-145.

65 Althausen AF, Prout GR, Daly JJ. Non-invasive papillary carcinoma of the bladder associated with carcinoma in situ. *J Urol* 1976;116(5):575-580.

66 Gibas Z, Prout GR, Connolly JG, *et al.* Nonrandom chromosomal changes in transitional cell carcinoma of the bladder. *Cancer Res* 1984;44(3):1257-1264.

67 Liebert M, Seigne J. Characteristics of invasive bladder cancers: histological and molecular markers. *Semin Urol Oncol* 1996;14(2):62-72.

68 Noone AM, Howlader N, Krapcho M, *et al.* SEER Cancer Statistics Review, 1975-2015, National Cancer Institute. Bethesda, MD, https://seer.cancer.gov/csr/1975_2015/ , based on November 2017 SEER data submission, posted to the SEER web site, April 2018.

69 Shinagare AB, Ramaiya NH, Jagannathan JP, *et al.* Metastatic pattern of bladder cancer: correlation with the characteristics of the primary tumor. *AJR Am J Roentgenol* 2011;196(1):117-122.

70 Sidransky D, Von Eschenbach A, Tsai YC, *et al.* Identification of p53 gene mutations in bladder cancers and urine samples. *Science* 1991;252(5006):706-709.

71 Tsai YC, Nichols PW, Hiti AL, *et al.* Allelic losses of chromosomes 9, 11, and 17 in human bladder cancer. *Cancer Res* 1990;50(1):44-47.

72 Habuchi T, Ogawa O, Kakehi Y, *et al.* Accumulated allelic losses in the development of invasive urothelial cancer. *Int J Cancer* 1993;53(4):579-584.

73 Hurst CD, Platt FM, Taylor CF, *et al.* Novel tumor subgroups of urothelial carcinoma of the bladder defined by integrated genomic analysis. *Clin Cancer Res* 2012;18(21):5865-5877.

74 Epstein JI, Amin MB, Reuter VR, *et al.* The World Health Organization/International Society of Urological Pathology consensus classification of urothelial (transitional cell) neoplasms of the urinary bladder. Bladder Consensus Conference Committee. *Am J Surg Pathol* 1998;22(12):1435-1448.

75 Mostofi, Fathollah Keshvar , Sobin, Leslie H , Torloni, Humberto & World Health Organization . (1973). Histological typing of urinary bladder tumours

76 Allard P, Bernard P, Fradet Y, *et al.* The early clinical course of primary Ta and T1 bladder cancer: a proposed prognostic index. *Br J Urol* 1998;81(5):692-698.

77 Kurth KH, Denis L, Bouffioux C, *et al.* Factors affecting recurrence and progression in superficial bladder tumours. *Eur J Cancer* 1995;31A(11):1840-1846.

78 Eble JN SG, Epstein JI, Sesterhenn IA. World Health Organiza- tion classification of tumours. Pathology and genetics of tumours of the urinary system and male genital organs. Lyon, France: IARC Press; 2004.

79 Yamashita H, Amponsa VO, Warrick JI, *et al.* On a FOX hunt: functions of FOX transcriptional regulators in bladder cancer. *Nat Rev Urol* 2017;14(2):98-106.

80 NCCN Guidelines. National Comprehensive Cancer Network Version 1.2018. Bladder Cancer. https://www.nccn.org/professionals/physician_gls/pdf/bladder.pdf. Accessed January 22, 2018.

81 Sylvester RJ, Oosterlinck W, van der Meijden AP. A single immediate postoperative instillation of chemotherapy decreases the risk of recurrence in patients with stage Ta T1 bladder cancer: a meta-analysis of published results of randomized clinical trials. *J Urol* 2004;171(6 Pt 1):2186-2190, quiz 2435.

82 Sylvester RJ, Brausi MA, Kirkels WJ, *et al.* Long-term efficacy results of EORTC genito-urinary group randomized phase 3 study 30911 comparing intravesical instillations of epirubicin, bacillus Calmette-Guérin, and bacillus Calmette-Guérin plus isoniazid in patients with intermediate- and high-risk stage Ta T1 urothelial carcinoma of the bladder. *Eur Urol* 2010;57(5):766-773.

83 Böhle A, Jocham D, Bock PR. Intravesical bacillus Calmette-Guerin versus mitomycin C for superficial bladder cancer: a formal meta-analysis of comparative studies on recurrence and toxicity. *J Urol* 2003;169(1):90-95.

84 Lamm DL, Blumenstein BA, Crissman JD, *et al.* Maintenance bacillus Calmette-Guerin immunotherapy for recurrent TA, T1 and carcinoma in situ transitional cell carcinoma of the bladder: a randomized Southwest Oncology Group Study. *J Urol* 2000;163(4):1124-1129.

85 Yates DR, Brausi MA, Catto JW, *et al.* Treatment options available for bacillus Calmette-Guérin failure in non-muscle-invasive bladder cancer. *Eur Urol* 2012;62(6):1088-1096.

86 Cookson MS, Herr HW, Zhang ZF, *et al.* The treated natural history of high risk superficial bladder cancer: 15-year outcome. *J Urol* 1997;158(1):62-67.

87 Svatek RS, Hollenbeck BK, Holmäng S, *et al.* The economics of bladder cancer: costs and considerations of caring for this disease. *Eur Urol* 2014;66(2):253-262.

88 Singer S, Ziegler C, Schwalenberg T, *et al.* Quality of life in patients with muscle invasive and non-muscle invasive bladder cancer. *Support Care Cancer* 2013;21(5):1383-1393.

89 Stein JP, Lieskovsky G, Cote R, *et al.* Radical cystectomy in the treatment of invasive bladder cancer: long-term results in 1,054 patients. *J Clin Oncol* 2001;19(3):666-675.

90 Herr HW, Dotan Z, Donat SM, *et al.* Defining optimal therapy for muscle invasive bladder cancer. *J Urol* 2007;177(2):437-443.

91 McConkey DJ, Choi W, Ochoa A, *et al.* Therapeutic opportunities in the intrinsic subtypes of muscle-invasive bladder cancer. *Hematol Oncol Clin North Am* 2015;29(2):377-394, x-xi.

92 Knowles MA. Novel therapeutic targets in bladder cancer: mutation and expression of FGF receptors. *Future Oncol* 2008;4(1):71-83.

93 Knowles MA, Platt FM, Ross RL, *et al.* Phosphatidylinositol 3-kinase (PI3K) pathway activation in bladder cancer. *Cancer Metastasis Rev* 2009;28(3-4):305-316.

94 Black PC, Brown GA, Inamoto T, *et al.* Sensitivity to epidermal growth factor receptor inhibitor requires E-cadherin expression in urothelial carcinoma cells. *Clin Cancer Res* 2008;14(5):1478-1486.

95 Powles T, Eder JP, Fine GD, *et al.* MPDL3280A (anti-PD-L1) treatment leads to clinical activity in metastatic bladder cancer. *Nature* 2014;515(7528):558-562.

96 Donin NM, Lenis AT, Holden S, *et al.* Immunotherapy for the Treatment of Urothelial Carcinoma. *J Urol* 2017;197(1):14-22.

97 Amin MB. Histological variants of urothelial carcinoma: diagnostic, therapeutic and prognostic implications. *Mod Pathol* 2009;22 Suppl 2:S96-S118.

98 Jozwicki W, Domaniewski J, Skok Z, *et al.* Usefulness of histologic homogeneity estimation of muscle-invasive urinary bladder cancer in an individual prognosis: a mapping study. *Urology* 2005;66(5):1122-1126.

99 Mitra AP, Bartsch CC, Bartsch G, *et al.* Does presence of squamous and glandular differentiation in urothelial carcinoma of the bladder at cystectomy portend poor prognosis? An intensive case-control analysis. *Urol Oncol* 2014;32(2):117-127.

100 Rogers CG, Palapattu GS, Shariat SF, *et al.* Clinical outcomes following radical cystectomy for primary nontransitional cell carcinoma of the bladder compared to transitional cell carcinoma of the bladder. *J Urol* 2006;175(6):2048-2053; discussion 2053.

101 López-Beltrán A, Martín J, García J, *et al.* Squamous and glandular differentiation in urothelial bladder carcinomas. Histopathology, histochemistry and immunohistochemical expression of carcinoembryonic antigen. *Histol Histopathol* 1988;3(1):63-68.

102 Kastritis E, Dimopoulos MA, Antoniou N, *et al.* The outcome of patients with advanced pure squamous or mixed squamous and transitional urothelial carcinomas following platinum-based chemotherapy. *Anticancer Res* 2006;26(5B):3865-3869.

103 Galsky MD, Iasonos A, Mironov S, *et al.* Prospective trial of ifosfamide, paclitaxel, and cisplatin in patients with advanced non-transitional cell carcinoma of the urothelial tract. *Urology* 2007;69(2):255-259.

104 Eble JN, Young RH. Carcinoma of the urinary bladder: a review of its diverse morphology. *Semin Diagn Pathol* 1997;14(2):98-108.

105 Billis A, Schenka AA, Ramos CC, *et al.* Squamous and/or glandular differentiation in urothelial carcinoma: prevalence and significance in transurethral resections of the bladder. *Int Urol Nephrol* 2001;33(4):631-633.

106 Zhai QJ, Black J, Ayala AG, *et al.* Histologic variants of infiltrating urothelial carcinoma. *Arch Pathol Lab Med* 2007;131(8):1244-1256.

107 Serretta V, Pomara G, Piazza F, *et al.* Pure squamous cell carcinoma of the bladder in western countries. Report on 19 consecutive cases. *Eur Urol* 2000;37(1):85-89.

108 Scosyrev E, Yao J, Messing E. Urothelial carcinoma versus squamous cell carcinoma of bladder: is survival different with stage adjustment? *Urology* 2009;73(4):822-827.

109 Erdem GU, Dogan M, Sakin A, *et al.* Non-Urothelial Bladder Cancer: Comparison of Clinicopathological and Prognostic Characteristics in Pure Adenocarcinoma and Non-Bilharzial Squamous Cell Carcinoma of the Bladder. *Oncol Res Treat* 2018;41(4):220-225.

110 Black PC, Brown GA, Dinney CPN. The impact of variant histology on the outcome of bladder cancer treated with curative intent *Urologic Oncology: Seminars and Original Investigations* 2009(27):5.

111 Visvader JE. Cells of origin in cancer. *Nature* 2011;469(7330):314-322.

112 Van Batavia J, Yamany T, Molotkov A, *et al.* Bladder cancers arise from distinct urothelial sub-populations. *Nat Cell Biol* 2014;16(10):982-991, 981-985.

113 Shin K, Lim A, Odegaard JI, *et al.* Cellular origin of bladder neoplasia and tissue dynamics of its progression to invasive carcinoma. *Nat Cell Biol* 2014;16(5):469-478.

114 McKenney JK, Desai S, Cohen C, *et al.* Discriminatory immunohistochemical staining of urothelial carcinoma in situ and non-neoplastic urothelium: an analysis of cytokeratin 20, p53, and CD44 antigens. *Am J Surg Pathol* 2001;25(8):1074-1078.

115 Dancik GM, Owens CR, Iczkowski KA, *et al.* A cell of origin gene signature indicates human bladder cancer has distinct cellular progenitors. *Stem Cells* 2014;32(4):974-982.

116 Burrell RA, McGranahan N, Bartek J, *et al.* The causes and consequences of genetic heterogeneity in cancer evolution. *Nature* 2013;501(7467):338-345.

117 Marusyk A, Polyak K. Tumor heterogeneity: causes and consequences. *Biochim Biophys Acta* 2010;1805(1):105-117.

118 Greaves M, Maley CC. Clonal evolution in cancer. *Nature* 2012;481(7381):306-313.

119 Harris AL, Neal DE. Bladder cancer--field versus clonal origin. *N Engl J Med* 1992;326(11):759-761.

120 Hafner C, Knuechel R, Stoehr R, *et al.* Clonality of multifocal urothelial carcinomas: 10 years of molecular genetic studies. *Int J Cancer* 2002;101(1):1-6.

121 Miyao N, Tsai YC, Lerner SP, *et al.* Role of chromosome 9 in human bladder cancer. *Cancer Res* 1993;53(17):4066-4070.

122 Gross K, Wronski A, Skibinski A, *et al.* Cell Fate Decisions During Breast Cancer Development. *J Dev Biol* 2016;4(1):4.

123 McGranahan N, Burrell RA, Endesfelder D, *et al.* Cancer chromosomal instability: therapeutic and diagnostic challenges. *EMBO Rep* 2012;13(6):528-538.

124 Marusyk A, Almendro V, Polyak K. Intra-tumour heterogeneity: a looking glass for cancer? *Nat Rev Cancer* 2012;12(5):323-334.

125 Fujimoto K, Yamada Y, Okajima E, *et al.* Frequent association of p53 gene mutation in invasive bladder cancer. *Cancer Res* 1992;52(6):1393-1398.

126 Cappellen D, Gil Diez de Medina S, Chopin D, *et al.* Frequent loss of heterozygosity on chromosome 10q in muscle-invasive transitional cell carcinomas of the bladder. *Oncogene* 1997;14(25):3059-3066.

127 Richter J, Wagner U, Schraml P, *et al.* Chromosomal imbalances are associated with a high risk of progression in early invasive (pT1) urinary bladder cancer. *Cancer Res* 1999;59(22):5687-5691.

128 Hartmann A, Schlake G, Zaak D, *et al.* Occurrence of chromosome 9 and p53 alterations in multifocal dysplasia and carcinoma in situ of human urinary bladder. *Cancer Res* 2002;62(3):809-818.

129 Sidransky D, Frost P, Von Eschenbach A, *et al.* Clonal origin of bladder cancer. *N Engl J Med* 1992;326(11):737-740.

130 Guo G, Sun X, Chen C, *et al.* Whole-genome and whole-exome sequencing of bladder cancer identifies frequent alterations in genes involved in sister chromatid cohesion and segregation. *Nat Genet* 2013;45(12):1459-1463.

131 Wu XR. Urothelial tumorigenesis: a tale of divergent pathways. *Nat Rev Cancer* 2005;5(9):713-725.

132 Wolff EM, Liang G, Jones PA. Mechanisms of Disease: genetic and epigenetic alterations that drive bladder cancer. *Nat Clin Pract Urol* 2005;2(10):502-510.

133 Hedegaard J, Lamy P, Nordentoft I, *et al.* Comprehensive Transcriptional Analysis of Early-Stage Urothelial Carcinoma. *Cancer Cell* 2016;30(1):27-42.

134 Sjödahl G, Lauss M, Lövgren K, *et al.* A molecular taxonomy for urothelial carcinoma. *Clin Cancer Res* 2012;18(12):3377-3386.

135 Lawrence MS, Stojanov P, Polak P, *et al.* Mutational heterogeneity in cancer and the search for new cancer-associated genes. *Nature* 2013;499(7457):214-218.

136 Morrison CD, Liu P, Woloszynska-Read A, *et al.* Whole-genome sequencing identifies genomic heterogeneity at a nucleotide and chromosomal level in bladder cancer. *Proc Natl Acad Sci U S A* 2014;111(6):E672-681.

137 Network CGAR. Comprehensive molecular characterization of urothelial bladder carcinoma. *Nature* 2014;507(7492):315-322.

138 Cairns P, Shaw ME, Knowles MA. Preliminary mapping of the deleted region of chromosome 9 in bladder cancer. *Cancer Res* 1993;53(6):1230-1232.

139 Kim J, Akbani R, Creighton CJ, *et al.* Invasive Bladder Cancer: Genomic Insights and Therapeutic Promise. *Clin Cancer Res* 2015;21(20):4514-4524.

140 Kim J, Mouw KW, Polak P, *et al.* Somatic ERCC2 mutations are associated with a distinct genomic signature in urothelial tumors. *Nat Genet* 2016;48(6):600-606.

141 Roberts SA, Lawrence MS, Klimczak LJ, *et al.* An APOBEC cytidine deaminase mutagenesis pattern is widespread in human cancers. *Nat Genet* 2013;45(9):970-976.

142 Nordentoft I, Lamy P, Birkenkamp-Demtröder K, *et al.* Mutational context and diverse clonal development in early and late bladder cancer. *Cell Rep* 2014;7(5):1649-1663.

143 Billerey C, Chopin D, Aubriot-Lorton MH, *et al.* Frequent FGFR3 mutations in papillary non-invasive bladder (pTa) tumors. *Am J Pathol* 2001;158(6):1955-1959.

144 López-Knowles E, Hernández S, Malats N, *et al.* PIK3CA mutations are an early genetic alteration associated with FGFR3 mutations in superficial papillary bladder tumors. *Cancer Res* 2006;66(15):7401-7404.

145 Przybojewska B, Jagiello A, Jalmuzna P. H-RAS, K-RAS, and N-RAS gene activation in human bladder cancers. *Cancer Genet Cytogenet* 2000;121(1):73-77.

146 Platt FM, Hurst CD, Taylor CF, *et al.* Spectrum of phosphatidylinositol 3-kinase pathway gene alterations in bladder cancer. *Clin Cancer Res* 2009;15(19):6008-6017.

147 Solomon DA, Kim JS, Bondaruk J, *et al.* Frequent truncating mutations of STAG2 in bladder cancer. *Nat Genet* 2013;45(12):1428-1430.

148 Cordon-Cardo C, Dalbagni G, Saez GT, *et al.* p53 mutations in human bladder cancer: genotypic versus phenotypic patterns. *Int J Cancer* 1994;56(3):347-353.

149 López-Knowles E, Hernández S, Kogevinas M, *et al.* The p53 pathway and outcome among patients with T1G3 bladder tumors. *Clin Cancer Res* 2006;12(20 Pt 1):6029-6036.

150 Chatterjee SJ, Datar R, Youssefzadeh D, *et al.* Combined effects of p53, p21, and pRb expression in the progression of bladder transitional cell carcinoma. *J Clin Oncol* 2004;22(6):1007-1013.

151 Mitra AP, Birkhahn M, Cote RJ. p53 and retinoblastoma pathways in bladder cancer. *World J Urol* 2007;25(6):563-571.

152 Cairns P, Evron E, Okami K, *et al.* Point mutation and homozygous deletion of PTEN/MMAC1 in primary bladder cancers. *Oncogene* 1998;16(24):3215-3218.

153 Aveyard JS, Skilleter A, Habuchi T, *et al.* Somatic mutation of PTEN in bladder carcinoma. *Br J Cancer* 1999;80(5-6):904-908.

154 Hurst CD, Alder O, Platt FM, *et al.* Genomic Subtypes of Non-invasive Bladder Cancer with Distinct Metabolic Profile and Female Gender Bias in KDM6A Mutation Frequency. *Cancer Cell* 2017;32(5):701-715.e707.

155 Robertson AG, Kim J, Al-Ahmadie H, *et al.* Comprehensive Molecular Characterization of Muscle-Invasive Bladder Cancer. *Cell* 2017;171(3):540-556.e525.

156 Egger G, Liang G, Aparicio A, *et al.* Epigenetics in human disease and prospects for epigenetic therapy. *Nature* 2004;429(6990):457-463.

157 Kandoth C, McLellan MD, Vandin F, *et al.* Mutational landscape and significance across 12 major cancer types. *Nature* 2013;502(7471):333-339.

158 Russo VEA MR, Riggs AD. Epigenetic mechanisms of gene regulation. Plainview, NY: Cold Spring Harbor Laboratory Press; 1996.

159 Kulis M, Esteller M. DNA methylation and cancer. *Adv Genet* 2010;70:27-56.

160 Jones PA. Functions of DNA methylation: islands, start sites, gene bodies and beyond. *Nat Rev Genet* 2012;13(7):484-492.

161 Baylin SB, Herman JG, Graff JR, *et al.* Alterations in DNA methylation: a fundamental aspect of neoplasia. *Adv Cancer Res* 1998;72:141-196.

162 Esteller M, Corn PG, Baylin SB, *et al.* A gene hypermethylation profile of human cancer. *Cancer Res* 2001;61(8):3225-3229.

163 Gonzalez-Zulueta M, Bender CM, Yang AS, *et al.* Methylation of the 5' CpG island of the p16/CDKN2 tumor suppressor gene in normal and transformed human tissues correlates with gene silencing. *Cancer Res* 1995;55(20):4531-4535.

164 Ribeiro-Filho LA, Franks J, Sasaki M, *et al.* CpG hypermethylation of promoter region and inactivation of E-cadherin gene in human bladder cancer. *Mol Carcinog* 2002;34(4):187-198.

165 Sánchez-Carbayo M. Hypermethylation in bladder cancer: biological pathways and translational applications. *Tumour Biol* 2012;33(2):347-361.

166 Gonzalgo ML, Hayashida T, Bender CM, *et al.* The role of DNA methylation in expression of the p19/p16 locus in human bladder cancer cell lines. *Cancer Res* 1998;58(6):1245-1252.

167 Cabello MJ, Grau L, Franco N, *et al.* Multiplexed methylation profiles of tumor suppressor genes in bladder cancer. *J Mol Diagn* 2011;13(1):29-40.

168 Marsit CJ, Houseman EA, Christensen BC, *et al.* Identification of methylated genes associated with aggressive bladder cancer. *PLoS One* 2010;5(8):e12334.

169 Wolff EM, Chihara Y, Pan F, *et al.* Unique DNA methylation patterns distinguish noninvasive and invasive urothelial cancers and establish an epigenetic field defect in premalignant tissue. *Cancer Res* 2010;70(20):8169-8178.

170 Reinert T, Modin C, Castano FM, *et al.* Comprehensive genome methylation analysis in bladder cancer: identification and validation of novel methylated genes and application of these as urinary tumor markers. *Clin Cancer Res* 2011;17(17):5582-5592.

171 Gui Y, Guo G, Huang Y, *et al.* Frequent mutations of chromatin remodeling genes in transitional cell carcinoma of the bladder. *Nat Genet* 2011;43(9):875-878.

172 Damrauer JS, Hoadley KA, Chism DD, *et al.* Intrinsic subtypes of high-grade bladder cancer reflect the hallmarks of breast cancer biology. *Proc Natl Acad Sci U S A* 2014;111(8):3110-3115.

173 Choi W, Czerniak B, Ochoa A, *et al.* Intrinsic basal and luminal subtypes of muscle-invasive bladder cancer. *Nat Rev Urol* 2014;11(7):400-410.

174 Chu PG, Lyda MH, Weiss LM. Cytokeratin 14 expression in epithelial neoplasms: a survey of 435 cases with emphasis on its value in differentiating squamous cell carcinomas from other epithelial tumours. *Histopathology* 2001;39(1):9-16.

175 Sjödahl G, Eriksson P, Liedberg F, *et al.* Molecular classification of urothelial carcinoma: global mRNA classification versus tumour-cell phenotype classification. *J Pathol* 2017;242(1):113-125.

176 Choi W, Porten S, Kim S, *et al.* Identification of distinct basal and luminal subtypes of muscle-invasive bladder cancer with different sensitivities to frontline chemotherapy. *Cancer Cell* 2014;25(2):152-165.

177 Prat A, Parker JS, Karginova O, *et al.* Phenotypic and molecular characterization of the claudin-low intrinsic subtype of breast cancer. *Breast Cancer Res* 2010;12(5):R68.

178 Dadhania V, Zhang M, Zhang L, *et al.* Meta-Analysis of the Luminal and Basal Subtypes of Bladder Cancer and the Identification of Signature Immunohistochemical Markers for Clinical Use. *EBioMedicine* 2016;12:105-117.

179 Rosenberg JE, Hoffman-Censits J, Powles T, *et al.* Atezolizumab in patients with locally advanced and metastatic urothelial carcinoma who have progressed following treatment with platinum-based chemotherapy: a single-arm, multicentre, phase 2 trial. *Lancet* 2016;387(10031):1909-1920.

180 Mariathasan S, Turley SJ, Nickles D, *et al.* TGFβ attenuates tumour response to PD-L1 blockade by contributing to exclusion of T cells. *Nature* 2018;554(7693):544-548.

181 Warrick JI, Sjödahl G, Kaag M, *et al.* Intratumoral Heterogeneity of Bladder Cancer by Molecular Subtypes and Histologic Variants. *Eur Urol* 2018.

182 Aine M, Eriksson P, Liedberg F, *et al.* On Molecular Classification of Bladder Cancer: Out of One, Many. *Eur Urol* 2015;68(6):921-923.

183 Cully M, You H, Levine AJ, *et al.* Beyond PTEN mutations: the PI3K pathway as an integrator of multiple inputs during tumorigenesis. *Nat Rev Cancer* 2006;6(3):184-192.

184 Cantley LC, Neel BG. New insights into tumor suppression: PTEN suppresses tumor formation by restraining the phosphoinositide 3-kinase/AKT pathway. *Proc Natl Acad Sci U S A* 1999;96(8):4240-4245.

185 Maehama T, Dixon JE. The tumor suppressor, PTEN/MMAC1, dephosphorylates the lipid second messenger, phosphatidylinositol 3,4,5-trisphosphate. *J Biol Chem* 1998;273(22):13375-13378.

186 Myers MP, Stolarov JP, Eng C, *et al.* P-TEN, the tumor suppressor from human chromosome 10q23, is a dual-specificity phosphatase. *Proc Natl Acad Sci U S A* 1997;94(17):9052-9057.

187 Tamura M, Gu J, Matsumoto K, *et al.* Inhibition of cell migration, spreading, and focal adhesions by tumor suppressor PTEN. *Science* 1998;280(5369):1614-1617.

188 Gildea JJ, Herlevsen M, Harding MA, *et al.* PTEN can inhibit in vitro organotypic and in vivo orthotopic invasion of human bladder cancer cells even in the absence of its lipid phosphatase activity. *Oncogene* 2004;23(40):6788-6797.

189 Hoadley KA, Yau C, Wolf DM, *et al.* Multiplatform analysis of 12 cancer types reveals molecular classification within and across tissues of origin. *Cell* 2014;158(4):929-944.

190 Sun CH, Chang YH, Pan CC. Activation of the PI3K/Akt/mTOR pathway correlates with tumour progression and reduced survival in patients with urothelial carcinoma of the urinary bladder. *Histopathology* 2011;58(7):1054-1063.

191 Yoo LI, Liu DW, Le Vu S, *et al.* Pten deficiency activates distinct downstream signaling pathways in a tissue-specific manner. *Cancer Res* 2006;66(4):1929-1939.

192 Puzio-Kuter AM, Castillo-Martin M, Kinkade CW, *et al.* Inactivation of p53 and Pten promotes invasive bladder cancer. *Genes Dev* 2009;23(6):675-680.

193 Tsuruta H, Kishimoto H, Sasaki T, *et al.* Hyperplasia and carcinomas in Pten-deficient mice and reduced PTEN protein in human bladder cancer patients. *Cancer Res* 2006;66(17):8389-8396.

194 Ahmad I, Morton JP, Singh LB, *et al.* β-Catenin activation synergizes with PTEN loss to cause bladder cancer formation. *Oncogene* 2011;30(2):178-189.

195 Foth M, Ahmad I, van Rhijn BW, *et al.* Fibroblast growth factor receptor 3 activation plays a causative role in urothelial cancer pathogenesis in cooperation with Pten loss in mice. *J Pathol* 2014;233(2):148-158.

196 Planchon SM, Waite KA, Eng C. The nuclear affairs of PTEN. *J Cell Sci* 2008;121(Pt 3):249-253.

197 Varley C, Bacon E, Holder J, *et al.* FOXA1 and IRF-1 intermediary transcriptional regulators of PPARc-induced urothelial
cytodifferentiation. *Cell Death and Differentiation* 2009;16:11.

198 Gao N, Ishii K, Mirosevich J, *et al.* Forkhead box A1 regulates prostate ductal morphogenesis and promotes epithelial cell maturation. *Development* 2005;132(15):3431-3443.

199 Kaestner KH. The FoxA factors in organogenesis and differentiation. *Curr Opin Genet Dev* 2010;20(5):527-532.

200 Bernardo GM, Lozada KL, Miedler JD, *et al.* FOXA1 is an essential determinant of ERalpha expression and mammary ductal morphogenesis. *Development* 2010;137(12):2045-2054.

201 Lin L, Miller CT, Contreras JI, *et al.* The hepatocyte nuclear factor 3 alpha gene, HNF3alpha (FOXA1), on chromosome band 14q13 is amplified and overexpressed in esophageal and lung adenocarcinomas. *Cancer Res* 2002;62(18):5273-5279.

202 Gerhardt J, Montani M, Wild P, *et al.* FOXA1 promotes tumor progression in prostate cancer and represents a novel hallmark of castration-resistant prostate cancer. *Am J Pathol* 2012;180(2):848-861.

203 Bernardo GM, Bebek G, Ginther CL, *et al.* FOXA1 represses the molecular phenotype of basal breast cancer cells. *Oncogene* 2013;32(5):554-563.

204 DeGraff D, Clark P, Cates J, *et al.* Loss of the Urothelial Differentiation Marker FOXA1 Is Associated with High Grade, Late Stage Bladder Cancer and Increased Tumor Proliferation. *PLoS ONE* 2012;7(5):13.

205 Reddy OL, Cates JM, Gellert LL, *et al.* Loss of FOXA1 Drives Sexually Dimorphic Changes in Urothelial Differentiation and Is an Independent Predictor of Poor Prognosis in Bladder Cancer. *Am J Pathol* 2015;185(5):1385-1395.

206 Cirillo LA, McPherson CE, Bossard P, *et al.* Binding of the winged-helix transcription factor HNF3 to a linker histone site on the nucleosome. *EMBO J* 1998;17(1):244-254.

207 Sekiya T, Muthurajan UM, Luger K, *et al.* Nucleosome-binding affinity as a primary determinant of the nuclear mobility of the pioneer transcription factor FoxA. *Genes Dev* 2009;23(7):804-809.

208 Motallebipour M, Ameur A, Reddy Bysani MS, *et al.* Differential binding and co-binding pattern of FOXA1 and FOXA3 and their relation to H3K4me3 in HepG2 cells revealed by ChIP-seq. *Genome Biol* 2009;10(11):R129.

209 Lupien M, Eeckhoute J, Meyer CA, *et al.* FoxA1 translates epigenetic signatures into enhancer-driven lineage-specific transcription. *Cell* 2008;132(6):958-970.

210 Lacroix M, Leclercq G. About GATA3, HNF3A, and XBP1, three genes co-expressed with the oestrogen receptor-alpha gene (ESR1) in breast cancer. *Mol Cell Endocrinol* 2004;219(1-2):1-7.

211 Ross-Innes CS, Stark R, Teschendorff AE, *et al.* Differential oestrogen receptor binding is associated with clinical outcome in breast cancer. *Nature* 2012;481(7381):389-393.

212 Gao N, Zhang J, Rao MA, *et al.* The role of hepatocyte nuclear factor-3 alpha (Forkhead Box A1) and androgen receptor in transcriptional regulation of prostatic genes. *Mol Endocrinol* 2003;17(8):1484-1507.

213 Warrick JI, Walter V, Yamashita H, *et al.* FOXA1, GATA3 and PPARɣ Cooperate to Drive Luminal Subtype in Bladder Cancer: A Molecular Analysis of Established Human Cell Lines. *Sci Rep* 2016;6:38531.

214 Badve S, Turbin D, Thorat MA, *et al.* FOXA1 expression in breast cancer--correlation with luminal subtype A and survival. *Clin Cancer Res* 2007;13(15 Pt 1):4415-4421.

215 Jin HJ, Zhao JC, Ogden I, *et al.* Androgen receptor-independent function of FoxA1 in prostate cancer metastasis. *Cancer Res* 2013;73(12):3725-3736.

216 Lehnertz B, Ueda Y, Derijck AA, *et al.* Suv39h-mediated histone H3 lysine 9 methylation directs DNA methylation to major satellite repeats at pericentric heterochromatin. *Curr Biol* 2003;13(14):1192-1200.

217 Jozwik KM, Chernukhin I, Serandour AA, *et al.* FOXA1 Directs H3K4 Monomethylation at Enhancers via Recruitment of the Methyltransferase MLL3. *Cell Rep* 2016;17(10):2715-2723.

218 Meyer KB, Carroll JS. FOXA1 and breast cancer risk. *Nat Genet* 2012;44(11):1176-1177.

219 Gabriel U, Bolenz C, Michel MS. Experimental models for therapeutic studies of transitional cell carcinoma. *Anticancer Res* 2007;27(5A):3163-3171.

220 Soloway MS. Intravesical and systemic chemotherapy of murine bladder cancer. *Cancer Res* 1977;37(8 Pt 2):2918-2929.

221 Summerhayes IC, Franks LM. Effects of donor age on neoplastic transformation of adult mouse bladder epithelium in vitro. *J Natl Cancer Inst* 1979;62(4):1017-1023.

222 Cohen SM, Yang JP, Jacobs JB, *et al.* Transplantation and cell culture of rat urinary bladder carcinoma. *Invest Urol* 1981;19(3):136-141.

223 van Bokhoven A, Varella-Garcia M, Korch C, *et al.* TSU-Pr1 and JCA-1 cells are derivatives of T24 bladder carcinoma cells and are not of prostatic origin. *Cancer Res* 2001;61(17):6340-6344.

224 DeGraff DJ, Robinson VL, Shah JB, *et al.* Current preclinical models for the advancement of translational bladder cancer research. *Mol Cancer Ther* 2013;12(2):121-130.

225 Williams PD, Lee JK, Theodorescu D. Molecular credentialing of rodent bladder carcinogenesis models. *Neoplasia* 2008;10(8):838-846.

226 Kobayashi T, Owczarek TB, McKiernan JM, *et al.* Modelling bladder cancer in mice: opportunities and challenges. *Nat Rev Cancer* 2015;15(1):42-54.

227 Druckrey H, Preussmann R, Ivankovic S, *et al.* Selective Induction of Bladder Cancer in Rats by DiButyl-and N-Butyl-N-Butanol(4)-Nitrosamine. *Z Krebsforsch* 1964;66:280-290.

228 Fukushima S, Hirose M, Tsuda H, *et al.* Histological classification of urinary bladder cancers in rats induced by N-butyl-n-(4-hydroxybutyl)nitrosamine. *Gan* 1976;67(1):81-90.

229 Vasconcelos-Nóbrega C, Colaço A, Lopes C, *et al.* Review: BBN as an urothelial carcinogen. *In Vivo* 2012;26(4):727-739.

230 Yamamoto S, Masui T, Murai T, *et al.* Frequent mutations of the p53 gene and infrequent H- and K-ras mutations in urinary bladder carcinomas of NON/Shi mice treated with N-butyl-N-(4-hydroxybutyl)nitrosamine. *Carcinogenesis* 1995;16(10):2363-2368.

231 Fantini D, Glaser AP, Rimar KJ, *et al.* A Carcinogen-induced mouse model recapitulates the molecular alterations of human muscle invasive bladder cancer. *Oncogene* 2018.

232 Zhang ZT, Pak J, Shapiro E, *et al.* Urothelium-specific expression of an oncogene in transgenic mice induced the formation of carcinoma in situ and invasive transitional cell carcinoma. *Cancer Res* 1999;59(14):3512-3517.

233 Cheng J, Huang H, Zhang ZT, *et al.* Overexpression of epidermal growth factor receptor in urothelium elicits urothelial hyperplasia and promotes bladder tumor growth. *Cancer Res* 2002;62(14):4157-4163.

234 Zhang ZT, Pak J, Huang HY, *et al.* Role of Ha-ras activation in superficial papillary pathway of urothelial tumor formation. *Oncogene* 2001;20(16):1973-1980.

235 Sharpless NE, Depinho RA. The mighty mouse: genetically engineered mouse models in cancer drug development. *Nat Rev Drug Discov* 2006;5(9):741-754.

236 Politi K, Pao W. How genetically engineered mouse tumor models provide insights into human cancers. *J Clin Oncol* 2011;29(16):2273-2281.

237 Chan E, Patel A, Heston W, *et al.* Mouse orthotopic models for bladder cancer research. *BJU Int* 2009;104(9):1286-1291.

238 Günther JH, Jurczok A, Wulf T, *et al.* Optimizing syngeneic orthotopic murine bladder cancer (MB49). *Cancer Res* 1999;59(12):2834-2837.

239 Oottamasathien S, Williams K, Franco OE, *et al.* Bladder tissue formation from cultured bladder urothelium. *Dev Dyn* 2006;235(10):2795-2801.

240 de Visser KE, Eichten A, Coussens LM. Paradoxical roles of the immune system during cancer development. *Nat Rev Cancer* 2006;6(1):24-37.

241 Jäger W, Xue H, Hayashi T, *et al.* Patient-derived bladder cancer xenografts in the preclinical development of novel targeted therapies. *Oncotarget* 2015;6(25):21522-21532.

242 Pan CX, Zhang H, Tepper CG, *et al.* Development and Characterization of Bladder Cancer Patient-Derived Xenografts for Molecularly Guided Targeted Therapy. *PLoS One* 2015;10(8):e0134346.

243 Rebouissou S, Bernard-Pierrot I, de Reyniès A, *et al.* EGFR as a potential therapeutic target for a subset of muscle-invasive bladder cancers presenting a basal-like phenotype. *Sci Transl Med* 2014;6(244):244ra291.

244 Hovelson DH, Udager AM, McDaniel AS, *et al.* Targeted DNA and RNA Sequencing of Paired Urothelial and Squamous Bladder Cancers Reveals Discordant Genomic and Transcriptomic Events and Unique Therapeutic Implications. *Eur Urol* 2018.

245 Thomsen MBH, Nordentoft I, Lamy P, *et al.* Comprehensive multiregional analysis of molecular heterogeneity in bladder cancer. *Sci Rep* 2017;7(1):11702.

246 Al-Ahmadie HA, Iyer G, Lee BH, *et al.* Frequent somatic CDH1 loss-of-function mutations in plasmacytoid variant bladder cancer. *Nat Genet* 2016;48(4):356-358.

247 Guo CC, Dadhania V, Zhang L, *et al.* Gene Expression Profile of the Clinically Aggressive Micropapillary Variant of Bladder Cancer. *Eur Urol* 2016;70(4):611-620.

248 Bertucci F, Finetti P, Birnbaum D. Basal breast cancer: a complex and deadly molecular subtype. *Curr Mol Med* 2012;12(1):96-110.

249 Knobbe CB, Lapin V, Suzuki A, *et al.* The roles of PTEN in development, physiology and tumorigenesis in mouse models: a tissue-by-tissue survey. *Oncogene* 2008;27(41):5398-5415.

250 Mermel CH, Schumacher SE, Hill B, *et al.* GISTIC2.0 facilitates sensitive and confident localization of the targets of focal somatic copy-number alteration in human cancers. *Genome Biol* 2011;12(4):R41.

251 Walter V, Du Y, Danilova L, *et al.* MVisAGe Identifies Concordant and Discordant Genomic Alterations of Driver Genes in Squamous Tumors. *Cancer Res* 2018;78(12):3375-3385.

252 Gao N, LeLay J, Vatamaniuk MZ, *et al.* Dynamic regulation of Pdx1 enhancers by Foxa1 and Foxa2 is essential for pancreas development. *Genes Dev* 2008;22(24):3435-3448.

253 Lesche R, Groszer M, Gao J, *et al.* Cre/loxP-mediated inactivation of the murine Pten tumor suppressor gene. *Genesis* 2002;32(2):148-149.

254 Mo L, Cheng J, Lee EY, *et al.* Gene deletion in urothelium by specific expression of Cre recombinase. *Am J Physiol Renal Physiol* 2005;289(3):F562-568.

255 Network CGAR. Comprehensive genomic characterization of squamous cell lung cancers. *Nature* 2012;489(7417):519-525.

256 Team RC. R: A language and environment for statistical computing. R Foundation for Statistical Computing, Vienna, Austria. http://www.R-project.org., 2018.

257 Thorat MA, Marchio C, Morimiya A, *et al.* Forkhead box A1 expression in breast cancer is associated with luminal subtype and good prognosis. *J Clin Pathol* 2008;61(3):327-332.

258 Bertram JS, Craig AW. Specific induction of bladder cancer in mice by butyl-(4-hydroxybutyl)-nitrosamine and the effects of hormonal modifications on the sex difference in response. *Eur J Cancer* 1972;8(6):587-594.

259 He Z, Kosinska W, Zhao ZL, *et al.* Tissue-specific mutagenesis by N-butyl-N-(4-hydroxybutyl)nitrosamine as the basis for urothelial carcinogenesis. *Mutat Res* 2012;742(1-2):92-95.

260 Miyamoto H, Yang Z, Chen YT, *et al.* Promotion of bladder cancer development and progression by androgen receptor signals. *J Natl Cancer Inst* 2007;99(7):558-568.

261 Nagao M, Suzuki E, Yasuo K, *et al.* Mutagenicity of N-butyl-N-(4-hydroxybutyl)nitrosamine, a bladder carcinogen, and related compounds. *Cancer Res* 1977;37(2):399-407.

262 Ohtani M, Kakizoe T, Nishio Y, *et al.* Sequential changes of mouse bladder epithelium during induction of invasive carcinomas by N-butyl-N-(4-hydroxybutyl)nitrosamine. *Cancer Res* 1986;46(4 Pt 2):2001-2004.

263 Oliveira PA, Palmeira C, Lourenço LM, *et al.* Evaluation of DNA content in preneoplastic changes of mouse urinary bladder induced by N-butyl-N-(4-hydroxybutyl) nitrosamine. *J Exp Clin Cancer Res* 2005;24(4):609-616.

264 Karoui M, Tresallet C, Julie C, *et al.* Loss of heterozygosity on 10q and mutational status of PTEN and BMPR1A in colorectal primary tumours and metastases. *Br J Cancer* 2004;90(6):1230-1234.

265 Drayton RM, Peter S, Myers K, *et al.* MicroRNA-99a and 100 mediated upregulation of FOXA1 in bladder cancer. *Oncotarget* 2014;5(15):6375-6386.

266 Espinal AC, Buas MF, Wang D, *et al.* FOXA1 hypermethylation: link between parity and ER-negative breast cancer in African American women? *Breast Cancer Res Treat* 2017.

267 Ghosh S, Gu F, Wang CM, *et al.* Genome-wide DNA methylation profiling reveals parity-associated hypermethylation of FOXA1. *Breast Cancer Res Treat* 2014;147(3):653-659.

268 Gong C, Fujino K, Monteiro LJ, *et al.* FOXA1 repression is associated with loss of BRCA1 and increased promoter methylation and chromatin silencing in breast cancer. *Oncogene* 2015;34(39):5012-5024.

269 He F, Melamed J, Tang MS, *et al.* Oncogenic HRAS Activates Epithelial-to-Mesenchymal Transition and Confers Stemness to p53-Deficient Urothelial Cells to Drive Muscle Invasion of Basal Subtype Carcinomas. *Cancer Res* 2015;75(10):2017-2028.

270 Warrick JI, Kaag M, Raman JD, *et al.* Squamous Dysplasia of the Urinary Bladder: A Consecutive Cystectomy Series. *Int J Surg Pathol* 2016;24(4):306-314.

271 Hedegaard J, Lamy P, Nordentoft I, *et al.* Comprehensive Transcriptional Analysis of Early-Stage Urothelial Carcinoma. *Cancer Cell* 2016;30(1):27-42.

272 Lin M, Pan J, Chen Q, *et al.* Overexpression of FOXA1 inhibits cell proliferation and EMT of human gastric cancer AGS cells. *Gene* 2018;642:145-151.

273 Gan HY, Li N, Zhang Q, *et al.* Silencing FOXA1 gene regulates liver cancer cell apoptosis and cell proliferation. *Eur Rev Med Pharmacol Sci* 2018;22(2):397-404.

274 Song L, Wei X, Zhang B, *et al.* Role of Foxa1 in regulation of bcl2 expression during oxidative-stress-induced apoptosis in A549 type II pneumocytes. *Cell Stress Chaperones* 2009;14(4):417-425.

275 Hanahan D, Weinberg RA. Hallmarks of cancer: the next generation. *Cell* 2011;144(5):646-674.

276 Coin F, Marinoni JC, Rodolfo C, *et al.* Mutations in the XPD helicase gene result in XP and TTD phenotypes, preventing interaction between XPD and the p44 subunit of TFIIH. *Nat Genet* 1998;20(2):184-188.

277 Furuta T, Ueda T, Aune G, *et al.* Transcription-coupled nucleotide excision repair as a determinant of cisplatin sensitivity of human cells. *Cancer Res* 2002;62(17):4899-4902.

278 Van Allen EM, Mouw KW, Kim P, *et al.* Somatic ERCC2 mutations correlate with cisplatin sensitivity in muscle-invasive urothelial carcinoma. *Cancer Discov* 2014;4(10):1140-1153.

279 Kelly PN, Strasser A. The role of Bcl-2 and its pro-survival relatives in tumourigenesis and cancer therapy. *Cell Death Differ* 2011;18(9):1414-1424.

280 Mani J, Vallo S, Rakel S, *et al.* Chemoresistance is associated with increased cytoprotective autophagy and diminished apoptosis in bladder cancer cells treated with the BH3 mimetic (-)-Gossypol (AT-101). *BMC Cancer* 2015;15:224.

281 Cordier F, Chaffotte A, Terrien E, *et al.* Ordered phosphorylation events in two independent cascades of the PTEN C-tail revealed by NMR. *J Am Chem Soc* 2012;134(50):20533-20543.

282 Chalasani V, Chin JL, Izawa JI. Histologic variants of urothelial bladder cancer and nonurothelial histology in bladder cancer. *Can Urol Assoc J* 2009;3(6 Suppl 4):S193-198.

283 Seiler R, Ashab HAD, Erho N, *et al.* Impact of Molecular Subtypes in Muscle-invasive Bladder Cancer on Predicting Response and Survival after Neoadjuvant Chemotherapy. *Eur Urol* 2017;72(4):544-554.

284 Ding J, Xu D, Pan C, *et al.* Current animal models of bladder cancer: Awareness of translatability (Review). *Exp Ther Med* 2014;8(3):691-699.

285 Day CP, Merlino G, Van Dyke T. Preclinical mouse cancer models: a maze of opportunities and challenges. *Cell* 2015;163(1):39-53.

286 Wu XR. Biology of urothelial tumorigenesis: insights from genetically engineered mice. *Cancer Metastasis Rev* 2009;28(3-4):281-290.

287 Okada M, Suzuki E, Hashimoto Y. Carcinogenicity of N-nitrosamines related to N-butyl-N-(4-hydroxybutyl)nitrosamine and N,N,-dibutylnitrosamine in ACI/N rats. *Gan* 1976;67(6):825-834.

288 Suzuki E, Anjo T, Aoki J, *et al.* Species variations in the metabolism of N-butyl-N-(4-hydroxybutyl) nitrosamine and related compounds in relation to urinary bladder carcinogenesis. *Gan* 1983;74(1):60-68.

289 Airoldi L, Bonfanti M, Magagnotti C, *et al.* Experimental model for investigating bladder carcinogen metabolism using the isolated rat urinary bladder. *IARC Sci Publ* 1987(84):159-161.

290 Hirose M, Fukushima S, Hananouchi M, *et al.* Different susceptibilities of the urinary bladder epithelium of animal species to three nitroso compounds. *Gan* 1976;67(2):175-189.

291 Shirai T, Murasaki G, Tatematsu M, *et al.* Early surface changes of the urinary bladder epithelium of different animal species induced by N-butyl-N-(4-hydroxybutyl)-nitrosamine. *Gan* 1977;68(2):203-212.

292 Suzuki E, Mochizuki M, Okada M. Relationship of urinary N-butyl-N-(3-carboxypropyl)nitrosamine to susceptibility of animals to bladder carcinogenesis by N-butyl-N-(4-hydroxybutyl)nitrosamine. *Gan* 1983;74(3):360-364.

293 Ohtani M, Kakizoe T, Sato S, *et al.* Strain differences in mice with invasive bladder carcinomas induced by N-butyl-N-(4-hydroxybutyl)nitrosamine. *J Cancer Res Clin Oncol* 1986;112(2):107-110.

294 Akagi G, Akagi A, Kimura M, *et al.* Comparison of bladder tumors induced in rats and mice with N-butyl-N-(4-hydroxybutyl)-nitrosoamine. *Gan* 1973;64(4):331-336.

295 Bonser G, Clayson D, Jull J. Some aspects of the experimental induction of tumours of the bladder. *Br Med Bull* 1958;14(2):146-152.

296 Becci PJ, Thompson HJ, Strum JM, *et al.* N-butyl-N-(4-hydroxybutyl)nitrosamine-induced urinary bladder cancer in C57BL/6 X DBA/2 F1 mice as a useful model for study of chemoprevention of cancer with retinoids. *Cancer Res* 1981;41(3):927-932.

297 Benavides F, Gomez G, Venables-Griffith A, *et al.* Differential susceptibility to chemically induced thymic lymphomas in SENCARB and SSIN inbred mice. *Mol Carcinog* 2006;45(7):543-548.

298 Maronpot RR. Biological Basis of Differential Susceptibility to Hepatocarcinogenesis among Mouse Strains. *J Toxicol Pathol* 2009;22(1):11-33.

299 Ritchie ME, Phipson B, Wu D, *et al.* limma powers differential expression analyses for RNA-sequencing and microarray studies. *Nucleic Acids Res* 2015;43(7):e47.

300 Huang dW, Sherman BT, Lempicki RA. Systematic and integrative analysis of large gene lists using DAVID bioinformatics resources. *Nat Protoc* 2009;4(1):44-57.

301 Huang dW, Sherman BT, Lempicki RA. Bioinformatics enrichment tools: paths toward the comprehensive functional analysis of large gene lists. *Nucleic Acids Res* 2009;37(1):1-13.

302 Saito R, Smith CC, Utsumi T, *et al.* Molecular subtype-specific immunocompetent models of high-grade urothelial carcinoma reveal differential neoantigen expression and response to immunotherapy. *Cancer Res* 2018.

303 Varley CL, Stahlschmidt J, Smith B, *et al.* Activation of peroxisome proliferator-activated receptor-gamma reverses squamous metaplasia and induces transitional differentiation in normal human urothelial cells. *Am J Pathol* 2004;164(5):1789-1798.

304 Sweis RF, Spranger S, Bao R, *et al.* Molecular Drivers of the Non-T-cell-Inflamed Tumor Microenvironment in Urothelial Bladder Cancer. *Cancer Immunol Res* 2016;4(7):563-568.

305 Thomas DG, Ward AM, Williams JL. A study of 52 cases of adenocarcinoma of the bladder. *Br J Urol* 1971;43(1):4-15.

306 Werling RW, Yaziji H, Bacchi CE, *et al.* CDX2, a highly sensitive and specific marker of adenocarcinomas of intestinal origin: an immunohistochemical survey of 476 primary and metastatic carcinomas. *Am J Surg Pathol* 2003;27(3):303-310.

307 Massard C, Gordon MS, Sharma S, *et al.* Safety and Efficacy of Durvalumab (MEDI4736), an Anti-Programmed Cell Death Ligand-1 Immune Checkpoint Inhibitor, in Patients With Advanced Urothelial Bladder Cancer. *J Clin Oncol* 2016;34(26):3119-3125.

308 Sharma P, Callahan MK, Bono P, *et al.* Nivolumab monotherapy in recurrent metastatic urothelial carcinoma (CheckMate 032): a multicentre, open-label, two-stage, multi-arm, phase 1/2 trial. *Lancet Oncol* 2016;17(11):1590-1598.

309 Leontyev D, Neschadim A, Branch DR. Cytokine profiles in mouse models of experimental immune thrombocytopenia reveal a lack of inflammation and differences in response to intravenous immunoglobulin depending on the mouse strain. *Transfusion* 2014;54(11):2871-2879.

310 Gerlinger M, Rowan AJ, Horswell S, *et al.* Intratumor heterogeneity and branched evolution revealed by multiregion sequencing. *N Engl J Med* 2012;366(10):883-892.

311 Gerlinger M, Catto JW, Orntoft TF, *et al.* Intratumour heterogeneity in urologic cancers: from molecular evidence to clinical implications. *Eur Urol* 2015;67(4):729-737.

312 Esserman LJ, Berry DA, Cheang MC, *et al.* Chemotherapy response and recurrence-free survival in neoadjuvant breast cancer depends on biomarker profiles: results from the I-SPY 1 TRIAL (CALGB 150007/150012; ACRIN 6657). *Breast Cancer Res Treat* 2012;132(3):1049-1062.

313 Esserman LJ, Berry DA, DeMichele A, *et al.* Pathologic complete response predicts recurrence-free survival more effectively by cancer subset: results from the I-SPY 1 TRIAL--CALGB 150007/150012, ACRIN 6657. *J Clin Oncol* 2012;30(26):3242-3249.

314 Kim JJ, Tannock IF. Repopulation of cancer cells during therapy: an important cause of treatment failure. *Nat Rev Cancer* 2005;5(7):516-525.

315 Stranger BE, Forrest MS, Dunning M, *et al.* Relative impact of nucleotide and copy number variation on gene expression phenotypes. *Science* 2007;315(5813):848-853.

316 Schreiber-Agus N, Chin L, Chen K, *et al.* An amino-terminal domain of Mxi1 mediates anti-Myc oncogenic activity and interacts with a homolog of the yeast transcriptional repressor SIN3. *Cell* 1995;80(5):777-786.

317 Eagle LR, Yin X, Brothman AR, *et al.* Mutation of the MXI1 gene in prostate cancer. *Nat Genet* 1995;9(3):249-255.

318 Wang DS, Rieger-Christ K, Latini JM, *et al.* Molecular analysis of PTEN and MXI1 in primary bladder carcinoma. *Int J Cancer* 2000;88(4):620-625.

319 Knudson AG. Two genetic hits (more or less) to cancer. *Nat Rev Cancer* 2001;1(2):157-162.

320 Berger AH, Knudson AG, Pandolfi PP. A continuum model for tumour suppression. *Nature* 2011;476(7359):163-169.

321 Tomlinson IP, Roylance R, Houlston RS. Two hits revisited again. *J Med Genet* 2001;38(2):81-85.

322 Whang YE, Wu X, Suzuki H, *et al.* Inactivation of the tumor suppressor PTEN/MMAC1 in advanced human prostate cancer through loss of expression. *Proc Natl Acad Sci U S A* 1998;95(9):5246-5250.

323 Cairns P, Okami K, Halachmi S, *et al.* Frequent inactivation of PTEN/MMAC1 in primary prostate cancer. *Cancer Res* 1997;57(22):4997-5000.

324 Goel A, Arnold CN, Niedzwiecki D, *et al.* Frequent inactivation of PTEN by promoter hypermethylation in microsatellite instability-high sporadic colorectal cancers. *Cancer Res* 2004;64(9):3014-3021.

325 García JM, Silva J, Peña C, *et al.* Promoter methylation of the PTEN gene is a common molecular change in breast cancer. *Genes Chromosomes Cancer* 2004;41(2):117-124.

326 Zhang HY, Liang F, Jia ZL, *et al.* mutation, methylation and expression in breast cancer patients. *Oncol Lett* 2013;6(1):161-168.

327 Agundez M, Grau L, Palou J, *et al.* Evaluation of the methylation status of tumour suppressor genes for predicting bacillus Calmette-Guérin response in patients with T1G3 high-risk bladder tumours. *Eur Urol* 2011;60(1):131-140.

328 Wang X, Trotman LC, Koppie T, *et al.* NEDD4-1 is a proto-oncogenic ubiquitin ligase for PTEN. *Cell* 2007;128(1):129-139.

329 Yang Z, Yuan XG, Chen J, *et al.* Reduced expression of PTEN and increased PTEN phosphorylation at residue Ser380 in gastric cancer tissues: a novel mechanism of PTEN inactivation. *Clin Res Hepatol Gastroenterol* 2013;37(1):72-79.

330 Stefansson OA, Moran S, Gomez A, *et al.* A DNA methylation-based definition of biologically distinct breast cancer subtypes. *Mol Oncol* 2015;9(3):555-568.

331 Frigola J, Song J, Stirzaker C, *et al.* Epigenetic remodeling in colorectal cancer results in coordinate gene suppression across an entire chromosome band. *Nat Genet* 2006;38(5):540-549.

332 Stransky N, Vallot C, Reyal F, *et al.* Regional copy number-independent deregulation of transcription in cancer. *Nat Genet* 2006;38(12):1386-1396.

333 Sutinen P, Rahkama V, Rytinki M, *et al.* Nuclear mobility and activity of FOXA1 with androgen receptor are regulated by SUMOylation. *Mol Endocrinol* 2014;28(10):1719-1728.

334 Ciriello G, Gatza ML, Beck AH, *et al.* Comprehensive Molecular Portraits of Invasive Lobular Breast Cancer. *Cell* 2015;163(2):506-519.

335 Eriksson P, Aine M, Veerla S, *et al.* Molecular subtypes of urothelial carcinoma are defined by specific gene regulatory systems. *BMC Med Genomics* 2015;8:25.

336 Böck M, Hinley J, Schmitt C, *et al.* Identification of ELF3 as an early transcriptional regulator of human urothelium. *Dev Biol* 2014;386(2):321-330.

337 DeGraff DJ, Grabowska MM, Case TC, *et al.* FOXA1 deletion in luminal epithelium causes prostatic hyperplasia and alteration of differentiated phenotype. *Lab Invest* 2014;94(7):726-739.

338 Camolotto SA, Pattabiraman S, Mosbruger TL, *et al.* FoxA1 and FoxA2 drive gastric differentiation and suppress squamous identity in NKX2-1-negative lung cancer. *Elife* 2018;7.

339 Shorning BY, Griffiths D, Clarke AR. Lkb1 and Pten synergise to suppress mTOR-mediated tumorigenesis and epithelial-mesenchymal transition in the mouse bladder. *PLoS One* 2011;6(1):e16209.

340 Lopez-Beltran A, Jimenez RE, Montironi R, *et al.* Flat urothelial carcinoma in situ of the bladder with glandular differentiation. *Hum Pathol* 2011;42(11):1653-1659.

341 Cordon-Cardo C. Molecular alterations associated with bladder cancer initiation and progression. *Scand J Urol Nephrol Suppl* 2008(218):154-165.

342 Mitra AP, Cote RJ. Molecular pathogenesis and diagnostics of bladder cancer. *Annu Rev Pathol* 2009;4:251-285.

343 Jung S, Wu C, Eslami Z, *et al.* The role of immunohistochemistry in the diagnosis of flat urothelial lesions: a study using CK20, CK5/6, P53, Cd138, and Her2/Neu. *Ann Diagn Pathol* 2014;18(1):27-32.

344 Okajima E, Hiramatsu T, Iriya K, *et al.* Effects of sex hormones on development of urinary bladder tumours in rats induced by N-butyl-N-(4-hydroxybutyl) nitrosamine. *Urol Res* 1975;3(2):73-79.

345 Hsu I, Chuang KL, Slavin S, *et al.* Suppression of ERβ signaling via ERβ knockout or antagonist protects against bladder cancer development. *Carcinogenesis* 2014;35(3):651-661.

346 Yao R, Lemon WJ, Wang Y, *et al.* Altered gene expression profile in mouse bladder cancers induced by hydroxybutyl(butyl)nitrosamine. *Neoplasia* 2004;6(5):569-577.

347 Mutant mice and neuroscience: recommendations concerning genetic background. Banbury Conference on genetic background in mice. *Neuron* 1997;19(4):755-759.

348 Smithies O, Maeda N. Gene targeting approaches to complex genetic diseases: atherosclerosis and essential hypertension. *Proc Natl Acad Sci U S A* 1995;92(12):5266-5272.

349 Li J, Yen C, Liaw D, *et al.* PTEN, a putative protein tyrosine phosphatase gene mutated in human brain, breast, and prostate cancer. *Science* 1997;275(5308):1943-1947.

350 Wolf I, Bose S, Williamson EA, *et al.* FOXA1: Growth inhibitor and a favorable prognostic factor in human breast cancer. *Int J Cancer* 2007;120(5):1013-1022.

351 Williamson EA, Wolf I, O'Kelly J, *et al.* BRCA1 and FOXA1 proteins coregulate the expression of the cell cycle-dependent kinase inhibitor p27(Kip1). *Oncogene* 2006;25(9):1391-1399.

352 Oltvai ZN, Milliman CL, Korsmeyer SJ. Bcl-2 heterodimerizes in vivo with a conserved homolog, Bax, that accelerates programmed cell death. *Cell* 1993;74(4):609-619.

353 Hu J, Lieb JD, Sancar A, *et al.* Cisplatin DNA damage and repair maps of the human genome at single-nucleotide resolution. *Proc Natl Acad Sci U S A* 2016;113(41):11507-11512.

354 Sidransky D. Nucleic acid-based methods for the detection of cancer. *Science* 1997;278(5340):1054-1059.

355 Chan MW, Chan LW, Tang NL, *et al.* Hypermethylation of multiple genes in tumor tissues and voided urine in urinary bladder cancer patients. *Clin Cancer Res* 2002;8(2):464-470.

VITA

Vasty Osei Amponsa

EDUCATION

2006-2009	B.Sc. in Biotechnology, Università degli Studi di Parma, Parma, Italy.
2009-2012	M.Sc. in Biotechnology Industry, Università degli Studi di Parma, Parma, Italy.
2013-2019	Ph.D. in Biomedical Sciences and Clinical and Translational Sciences, Pennsylvania State University College of Medicine, Hershey, PA.

HONORS AND AWARDS

Dean's Travel Award, Pennsylvania State University College of Medicine

SELECTED PEER-REVIEWED PUBLICATIONS

1. Warrick JI, Walter V, Yamashita H, Chung E, Shuman L, **Osei-Amponsa V**, Zheng Z, Chan W,Whitcomb TL, Yue F, Iyyanki T, Kawasawa YI, Kaag M, Guo W, Raman JD, Park JS and DeGraff DJ. (2016). FOXA1, GATA3 and PPARɣ Cooperate to Drive Luminal Subtype in Bladder Cancer: A Molecular Analysis of Established Human Cell Lines. Sci Rep. 6:38531.

2. **Osei-Amponsa V**, Shuman L, Ellis J, Wang E, Walter V, Zaleski M, Warrick JI, Raman JD, and DeGraff DJ. Carcinogen-induced bladder cancer in the FVB mouse strain is associated with glandular differentiation and increased Cd274/Pdl-1 expression. [*Under revision*]

3. **Osei-Amponsa V***, Buckwalter JM*****, Shuman L, Zheng Z, Yamashita H, Walter V, Ellis J, Liu C, Warrick JI, Shantz LM, Feehan RP, Al-Ahmadie H, Mendelsohn C, Kaestner KH, Wu XR, DeGraff DJ. Hypermethylation of *FOXA1* and Allelic Loss of *PTEN* Drive Squamous Differentiation and Promote Heterogeneity in Bladder Cancer. *co-first authors. [*Manuscript submitted*]

SELECTED SCIENTIFIC MEETING PRESENTATIONS

1. **Osei-Amponsa V**, Zheng Z, Bouza S, Warrick J, Mendelsohn C, Kaestner K, Wu X and DeGraff D. "Combined Loss of Foxa1 and Pten Accelerates Tumor Progression in a Mouse Model of Carcinogen-Induced Bladder Cancer" at the Society for Basic Urologic Research (SBUR) Fall Symposium. Scottsdale, AZ, 2016 [Poster presentation]

2. **Osei-Amponsa V**, Zheng Z, Walter V, Warrick J, Mendelsohn C, Kaestner K, Wu X, Raman J and DeGraff D. "Novel transgenic knockout model of basal-squamous bladder cancer" at The American Society of Clinical Oncology (ASCO) Genitourinary Cancers Symposium. San Francisco, CA, 2018 [Poster presentation #459]